

**BUILDING DESIGN AND OPERATION FOR IMPROVING  
THERMAL COMFORT IN NATURALLY VENTILATED BUILDINGS IN  
A HOT-HUMID CLIMATE**

A Dissertation

by

ATCH SRESHTHAPUTRA

Submitted to the Office of Graduate Studies of  
Texas A&M University  
in partial fulfillment of the requirements for the degree of

DOCTOR OF PHILOSOPHY

May 2003

Major Subject: Architecture

UMI Number: 3088186

**UMI**<sup>®</sup>

---

UMI Microform 3088186

Copyright 2003 by ProQuest Information and Learning Company.

All rights reserved. This microform edition is protected against  
unauthorized copying under Title 17, United States Code.

ProQuest Information and Learning Company  
300 North Zeeb Road  
P.O. Box 1346  
Ann Arbor, MI 48106-1346

**BUILDING DESIGN AND OPERATION FOR IMPROVING  
THERMAL COMFORT IN NATURALLY VENTILATED BUILDINGS IN  
A HOT-HUMID CLIMATE**

A Dissertation

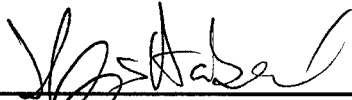
by

ATCH SRESHTHAPUTRA

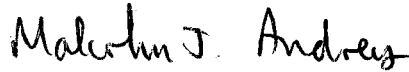
Submitted to Texas A&M University  
in partial fulfillment of the requirements  
for the degree of

DOCTOR OF PHILOSOPHY

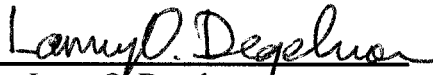
Approved as to style and content by:



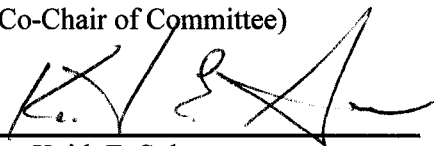
Jeff S. Haberl  
(Co-Chair of Committee)



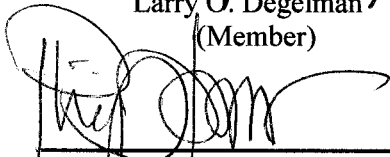
Malcolm J. Andrews  
(Co-Chair of Committee)



Larry O. Degelman  
(Member)



Keith E. Sylvester  
(Member)



Phillip J. Tabb  
(Head of Department)

May 2003

Major Subject: Architecture

## ABSTRACT

Building Design and Operation for Improving Thermal Comfort in Naturally Ventilated Buildings in a Hot-Humid Climate.

(May 2003)

Atch Sressthaputra, B. Arch., Chulalongkorn University, Bangkok, Thailand;

M.S., Georgia Institute of Technology

Co-Chairs of Advisory Committee: Dr. Jeff S. Haberl

Dr. Malcolm J. Andrews

The goal of this research was to develop new techniques for designing and operating unconditioned buildings in a hot-humid climate that could contribute to an improvement of thermal performance and comfort condition. The recommendations proposed in this research will also be useful for facility managers on how to maintain unconditioned buildings in this climate. This study investigated two unconditioned Thai Buddhist temples located in the urban area of Bangkok, Thailand. One is a 100-year-old, high-mass temple. The other is a 5-year-old, lower-mass temple. The indoor measurements revealed that the thermal condition inside both temples exceeded the ASHRAE-recommended comfort zone. Surprisingly, the older temple maintained a more comfortable indoor condition due to its thermal inertia, shading, and earth contacts.

A baseline thermal and airflow model of the old temple was established using a calibrated computer simulation method. To accomplish this, HEATX, a 3-D Computational Fluid Dynamics (CFD) code, was coupled with the DOE-2 thermal simulation program. HEATX was used to calculate the airflow rate and the surface convection coefficients for DOE-2, and DOE-2 was used to provide physical input variables to form the boundary conditions for HEATX. In this way calibrated DOE-2/CFD simulation model was accomplished, and the baseline model was obtained.

To investigate an improved design, four design options were studied: 1) a reflective or low-solar absorption roof, 2) R-30 ceiling insulation, 3) shading devices, and 4) attic ventilation. Each was operated using three modes of ventilation. The low-absorption roof and the R-30

ceiling insulation options were found to be the most effective options, whereas the shading devices and attic ventilation were less effective options, regardless of which ventilation mode was applied. All design options performed much better when nighttime-only ventilation was used.

Based on this analysis, two prototype temples were proposed (i.e., low-mass and high-mass temples). From the simulation results of the two prototypes, design and operation guidelines are proposed, which consist of: 1) increased wall and ceiling insulation, 2) white-colored, low-absorption roof, 3) slab-on-ground floor, 4) shading devices, 5) nighttime-only ventilation, 6) attic ventilation, and 7) wider openings to increase the natural ventilation air flow windows, wing walls, and vertical fins..

## **DEDICATION**

To my parents, my sister, and my wife, for their love and support.

## ACKNOWLEDGMENTS

I would like to express my sincere appreciation to the advisory committee. This research would not have been accomplished without their guidance. My sincerest gratitude goes to Dr. Jeff Haberl who guided me with his dedicated attention, expertise, and knowledge throughout the process of this dissertation; to Dr. Malcolm Andrews who provided me with numerous insightful and comprehensible instructions of using CFD in this research; to Prof. Larry Degelman who provided me with his intuitive suggestions about the methodology and results throughout the course of investigation; and to Dr. Keith Sylvester who gave me constructive suggestions about the DOE-2 simulations in building design.

I feel greatly in debt to the Royal Thai Government who has provided financial support for my study throughout the past several years in this country. In addition to that, I would like to express my sincere gratitude to the American Society of Heating, Refrigerating, and Air-Conditioning Engineers (ASHRAE) and the College of Architecture, Texas A&M University for providing me with financial aid through the ASHRAE Grant-in-Aid and a CARC Research Grant, respectively. Support from the Energy Systems Laboratory at Texas A&M University, and the Houston Chapter of ASHRAE who provides financial aids through the research assistantship and scholarship are also acknowledged.

My special gratitude is given to Monk Panya Kittipunyo at Pathum-wanaram Temple and Monk Wichai at Rama IX Temple for providing convenient access to the case study temples, including securing the data-loggers used for the measurements. Special thanks to Thanjira Sreshthaputra for maintaining the data-loggers and sending the data files to me every month for almost two years; and to Jaruroj Phooprasert and Kietnarin Istaprasert for their assistance with the data collection and measurements.

My heartfelt gratitude is given to my beloved parents who always support me with everything they have; my sister who offers to help me with everything she can; and my wife who loves and understands everything I do. Lastly, thank Lord Buddha for giving me strength, concentration, patience, and wisdom to overcome all of the difficulties I have faced.

## TABLE OF CONTENTS

	Page
ABSTRACT.....	iii
DEDICATION.....	v
ACKNOWLEDGMENTS .....	vi
TABLE OF CONTENTS.....	vii
LIST OF FIGURES .....	xi
LIST OF TABLES.....	xxi
NOMENCLATURE .....	xxii
CHAPTER	
I INTRODUCTION.....	1
1.1 Background.....	1
1.2 Objectives .....	2
1.3 Organization of the Dissertation.....	3
II LITERATURE REVIEW.....	5
2.1 Passive Cooling Techniques for Hot-humid Climates.....	5
2.2 Thermal Comfort and Adaptation in Hot-humid Climates.....	9
2.2.1 ASHRAE Comfort Charts.....	10
2.2.2 Olgyay’s Bio-Climatic Chart .....	16
2.2.3 Givoni’s Building Bio-Climatic Chart.....	16
2.2.4 Fanger’s Heat Balance Equation and Predicted Mean Vote (PMV).....	18
2.2.5 Other Significant Studies on Thermal Comfort .....	19
2.3 Thermal Simulation Techniques in Building Designs.....	22
2.3.1 The DOE-2 Simulation Program .....	22
2.3.2 Other Thermal Simulation Programs .....	23
2.3.3 Calibrated Thermal Simulations .....	25
2.4 Air Flow Simulation and Visualization Techniques in Building Designs.....	26
2.5 Combined CFD and Thermal Simulation.....	28
2.6 Field Measurements of an Indoor Environment .....	30
2.6.1 Calibrated Field Measurements .....	30
2.6.2 Standardized Calibration Procedures .....	31



CHAPTER	Page
2.7 Summary of Literature Review .....	33
III SIGNIFICANCE OF THE STUDY .....	35
3.1 Expected Contributions of This Research .....	35
3.2 Scope and Limitations of This Research .....	36
IV METHODOLOGY .....	37
4.1 Survey of Case-Study Temples .....	37
4.1.1 The New Temple .....	39
4.1.2 The Old Temple .....	39
4.1.3 Operating Schedules .....	46
4.2 Measurements and Data Collections .....	46
4.2.1 Bangkok Weather Data .....	46
4.2.2 Instrumentation and Calibration .....	49
4.3 Calibrated DOE-2/CFD Simulations .....	52
4.3.1 DOE-2 Thermal Simulations .....	52
4.3.1.1 DOE-2 Analyses of Unconditioned Buildings .....	52
4.3.1.2 Processing a DOE-2 Weather File Using the Bangkok Weather Data .....	53
4.3.1.3 Creating a DOE-2 Input File to Simulate the Old Temple .....	55
4.3.2 Computational Fluid Dynamics (CFD) .....	56
4.3.2.1 HEATX Governing Equations .....	56
4.3.2.2 CFD Analysis of the Old Temple Using HEATX .....	61
4.3.2.3 Creating a HEATX Input File to Simulate the Old Temple .....	65
4.3.2.4 Boundary Conditions .....	65
4.3.3 Calibrations of the Simulation Model .....	66
4.3.3.1 Combined DOE-2 and CFD Simulations .....	67
4.3.3.2 Calculation of Surface Convective Heat Transfer Coefficients .....	68
4.3.3.3 Calculation of the Air Exchange Rate .....	71
4.3.3.4 Calibrations of the Hourly DOE-2 Simulations for a Whole-Year Period .....	72
4.4 Summary of Methodology .....	74

CHAPTER	Page
V RESULTS .....	76
5.1 Data Collection and Measurements of the Case-Study Buildings.....	76
5.1.1 Bangkok Weather Data.....	76
5.1.2 Measurement Results of the Case-Study Buildings.....	79
5.2 Calibrated DOE-2/CFD Simulation Results.....	86
5.2.1 First Calibration.....	89
5.2.2 Second Calibration.....	91
5.2.3 Third Calibration.....	101
5.2.4 Fourth Calibration.....	101
5.2.5 Fifth Calibration.....	102
5.3 Analysis and Discussion of Simulation Results .....	106
5.4 Summary of Results.....	112
VI OPTIONAL DESIGNS AND OPERATIONS .....	114
6.1 Introduction .....	114
6.2 Option 1: As-Is Temple with Nighttime-Only Ventilation.....	116
6.3 Option 2: Low Solar-Absorption Roof Surfaces .....	119
6.4 Option 3: R-30 Ceiling Insulation .....	123
6.5 Option 4: Shading Devices .....	128
6.6 Option 5: Attic Ventilation.....	135
6.7 Summary of Optional Designs and Operations .....	143
VII GUIDELINES FOR IMPROVED BUILDING DESIGN AND OPERATION .....	151
7.1 Introduction .....	151
7.2 Prototype I: High-Mass Temple .....	152
7.3 Prototype II: Low-Mass Temple.....	160
7.4 Analysis of the Prototype Buildings .....	165
7.5 Guidelines for Building Designs and Operations .....	166
7.5.1 Guidelines for New Buildings .....	173
7.5.2 Guidelines for the Renovation of Old Buildings .....	176
7.6 Summary.....	177
VIII SUMMARY AND FUTURE RECOMMENDATIONS .....	179
8.1 Summary of Study Objectives .....	179

	Page
8.2 Summary of Methodology.....	179
8.3 Summary of Results.....	180
8.4 Summary of Design and Operation Guidelines .....	180
8.5 Recommendations for Future Research.....	182
REFERENCES .....	184
APPENDIX A DETAILS OF THE CASE-STUDY TEMPLES.....	193
APPENDIX B CLIMATE CHARACTERISTICS OF BANGKOK .....	202
APPENDIX C MEASUREMENT RESULTS OF THE CASE-STUDY TEMPLES .....	215
APPENDIX D DOE-2 SIMULATION.....	222
APPENDIX E CFD SIMULATION.....	242
APPENDIX F CALIBRATION OF THE INSTRUMENTS.....	259
APPENDIX G PREPARATION OF THE BANGKOK TRY FILE USING LS2TRY .....	266
VITA.....	269

## LIST OF FIGURES

	Page
Figure 2.1a ASHRAE Effective Temperature I .....	11
Figure 2.1b ASHRAE Effective Temperature II .....	12
Figure 2.2 ASHRAE Comfort Chart: Standard 55-1981 .....	13
Figure 2.3 ASHRAE Comfort Chart: Standard 55-1992 .....	14
Figure 2.4 ASHRAE Comfort Chart: Standard 55-1994 .....	15
Figure 2.5 Olgyay's Bio-Climatic Chart .....	17
Figure 2.6 Givoni's Building Bio-Climatic Chart .....	18
Figure 2.7 Fanger's Predicted Mean Vote (PMV) .....	19
Figure 2.8 Tanabe's Comfort Study of Preferred Airspeed at Higher Temperature .....	20
Figure 4.1 Survey Information Obtained for the Case-Study Buildings .....	38
Figure 4.2 Exterior View of the New Temple .....	40
Figure 4.3 Interior View of the New Temple .....	41
Figure 4.4 Exterior View of the Old Temple .....	42
Figure 4.5 Interior View of the Old Temple .....	43
Figure 4.6a Floor Plan of the New Temple .....	44
Figure 4.6b Section View of the New Temple .....	44
Figure 4.7a Floor Plan of the Old Temple .....	45
Figure 4.7b Section View of the Old Temple .....	45
Figure 4.8 Daily Occupancy Profiles on Weekdays and Weekends .....	47
Figure 4.9 Daily Lighting Profiles on Weekdays and Weekends .....	47
Figure 4.10 Daily Electrical Equipment Profiles on Weekdays and Weekends .....	48
Figure 4.11 Daily Natural Ventilation Profiles on Weekdays and Weekends .....	48
Figure 4.12a Portable Indoor Temperature/Relative Humidity Sensor Placed in a Secure Box .....	49
Figure 4.12b Vertical Positioning of the Temperature/Relative Humidity Sensors in the Old Temple .....	50
Figure 4.12c Vertical Positioning of the Temperature/Relative Humidity Sensors in the New Temple .....	50

	Page
Figure 4.13 Floor Surface Temperature Measurement Using a Portable Data Logger with an External Thermocouple-Type Sensor.....	51
Figure 4.14 Wall/Ceiling Surface Temperature Measurement Using an Infrared Thermometer .....	51
Figure 4.15 Flowchart Diagram Showing the DOE-2 Weather Data Processing.....	55
Figure 4.16 Input Diagram of the DOE-2 Building Description Language (BDL).....	57
Figure 4.17 Image of the Old Temple Simulation Input Using the DrawBDL Program .....	58
Figure 4.18 HEATX Calculation Procedure.....	59
Figure 4.19a Non-uniform Grid Setting for a CFD Simulation of the Old Temple: Plan View.....	62
Figure 4.19a Non-uniform Grid Setting for a CFD Simulation of the Old Temple: Section View .....	63
Figure 4.20 Thermal Network Diagram Showing the Heat Transfer Calculations in HEATX .....	64
Figure 4.21 Flowchart Diagram Showing the DOE-2/CFD Calibration Process for a 24-Hour Run Period .....	69
Figure 4.22 Flowchart Diagram Showing the Calibration Process of the Hourly DOE-2/CFD Simulations for a One-Year Period.....	73
Figure 5.1a Outdoor Temperatures for Bangkok, Thailand During 1999 .....	77
Figure 5.1b Outdoor Relative Humidity for Bangkok, Thailand During 1999 .....	77
Figure 5.1c Sun Path Diagram of Bangkok Created by SOLRPATH (Oh 2000) .....	79
Figure 5.2a Indoor Temperature of the New Temple During 1999 .....	81
Figure 5.2b Indoor Relative Humidity of the New Temple During 1999 .....	81
Figure 5.3a Indoor Temperature of the Old Temple During 1999 .....	82
Figure 5.3b Indoor Relative Humidity of the Old Temple During 1999 .....	82
Figure 5.4a Psychrometric Plot of the Indoor Conditions in the New Temple in the Summer .....	84
Figure 5.4b Psychrometric Plot of the Indoor Conditions in the New Temple in the Winter.....	84
Figure 5.5a Psychrometric Plot of the Indoor Conditions in the Old Temple in the Summer .....	85

	Page
Figure 5.5b Psychrometric Plot of the Indoor Conditions in the Old Temple in the Winter.....	85
Figure 5.6 Comparison of the DOE-2 Simulated and Measured Indoor Temperatures: Uncalibrated Simulation.....	88
Figure 5.7 Comparison of the DOE-2 Simulated and Measured Indoor Temperatures: 1 <sup>st</sup> Calibration .....	90
Figure 5.8 Vector Plot Showing the CFD-Simulated Airflow Through the Building on 04/01/99 at Noon (Floor Plan) .....	93
Figure 5.9 Vector Plot Showing the CFD-Simulated Airflow Through the Building on 04/01/99 at Noon (Section A-A).....	94
Figure 5.10 Contour Plot Showing the CFD-Simulated Air Pressure Across the Building on 04/01/99 at Noon.....	95
Figure 5.11a Contour Plot Showing CFD-Simulated Temperatures of the Air Passing Through the Building on 04/01/99 at Noon (Section A-A).....	96
Figure 5.11b Comparison of the DOE-2 and the Transient CFD-Simulated Indoor Temperatures of the Old Temple on a Summer Day (04/01/99).....	97
Figure 5.11c Comparison of the DOE-2 and the Transient CFD-Simulated Attic Temperatures of the Old Temple on a Summer Day (04/01/99).....	97
Figure 5.12 Comparison of the DOE-2 Simulated and Measured Indoor Temperatures: 2 <sup>nd</sup> Calibration .....	100
Figure 5.13 Comparison of the DOE-2 Simulated and Measured Indoor Temperatures: 3 <sup>rd</sup> Calibration.....	103
Figure 5.14 Comparison of the DOE-2 Simulated and Measured Indoor Temperatures: 4 <sup>th</sup> Calibration.....	104
Figure 5.15 Comparison of the DOE-2 Simulated and Measured Indoor Temperatures: 5 <sup>th</sup> Calibration.....	105
Figure 5.16a Comparison of the Simulated and Measured Indoor Air Temperatures During a 2-Week Period of the Summer of 1999.....	107
Figure 5.16b Comparison of the Simulated and Measured Indoor Air Temperatures During a 2-Week Period of the Winter of 1999 .....	107

	Page
Figure 5.17 CV-RMSE and NMBE Comparisons of the Simulated and Measured Indoor Air Temperatures.....	108
Figure 5.18a DOE-2 Simulated Indoor/Outdoor Conditions of the Old Temple During a 2-Week Period of the Summer: AS-IS Condition .....	110
Figure 5.18b DOE-2 Simulated Indoor/Outdoor Conditions of the Old Temple During a 2-Week Period of the Winter: AS-IS Condition.....	111
Figure 6.1a DOE-2 Simulated Hourly Indoor Temperatures of the Old Temple for a 2-Week Period of the Summer: As-Is Conditions with Daytime and Nighttime Space Ventilation Modes .....	117
Figure 6.1b DOE-2 Simulated Hourly Indoor Temperatures of the Old Temple for a 2-Week Period of the Winter: As-Is Conditions with Daytime and Nighttime Space Ventilation Modes .....	117
Figure 6.2 Daily Average DOE-2 Simulated Indoor Temperatures of the Old Temple for One-Year Period: As-Is Conditions with Daytime and Nighttime Space Ventilation Modes.....	118
Figure 6.3 DOE-2 Simulated Indoor Temperatures of the Old Temple for a One-Year Period: As-is Condition VS Option 2, Low-Absorption Roof with Nighttime-Only Space Ventilation.....	120
Figure 6.4a DOE-2 Simulated and Measured Indoor/Outdoor Conditions of the Old Temple During a 2-week Period of the Summer: Option 2, Low-Absorption Roof .....	121
Figure 6.4b DOE-2 Simulated and Measured Indoor/Outdoor Conditions of the Old Temple During a 2-week Period of the Winter: Option 2, Low-Absorption Roof.....	121
Figure 6.5a DOE-2 Simulated Attic Temperature of the Old Temple During a 2-Week Period of the Summer: Option 2, Low-Absorption Roof .....	122
Figure 6.5b DOE-2 Simulated Attic Temperature of the Old Temple During a 2-week Period of the Winter: Option 2, Low-Absorption Roof.....	122
Figure 6.6 DOE-2 Simulated Indoor Temperatures of the Old Temple for a One-Year Period: As-is Condition VS Option 3, R-30 Ceiling Insulation with Nighttime-Only Space Ventilation.....	125

	Page
Figure 6.7a DOE-2 Simulated and Measured Indoor/Outdoor Conditions of the Old Temple During a 2-week Period of the Summer: Option 3, R-30 Ceiling Insulation .....	126
Figure 6.7b DOE-2 Simulated and Measured Indoor/Outdoor Conditions of the Old Temple During a 2-week Period of the Winter: Option 3, R-30 Ceiling Insulation .....	126
Figure 6.8a DOE-2 Simulated Attic Temperature of the Old Temple During a 2-week Period of the Summer: Option 3, R-30 Ceiling Insulation.....	127
Figure 6.8b DOE-2 Simulated Attic Temperature of the Old Temple During a 2-week Period of the Winter: Option 3, R-30 Ceiling Insulation .....	127
Figure 6.9a Section View of the Old Temple with the Additional Shading Devices.....	129
Figure 6.9b DrawBDL Image of the Old Temple with the Additional Shading Devices.....	130
Figure 6.10 DOE-2 Simulated Indoor Temperatures of the Old Temple for a One-Year Period: As-is Condition VS Option 4, Shading Devices with Nighttime-Only Space Ventilation.....	131
Figure 6.11a DOE-2 Simulated and Measured Indoor/Outdoor Conditions of the Old Temple During a 2-week Period of the Summer: Option 4, Shading Devices.....	132
Figure 6.11b DOE-2 Simulated and Measured Indoor/Outdoor Conditions of the Old Temple During a 2-week Period of the Winter: Option 4, Shading Devices.....	132
Figure 6.12a DOE-2 Simulated Attic Temperature of the Old Temple During a 2-week Period of the Summer: Option 4, Shading Devices.....	133
Figure 6.12b DOE-2 Simulated Attic Temperature of the Old Temple During a 2-week Period of the Winter: Option 4, Shading Devices .....	133
Figure 6.13a Section View of the Old Temple with Attic Ventilation.....	136
Figure 6.13b DrawBDL Image of the Old Temple with Attic Ventilation.....	137
Figure 6.13c Vector Plot Showing the Simulated Airflow Through the Building on 03/30/99 at Noon: Option 5, Attic Ventilation.....	138
Figure 6.13d Contour Plot Showing the Simulated Temperatures of the Air Passing Through the Building on 03/30/99 at Noon: Option 5, Attic Ventilation .....	139



	Page
Figure 6.14 DOE-2 Simulated Indoor Temperatures of the Old Temple for a One-Year Period: As-is Condition VS Option 5, Attic Ventilation with Nighttime-Only Space Ventilation.....	140
Figure 6.15a DOE-2 Simulated and Measured Indoor/Outdoor Conditions of the Old Temple During a 2-week Period of the Summer: Option 5, Attic Ventilation.....	141
Figure 6.15b DOE-2 Simulated and Measured Indoor/Outdoor Conditions of the Old Temple During a 2-week Period of the Winter: Option 5, Attic Ventilation.....	141
Figure 6.16a DOE-2 Simulated Attic Temperature of the Old Temple During a 2-week Period of the Summer: Option 5, Attic Ventilation .....	142
Figure 6.16b DOE-2 Simulated Attic Temperature of the Old Temple During a 2-week Period of the Winter: Option 5, Attic Ventilation.....	142
Figure 6.17a Comparison of the DOE-2 Simulated Indoor Temperatures of All Design Options with Nighttime-Only Space Ventilation for a 2-Week Period of the Summer .....	145
Figure 6.17b Comparison of the DOE-2 Simulated Indoor Temperatures of All Design Options with Nighttime-Only Space Ventilation for a 2-Week Period of the Winter.....	146
Figure 6.18a Comparison of the DOE-2 Simulated Indoor Temperatures of All Design Options with Daytime-Only Space Ventilation for a 2-Week Period of the Summer .....	147
Figure 6.18b Comparison of the DOE-2 Simulated Indoor Temperatures of All Design Options with Daytime-Only Space Ventilation for a 2-Week Period of the Winter.....	148
Figure 6.19a Annual Average Indoor Temperatures of All Design Options.....	149
Figure 6.19b Annual Maximum Indoor Temperatures of All Design Options .....	149
Figure 6.19c Annual Average Indoor Temperature Deviations from Outdoor Temperature of All Design Options .....	150
Figure 6.19d Annual Average Indoor Temperature Deviations from Ground Temperature of All Design Options .....	150

	Page
Figure 7.1a	Section View of the Prototype I Temple.....153
Figure 7.1b	Vector Plot Showing the Simulated Airflow through the Building on 03/30/99 at Noon: Prototype I, High-Mass Design.....155
Figure 7.1c	Contour Plot Showing the Simulated Temperatures of the Air Passing Through the Building on 03/30/99 at Noon: Prototype I, High-Mass Design ....156
Figure 7.2	Comparison of the DOE-2 Simulated Indoor Air Temperature of the As-Is Design and Prototype I (High-Mass Design) .....157
Figure 7.3a	DOE-2 Simulated Indoor Temperature of Prototype I (High-Mass Design) for a 2-Week Period of the Summer .....158
Figure 7.3b	DOE-2 Simulated Indoor Temperature of Prototype I (High-Mass Design) for a 2-Week Period of the Winter.....158
Figure 7.3c	Psychrometric Plot of the Indoor Conditions of the High-Mass Prototype in the Summer .....159
Figure 7.3d	Psychrometric Plot of the Indoor Conditions of the High-Mass Prototype in the Winter.....159
Figure 7.4a	Section View of the Prototype II Temple.....161
Figure 7.4b	Exterior Wall Detail of the Prototype II Temple.....162
Figure 7.5	Comparison of the DOE-2 Simulated Indoor Air Temperature of the As-Is Design and Prototype II (Low-Mass Design).....163
Figure 7.6a	DOE-2 Simulated Indoor Temperature of Prototype II (Low-Mass Design) for a 2-Week Period of the Summer .....164
Figure 7.6b	DOE-2 Simulated Indoor Temperature of Prototype II (Low-Mass Design) for a 2-Week Period of the Winter .....164
Figure 7.7a	Comparison of the DOE-2 Simulated Indoor Temperature of Both Prototypes for a 2-Week Period of the Summer .....167
Figure 7.7b	Comparison of the DOE-2 Simulated Indoor Temperature of Both Prototypes for a 2-Week Period of the Winter.....168
Figure 7.8a	Annual Average Indoor Temperatures of Individual Options and of Both Prototypes.....169
Figure 7.8b	Annual Maximum Indoor Temperatures of Individual Options and of Both Prototypes.....169

	Page
Figure 7.8c Annual Average Indoor Temperature Deviations from the Outdoor Temperature of Individual Options and of Both Prototypes .....	170
Figure 7.8d Annual Average Indoor Temperature Deviations from the Ground Temperature of Individual Options and of Both Prototypes .....	170
Figure 7.9a Average 24-Hour Profile of Indoor Temperatures for the Period of 03/01/99 to 05/30/99 (Summer): As-Is Temple .....	171
Figure 7.9b Average 24-Hour Profile of Indoor Temperatures for the Period of 03/01/99 to 05/30/99 (Summer): Prototype I Temple.....	171
Figure 7.9c Average 24-Hour Profile of Indoor Temperatures for the Period of 03/01/99 to 05/30/99 (Summer): Prototype II Temple.....	171
Figure 7.10a Average 24-Hour Profile of Indoor Temperatures for the Period of 11/01/99 to 12/31/99 (Winter): As-Is Temple.....	172
Figure 7.10b Average 24-Hour Profile of Indoor Temperatures for the Period of 11/01/99 to 12/31/99 (Winter): Prototype I Temple .....	172
Figure 7.10c Average 24-Hour Profile of Indoor Temperatures for the Period of 11/01/99 to 12/31/99 (Winter): Prototype II Temple.....	172
Figure A.1 Exterior View of the Old Temple Showing a Series of Windows on the North Side of the Building .....	195
Figure A.2 Interior View of the Old Temple Showing the Wooden Ceiling, a Chandelier, Ceiling Lamps, and a Ceiling Fan.....	196
Figure A.3 Interior View of the Old Temple Showing the Interior Corridor.....	197
Figure A.4 Moisture Problem in the Old Temple.....	198
Figure A.5 Exterior View of the New Temple Showing the Front Entrance .....	199
Figure A.6 Exterior View of the New Temple Showing the South Side of the Building .....	200
Figure A.7 Interior View of the New Temple Showing the Interior Wall at the South Side of the Building .....	200
Figure A.8 A Window on the North Side Wall of the New Temple .....	201
Figure B.1.1 Monthly Average Dry-Bulb Temperature of Bangkok During 1985-1995.....	203
Figure B.1.2 Monthly Average Relative Humidity of Bangkok During 1985-1995.....	203
Figure B.2.1 Outdoor Dry-Bulb Temperature in Bangkok in 1999 .....	205
Figure B.2.2 Outdoor Relative Humidity in Bangkok in 1999 .....	206

	Page
Figure B.2.3 Global Horizontal Solar Radiation in Bangkok in 1999 .....	207
Figure B.2.4a Bangkok's Hourly Wind Speed in 1999 .....	208
Figure B.2.4b Bangkok's 12-Hour Running Average Wind Speed in 1999.....	209
Figure B.2.5 Bangkok's Hourly Wind Direction in 1999 .....	210
Figure B.2.6a Hourly Average Daily Wind Speed in the Summer of 1999.....	211
Figure B.2.6b Hourly Average Daily Wind Speed in the Winter of 1999.....	211
Figure B.2.7a Summer Wind Directions (March-April).....	212
Figure B.2.7b Hourly Wind Directions Frequency During the Summer of 1999.....	212
Figure B.2.8a Winter Wind Directions (November-December).....	213
Figure B.2.8b Hourly Wind Directions Frequency During the Winter of 1999 .....	213
Figure C.1.1 Indoor Air Temperature of the Old Temple During Jan 12-Dec 31, 1999.....	216
Figure C.1.2 Indoor Air Relative Humidity of the Old Temple During Jan 12-Dec 31, 1999.....	216
Figure C.1.3 Floor Surface Temperature of the Old Temple During Aug 1999-May, 2000.....	217
Figure C.1.4 Wall Surface Temperatures of the Old Temple During Jan 17-21, 2000.....	217
Figure C.1.5 Indoor Temperatures of the Old Temple at the Floor and Ceiling Levels During the Summer. ....	218
Figure C.1.6 Indoor Relative Humidity of the Old Temple at the Floor and Ceiling Levels During the Summer. ....	218
Figure C.2.1 Indoor Air Temperature of the New Temple During Jan 12-Dec 31, 1999 .....	219
Figure C.2.2 Indoor Air Relative Humidity of the New Temple During Jan 12-Dec 31, 1999.....	219
Figure C.2.3 Floor Surface Temperature of the New Temple During Aug 1999-May, 2000.....	220
Figure C.2.4 Wall Surface Temperatures of the New Temple During Nov 8-12, 1999 .....	220
Figure C.2.5 Indoor Temperatures of the New Temple at the Floor and Ceiling Levels During the Summer. ....	221
Figure C.2.6 Indoor Relative Humidity of the New Temple at the Floor and Ceiling Levels During the Summer. ....	221
Figure D.1.1 DrawBDL Output of the Base-Case Temple.....	222

	Page
Figure E.7.1 Example of a HEATX Output File in Text Format.....	257
Figure E.7.2 HEATX Simulation Results in a Vector Plot Generated by TECPLOT.....	258
Figure E.7.3 HEATX Simulation Results in a Contour Plot Generated by TECPLOT.....	258
Figure F.1 Calibration Results of the Temperature Sensors at a Room Condition.....	260
Figure F.2 Calibration Results of the Relative Humidity Sensors at a Room Condition.....	260
Figure F.3 Calibration Results of the Temperature Sensors at a Low-Temperature Condition.....	261
Figure F.4 Calibration Results of the Relative Humidity Sensors at a Low-Temperature Condition.....	261
Figure F.5 Calibration Results of the Temperature Sensors at a High-Temperature Condition.....	262
Figure F.6 Calibration Results of the Relative Humidity Sensors at a High-Temperature Condition.....	262
Figure F.7 Calibration Results of the Temperature Sensors Using Spot Checks Against a Calibrated Vaisala Handheld Temperature/RH Sensor and a Calibrated Sling Psychrometer .....	263
Figure F.8 Calibration Results of the Relative Humidity Sensors Using Spot Checks Against a Calibrated Vaisala Handheld Temperature/RH Sensor and a Calibrated Sling Psychrometer.....	263
Figure F.9 Comparisons of the Temperature Measured by the Instrument Used in the Research (Box-1) Against Those Measured by the ESL Canary Boxes. ....	264
Figure F.10 Comparisons of the Relative Humidity Measured by the Instrument Used in the Research (Box-1) Against Those Measured by the ESL Canary Boxes. ....	264
Figure F.11 Comparisons of the Temperature Measured by the Instrument Used in the Research (Box-2) Against Those Measured by the ESL Canary Boxes. ....	265
Figure F.12 Comparisons of the Relative Humidity Measured by the Instrument Used in the Research (Box-2) Against Those Measured by the ESL Canary Boxes. ....	265

## LIST OF TABLES

		Page
Table 4.1	Coordinate Source Terms and Diffusion Coefficients .....	60
Table 5.1	The ASHRAE Combined Inside Surface Resistances .....	86
Table 5.2	Comparison of Surface Convection Coefficients.....	99
Table 5.3	Comparison of the Inside Film Resistances .....	99
Table 5.4	Summary of the Calibration Steps .....	108
Table 5.5	Thermal Properties of Building Materials.....	112
Table 5.6	DOE-2 Calculated Building Peak Cooling Load Components .....	113
Table 6.1	Simulation Results of Design Options with Three Ventilation Modes .....	115
Table 7.1	Comparisons of the Simulation Results of Prototype I and the As-Is Temple....	154
Table 7.2	Comparisons of the Simulation Results of Prototype I, Prototype II, and the As-Is Temple .....	165
Table F.1	Statistical Errors between the Temperature/Relative Humidity Measured by the Sensors Used in the Research and those measured by the ESL Canary Boxes .....	259

## NOMENCLATURE

$A_S$	Surface Area ( $m^2$ ) [ft <sup>2</sup> ]
$A_{win}$	Window Area ( $m^2$ ) [ft <sup>2</sup> ]
$C_p$	Specific Heat of Air (1.02 kJ/kg · K) [0.24 Btu/(lb <sub>m</sub> · °F)]
$D$	Building Length (m) [ft]
$f_V$	Volumetric Porosity
$f_S$	Surface Permeability
$g$	Gravitational Force ( $m/s^2$ ) [ft/s <sup>2</sup> ]
$H$	Enthalpy (J/kg) [Btu/lb <sub>m</sub> ]
$h$	Heat Transfer Coefficient ( $W/m^2 \cdot K$ ) [Btu/h · ft <sup>2</sup> · °F]
$I_0$	Extraterrestrial Solar Radiation ( $W/m^2$ ) [Btu/ (h · ft <sup>2</sup> )]
$I_{dif}$	Diffuse Solar Radiation ( $W/m^2$ ) [Btu/ (h · ft <sup>2</sup> )]
$I_{glo}$	Global Horizontal Solar Radiation ( $W/m^2$ ) [Btu/ (h · ft <sup>2</sup> )]
$k$	Turbulence Kinetic Energy ( $m^2/s^2$ ) [ft <sup>2</sup> /h <sup>2</sup> ]
$K$	Fluid Thermal Conductivity ( $W/m \cdot K$ ) [Btu/h · ft · °F]
$k_{roof}$	Roof/Wall Thermal Conductivity ( $W/m \cdot K$ ) [Btu/h · ft · °F]
$k_T$	Hourly Clearness Index
$L$	Characteristic Length (m) [ft]
$Nu$	Nusselt Number
$P$	Pressure ( $N/m^2$ ) [psi]
$\bar{p}$	Modified Pressure ( $N/m^2$ ) [psi]
$Pr$	Prandtl Number
$Ra$	Rayleigh Number
$Re$	Reynolds Number
$S$	Source Term
$U_o$	Overall Heat Transfer Coefficient ( $W/m^2K$ ) [Btu/h · ft <sup>2</sup> · °F]
$u$	X-direction Velocity (m/s) [ft/h]
$v$	Y-direction Velocity (m/s) [ft/h]
$V_{inlet}$	Inlet Air Velocity (m/s) [ft/h]
$V_{win}$	Air Velocity across the Windows (m/s) [ft/h]

$w$	Z-direction Velocity (m/s) [ft/h]
$z$	Z-direction
$\Delta r_{\text{roof}}$	Roof Thickness (m) [ft]
$\varepsilon$	Turbulence Kinetic Energy Dissipation Rate ( $\text{m}^2/\text{s}^3$ ) [ $\text{ft}^2/\text{h}^3$ ]
$\Gamma$	Diffusion Coefficient
$\mu$	Laminar Viscosity ( $\text{Pa} \cdot \text{s}$ ) [ $\text{lb}_m/\text{ft} \cdot \text{h}$ ]
$\mu_{\text{eff}}$	Effective Viscosity (Laminar + Turbulent) ( $\text{Pa} \cdot \text{s}$ ) [ $\text{lb}_m/\text{ft} \cdot \text{h}$ ]
$\mu_{\infty}$	Dynamic Viscosity of Fluid ( $\text{Pa} \cdot \text{s}$ ) [ $\text{lb}_m/\text{ft} \cdot \text{h}$ ]
$\rho$	Fluid Density ( $\text{kg}/\text{m}^3$ ) [ $\text{lb}_m/\text{ft}^3$ ]
$\theta_S$	Zenith Angle of the Sun (Degree)
$\beta$	Thermal Expansion Coefficient ( $\text{K}^{-1}$ ) [ $\text{R}^{-1}$ ]
$\nu$	Fluid Kinematic Viscosity ( $\text{m}^2/\text{s}$ ) [ $\text{ft}^2/\text{h}$ ]
$\alpha$	Fluid Thermal Diffusivity ( $\text{m}^2/\text{s}$ ) [ $\text{ft}^2/\text{h}$ ]



# CHAPTER I

## INTRODUCTION

### 1.1 Background

In hot-humid climates, particularly in developing countries, air-conditioners are becoming more common in both residential and commercial buildings. However, there are buildings such as the Thai Buddhist temples that do not use air-conditioners for various reasons, including vows of poverty and religious constraints. Therefore, these buildings must rely only on passive cooling by means of natural ventilation in order to achieve comfort conditions. Passive cooling design strategies in hot/humid regions are difficult to accomplish, however, because of the excessive amount of moisture in the air. For this reason, passive cooling designs in hot-humid climates need to pay careful attention to building design, orientation, planning, material selection, window treatments, ventilation, including proper facility planning and management. Unfortunately, a modern day education in architecture orients students toward designs with air-conditioning systems. Practical advice for buildings without air-conditioning systems in hot-humid climates is not always available, since most passive cooling techniques were developed for either hot-arid or temperate climates where outdoor air has a lower humidity, which allows buildings to take advantage of large diurnal temperature swings.

Without a proper understanding of hourly and daily climate patterns, architects continue to design open-planned buildings, and facility managers open all windows to obtain a maximum of natural ventilation at all times. Unfortunately, in hot-humid climates, 24-hour natural ventilation during the cooling season can bring in unwanted heat and moisture from the outside, which decreases the indoor comfort condition. To make matters worse, computerized design tools that could help architects design naturally ventilated buildings are rarely used in these types of design applications. Advanced computer software such as Computational Fluid Dynamics programs (CFD) has been used for years to simulate fluid flows, heat transfer, and related phenomena through the use of numerical techniques. Although CFD simulations have become an

integral part of engineering design in both the aerospace and automotive industries, they have only recently been used for building design.

An accurate assessment of naturally ventilated buildings in hot-humid regions is best accomplished through an in-depth thermal and CFD analysis that uses a combination of advanced simulation tools. Detailed investigations of space planning, building material, the configuration of openings, the simulated movement of natural air flow, and operation schedules are essential for developing and testing practical passive cooling techniques for unconditioned buildings in hot-humid climates.

## **1.2 Objectives**

The main objective of this research is to develop guidelines and new techniques for designing and operating unconditioned buildings in hot-humid climates that will enhance indoor comfort conditions. This will allow building designers, building operators, and facility managers to build and maintain unconditioned buildings in this region that will have improved thermal performance and greater thermal comfort. To achieve this goal, the following tasks are defined:

- 1) To investigate the indoor thermal conditions of naturally ventilated buildings in a hot humid climate using Thai Buddhist temples as a case-study building type.
- 2) To analyze the indoor thermal conditions and airflow characteristics of the case-study buildings by using computer simulations that are calibrated with measured data from the case-study buildings themselves.
- 3) To develop design guidelines and operating strategies for naturally ventilated buildings in hot-humid regions by using Bangkok as a case-study city, and Thai Buddhist Temples as an unconditioned building type.
- 4) To evaluate the effectiveness of the proposed guidelines in terms of indoor thermal comfort by using computer simulations of the prototype buildings, and comparing the results with the measured data from the case-study buildings.

### **1.3 Organization of the Dissertation**

This chapter has discussed the background and objectives of the proposed research. Chapter II reviews and discusses the previous studies related to this research, in order to provide a basis for conducting this research. This literature review includes information on passive cooling techniques for buildings in hot-humid climates, human thermal comfort and adaptation in hot-humid climates, thermal and air flow simulation techniques in building design, combined CFD and thermal simulations, and field measurements of indoor environments.

Chapter III discusses the significance of the research and its contribution to the research area. The scope and limitations of the research, including development of procedures used in this research, are also discussed in this chapter.

Chapter IV discusses the methodology applied to this research. It includes a survey of the case-study temples, the measurements and data collection, and the calibrated DOE-2/CFD simulations.

Chapter V discusses the results of this investigation, which include the measurement results of the case-study temples, and the Bangkok weather data obtained from on-site measurements and from the Thai Government's weather measurements. This chapter also discusses the results and analyses of the calibrated DOE-2/CFD simulations of case-study temples.

Chapter VI discusses the analyses of new, improved designs and operations, which include nighttime-only ventilation, low-solar absorption roofs, R-30 ceiling insulation, attic ventilation, shading devices, and combinations of these strategies.

Chapter VII presents the guidelines for building design and operation through the simulations of two proposed prototypes (i.e., high mass and low mass), which are designed and operated using combinations of the strategies suggested in Chapter VI. This chapter also suggests guidelines for both the design of new temples and the renovation of old temples.

Finally, Chapter VIII summarizes this research and proposes recommendations for future research in this area.

## **CHAPTER II**

### **LITERATURE REVIEW**

The categories of previous literature related to this research include: passive cooling techniques for hot-humid climates, thermal comfort and adaptation in hot-humid climates, thermal simulation techniques in building design, and airflow simulation and visualization techniques in building design. Previous work involving combined CFD and thermal simulations and field measurements of indoor environments will also be reviewed. The sources used mainly included Cook (1989), the ASHRAE Fundamental Handbooks, ASHRAE Transactions, the Proceedings of the International Building Performance Simulation Association (IBPSA), the American Society of Testing and Materials (ASTM) Standards and Manuals, and the DOE-2.1E Version 110 User Manual.

#### **2.1 Passive Cooling Techniques for Hot-humid Climates**

The term “passive cooling” was clearly defined by Jeffrey Cook (1989) as any building design technique that not only avoids outdoor heat, but also transfers indoor heat to natural heat sinks. The most complete summaries in passive cooling research can be found in Cook (1989) and Abrams (1986), where passive cooling techniques are categorized into five major methods. These methods are: 1) heat avoidance, 2) radiative cooling, 3) evaporative cooling, 4) earth coupling, and 5) ventilative cooling. As described in Balaras (1996), heat avoidance consists of the use of shading devices, proper building orientation and the use of local vegetation as a simple means of reducing heat gain. For the current research, site and climate will be gathered in order to determine the best way to apply such information about the local climate and vegetation to new building designs.

Radiative cooling, as explained in Martin (1989; ref. Cook 1989, p.139), is the process whereby heat is absorbed by buildings in the daytime, and then radiated later to the cooler, night sky in the form of infrared radiation. This technique works best in arid climates where diurnal temperature swings are significant. For hot-humid regions, such as those examined by this research, high humidity and cloud cover usually slows the rate of nighttime radiative heat

transfer, thus trapping heat inside the buildings that would have otherwise radiated to the night sky.

Evaporative cooling is another technique that is currently used in passively cooled buildings in hot-arid regions. Unfortunately for hot-humid regions, high humidity prevents evaporative cooling from being effective. As described by Yellott (1989; ref. Cook 1989, p.85), “evaporative cooling works when the sensible heat in an air stream is exchanged for the latent heat of water droplets or wetted surfaces.” However, in hot-humid climates like Thailand, cooling with outdoor air without first removing moisture (such as with a desiccant cooler) causes the indoor air to be too humid or even to condense on surfaces, and thus causes mold and mildew to form.

Regarding earth coupling techniques, Kenneth Labs (1989; ref. in Cook 1989, p.197) has summarized that in earth-coupled buildings, the interior space is thermally coupled to the subsoil by conduction-convection through the building slab. This requires that the ground temperature be within the comfort zone (i.e., 68 – 78 °F) so that the ground can act as a heat sink (Labs, 1989). This technique is useful in temperate climates where the average ground temperature is within the comfort zone (Kreider and Rabl 1994). For Bangkok, Thailand, the annual average ground temperature is in the range of 78 °F (25.6 °C) and 84 °F (28.9 °C), which is in the upper limit of the comfort zone recommended by ASHRAE (ASHRAE 2001). Therefore, for this research, earth coupling will be investigated in order to see if it can be used effectively as a heat sink.

In ventilative cooling, as mentioned in Abrams (1986), a cooling effect occurs by means of convection by using surrounding air as a heat sink. Ventilative cooling has also been used in hot-humid locations where ventilation can make summers without air-conditioning at least more tolerable if not perfectly comfortable. For this research, ventilative cooling will be analyzed for its possible application to the temples since this method of cooling is traditionally used in this country, and it conforms to the chaste lifestyle of the Buddhist monks.

One of the most significant sources of research on ventilative cooling in hot-humid climates is the Florida Solar Energy Center (FSEC), directed by Subrato Chandra. FSEC has

produced much of the research in this area. The concept of ventilative cooling as presented by Chandra (1989) states that natural ventilation in a building needs to produce air exchanges at 5-500 air-changes per hour (ACH) between a room and the outside in order to provide comfort in hot-humid climates. This concept will also be considered for use in the case study temples.

Chandra conducted a test for hot-humid climates at the Passive Cooling Laboratory (PCL) in the Florida Solar Energy Center, which confirms that natural ventilation can be used to cool buildings in hot and humid climates. The concept uses air exchanges with outside air to cool buildings, and indoor air speed to cool people (Chandra 1989). To predict and test the effect of natural ventilation on indoor conditions in hot-humid climates, Chandra has conducted several experimental studies using a full-scale house with 3-bedroom, slab-on-grade, frame construction with typical insulation in Florida (Chandra et al. 1983). The results have shown that with a constant air exchange rate of 15 ACH, on the average, the indoor temperature could be maintained at 2.5 °F (1.4 °C) higher than the ambient outdoor temperature. If the air exchange rate was increased to 30 ACH, the indoor temperature could be maintained at the average ambient outdoor temperature. Increasing the air exchange rate helps lower the average indoor temperature. Chandra also recommended using night ventilation at the rate of at least 30 ACH for massive building in hot-humid climates. This suggests that ventilating the indoors at night with outdoor air at the rate recommended by Chandra could cool down the case-study buildings used for this research.

A consideration of the concept of year round ventilative cooling leads to a study conducted by Tantasawasdi et al. (2001), who investigated the periods in which natural ventilation could be effectively used in air-conditioned houses in Thailand. He found that only during the winter months (i.e., November – February) could buildings be open to the outdoors for daytime comfortable ventilation. His comfort zone was based on the 1992 ASHRAE comfort chart. In the summer, ventilation can be used only during the night, especially after 7 p.m., but to accomplish this, buildings need to be carefully designed. Although Tantasawasdi suggested ventilating buildings at night, he did not test the effect of nighttime-only ventilation on the building he studied. Therefore, in light of this work, diurnal and seasonal ventilation schedules will also be taken into consideration here.

The above investigations provide significant information on the potential use of natural ventilation, in terms of indoor heat removal, when the ambient air is cooler than the indoor air. However, only a few studies have investigated the use of varying ventilation rates to take advantage of diurnal temperature swings. One such study by Baer (1983, 1984) investigated a night ventilation approach in a hot-arid climate. He recommended that houses in hot-arid climates be protected against outdoor heat during the day and reject the heat stored in massive walls during the night. Such designs utilize three concepts: 1) proper shade and orientation, 2) high mass walls that reduce heat conduction from the outside, and 3) nighttime ventilation. At night, the heat trapped in massive exterior walls should reradiate and convect back to the ambient air. This concept was developed further for buildings in hot-humid climates at the FSEC by Chandra (1989), who used a ceiling fan to raise the indoor convective heat transfer coefficient and increase the night ventilation rate. For this research, night ventilation seems to be the most promising concept to use for heat removal. However, most temples are usually closed during the evening and therefore do not take advantage of night ventilation, thus limiting the access to experimental measured data. Nonetheless, this research will investigate the effects of night ventilation for cooling the case study temples by using simulation methods.

In addition to the night ventilation techniques discussed above, there are several investigations that have been conducted using attic ventilation. In 1981, Fairey and Battencourt proposed a rooftop ventilation device called "La Sucka" to ventilate hot air from attic spaces and reduce the peak indoor temperature (Fairey and Battencourt, 1981). Later, ASHRAE (1981a) and Bliss (1984) also proposed practical solutions to attic ventilation requirements for the purpose of moisture control. In addition, Cleary (1985) has conducted both tests and measurements of attic ventilation rates and compared them to moisture levels. It was found that attic ventilation not only helps to reduce the daytime peak indoor temperature, but also helps to remove moisture from the attic during the day. The studies mentioned above are useful for the current research, because the peak indoor temperature in the afternoon has a direct impact on the thermal comfort in the unconditioned buildings examined in this research. In addition, the preliminary observations of the old case-study temples revealed that many Buddhist temples in Thailand have a moisture problem. Therefore, attic ventilation will be investigated for use as a design improvement option for the case-study buildings in this research.



Even though the above studies have indicated the effectiveness of attic ventilation on reducing the daytime peak indoor temperature, including the amount of moisture, several studies have been performed and found that attic ventilation is not the most effective means of reducing the attic heat gain to an interior space. McQuiston, Der and Sandoval (1984) have shown that attic ventilation was a less effective means of cooling a house than ceiling insulation or radiant barriers. This corresponds to the studies conducted by Fairey (1984) and Medina et al. (1992) who have demonstrated that radiation is the predominant mode of heat transfer to occur in the attic space during summertime conditions. Medina has revealed that ceiling insulation and radiant barriers made of aluminum foil within an air space are the most effective means of reducing heat gain through attics in the summer. For the current research, the temples are designed with large attic spaces that have no radiant barriers, roof/ceiling insulation, or attic ventilation. The techniques supplied by Medina and Fairey seem to provide a promising possibility for improving the indoor air condition of the case study buildings. Therefore, this research will investigate the thermal performance of an insulated attic both with and without attic ventilation.

In conclusion, the literature reviews on passive cooling provide some guidance on passive cooling design strategies that could be adopted and developed further in this research, in terms of the design and operation guidelines for naturally ventilated buildings in hot-humid climates. Night ventilation, earth coupling, ceiling insulation, radiant barriers, and heat avoidance through shading devices seem to be the most relevant passive cooling techniques that could be adapted in this research.

## **2.2 Thermal Comfort and Adaptation in Hot-humid Climates**

One of the simplest definitions of thermal comfort is given by Givoni (1998), who explained that thermal comfort could be defined as the range of climatic conditions considered comfortable and acceptable to humans. This implies an absence of two basic sensations of discomfort: a thermal sensation of heat, and a sensation of skin wetness (Givoni 1998). Studies of human response to a thermal environment have been conducted by ASHRAE since the 1920s. Some significant studies in this area include the ASHRAE Comfort Charts (ASHRAE 1967; 1981b; 1985; 1992; 1997), Olgyay's Bio-climatic Chart (Olgyay 1963), Givoni's Building Bio-

climatic Chart (Givoni 1976), and Fanger's Predicted Mean Vote (Fanger 1972). Other recent studies on thermal comfort were also reviewed. These include studies by deDear and Auliciums (1985), Baillie et al. (1987), Tanabe (1988), Wu (1988), Griffiths (1990), Schiller (1990), Busch (1990), Humphreys (1992), Tantasawasdi et al. (2001), and Jitkhajornwanich et al. (1998).

### 2.2.1 ASHRAE Comfort Charts

The first attempt at developing comfort standards for use in HVAC applications was initiated by ASHRAE from 1923 to 1925. This effort introduced the Effective Temperature (ET) index (Figure 2.1a), which expresses in a single index air temperature, humidity, and air speed. This index proposed the concept of using the skin wettedness ( $w$ ) as a predictor of discomfort. The definition of the skin wettedness is the ratio of the actual evaporative loss at the skin surface to the maximum loss that could occur in the same environment, i.e. when the skin is completely wet (ASHRAE 1985). This chart suggested the neutral comfort zone at 74.3 °F (23.5 °C) dry-bulb temperature, 50 % relative humidity, and 0.06 skin wettedness (i.e., no sweating). Even though this chart was straightforward and easy to use, it had a limitation on the types of clothing (i.e., light clothing only).

Later in 1967, ASHRAE proposed another comfort index that took into account the differences between summer and winter comfort preferences. This comfort chart was published in the 1967 Handbook of Fundamentals (ASHRAE 1967) as shown in Figure 2.1b. This effective temperature index was widely used until 1981, when it was adjusted to consider an effect of mean radiant temperature (MRT). The new MRT-adjusted index was superimposed on the psychrometric chart and first published in the 1981 ASHRAE Fundamental Handbook (ASHRAE 1981b), as shown in Figure 2.2. This index was constructed mainly for use in air-conditioned office buildings in developed countries; therefore, it limits the maximum acceptable indoor air speed to 160 fpm (0.8 m/s). Higher indoor air speeds, however, are common in naturally ventilated buildings (Tanabe 1988).

In 1992, ASHRAE developed another comfort index and published it in the ASHRAE Standard 55-1992 (ASHRAE 1992), as shown in Figure 2.3. This ASHRAE comfort index takes into account different "clo" values for summer and winter, which are 0.5 and 0.9 respectively,

where the “clo” value is the insulation value of clothing. The clo value of 0.0 compares to a completely exposed body (i.e., naked), and 1.0 is equal to dressing with trousers, a long-sleeved shirt, a long-sleeved sweater, and T-shirt (ASHRAE 2001). The “clo” value appeared in the 1981 chart, and has been used later in the 1992 and 1994 chart. In this chart, ASHRAE set the maximum relative humidity at 60 % as mold and mildew start to grow beyond this limit.

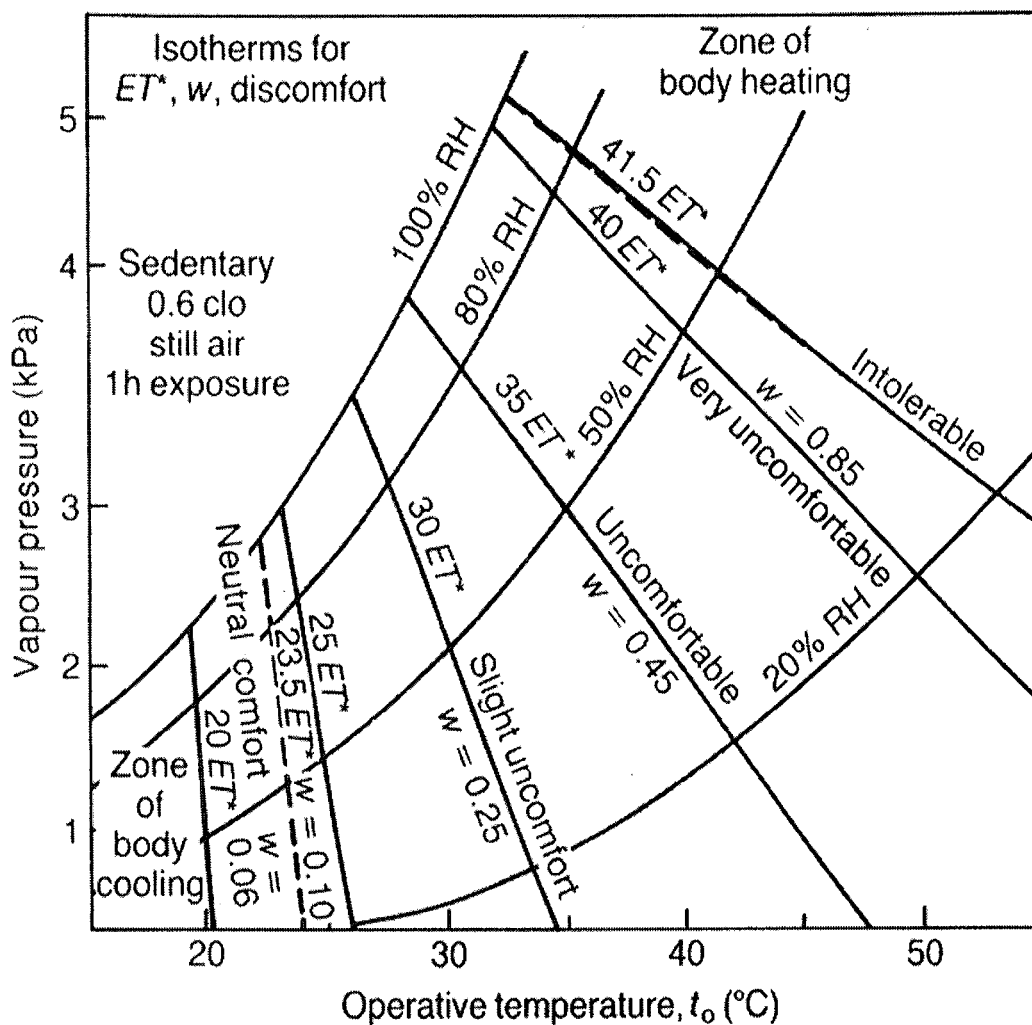


**Figure 2.1a** ASHRAE Effective Temperatures I. (Source: ASHRAE. 2001. Handbook of Fundamentals. Atlanta, GA: American Society of Heating, Refrigerating, and Air-Conditioning Engineers, p. 8.20. Reprinted with permission).

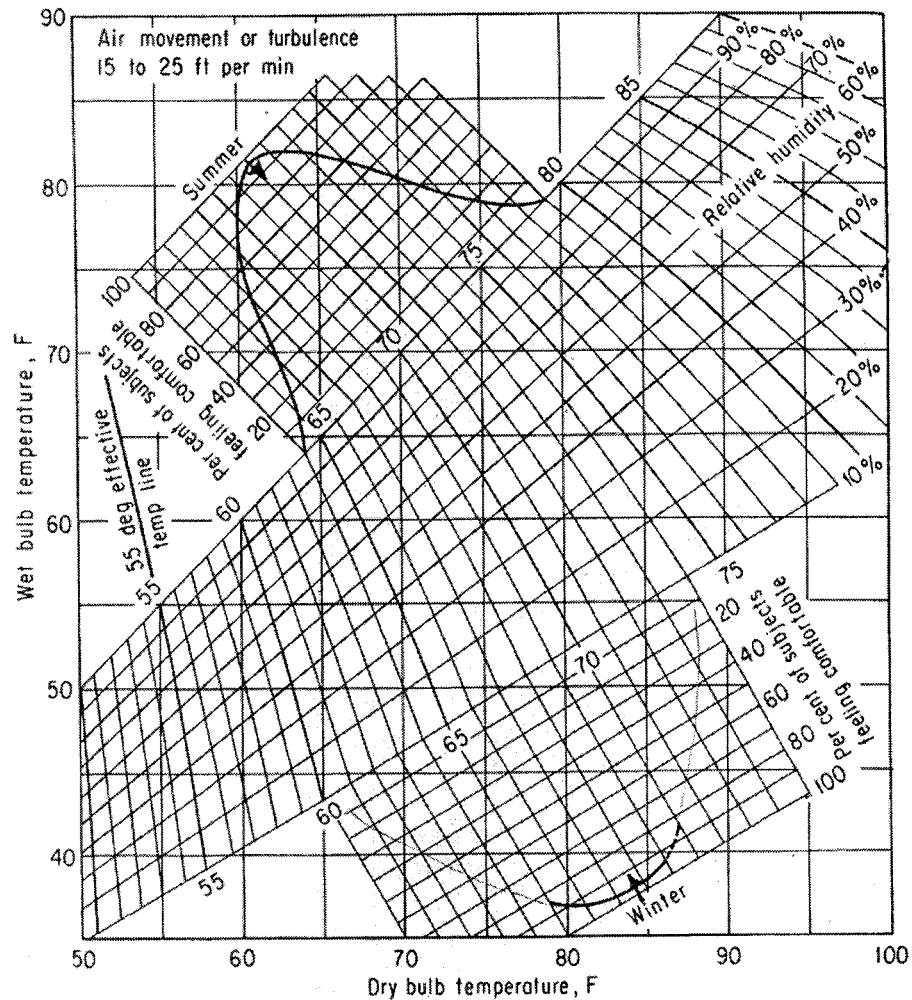


**Figure 2.1b** ASHRAE Effective Temperatures II. (Source: ASHRAE. 1967. *Handbook of Fundamentals*. Atlanta, GA: American Society of Heating, Refrigerating, and Air-Conditioning Engineers, p. 8.13. Reprinted with permission). These data are superseded by current ASHRAE Handbook information and are not intended for use in design.

In 1994, ASHRAE proposed another version of comfort index to accommodate evaporative air conditioning, which allows slightly higher regions of humidity (ASHRAE 1994), as shown in Figure 2.4. This index uses two wet-bulb temperature lines (i.e., 64.4 °F (18 °C) and 68 °F (20 °C)) to set the limits of winter and summer comfort zones, respectively. For this research, the ASHRAE comfort index needed to be adjusted for use in developing countries like

Thailand. The idea of adjusting the comfort zone for developing countries in hot-humid regions is supported by the studies of Humphreys (1975), Nicol, et al. (1994), and Tanabe (1988), who demonstrated that people in hot-humid developing countries regularly live in unconditioned buildings. According to these studies, the building occupants are acclimatized to, and therefore able to tolerate both higher temperatures and humidity. Importantly, these studies showed significant differences in building designs. For example, buildings in developing countries usually have less insulation, air tightness, and moisture controls than do buildings in developed countries.

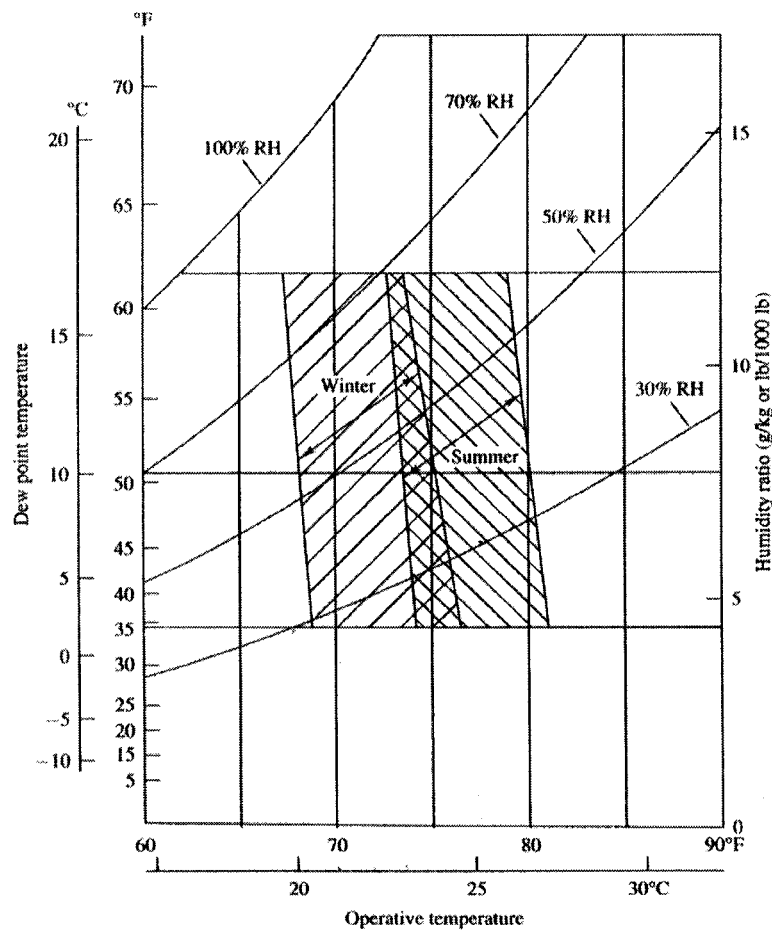


**Figure 2.2** *ASHRAE Comfort Chart: Standard 55-1981. (Source: ASHRAE. 1981b. Thermal Environmental Conditions for Human Occupancy. Standard 55-1981, Atlanta, GA: American Society of Heating, Refrigerating, and Air-Conditioning Engineers, p. 8.17. Reprinted with permission).*

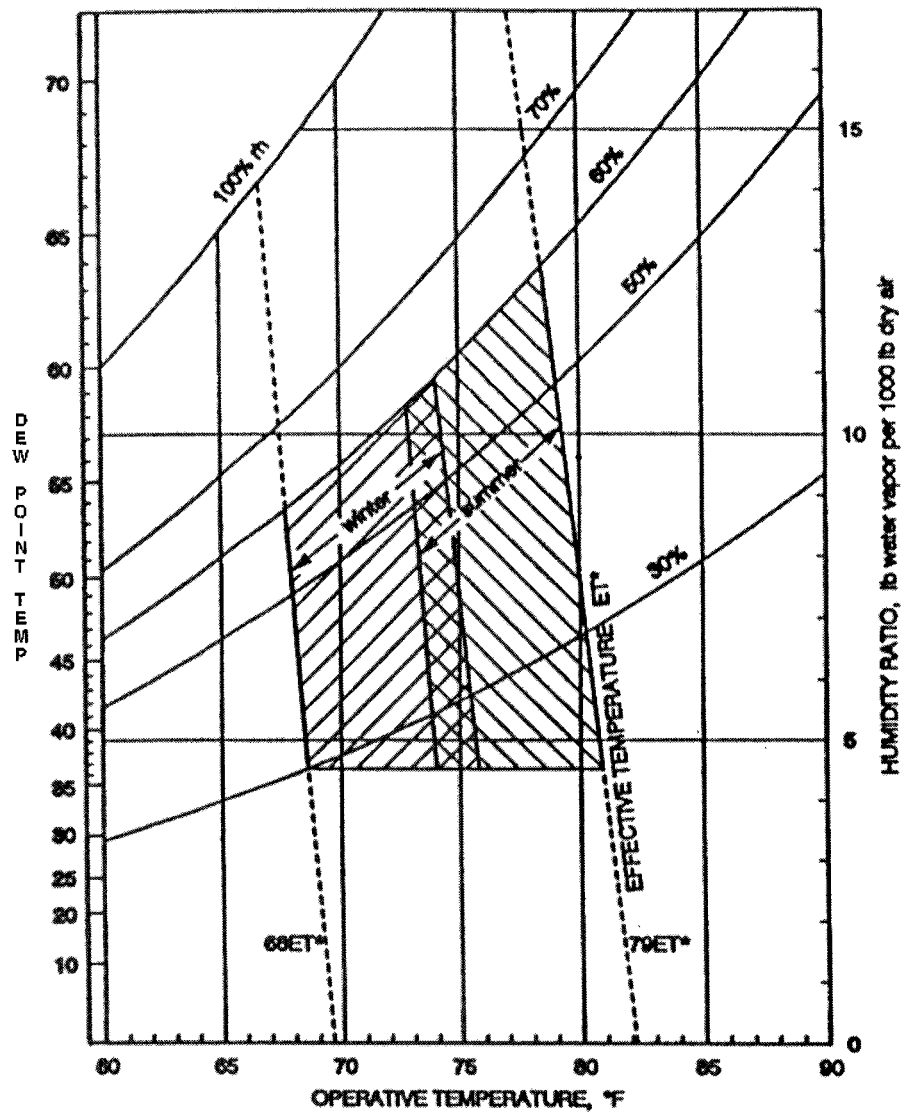


**Figure 2.3** *ASHRAE Comfort Chart: Standard 55-1992. (Source: ASHRAE. 1992. Thermal environmental conditions for human occupancy. Standard 55-1992. Atlanta, GA: American Society of Heating, Refrigerating, and Air-Conditioning Engineers, p.8.17. Reprinted with permission).*

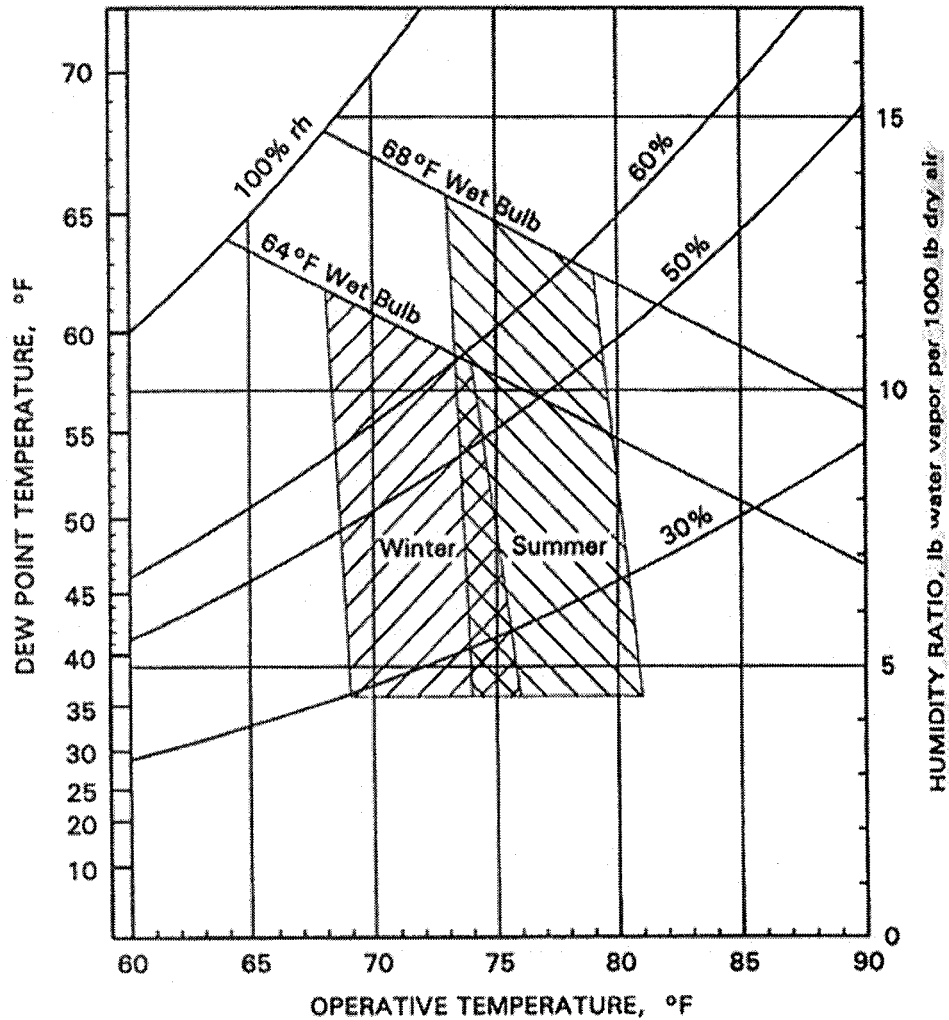


**Figure 2.4** *ASHRAE Comfort Chart: Standard 55-1994. (Source: ASHRAE. 1994. Thermal environmental conditions for human occupancy. Standard 55-1994. Atlanta, GA: American Society of Heating, Refrigerating, and Air-Conditioning Engineers, p.8.17. Reprinted with permission).*

### **2.2.2 Olgyay's Bio-Climatic Chart**

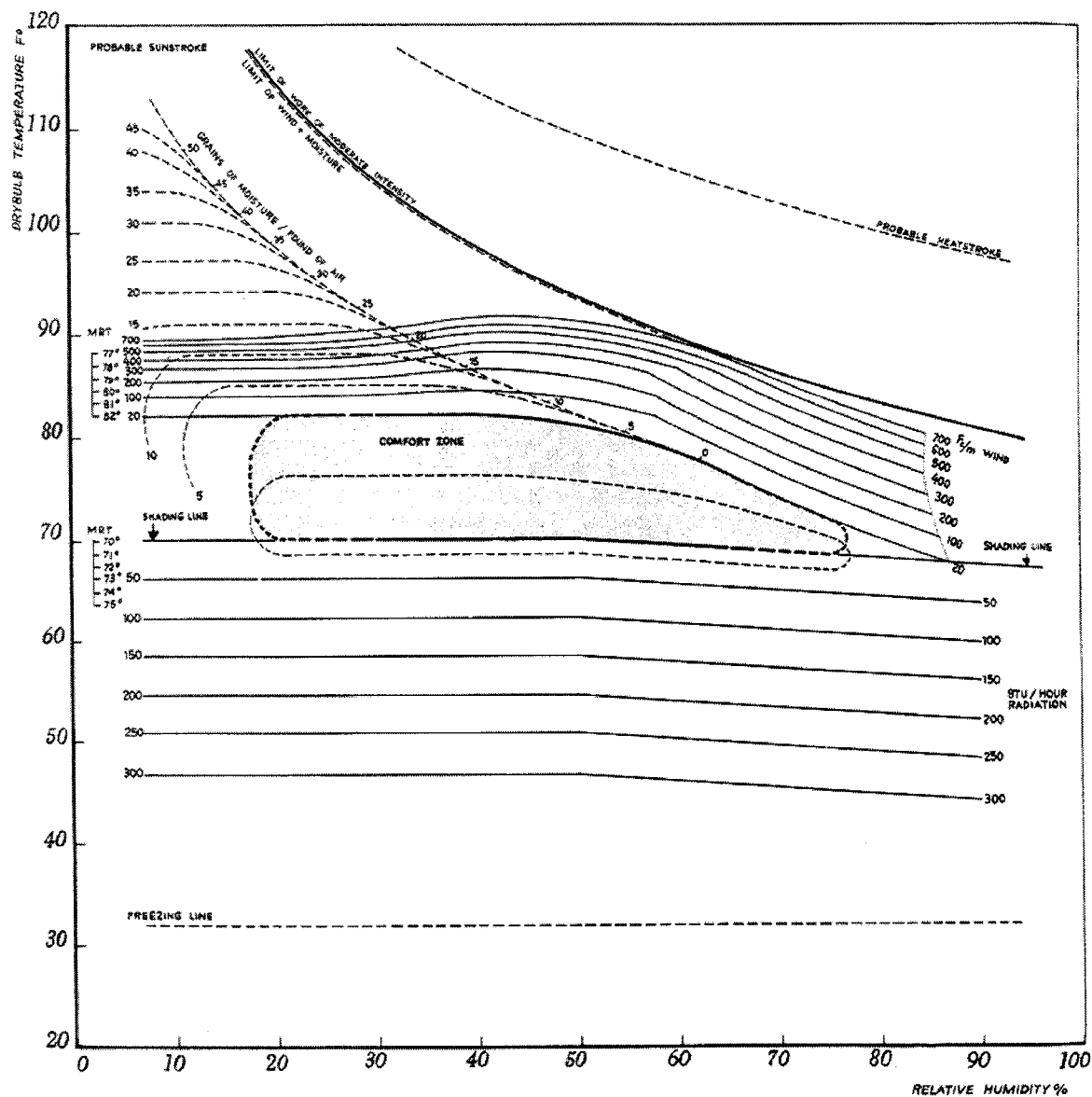
Another well-documented effort at establishing a thermal comfort index was conducted in 1963 by Olgyay, who published the first graphical comfort index called the "Bio-Climatic Chart"(Olgyay 1963), as shown in Figure 2.5. The comfort range is presented in an XY plot of temperature (Y-axis) and relative humidity (X-axis). This comfort index was intended to apply to unconditioned buildings with natural ventilation, and suggests that a summer comfort range could be shifted to a higher temperature and relative humidity as wind speeds increase. The maximum acceptable wind speed also exceeds that of the ASHRAE's 1981 Effective Temperature Index. During the 1970s, Olgyay's comfort chart was further investigated by Givoni (1976), who proposed that Olgyay's Bio-Climatic chart was only effective for lightweight buildings in humid regions because it assumed an indoor temperature very close to the outdoor level (Givoni 1976). Unfortunately, the Thai Buddhist temples used in this research are designed and constructed with high-mass walls. Thus ventilating the building during the daytime, as suggested in Olgyay's chart, may result in unwanted heat storage within the building's mass from elevated daytime temperatures. This stored heat would then be released into the indoor space during the evening, further increasing thermal discomfort.

### **2.2.3 Givoni's Building Bio-Climatic Chart**

In an attempt to work around the negative aspects of Olgyay's Bio-climatic Chart (i.e., that Olgyay's chart assumed an indoor temperature very close to the outdoor level), in 1976 Givoni developed the "Building Bio-Climatic Chart (BBCC)" (Givoni 1976), shown in Figure 2.6. Instead of using outdoor temperatures to construct the comfort index, as in Olgyay's chart, Givoni estimated the indoor temperatures that would be affected by different passive design strategies consisting of daytime ventilation, thermal mass, and evaporative cooling. The BBCC also suggests how passive cooling could provide indoor comfort in hot climates without the use air conditioning (Givoni 1998). This index is useful for this research because the proposed comfort zone was adjusted for unconditioned building in developing hot and humid countries. Compared with ASHRAE's 1992 comfort zone, the BBCC index allows a condition at higher indoor relative humidity and temperature to be comfortable if the building uses natural ventilation. In this research, the BBCC comfort index will be consulted along with ASHRAE's



comfort zone for an evaluation of passive cooling design strategies in hot-humid climates like Thailand.



45. Bioclimatic Chart, for U.S. moderate zone inhabitants.

**Figure 2.5** *Olgyay's Bio-Climatic Chart.* (Source: Olgyay, V. 1963. *Design with climate: A bioclimatic approach to architectural regionalism.* Princeton, N.J.: Princeton University Press, p.35. Reprinted with permission).

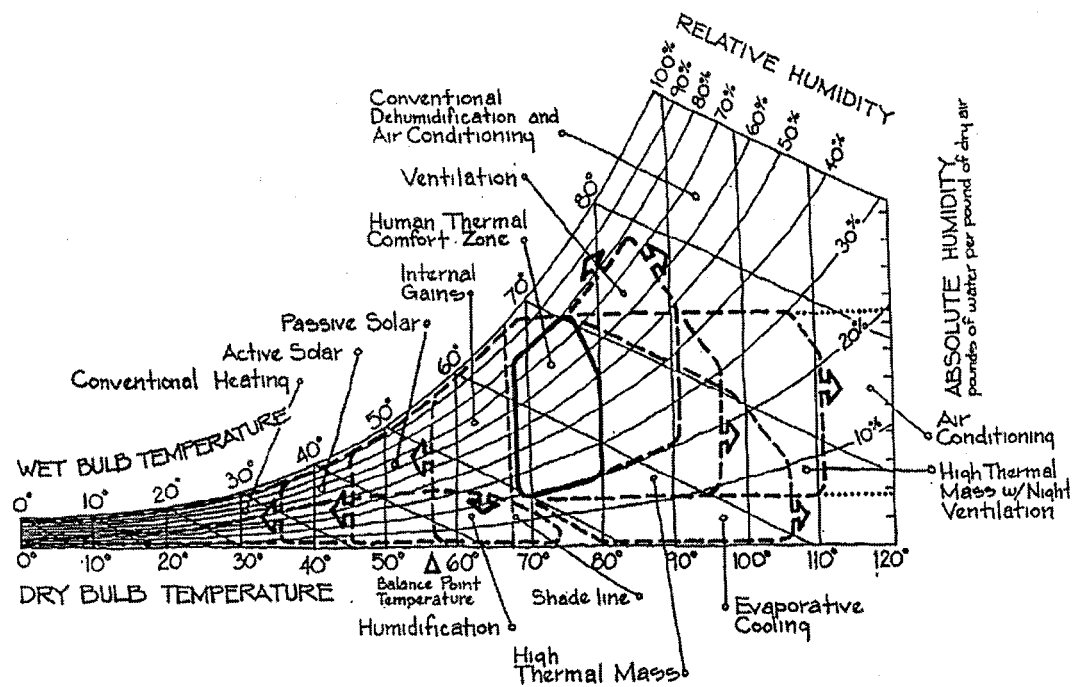


**Figure 2.6** Givoni's Building Bio-Climatic Chart. (Source: Givoni, B. 1998. *Climate Considerations in Building and Urban design*. New York: Van Nostrand Reinhold, p.45).

#### 2.2.4 Fanger's Heat Balance Equation and Predicted Mean Vote (PMV)

All of the comfort indices mentioned earlier have used a graphical presentation to display their results. Several of these methods (i.e., ASHRAE's and Givoni's BBCC) superimposed these results on top of a psychrometric chart. Unfortunately, this limits the possible uses of these methods. An alternative, proposed by the Danish scientist, P.O. Fanger, in 1972 used a mathematical model for assessing human comfort conditions. Fanger proposed that human thermal comfort could be derived from a heat balance equation. According to Fanger, the range of comfort could be defined by a subject's vote on a seven-point scale (Fanger 1972). From his proposed comfort equation, Fanger also proposed a "Predicted Mean Vote" (PMV) and "Predicted Percentage of Dissatisfied" (PPD), which is shown in Figure 2.7. Fanger's heat balance equation and PMV is useful for this research in terms of how the measured and simulated environmental parameters can be used to predict the comfort level in a space.

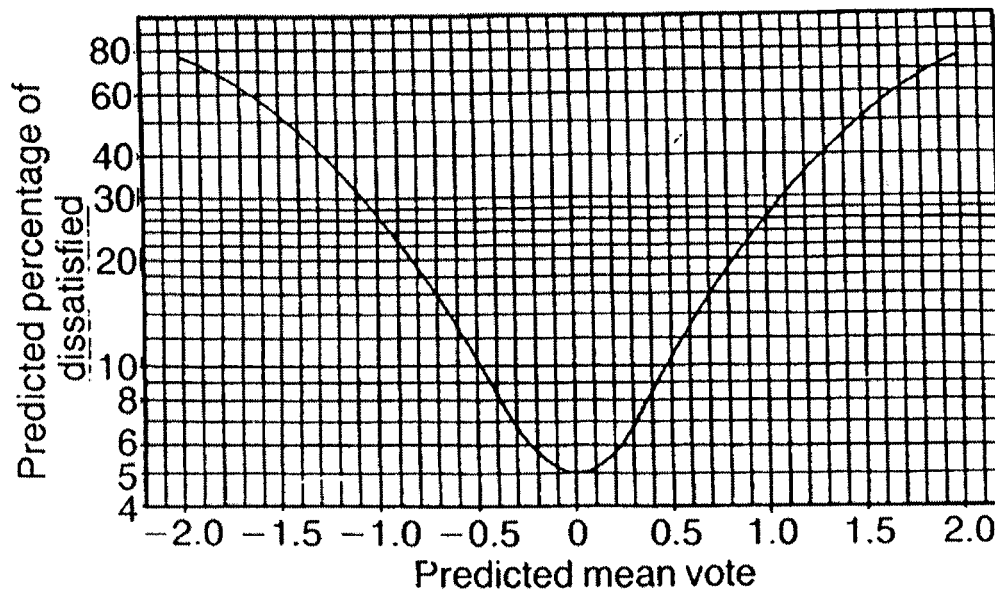


**Figure 2.7** *Fanger's Predicted Mean Vote (PMV). (Source: ASHRAE. 2001. Handbook of Fundamentals. Atlanta, GA: American Society of Heating, Refrigerating, and Air-Conditioning Engineers, p. 8.13. Reprinted with permission).*

### 2.2.5 Other Significant Studies on Thermal Comfort

All of the above comfort indices (i.e., Olgyay's Bio-Climatic chart, Givoni's BBCC, ASHRAE's, and Fanger's PMV) were derived from experiments on subjects in developed countries. These indices are widely used today and some are recognized by international organizations such as the International Standard Organization (ISO) (ISO 1984). Currently, there are several works that are continuing to evaluate these indices. In 1988, Tanabe used field studies in monitoring Japanese subjects' responses to different indoor conditions and compared these responses to the calculated PMV. The results showed discrepancies between the PMV and the field study votes. Tanabe's results, as shown in Figure 2.8, also indicated that the PMV does not take into account that at high temperatures, an increase in the cooling effect can be attributed to an increase in air speed (Tanabe 1988). Tanabe's study agrees with the studies of Humphreys (1992), Baillie et al. (1987), deDear and Auliciems (1985), Griffiths (1990), and Schiller (1990) who also used field studies to determine the thermal comfort preference of subjects in hot-humid climates. Tanabe's work is very useful for this research because he developed a comfort index

that is sensitive to higher air velocities, such as those encountered in unconditioned buildings in hot and humid climates.

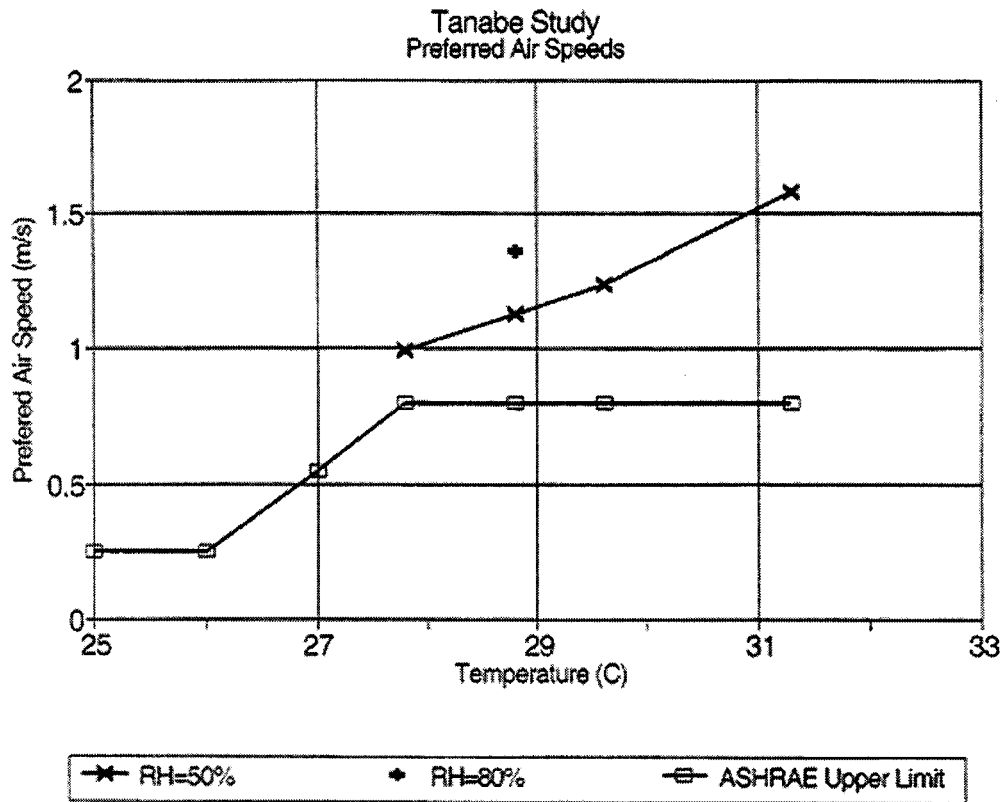


**Figure 2.8** *Tanabe's Comfort Study of Preferred Airspeed at Higher Temperature. (Source: Givoni, B. 1998. *Climate Considerations in Building and Urban design*. New York: Van Nostrand Reinhold, p.19).*

deDear and Auliciems (1985), Baillie et al. (1987), Griffiths (1990), Schiller (1990), and Humphreys (1992) also used field comfort studies and found that as the local average annual temperature of the location rises, so does the temperature that people consider acceptable. These studies agree with the studies of Busch (1990) and Jitkhajornwanich et al. (1998), which attempted to determine the thermal comfort preference of Thai people in both air-conditioned and unair-conditioned spaces. In performing a survey of the thermal comfort conditions of Thai citizens living in Bangkok, Busch collected data from four commercial buildings; two are

conditioned, the other two are naturally ventilated. The data were analyzed using different methods, including Fanger's PMV and ASHRAE's ET. The results of Busch's study are useful to this research because they indicate a broader range of comfort conditions for Bangkok condition, especially within unconditioned buildings as examined in this research. According to Busch, Thai conditions of thermal acceptability exist over a broad range of effective temperatures, from 71.6 °F (22 °C) to 86.9 °F (30.5 °C), pushing the summer comfort zone outward by 7.2 °F (4 °C). The neutral temperature of the whole sample was 77 °F (25 °C).

Recently, a number of studies on human comfort have focused on developing countries in hot and humid climates where people are used to living in unconditioned buildings. Wu demonstrated that for people acclimatized to hot and humid climates in developing countries, the suggested upper temperature limit with indoor airspeeds of 400 fpm (2 m/s) would be higher about 89.5 °F (32 °C) (Wu 1988). This conflicts with ASHRAE advice that at temperatures above 98.5 °F (37 °C), an increased air velocity actually increases the thermal sensation of heat (ASHRAE 1992). Wu's study is useful to this research because it suggests that the comfort range of occupants in the case study temples could shift to a higher temperature and a higher relative humidity with an increase in wind speed. However, during the summer in Bangkok, ventilating a building with the outdoor air during the daytime might bring discomfort. This hypothesis agrees with the study by Tantasawasdi (2001), who attempted to investigate the period during which natural ventilation could effectively be used in Thailand. He found that only during the winter months (i.e., November – February), could buildings be open to the outdoors for daytime comfort ventilation. Therefore, for this research, diurnal and seasonal ventilation schedules will also be taken into consideration.

In summary, the thermal comfort literature reviewed provides conflicting advice for assessing and predicting comfort levels in buildings. It demonstrates that, due to high humidity levels, high wind speeds, and acclimatization, no single universal comfort index has been developed for all people, all over the world, that does not need adjustments. Therefore, this research will not only consider both well-established comfort indices such as ASHRAE's comfort zone, Olgyay's Bio-climatic Chart, Givoni's BBCC, and Fanger's PMV, but also more recent research regarding possible shifts in the comfort range found in people in developing countries.

## **2.3 Thermal Simulation Techniques in Building Design**

Numerous thermal simulation computer programs for the purposes of new building design and existing building analysis have been developed worldwide. Generally, most simulation codes calculate dynamic heat transfer through building materials and evaluate overall building energy performance. Several general-purpose, energy simulations such as DOE-2 (LBNL 2001), BLAST (BSO 1993), TRNSYS (SEL 1995), and ESP-r (ESRU 1997) were initially developed for use on mainframe computers, which were available to government research centers in the 1970s and 1980s (Boyer et al. 1998). During the last decade, as the power of personal computers has increased, researchers have been able to translate general-purpose mainframe programs for use on PCs. Other high performance, easy-to-use computer codes have been developed such as Ener-Win (Degelman and Soebarto 1995), and SOLAR 5 (Milne et al. 1988). In addition to these general-purpose simulation codes, special purpose programs have also been developed for calculating heat transfer through fenestration systems, for example, Window 4.1 (Arastech et al. 1994), and OPAQUE (Abouella and Milne 1990). In this research, DOE-2 will be used as a design and analysis tool for simulating the thermal environment of the unconditioned case study temples.

### **2.3.1 The DOE-2 Simulation Program**

DOE-2 (LBNL 1982; 1994; 2001), developed by the Lawrence Berkeley National Laboratory, is an hourly-based thermal simulation program. This public domain simulation engine contains four subprograms: LOADS, SYSTEM, PLANT, and ECONOMICS. DOE-2 allows users to perform hourly simulations not only annually, but also for design days using hourly weather data available as the Typical Meteorological Year (TMY and TMY2), the Test Reference Year (TRY and TRY2), the California Climate Zone (CTZ), and the Weather Year for Energy Consumption (WYEC and WYEC2) file formats. In addition, simulation data can be calibrated with measured data by running the simulation with measured weather data converted into a DOE-2 readable format (Bronson 1992; Bou-Saada 1994; and Oh 2000). One of the most useful features of DOE-2 for this research is the hourly report. The variables of interest can be extracted into an hourly format for a maximum of one year, which can then be used for further analyses. This feature is very useful for this research, because several new variables (for

instance, exterior wall surface temperatures, solar radiation, pressure differences across a wall, and heat transfer from exterior walls to interior zones) can now be calculated and reported from the program. Moreover, the latest version of DOE-2.1E (i.e., Version 110) includes the thermal comfort feature, which provides an hourly report of the mean radiant temperatures along with the operative temperature of interior zones. In addition to the developments of DOE-2, many add-on programs have been created to assist in the use of DOE-2. One of the most useful DOE-2 add-on software programs is DrawBDL (Huang 1994), which allows users to visualize a building's geometry as it is described in the input file. DrawBDL will be used in this study to visualize the DOE-2 model of the case study temple.

### **2.3.2 Other Thermal Simulation Programs**

In addition to the DOE-2 simulation program, there are at least three other programs worth mentioning with regards to this thesis: 1) EnergyPlus, 2) ESP-r, and 3) HTB-2. EnergyPlus and ESP-r are considered public domain simulation tools, and are recognized by researchers worldwide. HTB-2 is a special purpose program used mostly for simulating passive cooling designs, especially those involving natural ventilation. More details of these programs follow.

EnergyPlus (DOE 2002) is the latest public domain software supported by the U.S. Department of Energy to be used to model building heating, cooling, lighting, ventilating, and other energy flows. This program builds upon the most widely used features and capabilities of BLAST and DOE-2. In addition, new innovative features have been integrated into the program; for example, the use of time steps of less than an hour, modular systems and plants integrated with zone simulations based on the heat balance method, multizone air flows, thermal comfort, and photovoltaic systems. One of the most useful features is the interoperability between EnergyPlus and CAD programs. EnergyPlus was designed to import a building's geometry from a CAD file directly into the program, and in the future it will be able to link to computational fluid dynamics programs. Currently, the program code is available as a stand-alone simulation engine without a user-friendly graphical user interface. More research on the program's validity, including third-party developments, is currently underway (DOE 2002).

ESP-r (ESRU 1997; Clarke et al. 1993) was developed in 1974 by the Energy Simulation Research Unit (ESRU) at the University of Strathclyde. In addition to performing thermal analyses of buildings, ESP-r is also integrated with modeling tools for simulating the visual, airflow, and acoustic performances of buildings. Currently, ESP-r has been developed to link with AutoCAD, Radiance, and CFD. This linkage makes the program the most versatile software available for overall building environmental analyses. ESP-r algorithms are based on a finite volume, conservation approach where a problem is transformed into a set of conservation equations representing energy, mass, momentum, etc., and then solved in successive time-steps. Even though ESP-r is a very powerful program for building environmental analyses, it is mostly used only by government and university research groups because it requires special knowledge of particular subjects, including the UNIX operating platform. This has placed the program out of reach for most building designers.

HTB2 (Lewis and Alexander 1990), developed by the Welsh School of Architecture at the University of Wales at Cardiff, is a dynamic finite difference thermal model that is capable of assessing the effects of a building's envelope, ventilation, solar gain and shading on internal thermal conditions. This program can be used to predict indoor temperatures in naturally ventilated buildings if passive designs are applied. In Jones et al. (1993), HTB2 was used to estimate the indoor air temperature of unconditioned traditional and modern Malaysian houses. The results show a reasonable agreement between the measured data and the modeled results, particularly where limited building data were available (Jones et al. 1993). Because the program was developed primarily for passive cooling designs, researchers do not widely use it for whole-building energy analyses.

For this research, the overall thermal performance of the case study temples was evaluated using DOE-2.1e, version 110. The simulated results were validated against the measured data obtained from field measurements taken at the case study temple over a 11-month period.



### 2.3.3 Calibrated Thermal Simulations

The purpose of calibrated thermal simulations is to develop baseline models for building thermal performances. In this approach, a thermal simulation is performed and its outputs are compared to measured data taken from the building. Through a calibration process, various physical input variables are changed so that the simulated outputs closely match the observed data. Once the baseline model results agree with the measured data, the calibration is complete. However, Krarti (2000) mentioned that, to date, there has been no general calibration procedure established for any building type, and the process relies mostly on user knowledge and expertise. Thus, ASHRAE is currently developing a procedure for calibrating whole-building simulation models (Krarti 2000). In addition to ASHRAE's effort, research on calibrated thermal simulations has been extensively conducted by Bronson et al. (1992), Corson (1992), Bou-Saada and Haberl (1995), Manke et al. (1996), Haberl and Thamilsaran (1996), Haberl et al. (1998), and Haberl and Bou-Saada (1998).

In an attempt to advance the calibrated simulation procedures, Haberl and Bou-Saada (1998) have suggested the use of statistical indicators to evaluate the goodness-of-fit of predicted results as compared to the observed data. Several statistical indicators, such as mean difference, mean biased error (MBE), and root mean square error (RMSE) were calculated for each calibration stage. These indicators are very helpful since they determine how well the simulated results match the measured data. The idea of using statistical indicators was also mentioned in Haberl and Thamilsaran (1996) in the results of the Great Energy Predictor Shootouts. In this research, the procedure of using statistical indicators suggested by Haberl and Bou-Saada has been adopted.

In researching calibrated simulations using DOE-2, Haberl et al. (1998) has examined the energy consumption of two Habitat for Humanity houses in Houston, Texas. The calibrated DOE-2 simulations were performed to evaluate residential energy conservation options. In order to obtain the baseline energy use models for these houses, several input parameters affecting the simulation discrepancies were tuned. Those included: 1) the thermal properties of the floor, 2) custom weighting factors, 3) roof absorptivity, 4) the window shading coefficient, 5) thermostat settings, 6) the performance curve-fit for the cooling system, and 7) the fan supply in kW. This

work is very useful to this research because it provided a general guideline for calibrating the DOE-2 simulations for the case-study temple by adjusting various input parameters.

#### **2.4 Air Flow Simulation and Visualization Techniques in Building Designs**

There are four techniques commonly used to study the air and heat flow in and around buildings—heat transfer correlations, inverted salt-gradients, wind tunnel testing (i.e., flow visualizations), and Computational Fluid Dynamics. The use of heat transfer correlations is the oldest method, and has been used since the 1600s. Even though this method provides a high degree of accuracy in specific cases such as laboratory setups, it is incapable of providing a visualization of the pattern of air movement that is normally helpful in designing the built environment (Boutet 1987). This shortcoming has led to the development of other techniques. One of the techniques currently used is known as the inverted salt-gradient visualization (Hunt et al. 1997). In this method, varying densities of colored salt solution are used to visualize fluid flow in a building.

For the air flow studies using wind tunnels, the simulations of air flows on buildings are performed for a number of different analyses: 1) to study wind load using a boundary-layer wind tunnel, 2) to study smoke and fire protection, and 3) to study air movement for natural ventilation studies. In the 1950s, a wind tunnel was used to study air movement in buildings at the Texas Engineering Experiment Station at Texas A&M University. Smith (1951) and Holleman (1951) used a uniform speed wind tunnel to study the effect of a fully open projection window, and its capability of directing air to the occupant level. They found that while the airflow was maximized by equal inlet and outlet areas, airspeeds in rooms were locally maximized if the outlet was slightly larger than the inlet. Later, in the 1970s, Givoni (1976) also conducted a study using a wind tunnel to test the effects of wing walls on the ventilation of a room. In Great Britain, the use of wind tunnels for building design has also gained popularity. Sobin (1983) conducted another comprehensive wind tunnel study at the Architectural Association of London. His study focused mainly on the effects of window shape on the airflow pattern in a space. However, wind tunnel testing is expensive and time-consuming. Over time, this type of testing has given way to another, newer method of studying air movement in buildings-Computational Fluid Dynamics (CFD).

Computational Fluid Dynamics, or CFD, as explained by Patankar (1980), is the simulation of a fluid flow and heat transfer processes through numerical methods in order to solve basic equations describing the conservation of mass, momentum, and heat in fluids. CFD has many advantages over the traditional, experimentally-based design methods because CFD is a fundamental approach that solves actual fluid flow equations. In addition, CFD provides a picture of the flow--unlike experimental results, which only provide visualization at a pre-selected position (Fawcett 1991).

Recently, several studies related to air movement in buildings have been performed using CFD. Awolesi et al. (1991) used CFD to predict the airflow pattern within a workshop and to compare the results with the actual measurements of that workshop. Yau and Whittle (1991) also used a combination of a CFD model and a reduced-scale physical model to simulate airflow characteristics inside an airport terminal. Vazquez (1991) used CFD to optimize the location of air inlets in an auditorium. Alamdari (1991) used a CFD code to simulate the effects of natural ventilation on an open atrium office building. All these previous studies are useful because they provide examples of how to set up the CFD calculations for the case-study temples. For this research, CFD will be applied to simulate the air movement in the case study temples using the HEATX program developed by Andrews and Prithiviraj (1997) at the Texas Engineering Experiment Station (TEES) at Texas A&M University. Details of HEATX will be included in Chapter 4.

In researching thermal comfort assessments, Awbi (1991a, 1991b) used CFD to simulate ventilation in a classroom. This thermal comfort prediction was performed using radiant heat transfer equations and Fanger's thermal comfort equation, which utilized the CFD-predicted air movement. The results were presented in contour plots of the Predicted Mean Vote (PMV) and Predicted Percentage of Dissatisfied (PPD). Awbi's method will be useful for this research in terms of how the measured and simulated environmental parameters (e.g., temperature, relative humidity, air speeds, and mean radiant temperatures) can be used to calculate PMV and then predict the comfort level for different location within a space.

## 2.5 Combined CFD and Thermal Simulation

In the last two decades, research on building simulations has been extensively performed using CFD to study the airflow in and around buildings. However, only recently has CFD been combined with thermal simulation programs. This is because researchers have begun to realize that a thermal simulation program alone cannot provide enough information about buildings operated using natural ventilation as a passive cooling system. Two main problems exist: 1) a difficulty in estimating the airflow rate, and 2) an incorrect estimation of heat transfer coefficients, which are based on the incorrect airflow rates (Kammerud et al. 1984). Since then, several studies have been conducted regarding how to couple CFD with thermal simulation codes. Significant research in this area includes Nagrao (1995), Sebric et al. (2000), and Graca et al. (2002).

Nagrao (1995) integrated a CFD code into the ESP-r program using the coupled modeling approach. The ESP-r program was used for both the whole-building and plant calculations, while CFD was used only for the simulation of a single interior room. The idea is that for each time-step, ESP-r performs a thermal calculation only for those variables necessary for CFD to establish boundary conditions. Once the CFD solution converges, it passes the results back to ESP-r to complete the whole-building and plant calculations. It was found that the success of this approach depends greatly upon the output of the thermal calculations to be passed on to CFD. Therefore, prior to calculating the airflow with CFD, a network airflow model was used in conjunction with ESP-r to calculate the inlet air velocity and temperature, including the surface heat flux. CFD then used these boundary conditions to calculate the detailed air velocity, air temperature, and surface convection coefficients. The surface convection coefficients from CFD were then fed back to ESP-r to perform the detailed heating and cooling load calculations, including surface temperature calculations for the entire building, while the CFD results of the air velocity and air temperature distributions were used in the comfort analyses. Nagrao's work is very useful for this research because it explained the coupling process in detail.

Sebric et al. (2000) also developed a coupled airflow and energy simulation program. In essence, a CFD code was coupled with the energy analysis program named ACCURACY (Chen and Kooi 1988), which calculates the hourly heating and cooling loads based upon the energy

balance method. At first, ACCURACY calculated the wall surface temperatures and A/C supply air velocity based on the cooling load required for that space, CFD then used those results to perform the airflow simulations and to calculate the convection coefficients for ACCURACY. Next, the air velocity, air temperature, wall temperatures, and air pressure were used to perform the thermal comfort analysis. Wall convection coefficients were then calculated using the difference between the wall temperature and the air temperature of the cells next to the wall, along with the heat flux calculated by ACCURACY. The results were then validated by the measurement data taken from experiments conducted in a test chamber.

Graca et al. (2002) performed a coupled CFD/thermal simulation of a wind-driven ventilative cooling system for apartment buildings in Beijing and Shanghai, China. CFD was used to calculate the wind-driven airflow through the building for a set of wind speeds and directions. The air velocity distribution near the interior walls and ceiling was used to calculate the surface convection coefficients using experimental correlations suggested by Chandra and Kerestecioglu (1984), originally intended for use with naturally ventilated buildings. Graca used isothermal CFD calculations to avoid the heavy computational burden of using CFD for detailed airflow and indoor surface temperatures. He stated that the temperature distribution in a building with wind-driven ventilation is uniform due to high airflow rates; therefore, this approach would be acceptable.

In considering the above studies, Nagrao's approach appears to be the most accurate, although time-consuming, because it is intended for use with multi-zone buildings where the inlet air velocity and temperature of each zone must be precisely calculated before the results are passed on to CFD. This is why the network airflow model was added into the thermal simulation process. However, this is not necessary for the current research because the case study temple only has one ventilated zone and there is no ducted HVAC system. Thus, only CFD will be used for these airflow calculations. Regarding Srebric's study, using heat-balance-based thermal simulation programs such as ACCURACY may not be appropriate for a building with high thermal mass. However, Srebric's method of calculating the convection coefficients using CFD is useful for this research. Graca's method, the method of calculating convection coefficients based on experimental correlations is also useful for the research because it is directly relevant to the simulations of the case study temples. However, using an isothermal CFD model is not

appropriate for the temple simulations because this method cannot simulate buoyancy effects inside the temple.

## **2.6 Field Measurements of an Indoor Environment**

### **2.6.1 Calibrated Field Measurements**

Field measurements in this research consist of measurements of air temperature, relative humidity, and surface temperature. The ASHRAE Handbook of Fundamentals (ASHRAE 2001) and the LoanSTAR Monitoring Workbook (Haberl et al. 1992) provide the basic, applications, instrumentations, and calibration methods necessary for field measurements of indoor/outdoor environmental conditions. For temperature measurements, the most used instruments consist of: 1) liquid-in-glass thermometers, 2) resistance thermometers, 3) thermocouples, 4) infrared radiometers, and 5) infrared thermography (ASHRAE 2001). For this research, thermocouples and infrared radiometers are used for the measurement of air temperatures and the surface temperature of the case study temples.

Regarding temperature measurements using thermocouples, a thermocouple is made of two wires of dissimilar metals that are joined by soldering, welding, or twisting to form a junction called a thermo-junction (ASHRAE 2001). The temperature of this junction creates an electromotive force (EMF) that can be recorded by a voltmeter. The measured EMF is a function of the temperature difference between the two junctions--therefore; at least one junction temperature must be known. The junction with a known temperature is usually called the "reference" junction, while the other is called the "measured" junction. Due to the low cost, moderate liability, and ease of use, thermocouple-type sensors will be used in this research to measure indoor and outdoor air temperatures, and the floor surface temperatures of the case study buildings.

In addition to the air temperature measurements, surface temperature measurements are also important for an indoor thermal analysis of the case study buildings. Infrared radiometers, also known as infrared thermometers, are the most popular devices used to measure the non-contact indoor/outdoor surface temperatures of buildings. In these instruments, radiant energy

flux from the surface being measured is received on an optical detector that generates an output signal, which can be read from a meter (ASHRAE 2001). This instrument is useful for this research because the ceiling and parts of the walls of the case study temples are in locations where it is impossible to attach thermocouples to these surfaces.

In measuring relative humidity, most measurements of humidity generally measure the “effects of moisture,” not the moisture content directly (Haberl et al. 1992) The devices used to measure relative humidity include psychrometers, dew-point hygrometers, mechanical hygrometers, electrical impedance and capacitance hygrometers, electrolytic hygrometers, piezoelectric sorption, radiation absorption hygrometers, and gravimetric hygrometers (ASHRAE 2001). For this research, electrical impedance hygrometers are used to measure the indoor and outdoor relative humidity of the case study temples because of their low cost, small size, fast response time, and good accuracy. These instruments measure changes in electrical impedance, when a particular substance built into the sensor absorbs or loses moisture due to humidity changes (ASHRAE 2001).

### **2.6.2 Standardized Calibration Procedures**

In order to maintain accurate measurements, an instrument must be regularly calibrated using the standardized calibration procedures suggested by the National Institute of Standards and Technology (NIST 2002; <http://www.nist.gov>) or the American Society for Testing and Materials (ASTM 2002; <http://www.astm.org>). The calibration procedures for thermometers, relative humidity sensors, and infrared thermometers used in this research are reviewed in the following section.

In general, the main purpose of a calibration is to compare the measurement results of an instrument with that of a standardized instrument, so that any necessary corrections or scaling can be applied. Once a calibration is successfully complete, the calibrated instrument can be used as a standard. As explained in McGee (1988), there are four classifications of standards: 1) the primary standard, 2) secondary standard, 3) tertiary standard, and 4) quaternary standard. A primary standard is obtained from the calibration of an instrument from which the fundamental equation is determined. A secondary standard is obtained from the calibration of an instrument

against another instrument that has been calibrated with a primary standard. A tertiary standard is obtained from the calibration of an instrument against a secondary standard instrument. This type of calibration is normally performed by NIST as a service to instrument companies. A quarterary standard is obtained from a calibration performed by instrument companies against a Bureau of Standards calibrated device (i.e., a tertiary standard). Quarterary standards are often provided by instrument companies with the statement “calibration traceable to the National Bureau of Standards” (e.g., NIST-Traceable Calibrations).

In this research, all instruments were new and had previously been tested by the manufacturers. However, they can only be classified as NIST-traceable calibration standards when the manufacturers perform the NIST calibration upon requests with service fees. To maintain the accuracy, the sensors needed to be recalibrated regularly during the course of measurements. The American Society of Testing and Materials (ASTM) has provided standardized test methods and guidelines for the calibration of thermometers, relative humidity sensors, and infrared thermometers, and these guidelines were followed when the need for calibration arose.

For thermometers, ASTM suggests three reference temperatures be used for the calibration of temperature sensors. These include: 1) the freezing point of water or the ice point (ASTM 2001a), 2) the freezing point of metals (ASTM 2001b), and 3) the triple point of water (ASTM 2001c). In addition to the mentioned ASTM procedures, Benedict (1984) suggests that the boiling point of water be used as a reference temperature, along with the application of electrically heated temperature-controlled baths. In terms of calibration methods, ASTM also provides a standardized test method for calibration of thermocouples through comparison techniques (ASTM 2001d), and a standardized guide for the testing of sheathed thermocouples (ASTM 2001e).

For relative humidity sensors, Greenspan (1977), NIST (1991), and ASTM (2001f) all suggest the method of using selected saturated salt solutions to provide a reference point for relative humidity. Once put inside a closed chamber, a specific water/salt solution determines the equilibrium water-vapor pressure above the solution, depending on the temperature. A corresponding relative humidity can then be obtained through calculation. ASHRAE (1994b) has



published a table that gives experimental correlations between the relative humidity and temperature of various salt solutions. This can be used for the calibration of humidity sensors used in this research.

For infrared thermometers, ASTM (2001g) suggests the method of using a blackbody or other stable isothermal radiant source of known, high emissivity as a reference temperature source. The temperature of the source and the infrared thermometer are recorded and compared, and from that the uncertainty can be calculated.

Calibration methods for other equipments used to measure indoor/outdoor environmental conditions are also suggested by NIST and ASTM. Pyranometers and anemometers are used to measure solar radiation and wind speed respectively at the Royal Thai Meteorological Department (2000). For solar radiation measurements using pyranometers, ASTM Standard G167-00 suggests the use of a reference pyrhelimeter to perform the calibration of a pyranometer (ASTM 2001h). For wind speed measurements using anemometers, NIST suggests the use of a wind tunnel equipped with pitot-static tubes and Laser Doppler anemometers (LDA) as a reference used to perform the calibration of an anemometer (Mease et al. 1992).

## **2.7 Summary of Literature Review**

This chapter has reviewed the previous work relevant to this research, including Cook (1989), the ASHRAE Fundamental Handbooks, ASHRAE Transactions, the Proceedings of the International Building Performance Simulation Association (IBPSA), the American Society of Testing and Materials (ASTM) Standards and Manuals, and the DOE-2.1E Version 110 User Manual. It has been found that very few studies addressed passive cooling designs in hot-humid climates, especially in developing countries. Moreover, only a few studies were concerned with the effects of combining ventilative cooling with earth coupling designs. In terms of building simulations, no previous studies were found that combined measured data, thermal simulation programs, and CFD to perform an analysis of a naturally ventilated, high mass building where thermal inertia plays an important role in the indoor comfort conditions. Additionally, no research was found to combine DOE-2 with a CFD program to perform simulations of naturally

ventilated buildings, particularly using a transient CFD calculation because of the lack of long-term measurements needed to validate the simulation models.

For passive cooling, previous studies provided useful guidance on passive cooling design strategies that could be adopted and developed further in this research, in terms of the design and operation guidelines for naturally ventilated buildings in hot-humid climates. Night ventilation, earth coupling, ceiling insulation, radiant barriers, and heat avoidance through shading devices seem to be the most relevant passive cooling techniques that could be adapted in this research.

In terms of thermal comfort, the previous studies demonstrated the historical development of the human thermal comfort preferences. It was found that most well-documented efforts on the human thermal comfort have been performed using subjects in developed countries in cold and temperate climates, where people live mostly in air-conditioned buildings. However, only recently were a growing number of studies performed on subjects in developing countries in hot-humid climates, where people are familiar with living in unconditioned buildings. These studies showed that due to high humidity levels, high wind speeds, and acclimatization, no single universal comfort index has been developed for all people, around the world, that does not need adjustments. Nonetheless, these studies are useful to this research because they indicate a broader range of thermal comfort preferences found in people in hot-humid, developing countries.

In summary, this research uses a combination of computer programs for both the thermal calculations (i.e., DOE-2) and the airflow simulation and visualization by using a CFD code to analyze the thermal comfort conditions in the case study temples. Using these techniques, the effects of design, construction, and operation schedules on the thermal performance and indoor comfort of the buildings will be analyzed.

## **CHAPTER III**

### **SIGNIFICANCE OF THE STUDY**

#### **3.1 Expected Contributions of This Research**

This research is intended to contribute to the development of design and operation guidelines for passively cooled, unconditioned buildings in a hot and humid climate. It has been found that few studies in this area are concerned with the passive cooling design of unconditioned buildings-particularly with the older historic buildings in hot and humid climates. New buildings are currently designed without consulting the performance of older buildings-their reaction with the environment and how they cope with ever-changing construction technologies. For this reason, this research is intended to provide the following contributions toward the development of a climate-responsive architectural design:

- 1) The development of design and operation guidelines for unconditioned buildings in a hot and humid climate.
- 2) The development of renovation guidelines for older, historic buildings in a hot and humid climate.
- 3) The development of a methodology to be used to combine the dynamic thermal and airflow simulations of unconditioned buildings.
- 4) The testing of the combined simulation using on-site temperature and humidity measurements from a well-documented case study site.
- 5) The development of new knowledge concerning the thermal and airflow performances and analyses of an old, historic building type in a tropical region.

### **3.2 Scope and Limitations of This Research**

This research is focused on the proposed designs of religious temples specifically, Thai Buddhist temples that retain the original design footprint of the case-study temple as a naturally ventilated building in a hot and humid climate. Therefore, the proposed building designs are simulated using the same building location and surroundings as that of the case study temples. This study does not investigate the effects of major changes to the configuration of the building in terms of building shape and form, orientation, size, or different window sizes and proportions.

In addition, the proposed designs are focused on how to enhance the overall thermal performance and comfort conditions of these buildings using only passive cooling designs. This research does not investigate the effects of using hybrid-cooling designs, which involve a combination of passive designs and supplemental HVAC systems.

In terms of comfort analysis, this research uses the comfort zones recommended by ASHRAE and Givoni as indicators of how comfortable an indoor condition is. It does not use the more complicated comfort index suggested by Fanger, the Predicted Mean Votes (PMV), although future work on the data generated by this research may indeed yield PMV values. In addition, this research does not investigate the comfort preferences of Thailand in particular. It assumes that universal human comfort preferences are based on worldwide research that can be appropriately applied to this group of occupants.

## CHAPTER IV

### METHODOLOGY

This chapter discusses the methodology used in this research. It contains descriptions of methods used to survey the case study buildings, measurements and data collection methods, and the calibrated DOE-2/CFD simulation methods.

#### **4.1 Survey of Case-Study Temples**

A survey of Thai Buddhist temples in Bangkok was performed from December of 1998 to January of 1999. The purpose was to select two case-study buildings that represent the typical Thai Buddhist temples in terms of architectural style, building design and construction, materials, age, and building use profiles. Other important criteria include the physical condition, availability of building information, and the possibility of further investigations. There needed to be one old and one new case-study temple, because there are significant differences in the architectural design and construction of the new temples built during the last 5-10 years, and the older temples constructed at least a century ago. In addition, this research intended to provide suggestions concerned not only with design guidelines for new temples, but also with renovation recommendations for older temples.

Figure 4.1 shows the survey information obtained for the case-study temples. In general, the building information required is: 1) the building design and construction, 2) all building documentation, and 3) building operations. In more detail, the data regarding the physical condition of both temples were collected through observation and discussions with the Buddhist monks and temple maintenance personnel. The data related to building design and construction include space planning, building orientation, construction systems and materials, HVAC systems, lighting and electrical systems, the surrounding conditions, and landscaping. The documents concerning the historical data and renovation records, including the as-built drawings, were obtained from the Department of Art and Architecture at the Ministry of Education in Thailand (DOAA 1998a; 1998b).

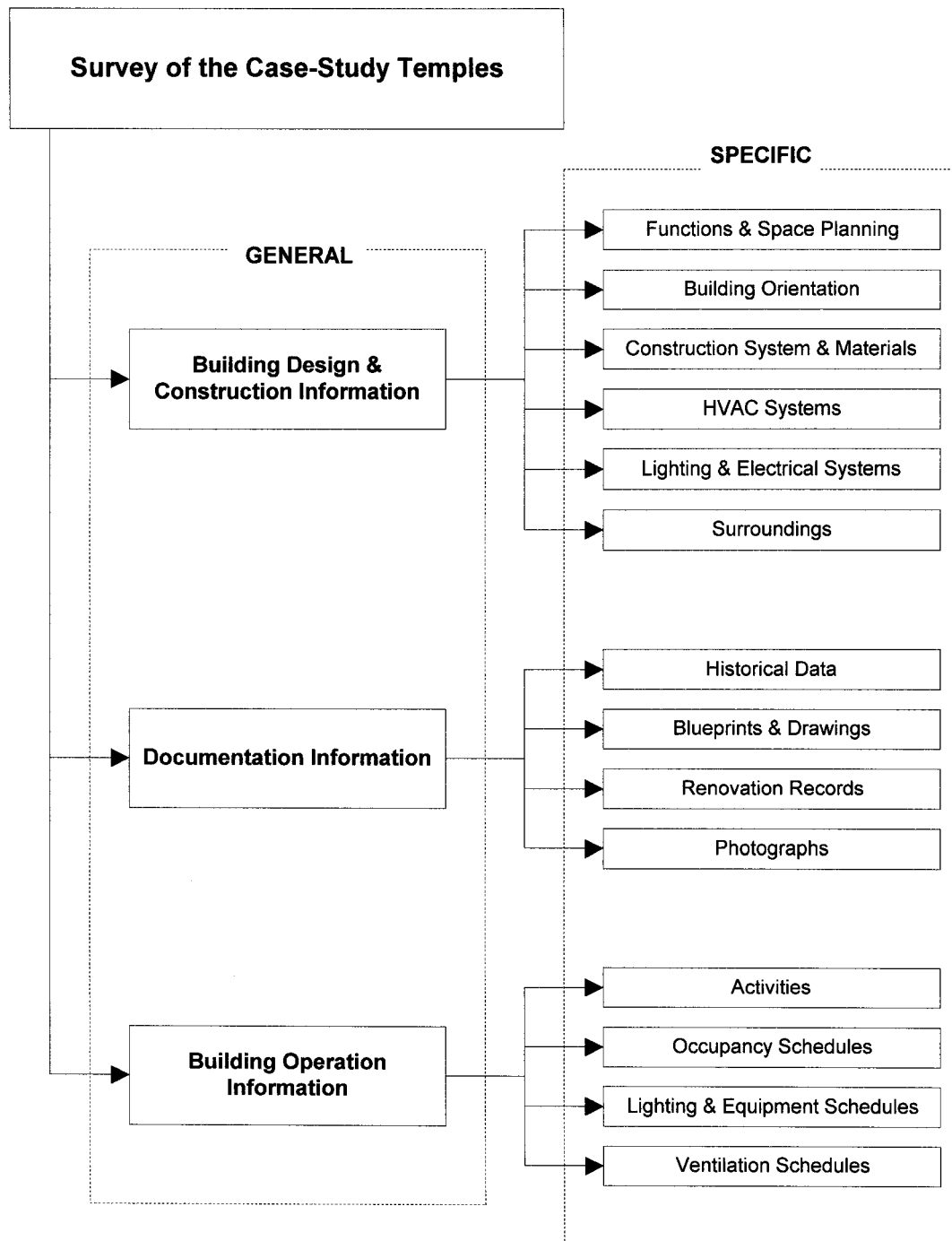


*Figure 4.1* Survey Information Obtained for the Case-Study Buildings.

Among the several temples that were visited, two temples were found suitable for further investigation. The first is a new temple named "King Rama IX Temple" (Figures 4.2 and 4.3) constructed in 1995. The second is an old temple named "Pathum Wanaram Temple" (Figures 4.4 – 4.7) constructed during the early 1900's. Both temples are located in the urban area of Bangkok and they have been considered to be under Royal Patronage, since they were built by the Kings of Thailand and preserved by the Royal Thai Government.

#### **4.1.1 The New Temple**

Figures 4.2 and 4.3 are photos of the new case-study temple taken during a site visit in January of 1999. This temple was designed by a group of architects at the Department of Art and Architecture at the Ministry of Education who were appointed in 1995 to work for the King Rama IX of Thailand. The primary design was intended to be the prototype for contemporary Thai Buddhist temples built in the future. The temple was constructed with 4" (0.10 m) masonry brick exterior walls, steel roof frames, a sheet metal roof, a 1" (0.025 m) wood ceiling, and a slab-on-beam concrete floor with granite toppings and a crawl space beneath the floor. The exterior walls and roof were painted white. Windows and doors are single-pane clear glass with aluminum frames. The building's main structural system is concrete post-and-beam. No wall or ceiling insulation was installed. No attic ventilation was used. During the site visit, it became clear that the windows were not adequately shaded. Details of this temple are included in Appendix A.2.

#### **4.1.2 The Old Temple**

Figures 4.4 and 4.5 show pictures of the old case-study temple taken during January of 1999. This temple was constructed during the early 1900's, and therefore the documents relating its original construction details and past renovations were not available. The as-built drawings prepared by the Department of Art and Architecture were the only sources of detailed construction documentation available. The construction consists of load-bearing masonry brick walls and columns, timber roof frames, a red clay-tile roof, a 1" (0.025 m) wood ceiling, and a stone slab-on-grade floor with marble toppings. Windows and doors are made of solid 1" (0.025 m) thick wood. The building's main structure is a load bearing wall system with 2.5-foot (0.80

m) thick walls that resulted in a limited size and number of openings. No wall or ceiling insulation was installed. No attic ventilation was used. During the site inspection, it was found that the windows were well shaded by the colonnade. Details of this temple are also included in Appendix A.1. Figures 4.6a, 4.6b, 4.7a, and 4.7b show floor-plan and section drawings of both temples.

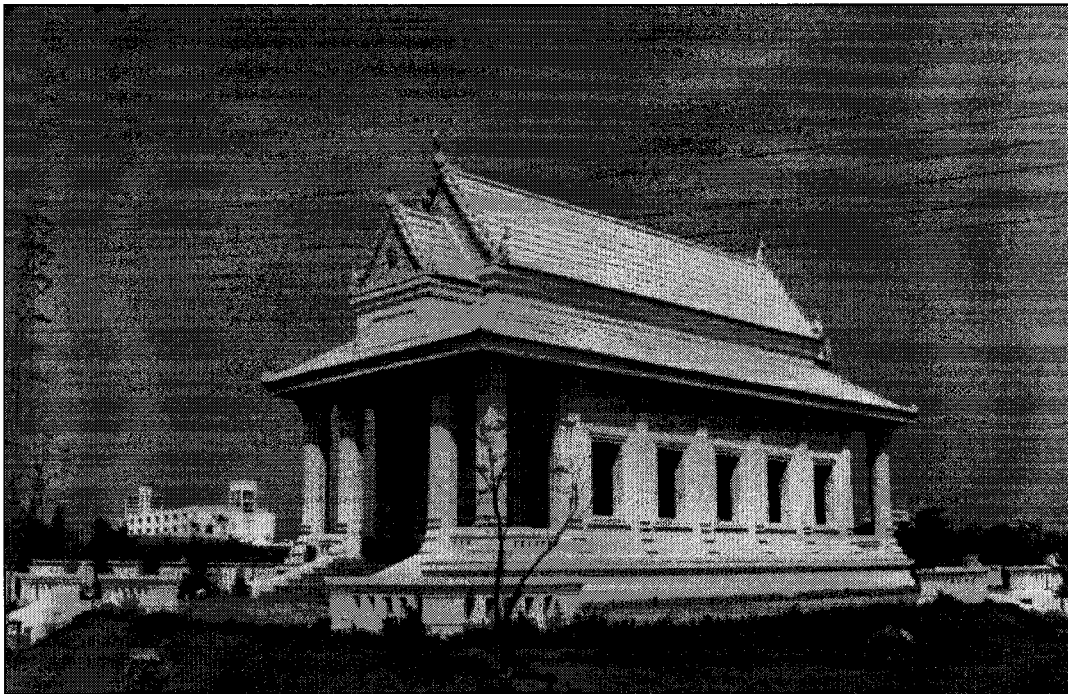


**Figure 4.2** *Exterior View of the New Temple. This photo was taken from the northeast direction at noon on January 6, 1999. Notice how the temple's windows are exposed to the direct sunlight. The temple was constructed with 4" (0.10 m) masonry brick exterior walls, steel roof frames, a sheet metal roof, a 1" (0.025 m) wood ceiling, and a slab-on-beam concrete floor with granite toppings and a crawl space beneath the floor. The exterior walls and roof are painted white. Windows and doors are single-pane clear glass with aluminum frames.*



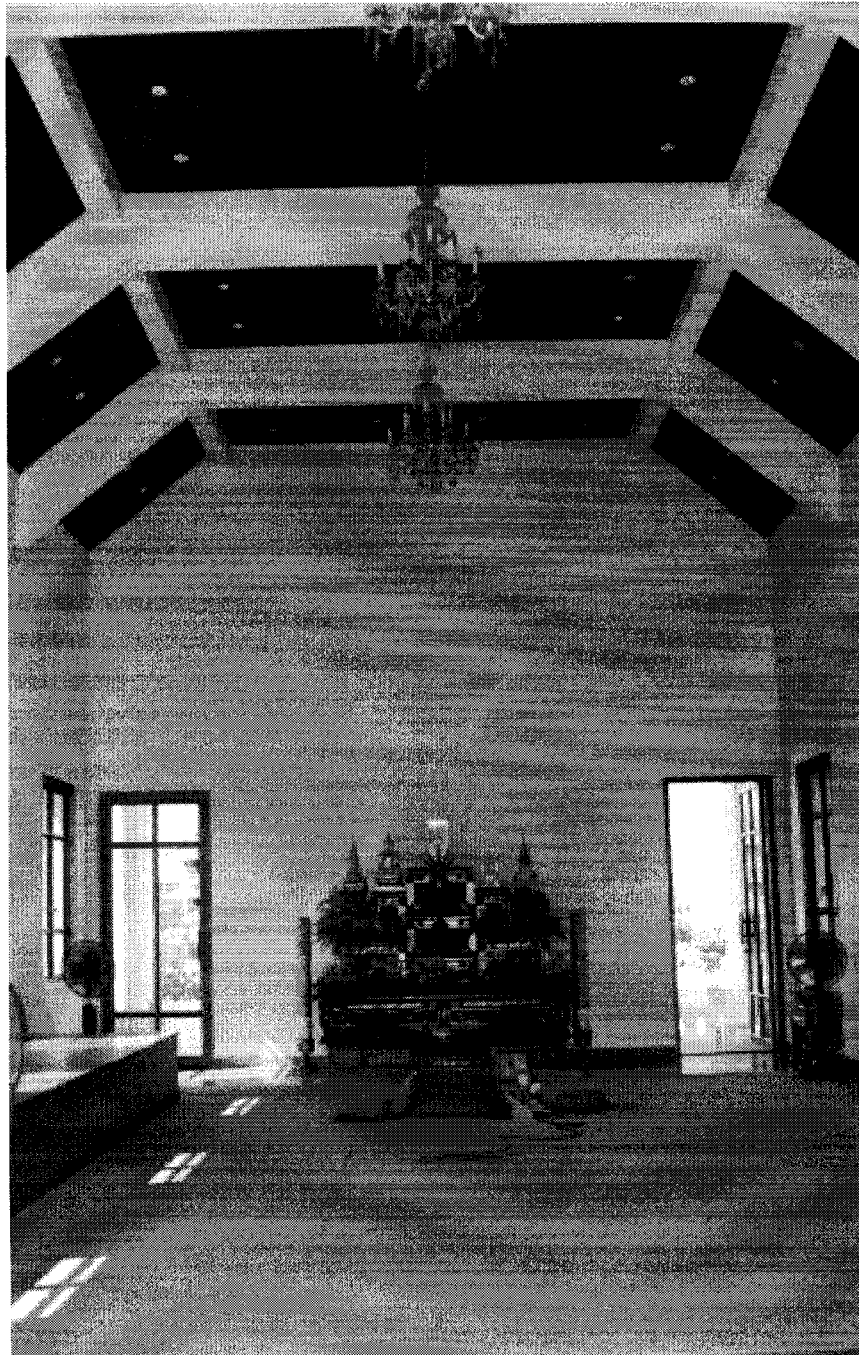


**Figure 4.3** *Interior View of the New Temple. This photo was taken from the front entrance at noon on January 6, 1999. It shows the altar at the back and bench-type seating for the monks on the side. Notice the solar radiation is seen penetrating directly into the building's interior.*

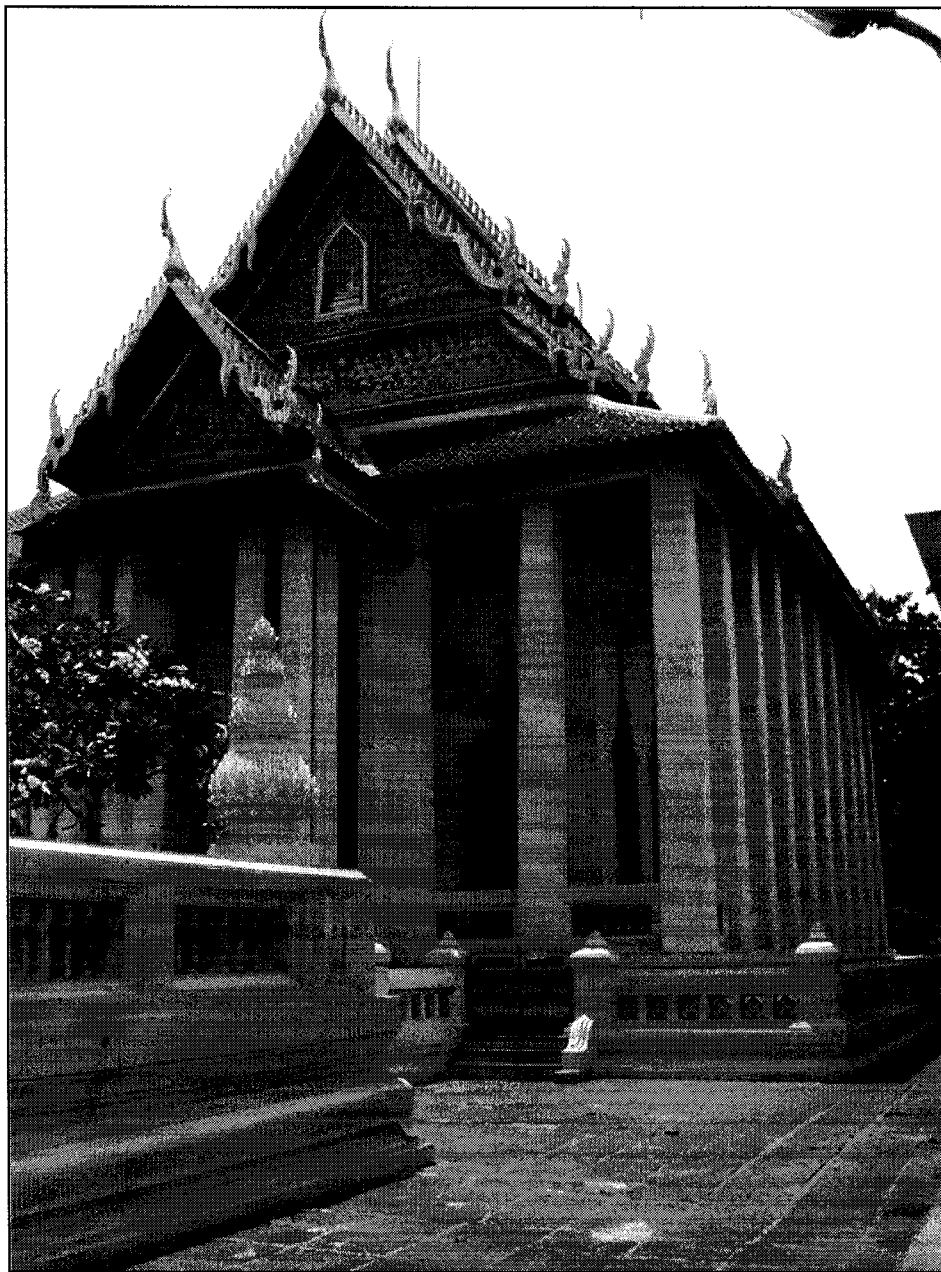


**Figure 4.4** *Exterior View of the Old Temple. This photo was taken from the northeast direction at noon on January 7, 1999. The construction consists of load-bearing masonry brick walls and columns, timber roof frames, a red clay-tile roof, a 1" (0.025 m) wood ceiling, and a stone slab-on-grade floor with marble toppings. Windows and doors are made of solid 1" (0.025 m) thick wood. The building's main structure is a load bearing wall system with 2.5-foot (0.80 m) thick walls. Notice how the exterior walls are completely shaded from the sun.*



*Figure 4.5* Interior View of the Old Temple. This figure shows the altar at the center. This photo was taken from the main entrance at noon on January 7, 1999.

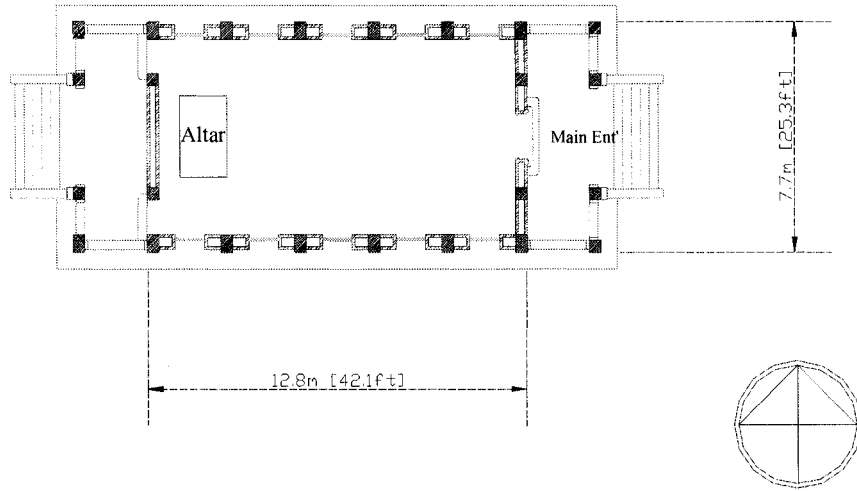


**Figure 4.6a** Floor Plan of the New Temple.

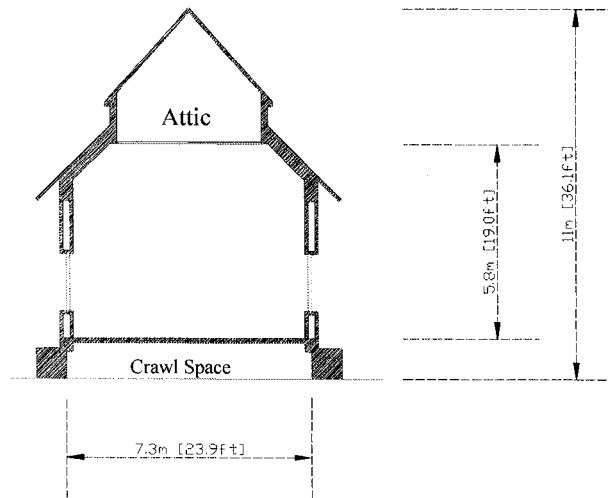


**Figure 4.6b** Section View of the New Temple.

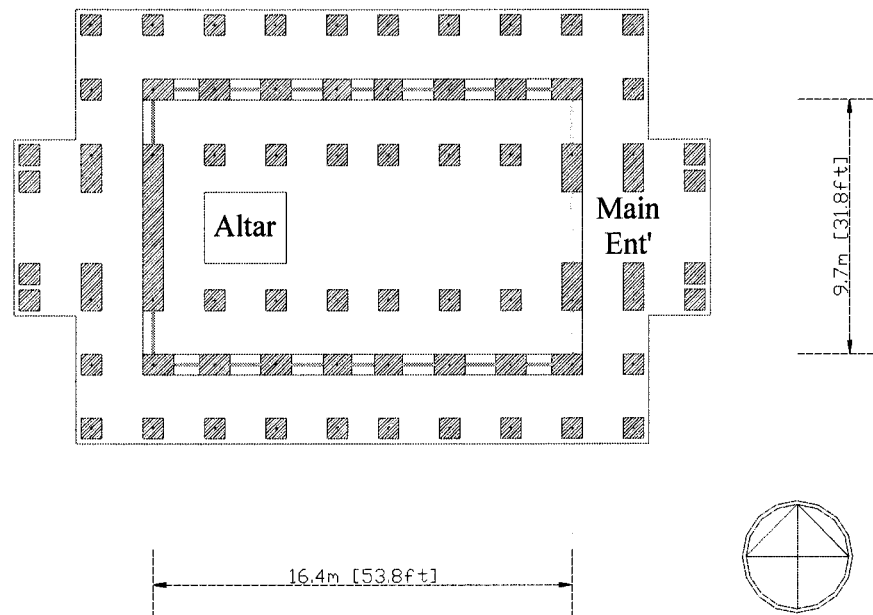


**Figure 4.7a** Floor Plan of the Old Temple.

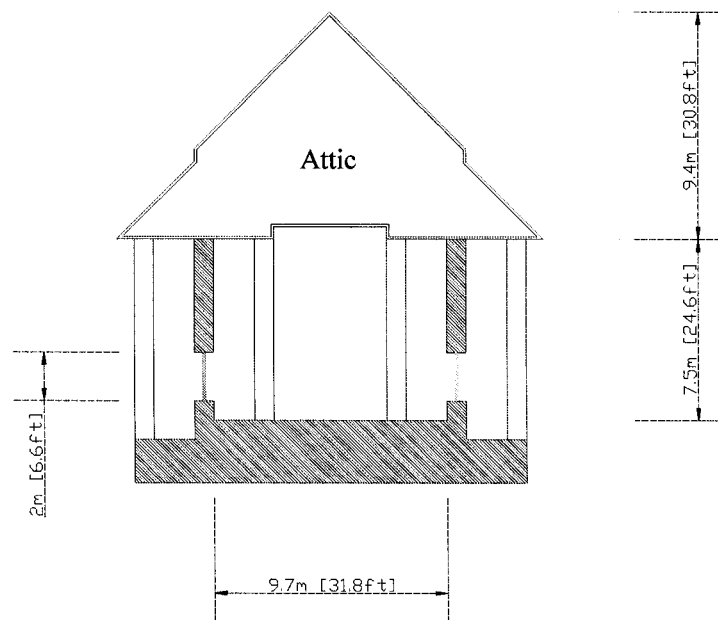


**Figure 4.7b** Section View of the Old Temple.

### **4.1.3 Operating Schedules**

Since all Buddhist temples in Thailand are considered government facilities, the major building operating schedules of both temples are not significantly different from one another because they follow the same regulations set out by the Thai government in terms of the hours of operation and activities allowed inside. Figures 4.8-4.11 show daily profiles of both temples. These two temples are open to the public at 6:00 a.m. and closed at 6:00 p.m. every day, including weekends and holidays. The highest occupancy periods are usually from 10:00 a.m. to 12:00 noon and 5:00 p.m. to 6:00 p.m., especially on Sundays and religious holidays. During the day, all doors and windows are normally left open, and they are completely closed at night for security reasons (Kittipunyo 1999). The newer temple has a smaller number of Buddhists visiting the temple on weekdays, and is therefore occasionally closed on weekday afternoons. In addition, due to religious reasons, most Buddhist temples do not have any kind of sophisticated HVAC systems installed. Only portable fans donated by faithful Buddhists are allowed.

## **4.2 Measurements and Data Collections**

### **4.2.1 Bangkok Weather Data**

The outdoor weather data collected from Bangkok during 1999 were obtained from two sources: 1) on-site measurements, and 2) weather data recorded by the Thai government. On-site measurements included outdoor dry-bulb temperatures and the relative humidity. These data were measured outside the temples using micro data-loggers from February to December in 1999. The weather data obtained from the Royal Thai Meteorological Department (RTMD) included: 1) the barometric pressure, 2) the dry-bulb temperature, 3) the wet-bulb temperature, 4) the relative humidity, 5) the wind speed, 6) wind direction, 7) rainfall, 8) global horizontal solar radiation, and 9) the sky conditions. The RTMD data were collected from the measurements taken at 11 sub-stations around Bangkok, and were averaged into a single set of data. All measurements except that of wind speed were taken manually. These hourly data were recorded by a single snapshot reading each hour. More details regarding the instruments and plots of data are presented in Appendix B.

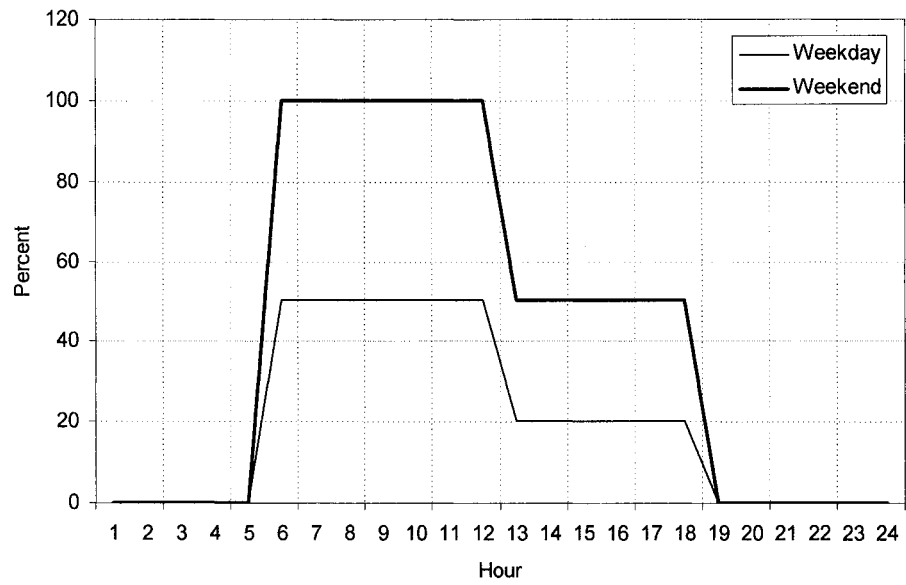


**Figure 4.8** Daily Occupancy Profiles on Weekdays and Weekends.

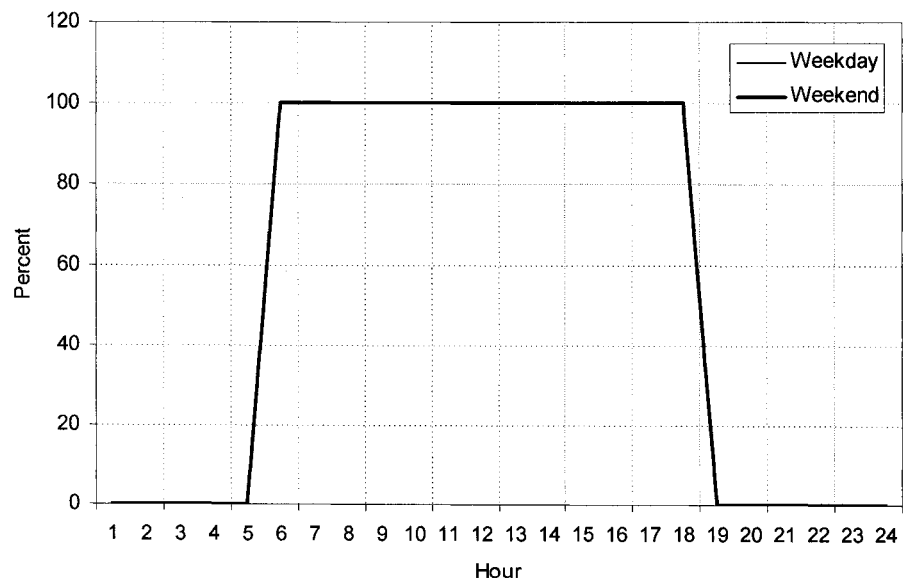


**Figure 4.9** Daily Lighting Profiles on Weekdays and Weekends.

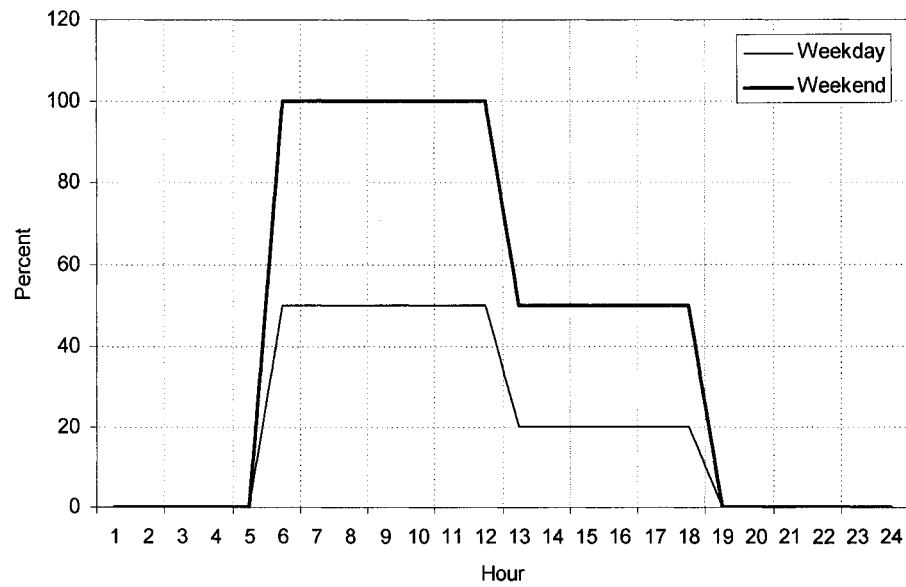


**Figure 4.10** *Daily Electrical Equipment Profiles on Weekdays and Weekends.*

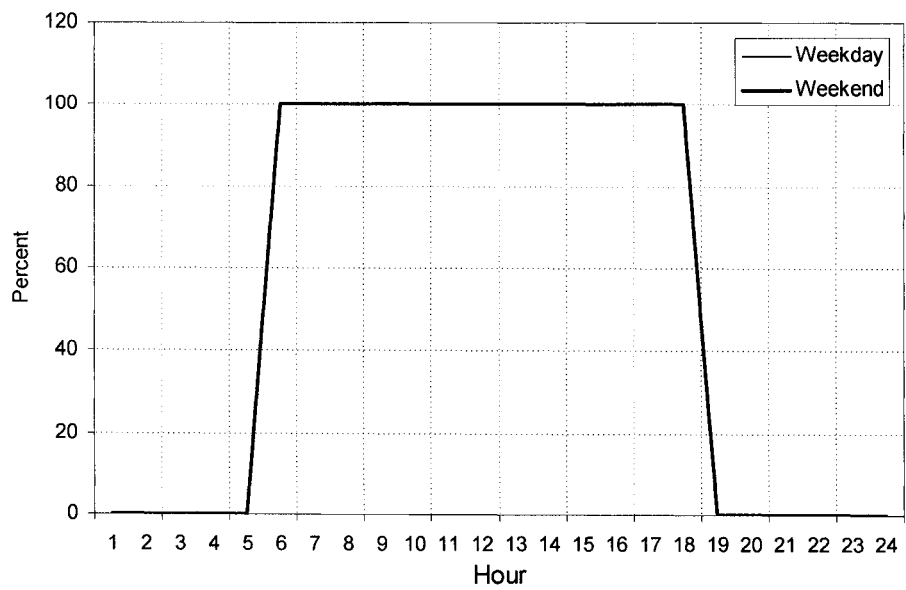


**Figure 4.11** *Daily Natural Ventilation Profiles on Weekdays and Weekends.*



#### 4.2.2 Instrumentation and Calibration

Figures 4.12a, 4.12b, 4.12c, and 4.13 show the portable temperature/relative humidity sensors placed inside both case-study temples. The indoor air temperature, relative humidity, and floor surface temperature of each case study temple were measured using micro data-loggers installed in secured boxes (Onset 2002). Six data-loggers were used to measure room and floor temperatures using a surface-mounted external sensor, as demonstrated in Figure 4.13. For each temple, the measurements included: 1) indoor air temperature and relative humidity at the floor level, 2) indoor air temperature and relative humidity at the ceiling level, and 3) the indoor floor surface temperature. The hourly data were retrieved once a month, beginning in February of 1999 and the data files emailed to the U.S. The wall surface temperatures were measured using a handheld infrared thermometer (Raytek 1999) from October of 1999 through January of 2000. Figure 4.14 shows the instrument used to take this measurement. All data-loggers were calibrated using a sling psychrometer, a glass thermometer, and a calibrated digital temperature/relative humidity sensor before being deployed at the sites, and they were recalibrated after the measurements were completed. Calibration procedures and results are included in Appendix F.



*Figure 4.12a* Portable Indoor Temperature/Relative Humidity Sensor Placed in a Secure Box.

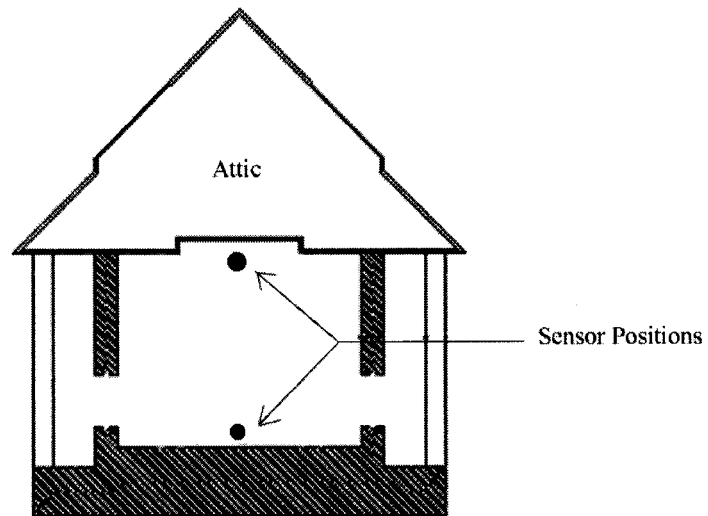


**Figure 4.12b** *Vertical Positioning of the Temperature/Relative Humidity Sensors in the Old Temple.*

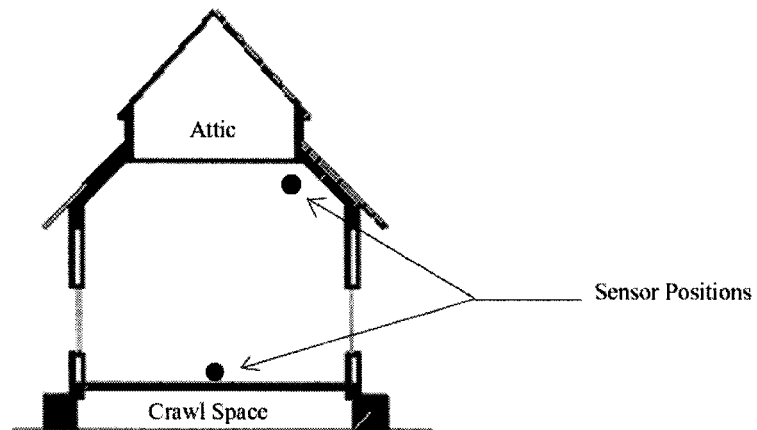


**Figure 4.12c** *Vertical Positioning of the Temperature/Relative Humidity Sensors in the New Temple.*



**Figure 4.13** *Floor Surface Temperature Measurement Using a Portable Data logger with an External Thermocouple-Type Sensor. The sensor is attached to the floor using duct tape.*



**Figure 4.14** *Wall/Ceiling Surface Temperature Measurement Using an Infrared Thermometer.*

### **4.3 Calibrated DOE-2/CFD Simulations**

To perform this study, the DOE-2.1e building simulation program (LBNL 1994; 2001) and a 3-D Computational Fluid Dynamic (CFD) program were used (Andrews and Prithiviraj, 1997). The DOE-2 program was chosen because of its ability to simulate the overall thermal performance of a building using specially prepared hourly weather files that contained Thai weather data for the 1999 period. CFD was used because of its ability to simulate the detailed airflow and physical processes occurring in the case study building. DOE-2 reports hourly variables needed for the CFD program to perform a simulation. Therefore, this research, the two simulation tools were coupled together because DOE-2 needs the air infiltration rates calculated by CFD in order to provide accurate thermal simulations of the temple, and CFD needs the information regarding the building envelop (such as the solar heat gain and the surface temperatures) from DOE-2 to establish the boundary conditions. Details of how the programs were coupled are presented in the following sections.

#### **4.3.1 DOE-2 Thermal Simulations**

DOE-2, developed by the Lawrence Berkeley National Laboratory, is an hourly-based thermal simulation program used to calculate multizone envelope, system, and plant loads. This public-domain simulation program allows users to perform hourly building energy simulations for a one-year period using ASHRAE's algorithms. The heat transfer by conduction and radiation through walls, roofs, floors, windows, and doors are calculated separately using response factors, in which the effects of thermal mass are carefully considered. In addition, interior surface convection is computed based on user-specified convection coefficients, while the exterior convection is calculated by the program itself, based on the surface roughness and outdoor wind speeds taken from the weather data.

##### **4.3.1.1 DOE-2 Analyses of Unconditioned Buildings**

DOE-2 was primarily designed to help building designers perform annual calculations of energy consumed by various heating and cooling systems. However, this research is concerned with buildings with no heating, ventilating, and air-conditioning (HVAC) systems, and are

instead operated with natural ventilation at all times. Therefore, to simulate the thermal effect of natural ventilation with DOE-2, the temple was first divided into two primary unconditioned zones (i.e., the indoor space and the attic space), where heat gains from the outside and inside cause the indoor temperature to float freely. In terms of the heat gains by natural ventilation, both spaces were treated like control volumes with outdoor air supplied to the spaces through air infiltrations. The amount of outside air infiltration is a very important variable, and is usually obtained either from experiment (i.e., blower door test) or a computer program (i.e., network airflow model). For this research, the air infiltration rates were computed by the CFD program by multiplying the opening area with an average velocity of the air passing through all windows. The details can be found in the following sections.

#### **4.3.1.2 Processing a DOE-2 Weather File Using the Bangkok Weather Data**

Figure 4.15 shows a flowchart diagram for the DOE-2 weather processing. The DOE-2 program was designed to calculate hourly building energy consumptions by using hourly weather data available in several file formats. The available types of weather files include the Test Reference Year (TRY and TRY2), the Typical Meteorological Year (TMY and TMY2), the California Climate Zone (CTZ), and the Weather Year for Energy Consumption (WYEC and WYEC2). However, before the DOE-2 simulation program can execute, users need to convert ASCII files into binary files recognizable by DOE-2. Recently, the Lawrence Berkeley National Laboratory (LBNL) has developed a sub-program, which converts an ASCII file into binary files. It is called the “DOE-2 weather processor” (LBNL 2001), or commonly known as the “DOE-2 Weather Packer.”

To pack the actual Bangkok weather data into a DOE-2 weather file, the hourly weather data from Bangkok must be in the TRY, TMY, TMY2, CTZ, or WYEC file formats. Since the TRY format contains all the data necessary for this research, this format was used to pack the Bangkok weather data into a DOE-2 weather file. The flowchart diagram in Figure 4.15 demonstrates how the raw hourly weather data obtained from the Bangkok Meteorological Department were converted into the TRY file needed by the DOE-2 weather packer. Initially, the hourly data containing dry-bulb temperature, relative humidity, wind speed, wind direction, global horizontal solar radiation, and atmospheric pressure were converted into an ASCII file in

the TRY format using the LS2TRY program developed by Bronson (1992). The global horizontal solar radiation was synthesized into the beam and diffuse components using the correlations developed by Erbs et al. (1982) as the following formulas:

$$\frac{I_{dif}}{I_{glo}} = 1.0 - 0.09k_T \quad \text{for } 0 \leq k_T \leq 0.22 \quad (4.1)$$

$$\frac{I_{dif}}{I_{glo}} = 0.9511 - 0.1604k_T + 4.388k_T^2 - 16.638k_T^3 + 12.336k_T^4 \quad \text{for } 0.22 \leq k_T \leq 0.80 \quad (4.2)$$

$$\frac{I_{dif}}{I_{glo}} = 0.165 \quad \text{for } 0.80 \leq k_T \quad (4.3)$$

Where  $I_{dif}$  is the diffuse solar radiation,  $I_{glo}$  is the global horizontal solar radiation, and  $k_T$  is the hourly clearness index (i.e., the ratio of terrestrial and extraterrestrial solar radiation), which was calculated by the following formula:

$$k_T = \frac{I_{glo}}{I_0 \cos \theta_s} \quad (4.4)$$

Where  $\theta_s$  is the zenith angle of the sun, which is the incidence angle on the horizontal surfaces;  $I_0$  is the extraterrestrial solar radiation, which was calculated using the following formula:

$$I_0 = \left( 1 + 0.033 \cos \frac{360^\circ \times n}{365.25} \right) \times 435.2 \text{ Btu/ (h} \cdot \text{ft}^2) \quad (4.5US)$$

$$I_0 = \left( 1 + 0.033 \cos \frac{360^\circ \times n}{365.25} \right) \times 1373 \text{ W/m}^2 \quad (4.5SI)$$

Where  $n$  is the day of year (e.g.,  $n = 1$  for January 1).

Once a Bangkok TRY file was prepared, the DOE-2 Weather Packer converted this TRY file into a binary file that DOE-2 could read.

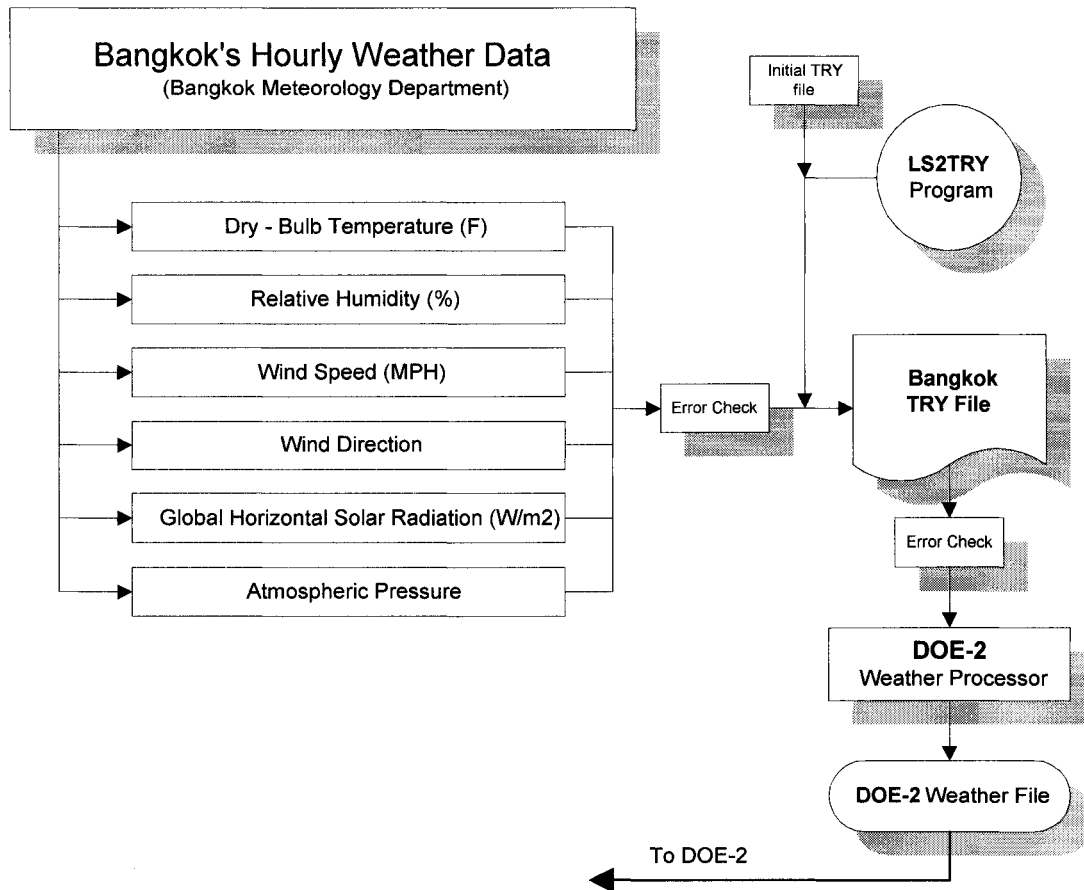


**Figure 4.15** Flowchart Diagram Showing the DOE-2 Weather Data Processing.

#### 4.3.1.3 Creating a DOE-2 Input File to Simulate the Old Temple

The case study buildings consist of the new temple and the old temple. Indoor measurements were performed for both temples. However, only the simulations made of the old temple were included in this research. Figure 4.16 demonstrates the process by which the building's descriptions were entered in to the DOE-2 input file. A DOE-2 input file generally contains a series of input variables assigned to four major DOE-2 sub-programs: LOADS, SYSTEM, PLANT, and ECONOMICS (LBNL 2001), however, for this research, only LOADS and SYSTEM sub-programs were used. In an input file, all variables are categorized into groups of input variables. These contain the building's location, materials and construction, schedules,

shade from the building's surroundings, general space definitions, building zones, and building systems. The case-study temple was divided into an interior space and an attic space, where heat gain from the outside and inside caused the indoor temperatures to float freely. The interior space is defined by four exterior walls, a floor, a ceiling, and series of doors and windows. The attic space is defined by four exterior walls, which are actually the four sides of the roof, and a ceiling next to the interior space below. The surrounding colonnades and buildings are defined as the building shades, which DOE-2 accounts for through shading calculations. Figure 4.17 illustrates the 3-dimensional geometry of the building created by the DOE-2 add-on program, DrawBLD (Huang 1994).

### **4.3.2 Computational Fluid Dynamics (CFD)**

The 3-D CFD simulations were performed with the HEATX code written by Andrews and reported in Prithiviraj and Andrews (1998a, 1998b). The HEATX code was originally written for the simulation of large shell-and-tube heat exchangers. However, since these devices have complex geometries, including many twisting flow passages, the code is well suited to the complex geometries of architectural design. Figure 4.18 demonstrates the calculation procedure embedded in HEATX. Basically, the code employs a modified two-equation  $k$ - $\epsilon$  turbulence model with source terms for turbulence generation and dissipation due to buoyancy. The formulation involves solving equations for pressure, three components of velocity, temperature, turbulence kinetic energy and its dissipation rate, both for steady and for transient problems. Table 4.1 shows the source terms and diffusion coefficients formulated inside the HEATX code. Due to the complex nature of the partial differential equations governing fluid flow and heat transfer, the CFD problem was solved by the iteration procedure shown in Figure 4.18.

#### **4.3.2.1 HEATX Governing Equations**

A statistical representation of turbulence was adopted to overcome the problem of representing the wide range of time and length scales in turbulent flows. The Reynolds stresses that originate from the statistical averaging were modeled using the Boussinesq (1877; ref. Andrews and Prithiviraj 1997, p.3) eddy viscosity approximation.



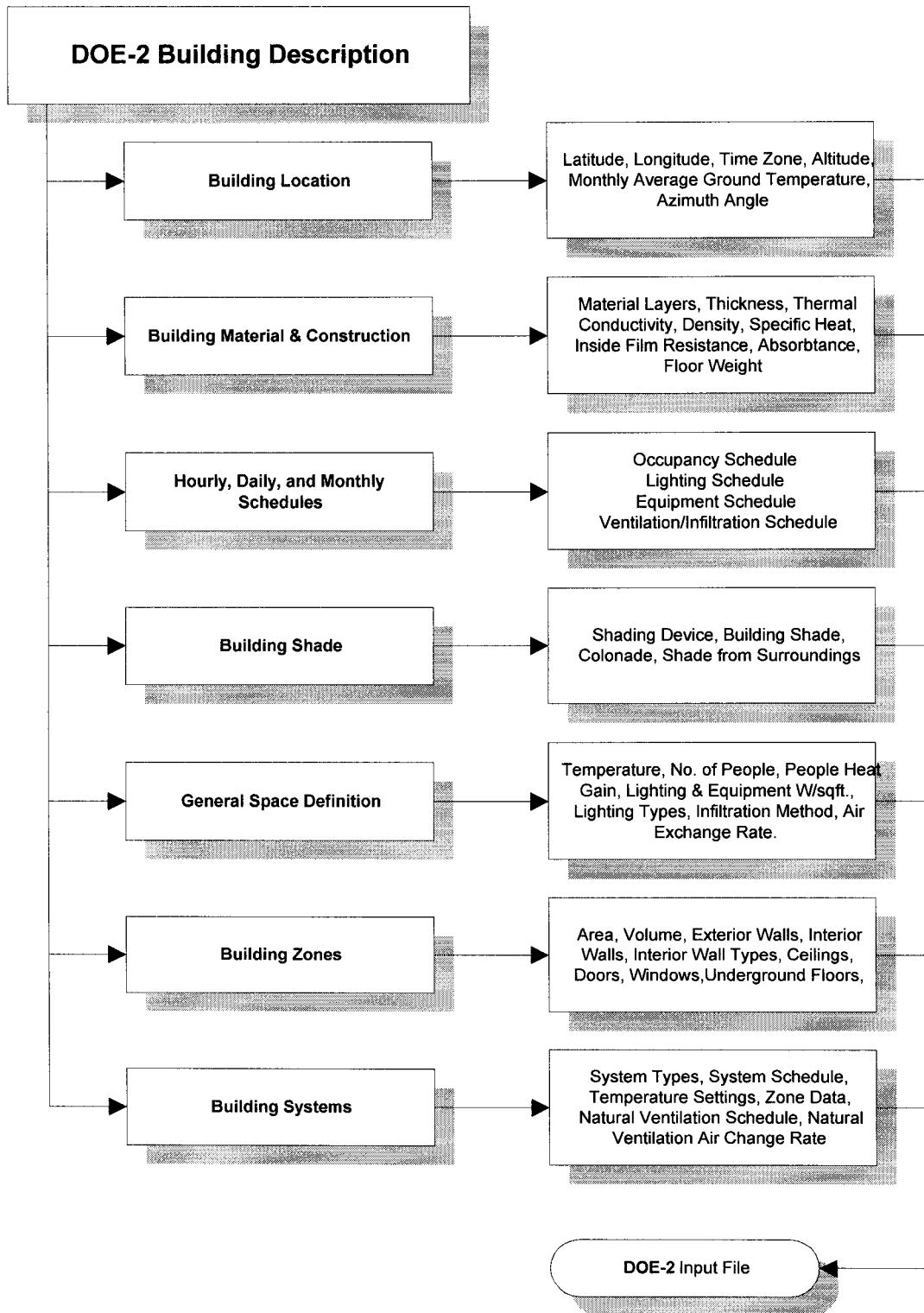


*Figure 4.16 Input Diagram of the DOE-2 Building Description Language (BDL).*

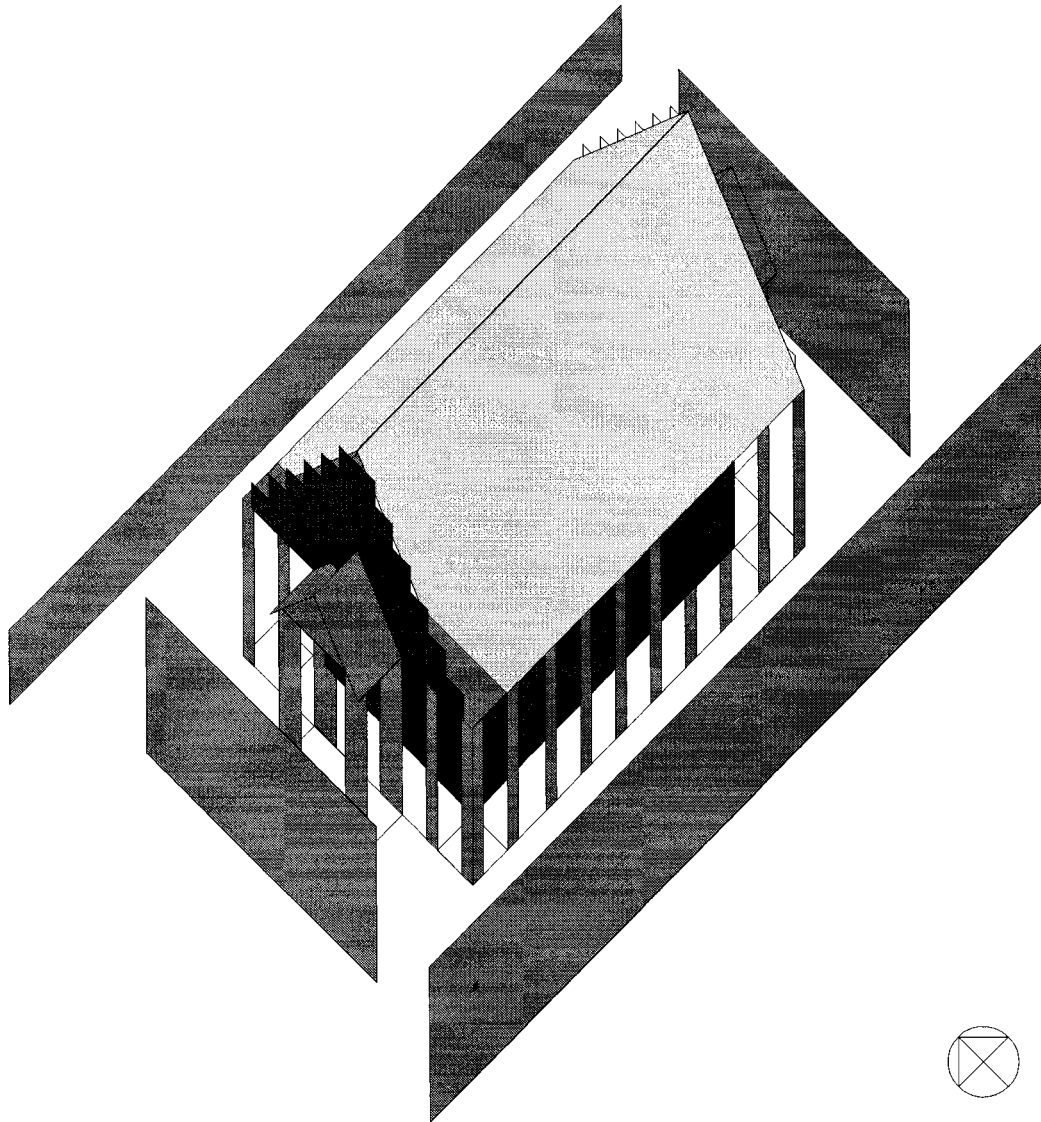


**Figure 4.17** *Image of the Old Temple Simulation Input Using the DrawBDL Program.*

A modified two-equation  $k-\epsilon$  turbulence model with source terms for turbulence generation and dissipation due to buoyancy was used (Snider and Andrews 1994). The reason to adopt the  $k-\epsilon$  model is due to a lack of detailed experimental knowledge of the turbulence field within the temple. Hence, it is better to use a turbulence model whose attributes are well known rather than a more sophisticated RNG or Reynolds stress model for which its need in modeling a temple is not known in the present context.

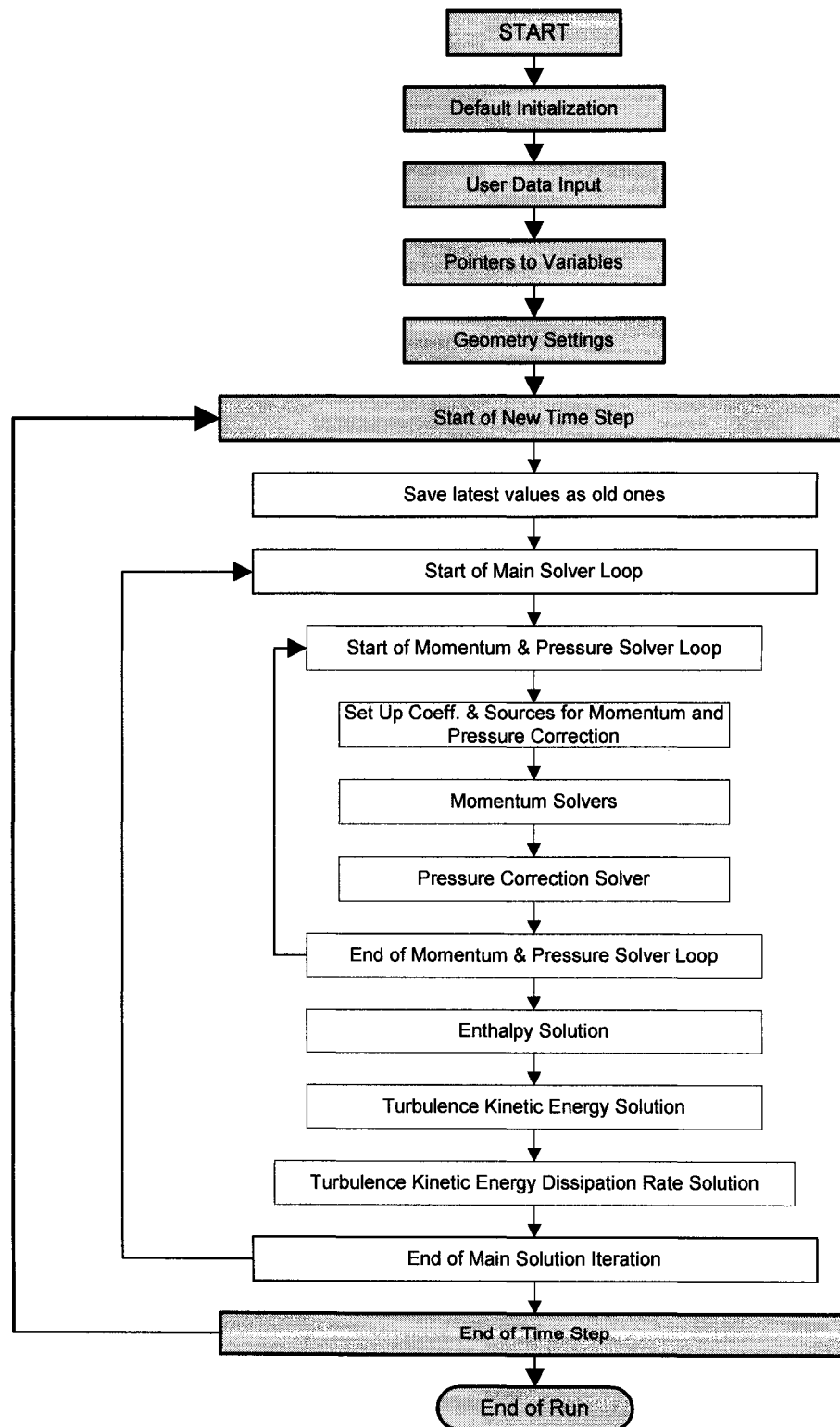


**Figure 4.18** HEATX Calculation Procedure.

The derivation of the equations governing fluid flow and heat transfer presented have been given in Prithiviraj and Andrews (1998a). The steady governing equation may be written:

$$\nabla \cdot (f\rho\phi\vec{V} - f\Gamma_\phi \nabla\phi) = fS_\phi \quad (4.6)$$

Where  $\Gamma_\phi$  is the diffusion coefficient,  $f$  the porosity, and  $S$  a source for variable  $\phi$ . The source terms for the various  $\phi$ 's and the diffusion coefficients  $\Gamma_\phi$  are given in Table 4.1.

**TABLE 4.1**  
**Coordinate Source Terms and Diffusion Coefficients**

$\phi$	$S_\phi$	$\Gamma_\phi$
u	$-\frac{\partial\bar{p}}{\partial x}$	$\mu_{\text{eff}}$
v	$-\frac{\partial\bar{p}}{\partial y}$	$\mu_{\text{eff}}$
w	$-\frac{\partial\bar{p}}{\partial z} + \rho g_z$	$\mu_{\text{eff}}$
$H_{\text{roof}}$	$\frac{U_o A_{\text{roof}}}{\text{Volume}} \left( \frac{H_{\text{outside cell}}}{C_p} - \frac{H_{\text{inside cell}}}{C_p} \right)$	$\frac{\mu}{Pr} + \frac{\mu_t}{Pr_t}$
k	$G - \rho\varepsilon$	$\frac{\mu_t}{\sigma_k}$
$\varepsilon$	$C_1 G \frac{\varepsilon}{k} - C_2 \rho \frac{\varepsilon^2}{k}$	$\frac{\mu_t}{\sigma_\varepsilon}$

For example, the continuity equation is expressed in the Cartesian (x-y-z) coordinates adopted for this simulation.

$$\frac{\partial(f_s \rho u)}{\partial x} + \frac{\partial(f_s \rho v)}{\partial y} + \frac{\partial(f_s \rho w)}{\partial z} = 0 \quad (4.7)$$

The effective viscosity  $\mu_{\text{eff}}$  is given by:

$$\mu_{\text{eff}} = \mu + \frac{\rho C_{\mu} k^2}{\varepsilon} \quad (4.8)$$

Where  $\mu$  is the laminar viscosity,  $k$  is the turbulence kinetic energy,  $\varepsilon$  is the turbulence dissipation rate, and  $\bar{p}$  is the modified pressure given as:

$$\bar{p} = p + \frac{2}{3}k \quad (4.9)$$

$Pr$  is the laminar Prandtl number.  $G$  is the production of turbulence kinetic energy from shear and buoyancy and  $C_1$ ,  $C_2$ ,  $C_{\mu}$ ,  $\sigma_k$ , and  $\sigma_{\varepsilon}$  are turbulence model constants from Launder and Spalding (1974).  $C_3$  was assigned by Snider and Andrews (1994).

#### 4.3.2.2 CFD Analysis of the Old Temple Using HEATX

The HEATX code solves the aforementioned governing equations using finite volumes (Patankar 1980), in which the temple and surrounding space is subdivided into finite-sized control volumes. The control volumes were chosen so that the surface of the temple corresponds to the surface of the control volumes. The control volumes were then used to form balances of mass, momentum and heat balances around a control volume and thus forms an algebraic equation that corresponds to the fundamental governing partial differential equations. The very complex geometry of a temple precludes the use of body-fitted coordinates; therefore a “porosity” formulation was used in which solid walls were assigned a porosity of 0.0, while open volumes were assigned a value of 1.0. This formulation restricts the accuracy of the simulation to the size of the cell, but this is also the limit of the numerical representation of gradients. Thus, the angled roof was represented by a set of steps. With a sufficient number of volumes, the geometries could then be well represented, as is aptly shown in Figures 4.19a and 4.19b. One

concern was the resolution offered to the small-scale details associated with items such as flows through windows, or small vents. Ideally, the grid should be locally refined around the detailed items. However, the complexity of the temple geometry, and in particular the number of windows, columns and vents, prevents such high-resolution calculations. Even though it should be recognized that the detailed flows around and through small-scale features such as windows might not be accurately represented, however, the overall performance of the temple is well simulated. Figure 4.20 demonstrates the thermal network diagram used to formulate the heat transfer process of the case-study temple.

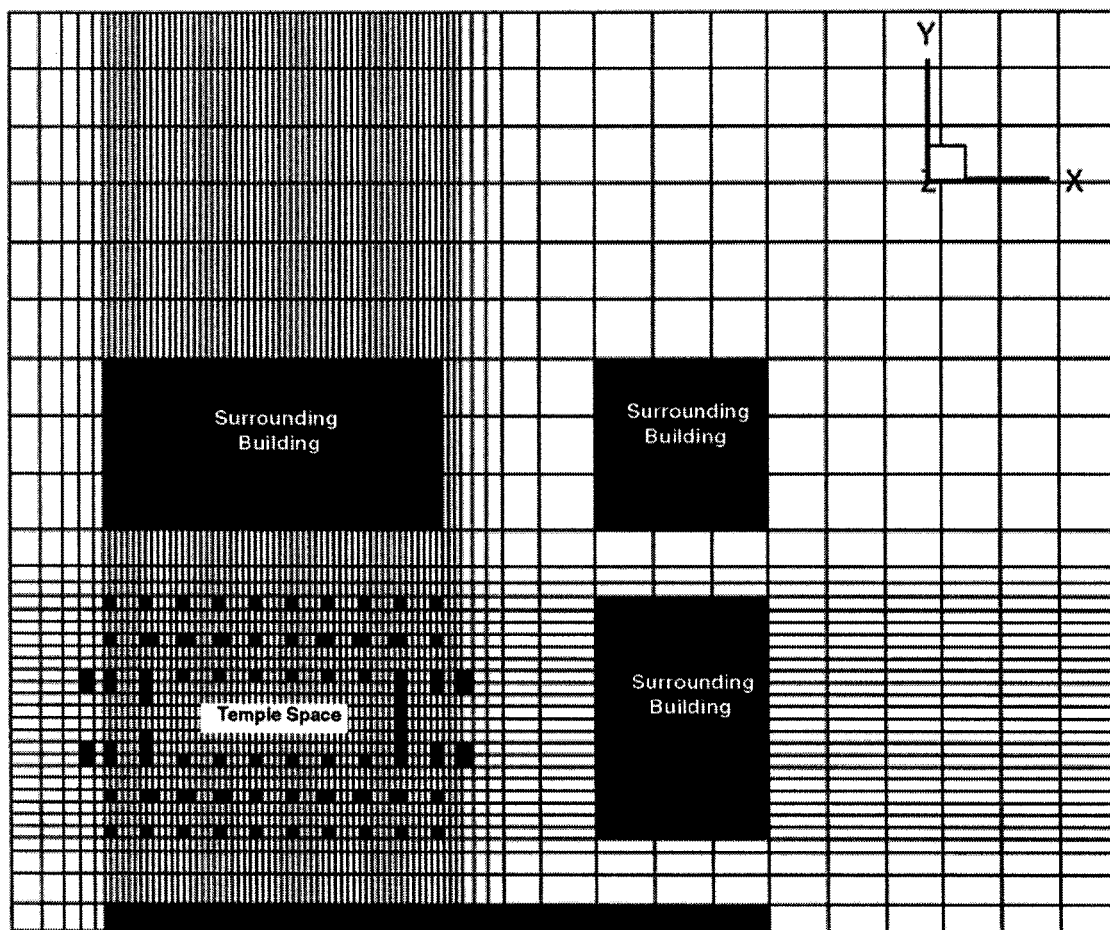


**Figure 4.19a** *Non-Uniform Grid Setting for a CFD Simulation of the Old Temple: Plan View.*

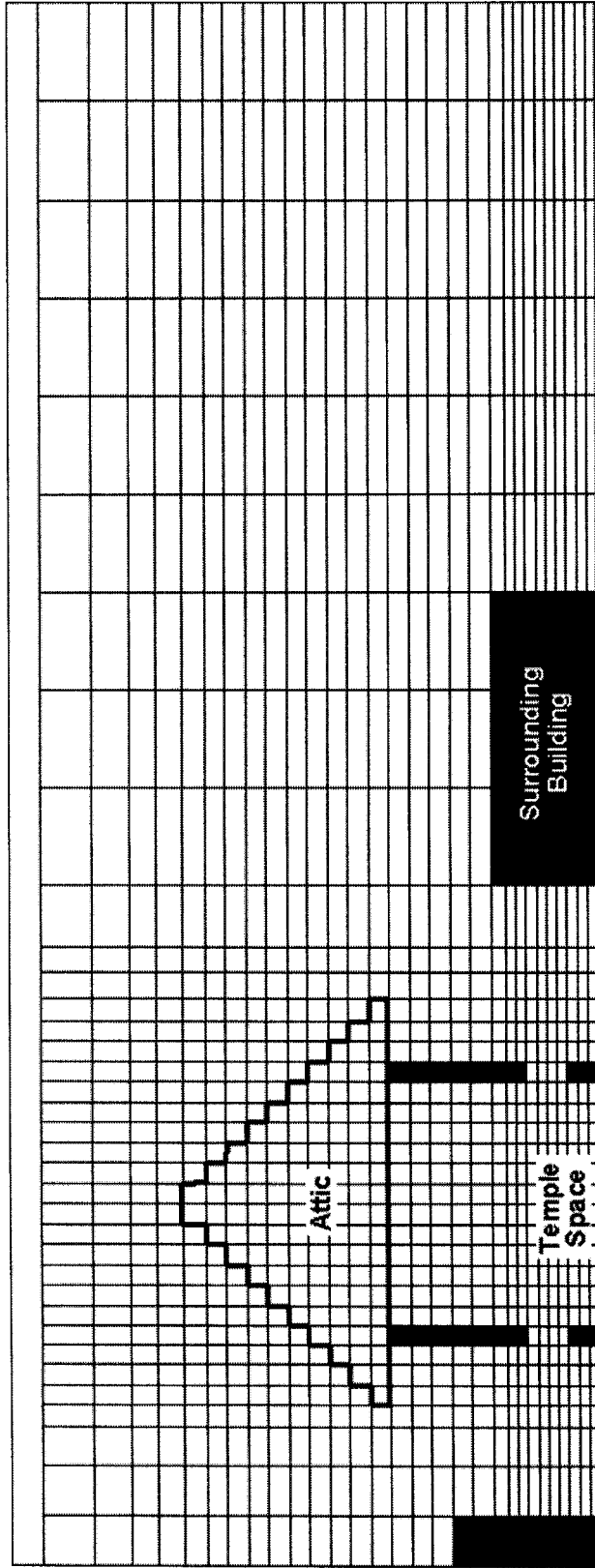


**Figure 4.19b** Non-Uniform Grid Setting for a CFD Simulation of the Old Temple: Section View.

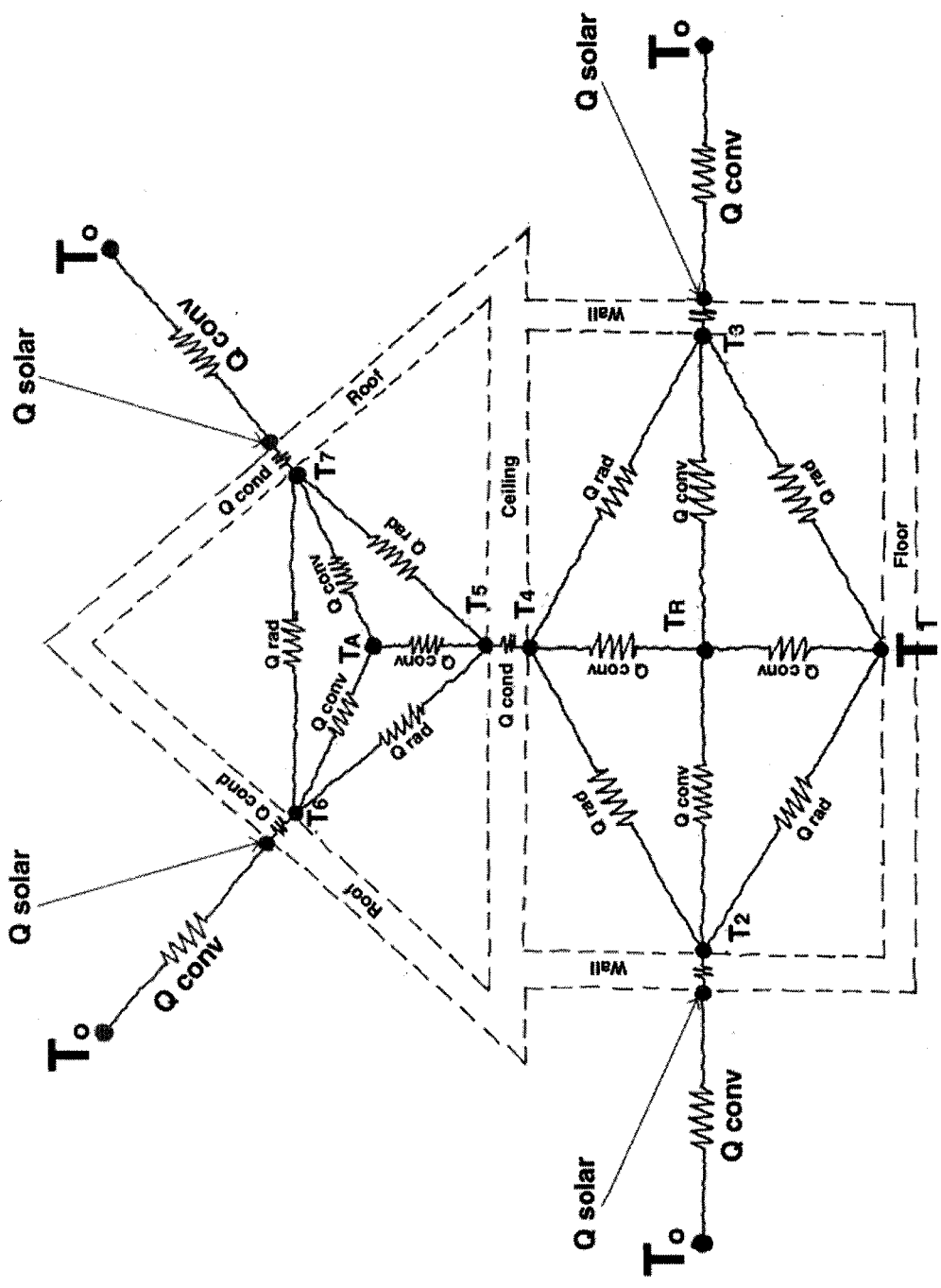


Figure 4.20 Thermal Network Diagram Showing the Heat Transfer Calculations in HEATX.



#### 4.3.2.3 Creating a HEATX Input File to Simulate the Old Temple

Figure 4.20 demonstrates the thermal network diagram used to formulate the heat transfer process of the case-study temple.  $T_O$  is the ambient outdoor temperature obtained from the weather tape.  $Q_{\text{solar}}$  is the total solar radiation received on each surface calculated by DOE-2 using the global horizontal solar radiation in the Thai weather data file, which is divided into beam and diffuse components using the correlations by Erbs et al. (1982).  $T_1, T_2, T_3, T_4, T_5, T_6,$  and  $T_7$  are the interior surface temperatures calculated by DOE-2.  $T_A$  is the attic temperature and  $T_R$  is the room temperature. Both DOE-2 and HEATX were used to calculate  $T_A$  and  $T_R$ . During the daytime, solar radiation heats up the building's exterior surfaces. A fraction of this surface heat is taken away by the outside air through convection, leaving the rest to be conducted through the exterior walls and roof. The heat conduction through the exterior envelope causes the interior surfaces to warm up during the day and transfers to the indoor air through a thermal convection process. A portion of the interior surface heat radiates to other surfaces through a radiation exchange process. The heat accumulated in the attic then transfers to the interior space through the ceiling. This thermal diagram was used to formulate the heat balance equations in the CFD code.

#### 4.3.2.4 Boundary Conditions

For the inflow boundary conditions, the outdoor weather data on one typical summer and winter day were put in to the CFD simulations. The turbulence kinetic energy ( $k$ ) and its dissipation rate ( $\epsilon$ ) were set according to the formulas:

$$k = (0.05V_{\text{inlet}})^2 \quad (4.10)$$

$$\epsilon = (0.09^{0.75} k^{1.5})/D \quad (4.11)$$

where  $V_{\text{inlet}}$  is the inflow velocity of the air, and  $D$  is the hydraulic diameter.

The solar radiation received on the roof's surface and the interior wall surface temperatures were obtained from DOE-2. The floor surface temperature was obtained from the

measurement. Computational grids are shown in Figure 4.19. The total number of computational cells is 313,000, which is considered a moderately high number of computational cells by current CFD standards.

The major heat gain to the building was the solar heat gain through the roof. In terms of the roof's heat exchange formulation, the variation of  $H_i$  across the roof appeared through a cell heat source  $q$ , given as:

$$q = U_o A_s \left( \frac{H_{out}}{C_p} - \frac{H_{in}}{C_p} \right) / \text{volume} \quad (4.12)$$

where  $U_o$  is the overall heat transfer coefficient,  $A_s$  is the cell surface area,  $C_p$  is the specific heat of the air, and  $H_{out}$  and  $H_{in}$  are enthalpies of air both outside and inside the roof, respectively.

#### 4.3.3 Calibrations of the Simulation Model

The calibration process began by first combining the two programs to simulate the indoor air temperatures of the case-study temple for various 24-hour periods on summer and winter days. Second, the average maximum air exchange rate and corresponding convection coefficients obtained from the 24-hour coupled DOE-2/CFD simulations were used only by DOE-2 for the annual hourly calculations. Third, the measured hourly indoor temperatures were then used as an indicator of how well the simulation model represented the real building. Since the indoor temperature measurements will be taken at two locations in the space (i.e., 1) on the floor level, and 2) at the ceiling level), the measured indoor temperature used for the comparison in the research will be the average temperatures of these two locations. With DOE-2's capability of generating the hourly output for one year, the simulated indoor temperatures were compared to the measured temperatures. Finally, once the simulated temperatures matched the measured data in a satisfactory way, the simulation model was then declared calibrated. More details concerning this process are discussed in the following sections. In terms of the statistical analyses concerning modeling uncertainty and error, the Coefficient of Variation for the Root Mean Squared Error (CV-RMSE) and the Normalized Mean Biased Error (NMBE) were used as

indices for the comparison (Kreider and Haberl, 1994). Their definitions are as follows:

$$\text{CV - RMSE} = 100 \times \left[ \sum (y_i - \hat{y}_i)^2 / (n-1) \right]^{1/2} / \bar{y} \quad (4.13)$$

$$\text{NMBE} = \frac{\sum_{i=1}^n (y_i - \hat{y}_i)}{(n-1) \times \bar{y}} \times 100 \quad (4.14)$$

where  $y_i$  is the measured indoor temperature at hour  $i$ ,  $\hat{y}_i$  is the simulated indoor temperature at hour  $i$ ,  $\bar{y}$  is the average indoor temperature from the measurement of  $n$  hours, and  $n$  is the number of hours - 8,760 for a one-year calculation.

#### 4.3.3.1 Combined DOE-2 and CFD Simulations

The flowchart in Figure 4.21 outlines the process through which DOE-2 and HEATX were combined to simulate the indoor air temperatures of the case-study temple for two 24-hour periods. The whole process began with the creation of the uncalibrated input files for both programs from the same building description data, measured data, and weather data. Two important variables were fed back and forth between the two programs during the calibration process. One was the amount of outside air infiltration, which is specified by the term “Air Exchange Rate” in DOE-2 (i.e., AIR-CHANGES/HR keyword), and the other was the interior surface convection coefficient for each surface, assigned to DOE-2 in terms of the “Inside Surface Film Resistance” (i.e., I-F-R keyword).

At first, the initial values of these variables were set based on the ASHRAE recommendations (ASHRAE 1998). By supplying the DOE-2 program with these initial values, the thermal conductivity, the hourly solar gain to the walls and roof, and the hourly surface temperatures could be calculated. These outputs were then used to set the boundary conditions in HEATX. HEATX calculated the velocity and temperatures of the air flowing through all openings, along with an average Nusselt number for each surface. In turns, the air velocity and the Nusselt numbers calculated by HEATX were then used to calculate the airflow rates and the

surface convection coefficients for DOE-2. The calibration loops continued until the indoor temperatures calculated by both programs agreed with the measured data, and the same surface convection coefficients were used in both programs. Using the convergence criteria suggested by Nagroa (1995), the coupled DOE-2/CFD simulation model in this research was declared calibrated when the error between the indoor temperature calculated by DOE-2 and that simulated by HEATX for each hour was within  $\pm 1$  °C ( $\pm 1.8$  °F). Since HEATX can calculate indoor temperatures for a number of locations in the space depending on the number of cells, to compare the HEATX results with those of DOE-2, the temperature of the cell at the center of the room will be used.

#### 4.3.3.2 Calculation of Surface Convective Heat Transfer Coefficients

In DOE-2, the surface convective heat transfer coefficients were specified in terms of the “Inside Film Resistance” at the interior surface of the walls (i.e., I-F-R keyword in the construction command of DOE-2). The convection coefficients of the outside surfaces were calculated by DOE-2 using the wind speed data taken from the Thai weather data. For this research, the convection coefficients at the inside surfaces of the walls, the ceiling, and the floor were calculated based on Incropera and De Witt (1996). Using an assumption of buoyancy-driven, fully developed turbulent flow, the convection coefficients were calculated using the following formula (Incropera and De Witt 1996, p.314):

$$h = \frac{\text{Nu}K}{L} \quad (4.15)$$

Where Nu is the Nusselt number, K is the fluid thermal conductivity, and L is the characteristic length of the surface (i.e., the height of the vertical plane, or the width of the horizontal plane).

For the vertical surfaces, which are the interior sidewalls of the temple, the Nusselt number was calculated using the formula suggested by Churchill and Chu (1975; ref. Incropera and De Witt 1996, p.493):

$$\text{Nu} = \left\{ 0.825 + \frac{0.387\text{Ra}^{1/6}}{\left[ 1 + (0.492/\text{Pr})^{9/16} \right]^{8/27}} \right\}^2 \quad (4.16)$$

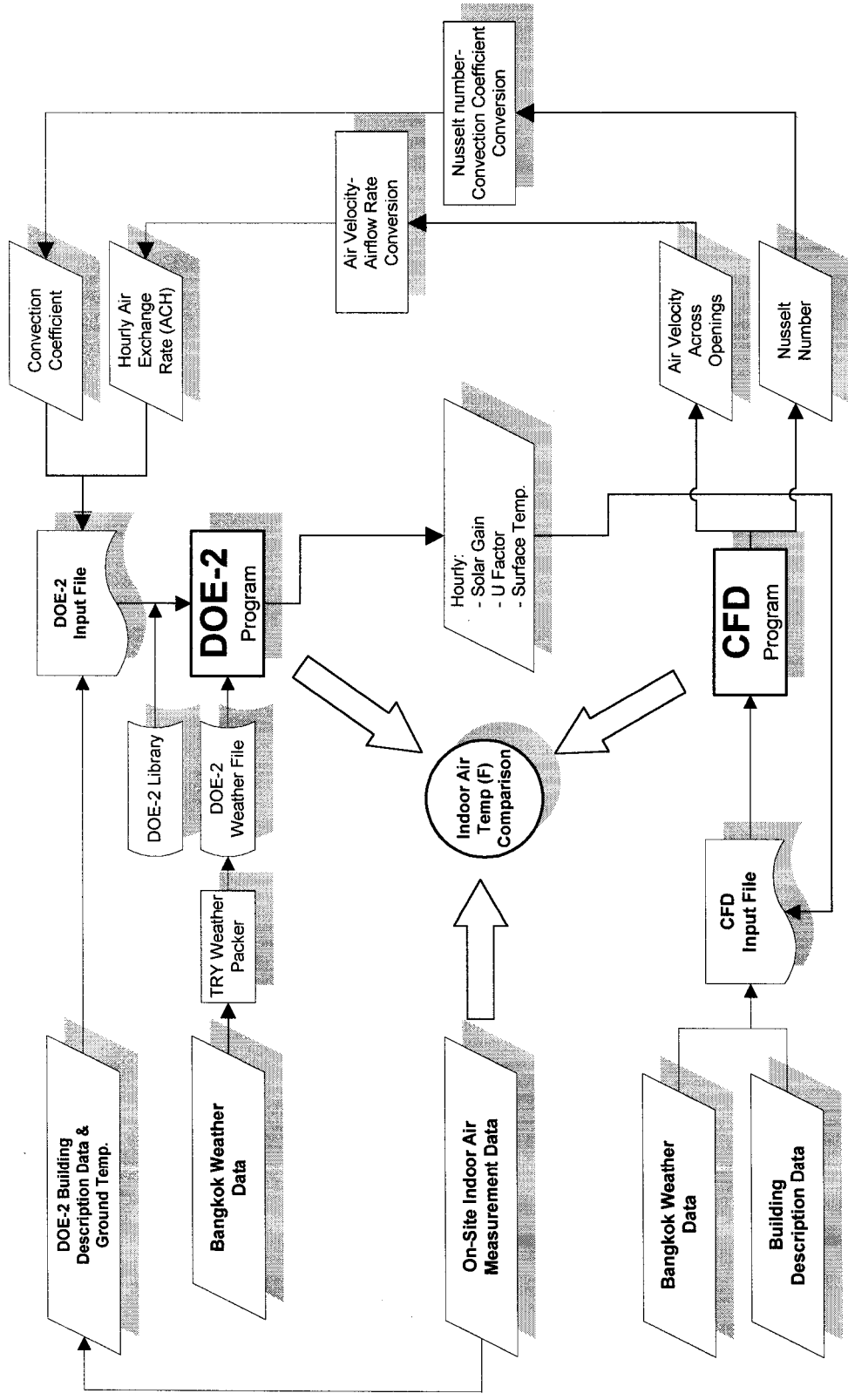


Figure 4.21 Flowchart Diagram Showing the DOE-2/CFD Calibration Process for a 24-Hour Run Period.

For the horizontal surfaces, the floor and the ceiling of the temple, the Nusselt number was calculated using the formula suggested by Lloyd and Moran (1974; ref. Incropera and De Witt 1996, p.498):

$$Nu = 0.27Ra^{1/4} \quad \text{for } 10^5 \leq Ra \leq 10^{10} \quad (4.17)$$

Where Pr is the Prandtl number, which is expressed as the following formula:

$$Pr = \frac{\mu_{\infty} C_p}{K} \quad (4.18)$$

Where  $\mu_{\infty}$  is the dynamic viscosity of the fluid,  $C_p$  is the specific heat of the fluid, and  $K$  is the fluid thermal conductivity.

Ra is the Rayleigh number, which is expressed as the following formula:

$$Ra = \frac{g\beta(T_s - T_{\infty})L^3}{\nu\alpha} \quad (4.19)$$

Where  $g$  is the gravitational force,  $\beta$  is the expansion coefficient,  $T_s$  is the surface temperature,  $T_{\infty}$  is the fluid temperature,  $L$  is the characteristic length,  $\nu$  is the fluid kinematic viscosity, and  $\alpha$  is the fluid thermal diffusivity.

Although the convection coefficients of the outside surfaces were calculated by DOE-2 using the wind speed data taken from the Thai weather data, to use HEATX to calculate the heat transfer through the walls and the roof of the case study temple, these coefficients need to be specified in HEATX. Therefore, the outside surface convection coefficients were calculated using Equation 4.15, however, a different formula was used for calculating the Nusselt number. Using an assumption of fully developed turbulent external flow, the local Nusselt numbers were calculated using the following formula (Incropera and De Witt 1996, p.355):

$$Nu = 0.0296Re^{4/5} Pr^{1/3} \quad \text{for } 0.6 < Pr < 60 \quad (4.20)$$

Where Pr is the Prandtl number, which was calculated using Equation 4.18, Re is the Reynolds number, which is expressed as the following formula (Incropera and De Witt, p.312):

$$\text{Re} = \frac{VL}{\nu} \quad (4.21)$$

Where V is the fluid velocity, L is the characteristic length, and  $\nu$  is the fluid kinematic viscosity.

#### 4.3.3.3 Calculation of the Air Exchange Rates

The DOE-2 program uses the term “Air Exchange Rate” (i.e., AIR-CHANGES/HR code word in the SPACE-CONDITIONS command in DOE-2) to specify the amount of air infiltration in a space. The air exchange rate is a very important variable in thermal calculations of unconditioned buildings, because it specifies the amount of outdoor air to be mixed with the indoor air. If the air exchange rate is too high in a naturally-ventilated building, the indoor temperatures will be maintained close to the outdoor temperatures, thus causing the indoor air to be either warmer or cooler depending on the outside conditions. There are three methods of specifying the air exchange rate (i.e., INF-METHOD code word) in DOE-2: 1) the residential method (i.e., INF-METHOD = RESIDENTIAL), 2) the crack method (i.e., INF-METHOD = CRACK), and 3) the air-change method (i.e., INF-METHOD = AIR-CHANGE). For the residential method, DOE-2 calculates the infiltration heat gain or loss by using the wind speed data taken from the weather tape, along with the outdoor-indoor temperature differentials and user-specified coefficients (i.e., RES-INF-COEF keyword) based on various construction types. For the crack method, DOE-2 calculates the infiltration rate by computing a pressure difference between the inside and outside of a building caused by the stack effect and the wind velocity. For the air-change method, the infiltration rate is directly specified in the DOE-2 input file as the total amount of air infiltration per unit of time. For this research, the air-change method was used because the infiltration rate could be accurately calculated by the CFD program, and then directly specified in the DOE-2 input file. There were two input alternatives used for assigning this variable to DOE-2: 1) the cubic feet of air per minute (i.e., INF-CFM/SQFT keyword), and 2) the air changes per hour (i.e., AIR-CHANGES/HR keyword). Both terms are interrelated in the following expression:

$$\text{ACH} = (\text{CFM} \times 60) / \text{Space Volume in ft}^3 \quad (4.22)$$

The definition of one air change per hour (ACH) is the infiltration rate of the outdoor air where the indoor air is completely replaced within one hour. For the old temple that has a volume of 54,000 ft<sup>3</sup>, one ACH was equal to 900 CFM. This means that 900 ft<sup>3</sup> of the outdoor air was ventilated into the interior space every minute. To calculate the infiltration rate in terms of CFM, the following expression is given:

$$\text{CFM} = V_{\text{win}} \times A_{\text{win}} \quad (4.23)$$

where  $V_{\text{win}}$  is the average air velocity across a window in ft/min.  $A_{\text{win}}$  is the window area in ft<sup>2</sup>. In this research the air velocity across each window is calculated by the CFD program. However, it should be realized that if the codeword INF-METHOD = AIR-CHANGE is used, DOE-2 will perform a wind speed correction each hour to the user-specified air changes per hour. As a result, the actual air exchange rate that DOE-2 uses will vary with the hourly wind speeds taken from the weather data. This benefits this research, however, because a proper wind-adjusted air exchange rate for each hour can be adjusted from a user-specified maximum air change per hour during one-year calculations.

#### 4.3.3.4 Calibrations of the Hourly DOE-2 Simulations for a Whole-Year Period

In an attempt to analyze the overall thermal performance of the case-study temple, the simulated indoor temperature for a one-year period was compared against the average measured temperature of the temple to judge how successful the simulation of this building was. Unfortunately, due to computing hardware limitations, it was impossible for this research to perform the coupled DOE-2/CFD hourly simulations for one full year (i.e., 8,760 hours) with an updated value for the airflow rate and the convection coefficients for each time-step (i.e., every hour changes in wind speed and direction), because the simulation process would have been very complicated and time-consuming. Using a non-networked Pentium III 500 MHz PC computer dedicated solely to this task, a typical steady-state computation took 1 day of CPU time, a 24-hour transient calculation took 2 days. A 8,760-hour transient calculation is estimated to take 730



days approximately, which is an unreasonable amount of time. Therefore, this research adopted the method where average values of the air exchange rates and the corresponding convection coefficients were obtained from the coupled DOE-2/CFD simulations of two selected days. These average values were then used by DOE-2 to perform the annual hourly calculations. Figure 4.22 demonstrates the process by which the combined DOE-2/CFD simulations were performed for the average summer and winter days. Then the average maximum air exchange rate was supplied to DOE-2 for one-year calculations.

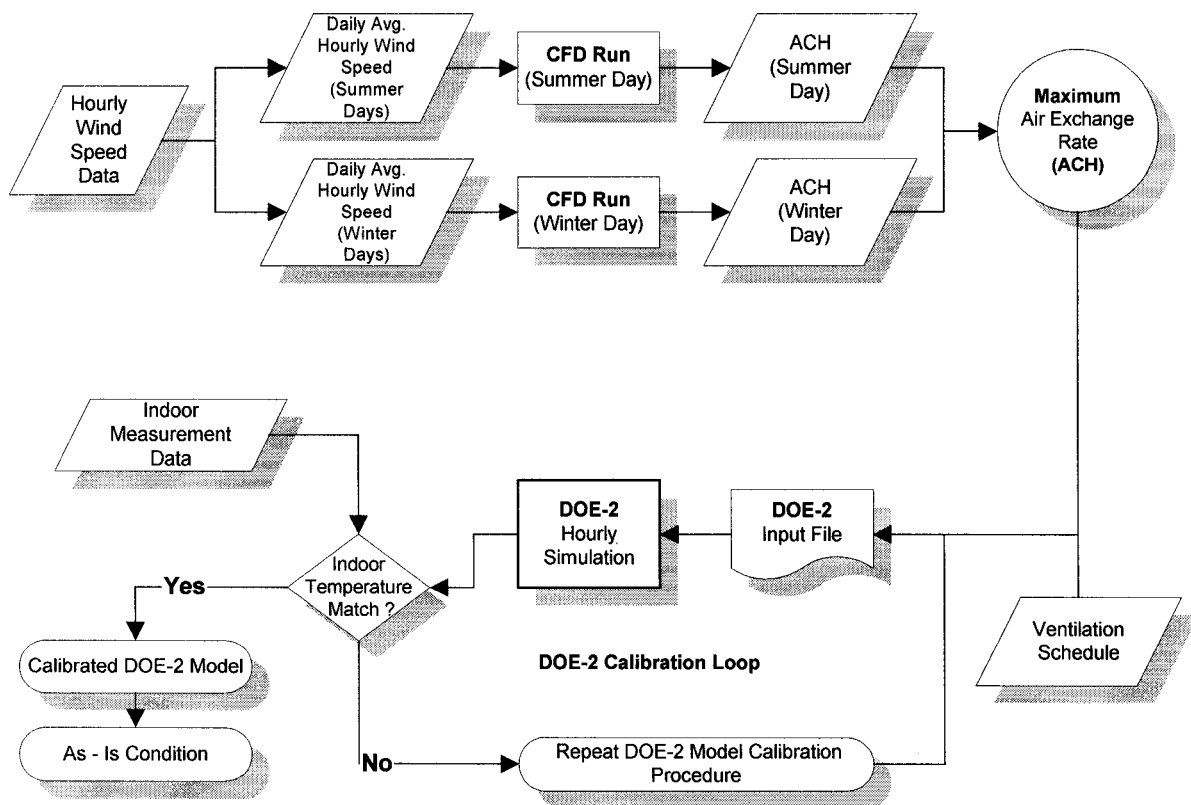


**Figure 4.22** Flowchart Diagram Showing the Calibration Process of the Hourly DOE-2/CFD Simulations for a One-Year Period.

Initially, the process began with the selection of two design days that represented average summer and winter days. The objective was to obtain one value for the hourly air

exchange rate that could be fed in to DOE-2. Because the hourly ventilation schedules are known, good estimates of the hourly airflow rates for DOE-2 could be obtained by combining the hourly schedule with the average maximum air exchange rate obtained from DOE-2/CFD simulations. The average maximum air exchange rate was then used throughout the calibration process for a whole-year period.

Once an estimation of the average airflow rate and convection coefficient was successfully performed, the next process used this value for the annual DOE-2 calibration. The measured average hourly indoor temperatures (i.e., the average of the measured indoor air temperatures at the floor and the ceiling levels) were used as an indicator of how well the simulation model represented the real building. With the DOE-2 capability of generating the hourly output reports for one year, the simulated indoor temperatures were then compared to the measured indoor temperatures, hour by hour. Once the simulated values matched with the measured data, the simulation model was then declared calibrated and used for further analyses.

#### **4.4 Summary of Methodology**

This chapter describes the overall process developed to create a simulation model of a Thai Buddhist temple that is well calibrated to the measurement data. The purpose was to obtain a simulation model that correctly represents the real building for its use as a base-case in the parametric analysis. To accomplish this, survey, measurement and data collection procedures were carefully designed and performed, along with an in-depth thermal and CFD analysis.

A survey of Thai Buddhist temples in Bangkok was performed in order to select two case-study buildings that represent the typical Thai Buddhist temples in terms of architectural style, building design and construction, materials, age, and building use profiles. Among the several temples that were visited, two temples were found suitable for further investigation. The first is a new temple constructed in 1995. The second is an old temple constructed during the early 1900's. Both temples are located in the urban area of Bangkok.

The indoor air temperature, relative humidity, and floor surface temperature of each case study temple were measured using micro data-loggers. Six data-loggers were used to

measure room and floor temperatures using surface-mounted external sensors. The wall surface temperatures were measured using a handheld infrared thermometer. The outdoor weather data collected from Bangkok during 1999 were obtained from two sources: 1) on-site measurements, and 2) a weather tape from the Thai government, which was used to create a DOE-2 weather file.

To perform this study, the DOE-2.1e building simulation program and a 3-D Computational Fluid Dynamic (CFD) program were used. The two simulation tools were coupled together because DOE-2 needs the air infiltration rates calculated by CFD in order to provide accurate thermal simulations of the naturally-ventilated temple, and CFD needs the information regarding the building envelop (such as the solar heat gain and the surface temperatures) from DOE-2 to establish the boundary conditions. The calibration process began by first combining the two programs to simulate the indoor air temperatures of the case-study temple for 24-hour periods on summer and winter days.

In an attempt to analyze the overall thermal performance of the case-study temple, the simulated indoor temperature for a one-year period was then compared against the average measured temperature of the temple to judge how successful the simulation of this building was. This research adopted the method where average values of the air exchange rates and the corresponding convection coefficients were obtained from the coupled DOE-2/CFD simulations of two selected days, and were used by DOE-2 only for one-year of hourly calculations. Because the hourly ventilation schedules are known, good estimates of the hourly airflow rates for DOE-2 could be obtained by combining the hourly schedule with the average maximum air exchange rate obtained from DOE-2/CFD simulations. The average maximum air exchange rate was then used throughout the calibration process for a whole-year period.

The measured hourly indoor temperatures were used as an indicator of how well the simulation model represented the real building. Finally, once the simulated temperatures matched the measured data in a satisfactory way, the simulation model was then declared calibrated.

## CHAPTER V

### RESULTS

This chapter discusses the results of the investigation, which include the data collection and measurement results of the case-study temples, and the coupled DOE-2/CFD calibrated simulation results. The data collection and measurements were performed on both temples. However, only the old temple was selected for the detailed thermal and airflow analysis using the coupled DOE-2/CFD simulations. Analysis of the results in terms of the thermal and airflow performances of the old case-study temple is also included in this chapter.

#### 5.1 Data Collection and Measurements of the Case-Study Buildings

##### 5.1.1 Bangkok Weather Data

The outdoor weather data of Bangkok during 1999 were obtained from two sources: 1) on-site measurements, and 2) a weather file from the Thai government (RTMD 2000). Figures 5.1a and 5.1b presents a statistical summary of the outdoor dry-bulb temperatures and relative humidity that were measured at the site using the micro data-loggers from February to December of 1999. Appendix B shows the outdoor weather data obtained from the Department of Meteorology in Thailand. The government weather file contained the hourly data of dry-bulb temperature, relative humidity, global horizontal solar radiation, wind speed, and wind direction. It was used to create the DOE-2 weather file using the LS2TRY program (Bronson 1992) mentioned in the previous chapter.

Figures 5.1a and 5.1b show that the outdoor temperatures were above the comfort zones recommended by ASHRAE (2001) throughout the year, except during a few short periods in December. The monthly average outdoor temperatures were between 72 and 88 °F. March through June were the summer months and included periods of high humidity. The hottest period occurring from late March through late April. September through November were warm, averaging 80 to 85 °F, but became more humid because of rainfall. January (not shown) and December were cool and dry.

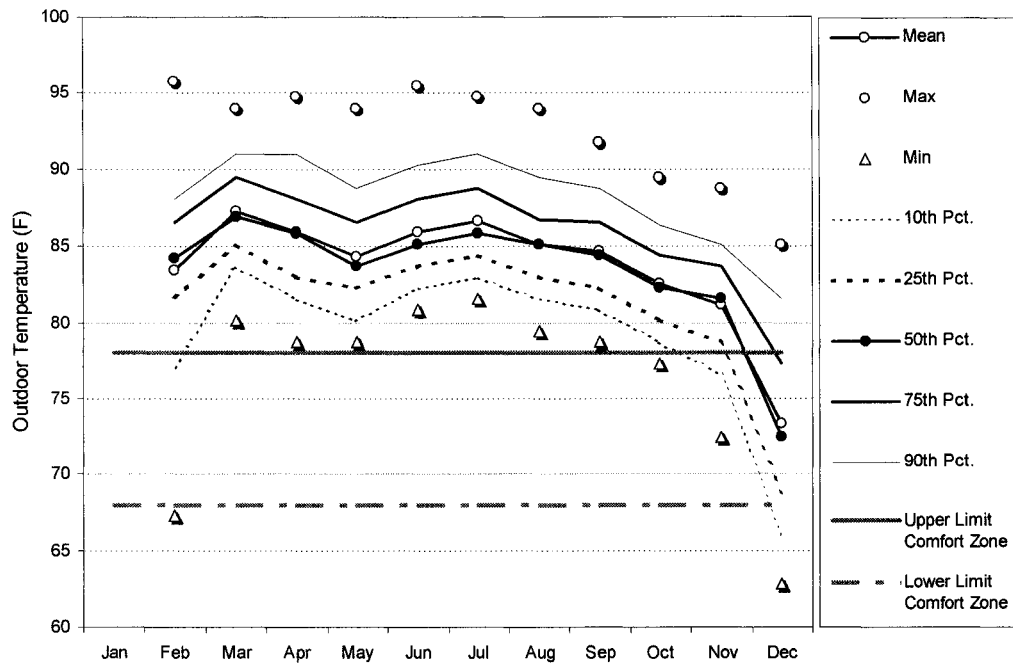


Figure 5.1a Outdoor Temperatures for Bangkok, Thailand During 1999.

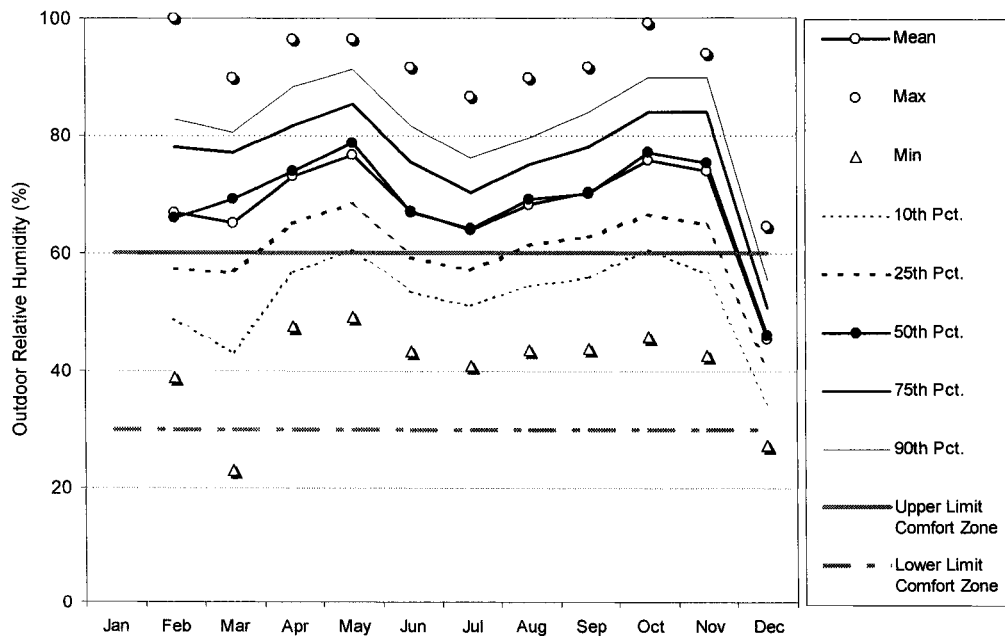


Figure 5.1b Outdoor Relative Humidity for Bangkok, Thailand During 1999.

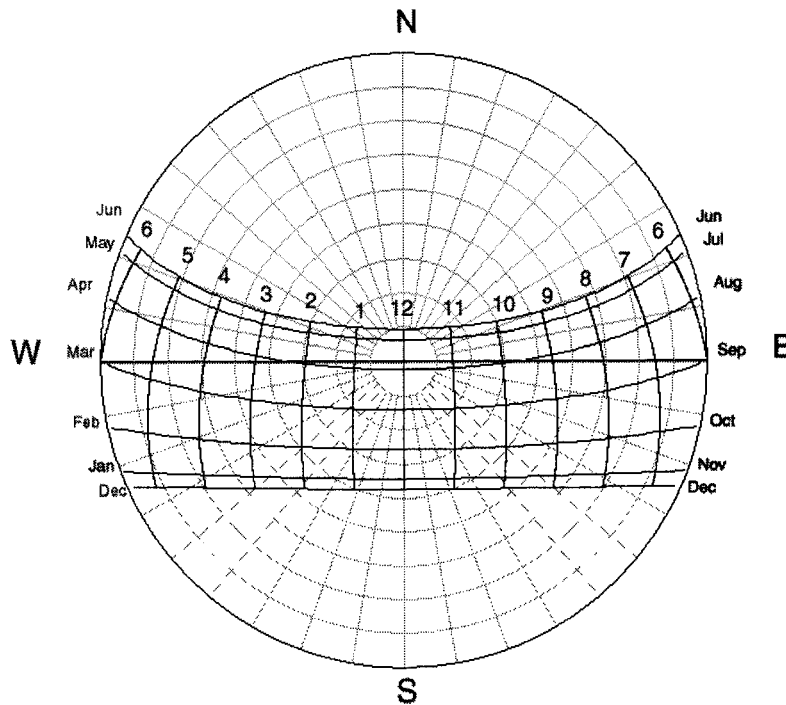
Throughout the year, the outdoor relative humidity was above 50 % with the means ranging from 50 % to 80 %. January and December were dryer, with an average relative humidity of 45 %. September through November represent Thailand's rainy season, where the relative humidity was between 70 % and 78 %. May was also humid, because of late afternoon thunderstorms. It was found that extreme hot-humid summer conditions usually occurred from March through May. The most comfortable periods were in December, when the outdoor conditions were cool and dry.

Figure B.2.3 shows the hourly global horizontal solar radiation data obtained from the Thai weather file. By using the SOLRPATH program developed by Oh (2000) to generate the Sun Path diagram for Bangkok's location (i.e., 14° north latitude), Figure 5.1c shows that the noon sun is perpendicular to the ground during April, thus resulting in the largest amount of solar radiation received on the building's horizontal surfaces during the early summer months. Therefore, a combination of high temperatures, high humidity, and solar radiation causes the summer conditions to be extreme. However, from May to October, the weather is cooler but more humid because of cloudy skies and rainfall.

Figures B.2.6a and B.2.6b show the hourly average wind speeds for the summer and winter days, respectively. It was found that the wind was usually calm at night, with an average speed of about 1-2 mph (0.45–0.89 m/s). The wind speed increased during the day to about 4-5 mph (1.8–2.2 m/s), and was stronger during the summer months. In terms of wind direction, Figures B.2.7 a, B.2.7b, B.2.8a, and B.2.8b show that there are usually two distinct wind directions for summer and winter. The summer wind usually came from the South and Southwest, while in the winter; the wind came from the North and Northeast.

From all the data collected and measured, it can be concluded that the Bangkok's climate in 1999 was generally hot and humid with a significant amount of solar radiation. Extremely hot-humid summer conditions occurred from March to May, warm-humid climates occurred from June to August, a wet climate occurred from September to November, and a cool and dry climate occurred in short periods during December and January. Wind came from the North to Northeast during the winter, and from the South to Southwest during the summer. Daytime wind speeds were higher than in the evening. The 1999 measured weather was similar

to the 10-year typical climate characteristics reported by the Department of Meteorology in Thailand (RTMD 1995). Therefore, the weather data of 1999 can be used to appropriately represent Bangkok's typical climate.



*Figure 5.1c Sun Path Diagram of Bangkok Created by SOLRPATH (Oh 2000).*

### 5.1.2 Measurement Results of the Case-Study Buildings

Figures 5.2a and 5.2b present the indoor measurement results of the newer case-study temple from February to December of 1999. It was found that throughout the year, the indoor temperatures were also above the comfort zone recommended by ASHRAE (2001). The monthly average indoor temperatures were between 82 and 88 °F, which were higher than those of the outdoors. The monthly average maximum indoor temperatures were primarily above 90 °F, with the hottest period recorded in April. The maximum indoor temperatures were high, which indicates higher daytime temperatures most likely from a lack of shading and ceiling insulation. The indoor relative humidity was normally above 50 % with the means ranging from 50 % to 80 % all year round. The indoor relative humidity followed the outdoor pattern shown in Figure

5.1b, but with smaller fluctuations. The maximum indoor relative humidity was lower than the outdoors, which correspond to higher indoor temperatures at night. The minimum indoor relative humidity was slightly higher than the outdoors, which correspond to slightly lower maximum indoor temperature. In terms of the building surface temperatures, Figure C.2.3 shows that the floor surface temperature of the newer temple fluctuated around an average of 85 °F. Regarding the inside surface temperatures of the exterior walls, Figure C.2.4 indicates that the wall surface temperature of the new temple on each side was different depending on the time of day. The south wall was the hottest at noon. The west wall was the hottest in the afternoon, and the east wall was hottest in the morning. These measurements emphasize the need to reduce the heat gain through exterior walls.

For the old temple, Figures 5.3a and 5.3b show that throughout the year, the indoor temperatures were also regularly above the comfort zone recommended by ASHRAE (2001). The average indoor temperatures were between 78 and 87 °F, year round. The monthly average maximum indoor temperatures were primarily above 87 °F, with the hottest period recorded in March. The indoor temperatures followed the outdoor pattern, but with smaller fluctuations. This indicates the increased thermal mass effect in the old temple. For the relative humidity plot in Figure 5.3b, the indoor relative humidity was normally above 50% with the mean ranging from 50 % to 80 %, year round. The indoor relative humidity followed the outdoor pattern shown, but with smaller fluctuations. The maximum indoor relative humidity was lower than the outdoors, which corresponds to higher indoor temperatures at night. The minimum indoor relative humidity was higher than the outdoors, which indicates lower indoor temperatures during the day. In terms of the building surface temperatures, Figure C.1.3 shows that the floor surface temperature of the older temple was more constant than that which was measured inside the newer temple. The average was 83 °F. Regarding the inside surface temperatures of the walls, Figure C.1.4 indicates that the wall surface temperature of the older temple at each side was relatively constant regardless of the time of day. These measurements indicated the effects of thermal inertia due to the mass of the exterior walls.



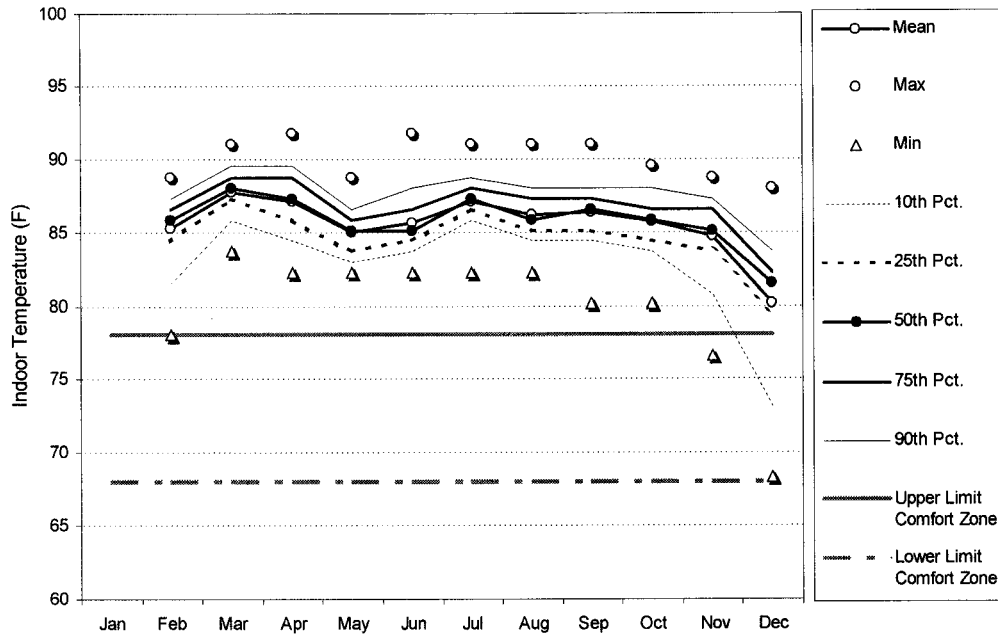


**Figure 5.2a** Indoor Temperature of the New Temple During 1999.

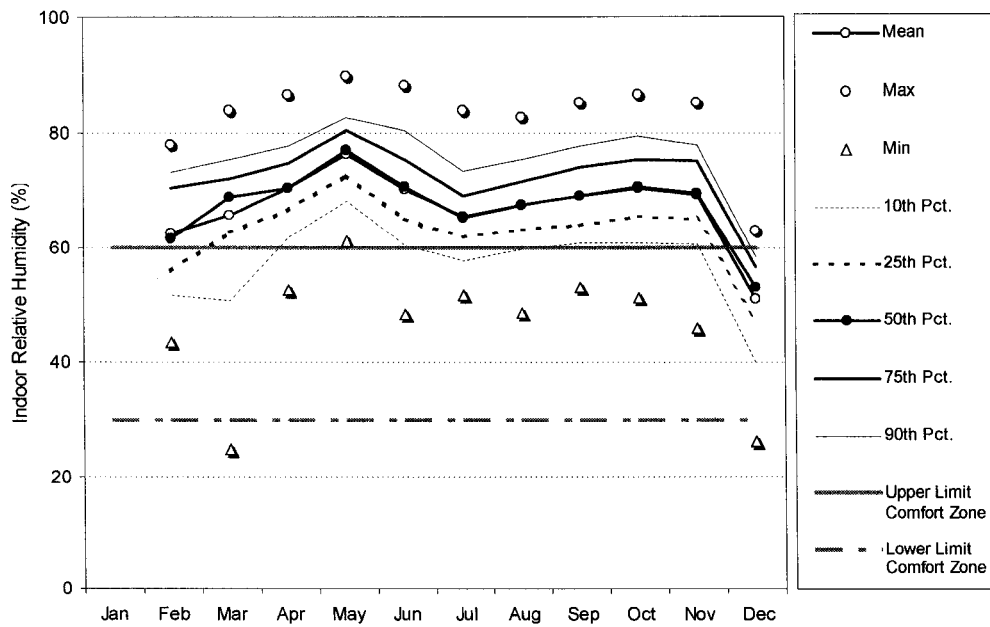


**Figure 5.2b** Indoor Relative Humidity of the New Temple During 1999.

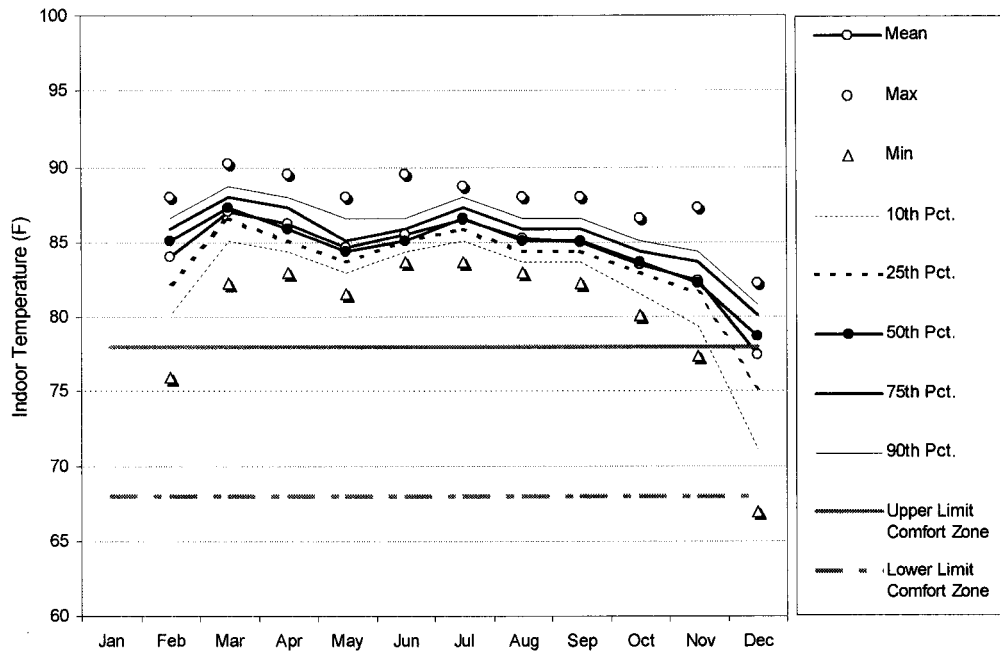


Figure 5.3a Indoor Temperature of the Old Temple During 1999.

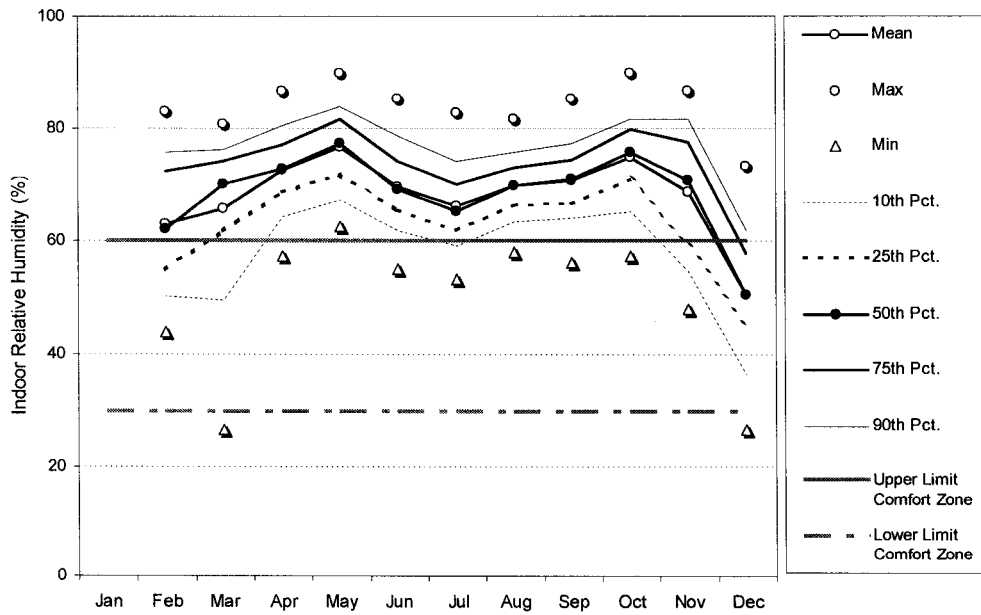


Figure 5.3b Indoor Relative Humidity of the Old Temple During 1999.

On the annual average, it was found that both temples were warmer than the outdoors, and the new temple was warmer than the old temple. Conversely, the relative humidity measurements showed that the old temple was more humid than the new temple.

To study the seasonal thermal comfort conditions, the indoor measurement results of both temples were plotted on psychrometric charts. Figures 5.4a and 5.4b indicate that during the summer, the conditions inside the newer temple were very hot and humid. The indoor temperatures ranged from 83 to 92 °F, and the relative humidity was between 50 % and 90 %. This condition exceeds the upper limit of both the ASHRAE comfort zone (ASHRAE 2001) and the comfort zone proposed by Givoni (1998). In the winter, the inside of the new temple was considered too warm by ASHRAE, but acceptable by Givoni. The indoor temperatures ranged from 72° to 89 °F, and the relative humidity was between 30 % and 85 %. There were periods in December when the indoor conditions were considered comfortable by both standards.

Figures 5.5a and 5.5b demonstrate that during the summer, the conditions inside the older temple were hot and humid. Indoor temperatures ranged from 82 to 90 °F, and the relative humidity was between 30 % and 85 %. This condition exceeds the upper limit of both the ASHRAE and Givoni comfort zones. In the winter, the inside of the older temple was considered too warm by ASHRAE, but acceptable by Givoni. The indoor temperatures ranged from 67° to 87 °F, and the relative humidity was between 30 % and 90 %. There were periods in December when the indoor conditions were considered comfortable by both standards.

When comparing the psychrometric plots of both temples for the same periods, it can be seen that the older temple is generally more comfortable than the newer temple. There are longer periods of time when the conditions inside the newer temple are out of the comfort zone, while the older temple can still be considered comfortable. Unfortunately, although the older temple is cooler, it tends to be more humid than the new temple. The evidence for this is the mold and mildew problem found inside the old temple as presented in Figure A.4.

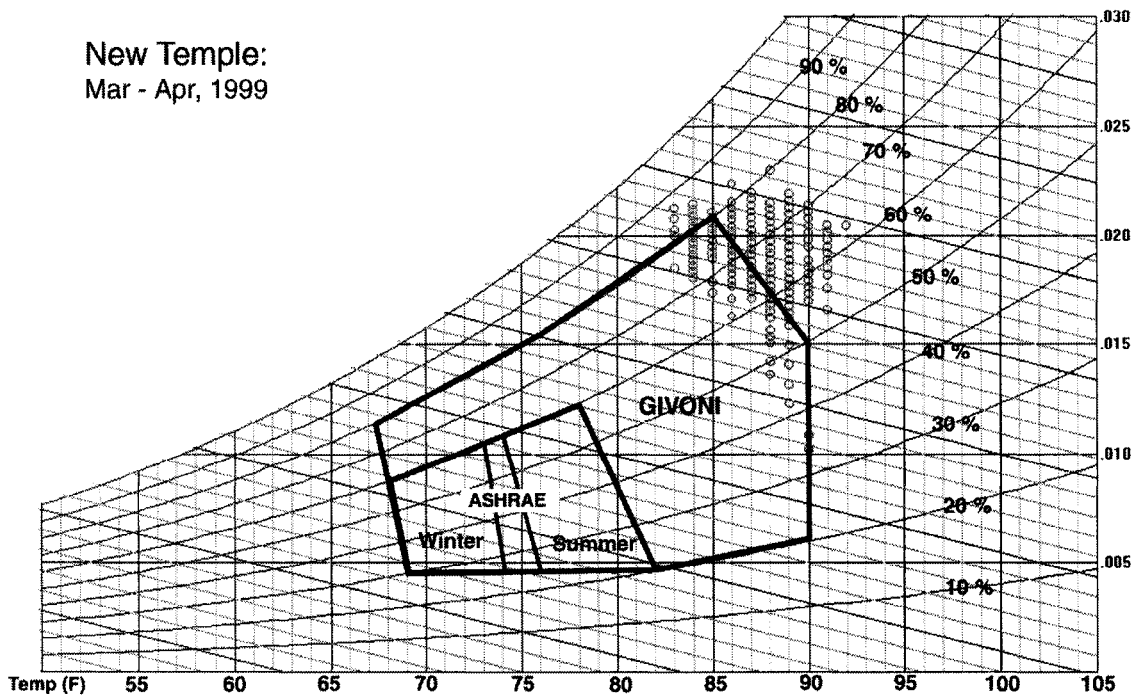


Figure 5.4a Psychrometric Plot of the Indoor Conditions in the New Temple in the Summer.

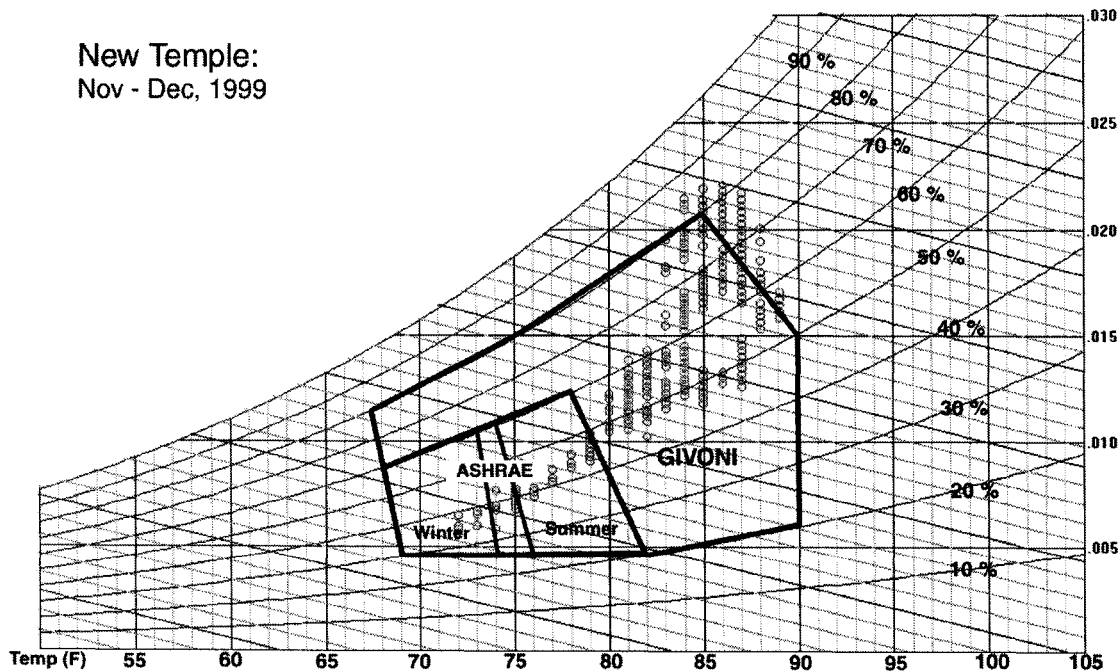


Figure 5.4b Psychrometric Plot of the Indoor Conditions in the New Temple in the Winter.

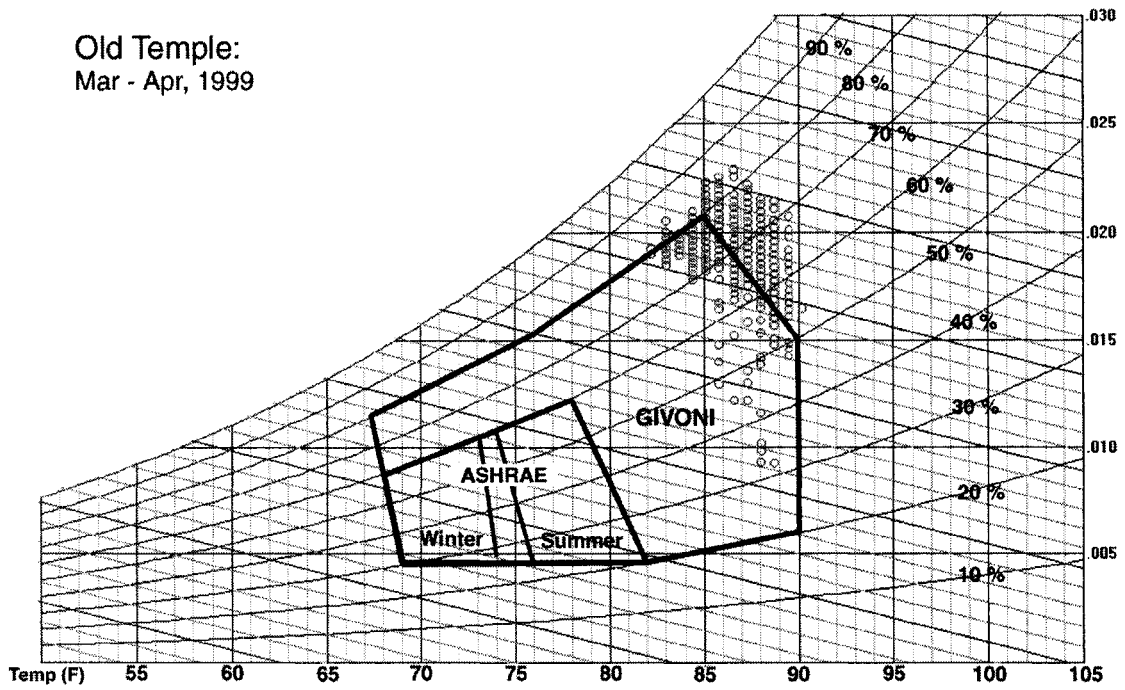


Figure 5.5a Psychrometric Plot of the Indoor Conditions in the Old Temple in the Summer.

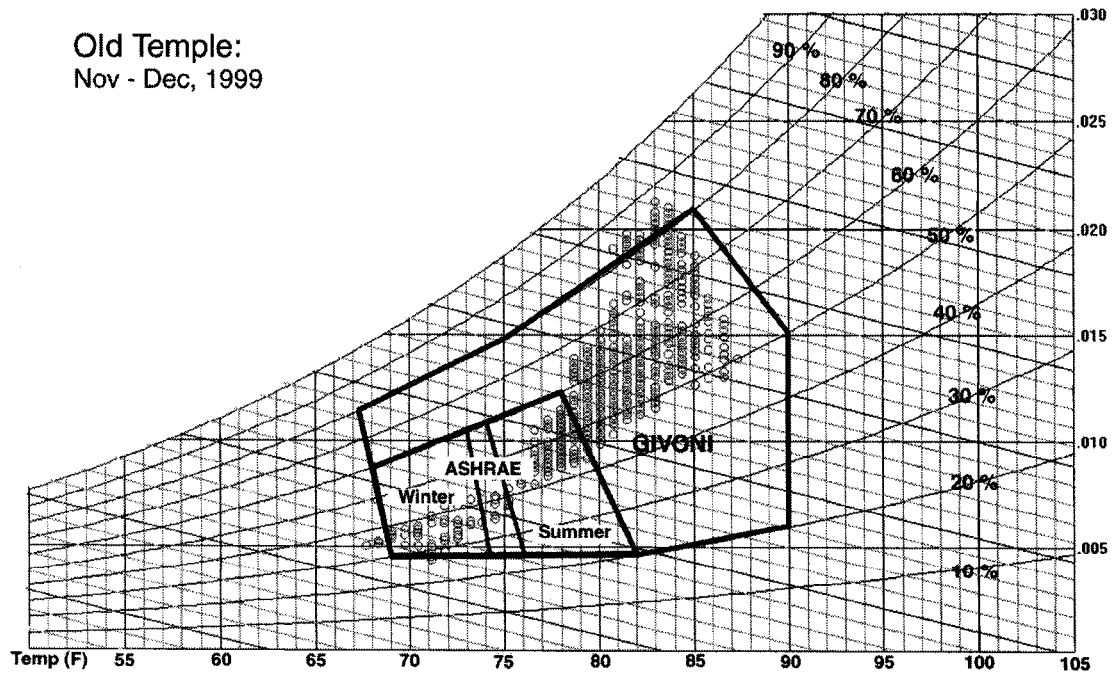


Figure 5.5b Psychrometric Plot of the Indoor Conditions in the Old Temple in the Winter.

## 5.2 Calibrated DOE-2/CFD Simulation Results

In order to develop a calibrated DOE-2/CFD simulation of the case study temple, a series of simulations were used to assess the improved accuracy. The first simulation was performed without input from the CFD calculations of the air exchange rates and the surface convection coefficients. The first DOE-2 calculation was performed using the air exchange rate of 100 ACH, and the ASHRAE-recommended indoor surface resistances of 0.68 hr-ft<sup>2</sup>-°F/Btu for the vertical walls, 0.62 hr-ft<sup>2</sup>-°F/Btu for the roof, 0.92 hr-ft<sup>2</sup>-°F/Btu for the floor, and 0.61 hr-ft<sup>2</sup>-°F/Btu for the ceiling (ASHRAE 1998; Table 4.2). Unfortunately, it should be noted that ASHRAE's surface resistances combine convection and radiation resistances, normally called "film resistances." Niles (1988; ref. Balcomb 1988, p.140), derived convection-only film resistances, and suggested 0.54 Btu/hr-ft<sup>2</sup>-°F for the vertical walls, 0.71 Btu/hr-ft<sup>2</sup>-°F for the lower surface of the ceiling, 0.68 Btu/hr-ft<sup>2</sup>-°F for the inside roof surfaces, and 0.17 Btu/hr-ft<sup>2</sup>-°F for the upper surface of the floor. Niles calculated the radiation portion of ASHRAE's combined film resistances to be 0.93 Btu/hr-ft<sup>2</sup>-°F equally, for all surfaces. It was found that Niles's radiation-only coefficient was about 64 % of the total combined coefficients for the vertical walls, 54 % for the lower surface of horizontal plane, and 85 % for the upper surface of horizontal plane. Table 5.1 presents the comparisons between the combined coefficients and the convection-only coefficients.

**TABLE 5.1**  
**The ASHRAE Combined Inside Surface Resistances**

	ASHRAE Combined Convection/Radiation Coefficients (Btu/hr-ft <sup>2</sup> -°F)	ASHRAE Combined Convection/Radiation Film Resistances (hr-ft <sup>2</sup> -°F/Btu)	Niles's Convection- only Coefficients (Btu/hr-ft <sup>2</sup> -°F)
Vertical walls	1.47	0.68	0.54
Lower surfaces of ceiling	1.64	0.61	0.71
Inside surface Roof (45°-slope)	1.61	0.62	0.68
Upper surface of floor/ceiling	1.09	0.92	0.17

In this simulation, the temple was divided into two adjacent zones, a temple space and an attic space. For DOE-2 to perform the calculations there must be at least one conditioned zone. Therefore, the temple space is set as a conditioned zone with a residential-type HVAC system (i.e., RESYS in DOE-2) assigned in DOE-2. The thermostat of this zone was set as high as 110 °F (43 °C), so that the cooling system would never turn on and the indoor temperatures would float freely. Since there is no HVAC system for the attic space, this zone was modeled as an adjacent unconditioned space. The hourly indoor temperatures were calculated and reported by using the DOE-2 hourly report capability.

The hourly indoor temperature comparison shown in Figure 5.6 demonstrates that there were vast differences between the uncalibrated simulated and the measured indoor temperatures in terms of the magnitude. The uncalibrated, simulated temperatures have more fluctuations than do the measured temperatures. A statistical analysis of error was used in this comparison. For this first simulation the Coefficient of Variation for the Root Mean Squared Error (CV-RMSE) was 6 %, and the Normalized Mean Biased Error (NMBE) was 1.02 %. This simulated temperature swing seemed to follow the outdoor pattern, which indicated too much outdoor airflow (i.e., 100 ACH) was specified for DOE-2. In addition, there were periods of time when the indoor temperatures dropped below the outdoor temperature for no apparent reason. To find the source of the problem, the DOE-2 “SYSTEM” hourly report was generated in order to check for errors. From an hourly report of the SYSTEM heat attraction rates, it was found that DOE-2 switched on the HVAC system even when indoor temperatures are below the 110 °F set point. This resulted from an error in the DOE-2 SYSTEM calculation because an unreasonable cooling set point is specified.

The first DOE-2 run indicated that the method of specifying unreasonably high cooling thermostat set points for unconditioned spaces caused an unacceptable error. This knowledge was useful for the subsequent DOE-2 calibrations. In the subsequent simulations, a fictitious, highly-insulated “small box” was created as the only conditioned zone, which was set next to the unconditioned temple space. This eliminated the unreasonably low zone temperatures. In all subsequent simulations this fictitious zone was used to trick DOE-2 into simulating a very small cooling load. Zone temperatures for only the unconditioned zones were then used.

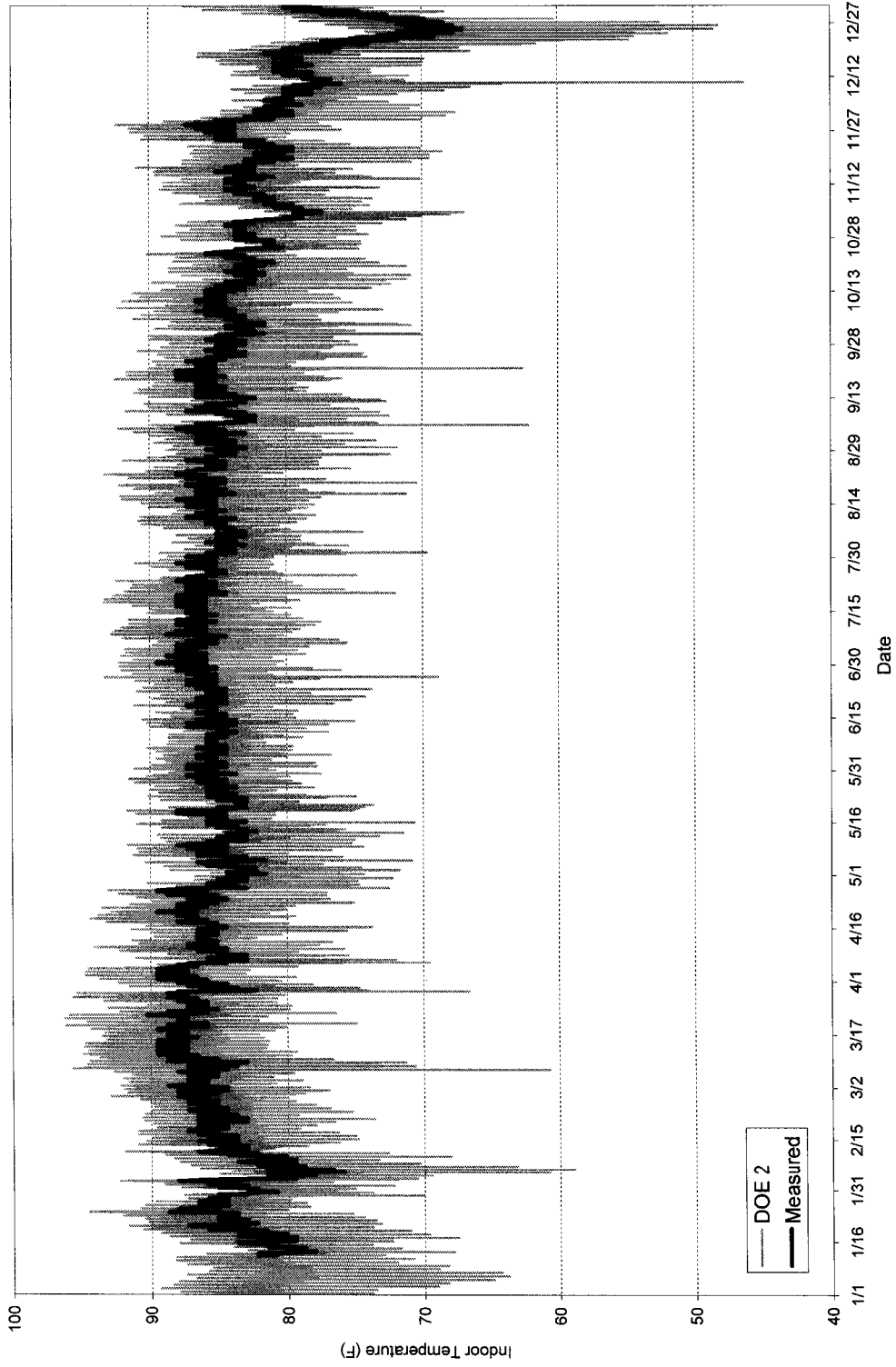


**Figure 5.6** Comparison of the DOE-2 Simulated and Measured Indoor Temperatures: Uncalibrated Simulation.



### 5.2.1 First Calibration

As mentioned earlier, the DOE-2 simulation program needs at least one conditioned zone in order to perform an accurate calculation of the unconditioned zones. Therefore, a small, well-insulated conditioned zone with a volume of one cubic foot was added to the building so that DOE-2 could perform its calculations. This small conditioned box was attached to the temple space; however, there was no heat transfer between these two zones because all of the interior walls of this box, including the ceiling, were set as adiabatic walls. Using this method, the HVAC system of the box was specified using the DOE-2 residential system (i.e., the RESYS system) with a normal cooling thermostat set point of 76 °F. Both the temple space and the attic space were simulated as unconditioned zones so that the indoor temperatures could float freely and be reported by the DOE-2's hourly report command. Only the results from unconditioned zones were used in the calibrated simulations.

For the first calibration, a starting air exchange rate of 100 ACH was used, along with the ASHRAE-recommended surface heat transfer coefficients of 0.54 Btu/hr-ft<sup>2</sup>-°F for the walls, 0.71 Btu/hr-ft<sup>2</sup>-°F for the ceiling, 0.68 Btu/hr-ft<sup>2</sup>-°F for the inside roof surfaces, and 0.17 Btu/hr-ft<sup>2</sup>-°F for the floor. The results, as shown in Figure 5.7, demonstrate that there were significant improvements between the simulated and measured indoor temperatures in terms of both magnitude and direction. However, significant differences still remained. The simulated temperatures not only had large fluctuations, but also floated about 10 °F higher than the measured temperatures. The Coefficient of Variation for the Root Mean Squared Error (CV-RMSE) was 5.53 %, and the Normalized Mean Biased Error (NMBE) was 4.56 %. It was also found that the temperature swings of this first calibration seemed to follow the outdoor pattern, which indicates that too much outdoor airflow rate (i.e., 100 ACH) was specified for DOE-2. In addition, the effects of thermal mass seemed to be insignificant as the temperature swings were too high. For the next calibration, a more accurate airflow rate using the CFD results was estimated and assigned to the DOE-2 program input. The method of using CFD in determining an appropriate DOE-2 air exchange rate was explained in Chapter 4.

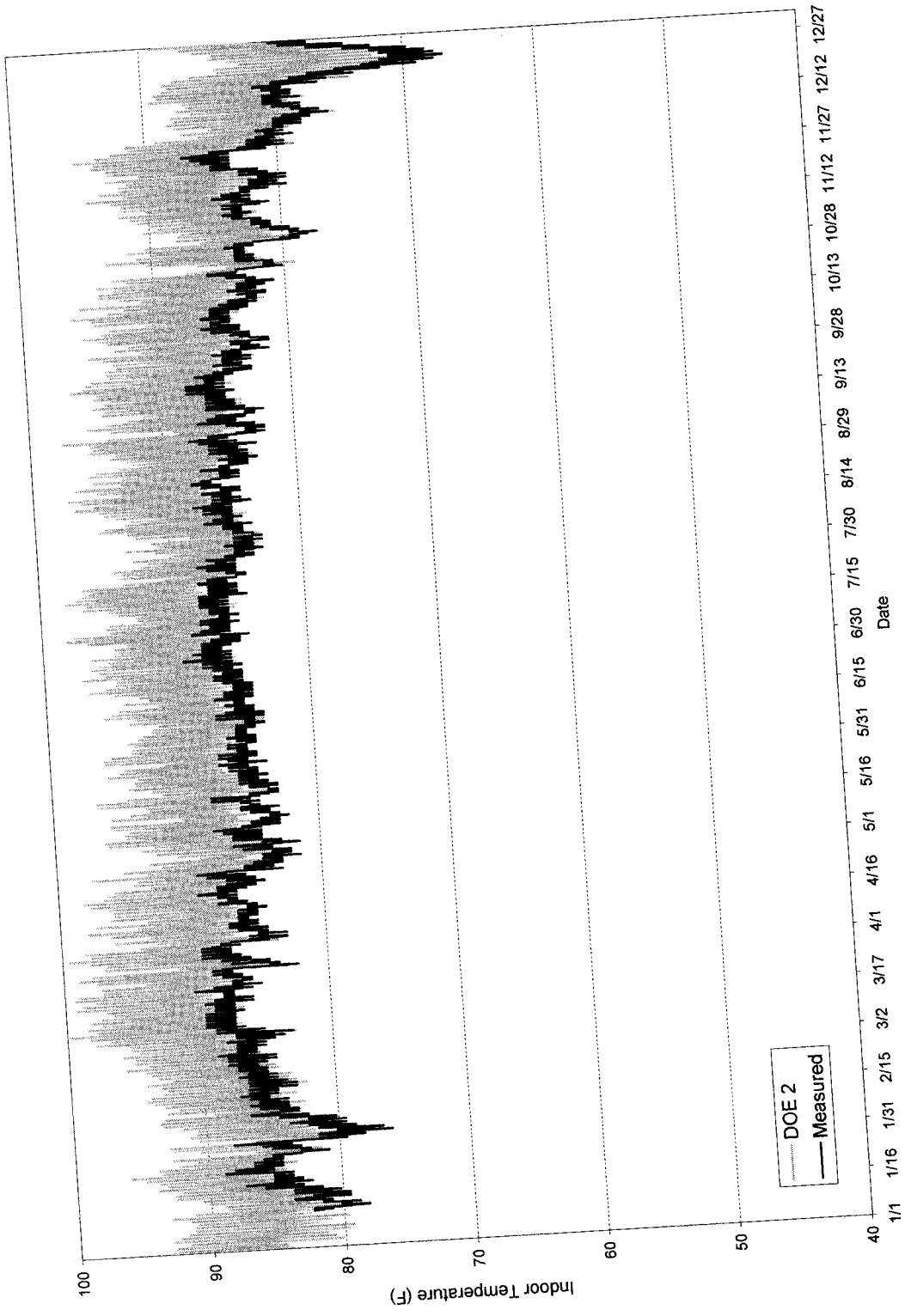


**Figure 5.7** Comparison of the DOE-2 - Simulated and Measured Indoor Temperatures: 1<sup>st</sup> Calibration.

### 5.2.2 Second Calibration

Prior to using the CFD simulations to calculate the ventilation rate and the surface convection coefficients, the starting air exchange rate of 100 ACH was used along with the ASHRAE-recommended surface heat transfer coefficients of 0.54 Btu/hr-ft<sup>2</sup>-°F for the walls, 0.71 Btu/hr-ft<sup>2</sup>-°F for the ceiling, 0.68 Btu/hr-ft<sup>2</sup>-°F for the inside roof surfaces, and 0.17 Btu/hr-ft<sup>2</sup>-°F for the floor. These variables were initially assigned to the DOE-2 program so that the program could run and the three hourly variables: 1) the hourly envelope solar heat gain, 2) the envelope thermal resistance, and 3) the surface temperatures could be reported and assigned as the boundary conditions for the CFD calculation. As demonstrated in Chapter 4, the coupled DOE-2/CFD simulation loop began at this point, where the updated airflow rate and convection coefficients calculated by CFD were then fed back into the DOE-2 program as inputs. The DOE-2/CFD calibration loops were then performed successfully, and the outputs are presented in Figures 5.8 through 5.12.

Figure 5.8 shows the CFD - simulated airflow across the building. These simulated air flows were confirmed with site observations and the Bangkok weather data revealed that the outdoor air moved across the temple at a 45° angle to the front entrance, passing through the front exterior colonnades, through the interior space, and exiting in the rear of the temple. It was found from the CFD velocity plot that the airspeeds increased significantly on the outside corners and at the side openings. This agrees with the observations recorded at the site, where increasing airspeeds at the windows were noticeable, thus producing a slightly more comfortable condition. However, inside the temple space where the major indoor religious activities take place, the CFD simulation showed the air velocities decrease greatly. Air stagnation in the interior space caused the indoor conditions to be stuffy and less comfortable. This agrees with the site observations, where it was also observed that smoke produced by candles and incense was trapped inside the space, which further deteriorated the indoor air quality. The results obtained from the CFD simulation showed that there is a need to redesign the proper sizes and locations of vents that would produce more airflow across the building in the evening.

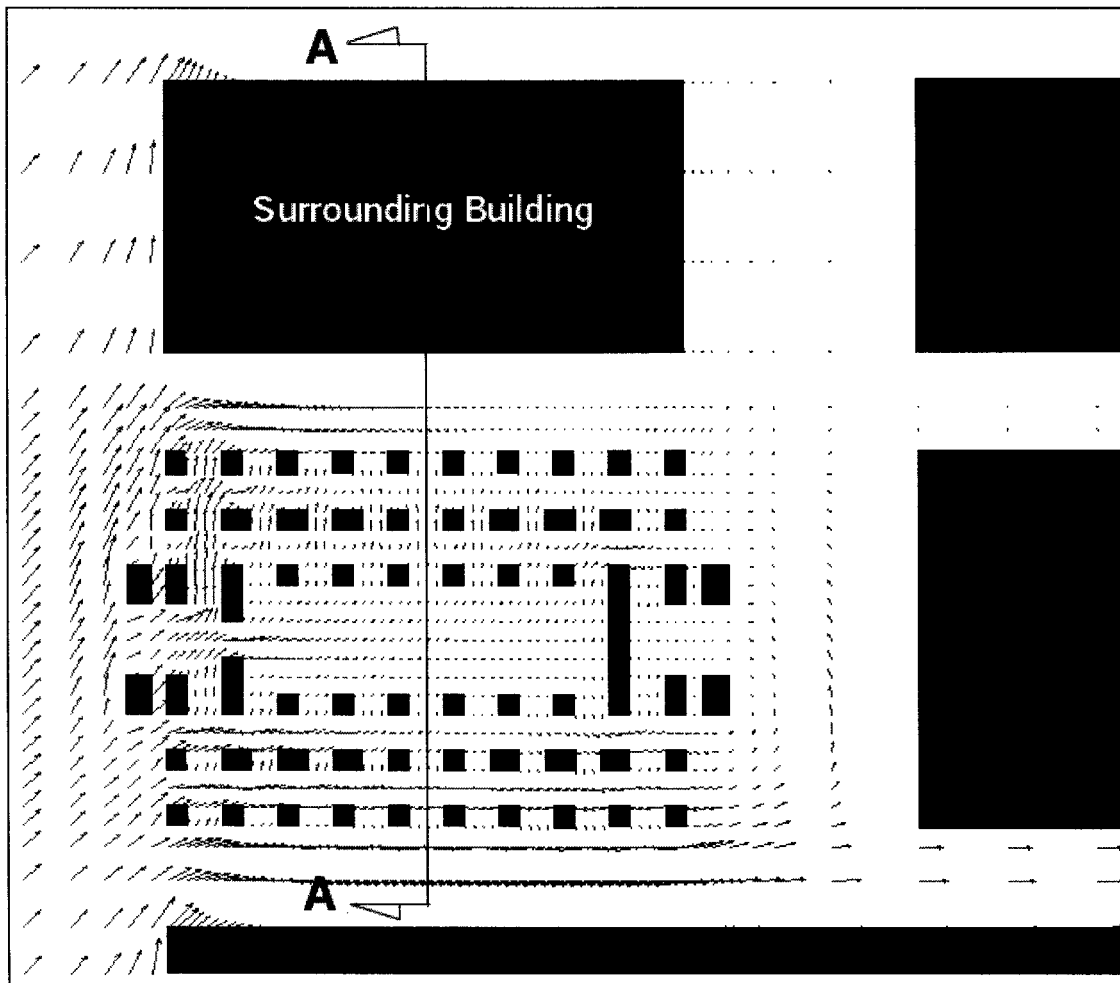
Figure 5.9 shows a cross section of incoming air flowing through the building. In this simulated velocity plot, the airspeeds increase significantly across the openings with vortices

occurring right above and below the window levels, although the total airflow through the building remains small. Close examination of the plots reveals significant stagnation just below the ceiling. Based on the observations made at the site, this condition leads to two undesirable outcomes in the case-study building. First, smoke produced by incenses rises, and it is trapped at the ceiling level. This caused the ceiling and interior decorations (e.g. wall paintings, chandeliers) to become stained over time. Second, since the ceiling is hot during the day, air stagnation tends to decrease the thermal convection, which traps the heat in the ceiling. The hot ceiling then radiates heat to occupants, which contributes to the already uncomfortable conditions. Ventilating the air at the ceiling level should help to alleviate these problems. However, designers must keep in mind that stirring hot air from the ceiling down to the occupancy level might not produce a desirable effect; therefore ceiling fans, which blow down might not be a good option.

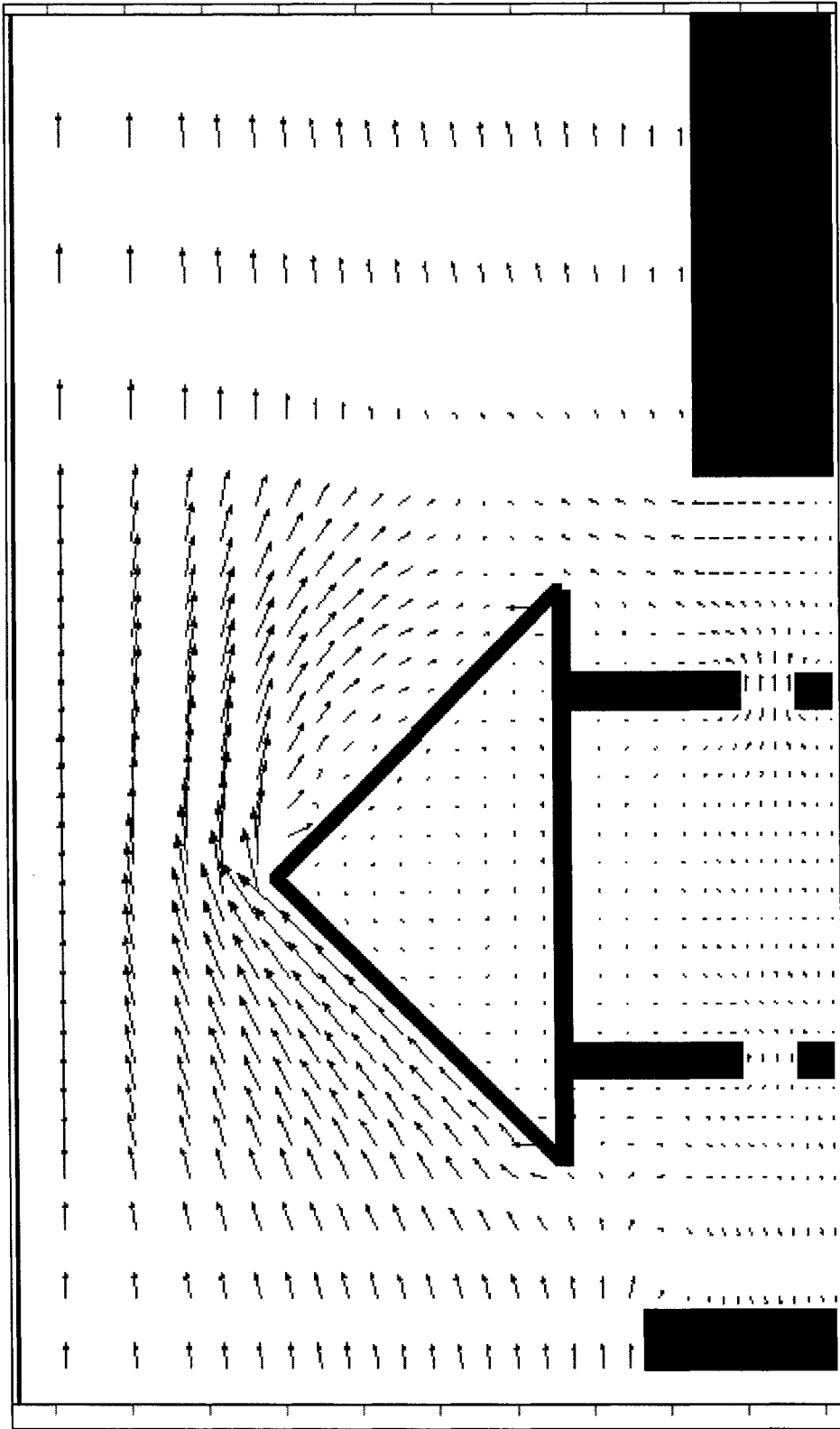
Figure 5.10 shows the air pressure profiles along the flow domain. In this figure, it is clear that the building becomes an obstacle to the flow field. Positive pressure occurs at the location where the air first reaches the building, and negative pressure occurs where the air leaves the building. The negative pressure can also be clearly seen at the openings where air is passing through with high velocities, as seen in Figure 5.9. These pressure differentials play a major role in ventilating the building because they provide suction that drives the airflow across the openings at a higher speed. However, the high positive pressure at the inflow also indicates that the building is not oriented properly for the outdoor air to pass through at the maximum ventilation rate. If the new design needs more ventilation, redesigning the building with respect to proper orientation to the direction of the prevailing wind could provide more desirable effects. This problem might also be solved by adding building components (e.g., fins, overhangs) that help direct the incoming air to the inside of the building.

Figure 5.11a shows plots of the temperature of the air passing through the building with the buoyancy effects considered. Solar radiation heats up the outside roof surface, and this heat is transferred to the attic. This causes the attic to be hotter, especially in the area right beneath the roof. Inside the attic, buoyancy causes the hot attic air to accumulate at the top of the attic. This stirs hot air from the inside surface of the roof with the cooler air at the ceiling. At the outside roof surface, it was found that the back roof (i.e., leeward) was hotter than the front (i.e.,

windward). This is because the incoming air convects away heat from the windward roof surface, while at the back roof a re-circulation of air occurs and that reduces the local convection heat transfer. Hot air vortices in the leeward side also trap the heated air near the roof surface, and thus add to the heating up of the outside back roof.



**Figure 5.8** *Vector Plot Showing the CFD-Simulated Airflow Through the Building on 04/01/99 at Noon (Floor Plan).*



**Figure 5.9** Vector Plot Showing the CFD-Simulated Airflow Through the Building on 04/01/99 at Noon (Section A-A).

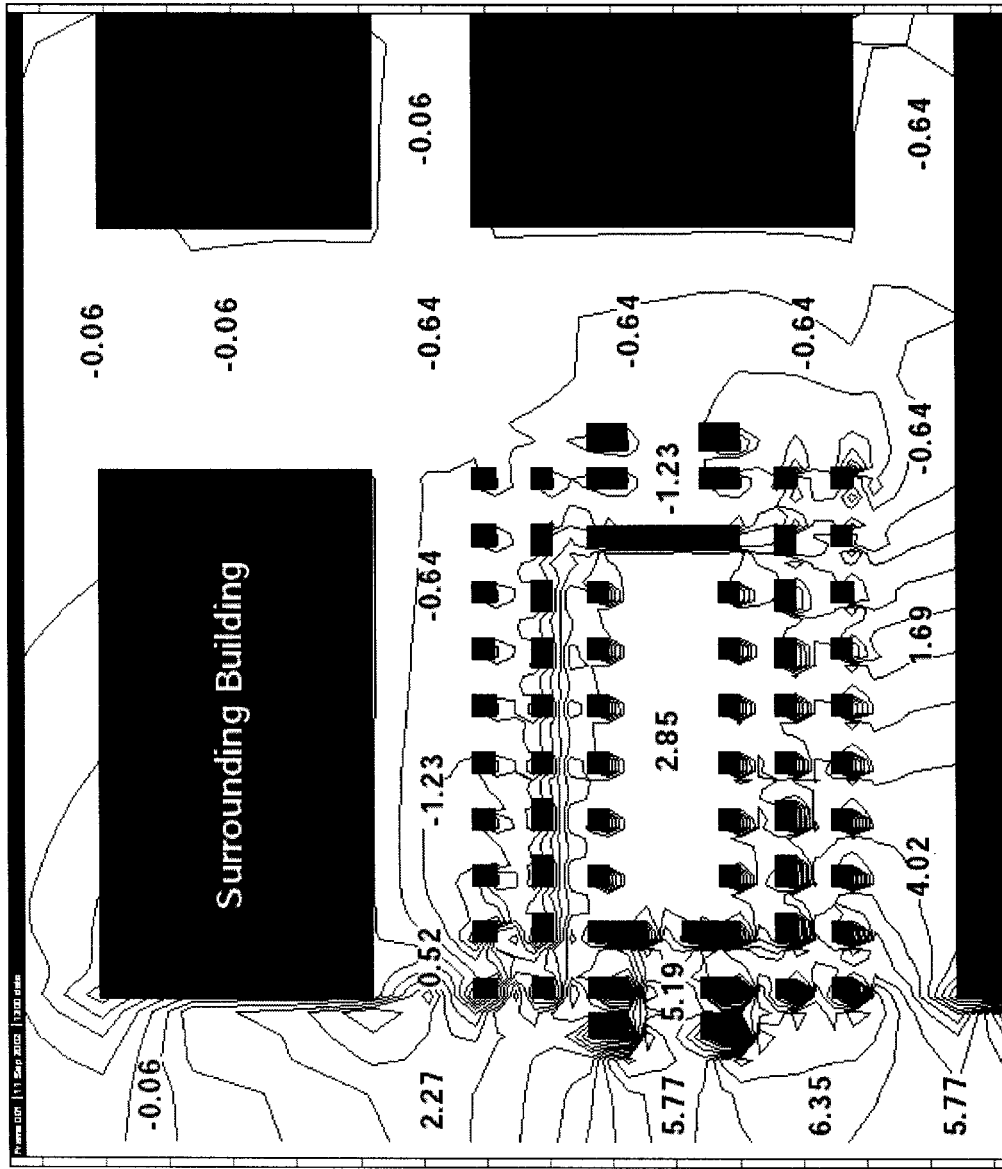


**Figure 5.10** Contour Plot Showing the CFD-Simulated Air Pressure Across the Building on 04/01/99 at Noon.

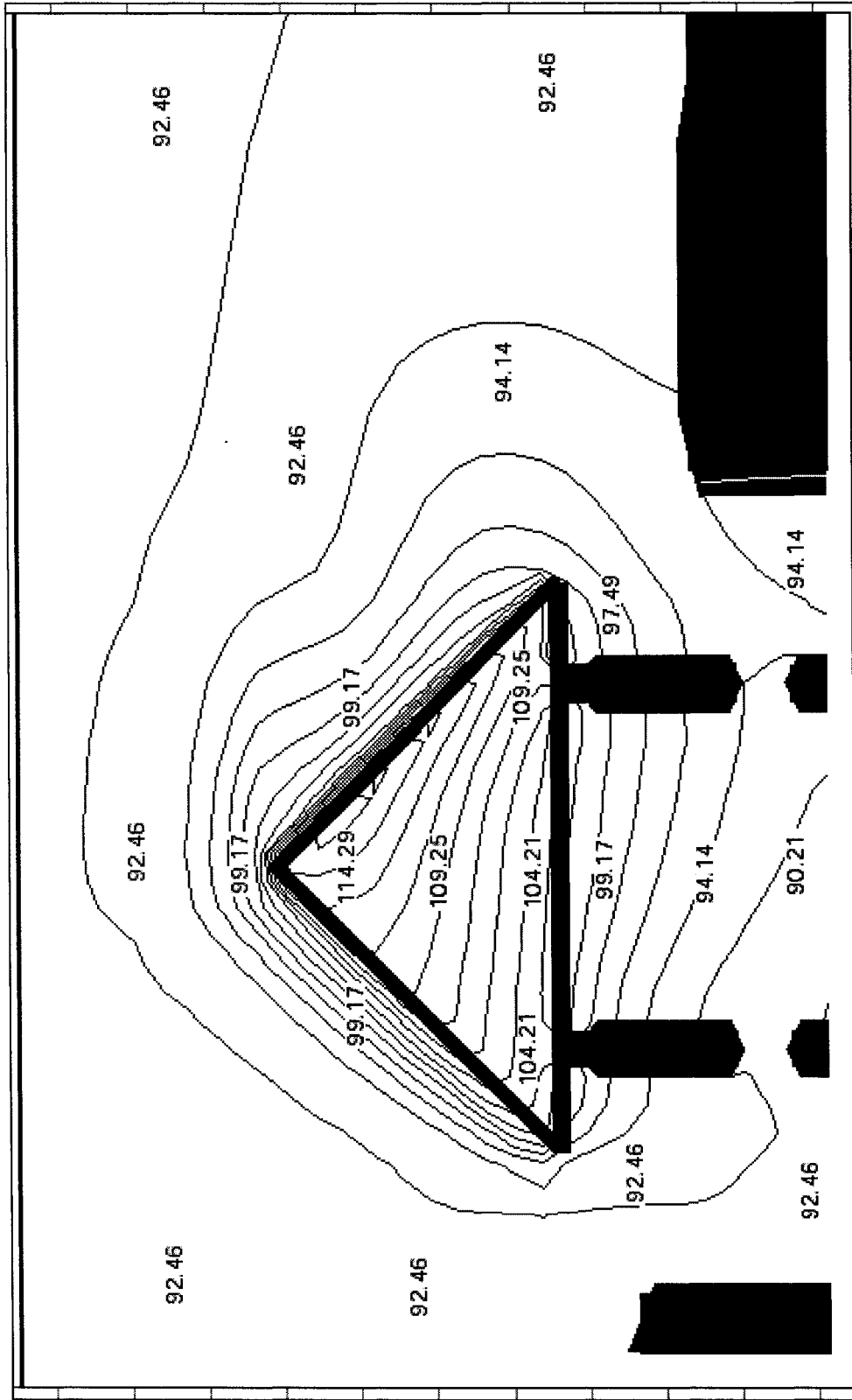


**Figure 5.11a** Contour Plot Showing CFD-Simulated Temperatures of the Air Passing Through the Building on 04/01/99 at Noon (Section A-A).



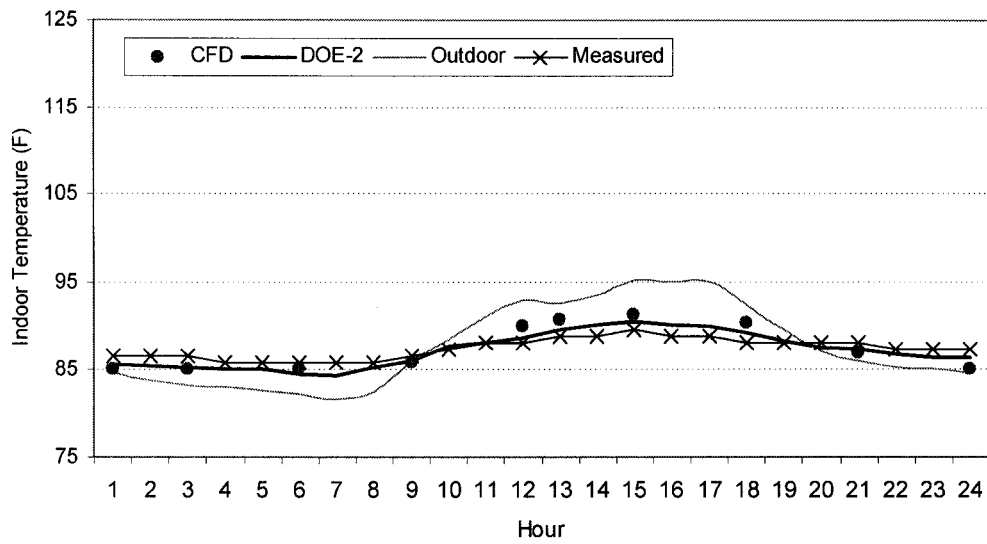


**Figure 5.11b** Comparison of the DOE-2 and the Transient CFD-Simulated Indoor Temperatures of the Old Temple on a Summer Day (04/01/99).

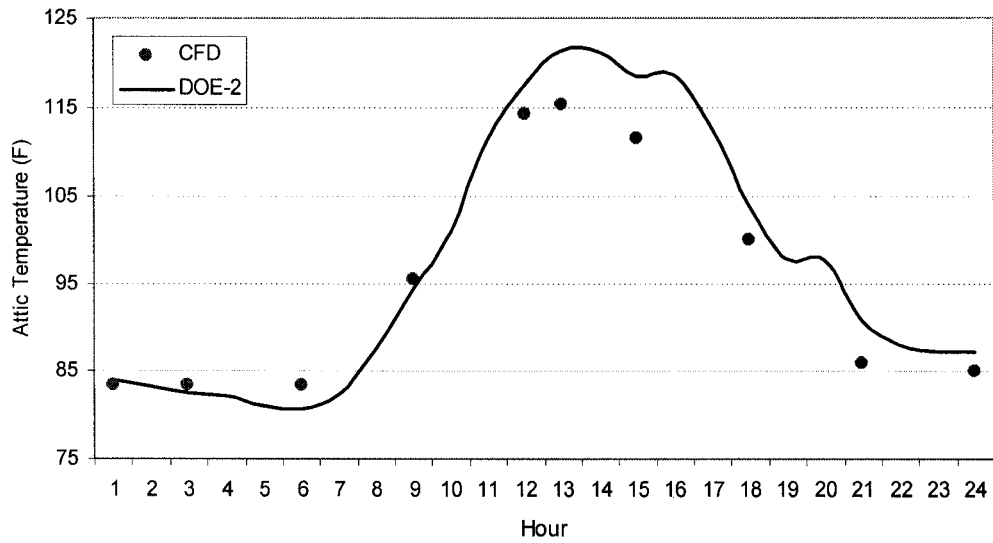


**Figure 5.11c** Comparison of the DOE-2 and the Transient CFD-Simulated Attic Temperatures of the Old Temple on a Summer Day (04/01/99).

For the DOE-2/CFD calibration, Figures 5.11b and 5.11c show the simulation results of a coupled DOE-2/CFD transient calculation of the old temple for a 24-hour period on a summer day (i.e., April 1, 1999). The comparison of the simulation results of DOE-2 with those from CFD improved.

Once a coupled DOE-2/CFD simulation was performed, the maximum ventilation rate to be supplied to DOE-2 was calculated by multiplying the maximum air velocity across the windows with the total area of the windows. The maximum ventilation rate in terms of the air exchange per hour (ACH) in DOE-2 was found to be 20 ACH, as compared to the pre-CFD estimated value of 100 ACH. In addition, it was found that maximum ventilation occurs mostly during the afternoon, especially in the summer when the outdoor wind speeds are at the highest, and all the windows are left open. Unfortunately, this causes the temperatures inside the temple to rise as the cooler air inside the temple was replaced with hotter outside air.

In terms of the surface convection coefficients, the CFD results of the space temperature distribution and air velocity were used to calculate the convection heat transfer coefficients using equations 4.15 – 4.21. For each inside surface, the wall temperature and the air temperature of the area next to the wall were used to establish the temperature difference needed for the calculation of the Rayleigh number in equation 4.19. For each outside surface, the air velocity at the surface was used to calculate the Reynolds number in equation 4.21, which was then used to calculate the Nusselt number in equation 4.20. The convection heat transfer coefficients for all surfaces are presented in Table 5.2. From the CFD calculation, it was found that the convection coefficients calculated in the current research were lower than those suggested by ASHRAE (1998: Table 4.2, p.50). However, these results agreed more closely to the study of Gadgil et al. (1982; ref. Balcomb ed. 1988: p.141), who performed a finite-difference calculation of the Navier-Stokes equations in order to determine the convection coefficients in a room. His results are presented in Table 5.2. Gadgil argued that the ASHRAE convection coefficients were too large, and that smaller values could be expected if calculated using a numerical model. Once the convection coefficients were obtained, the combined convection/radiation film resistances could be estimated based on Niles et al. (1988: ref. Balcomb ed. 1988). The inside surface film resistances to be specified for DOE-2 are presented in Table 5.3.

**TABLE 5.2**  
**Comparison of Surface Convection Coefficients**

	ASHRAE (1998) (Btu/hr-ft <sup>2</sup> -°F)	Gadgil et al. (1982) (Btu/hr-ft <sup>2</sup> -°F)	The Old Temple (Btu/hr-ft <sup>2</sup> -°F)
Vertical walls	0.54	0.48	0.32
Lower surface of ceiling	0.71	0.30	0.23
Inside roof surface (slope-45)	0.68	N/A	0.47
Upper surface of floor/ceiling	0.17	N/A	0.16

**TABLE 5.3**  
**Comparison of Inside Film Resistances**

	ASHRAE (1998) (hr-ft <sup>2</sup> -°F/Btu)	The Old Temple (hr-ft <sup>2</sup> -°F/Btu)
Vertical walls	0.68	0.80
Lower surface of ceiling	0.61	0.86
Inside roof surface (slope-45)	0.62	0.71
Upper surface of floor/ceiling	0.92	0.93

Unfortunately, although the CFD-calculated inside film resistances and air change rates improved the simulations, as shown in Figure 5.12, major differences still remained between the simulated and measured indoor temperatures (i.e., the simulated temperatures had more fluctuation). Nonetheless, the CV-RMSE was reduced to 3.16 %, and the NMBE reduced to -1.77 %. On average it was found that DOE-2 calculated the indoor space temperatures to be higher than the measured temperatures by about 5° to 10 °F. This occurred mostly during the daytime, and was most likely caused from an over-estimation of space heat gain. Therefore, the next calibration step focused on adjusting the daytime heat gain to the indoor space, including a reduction of the internal heat gain and solar heat gain through the attic.

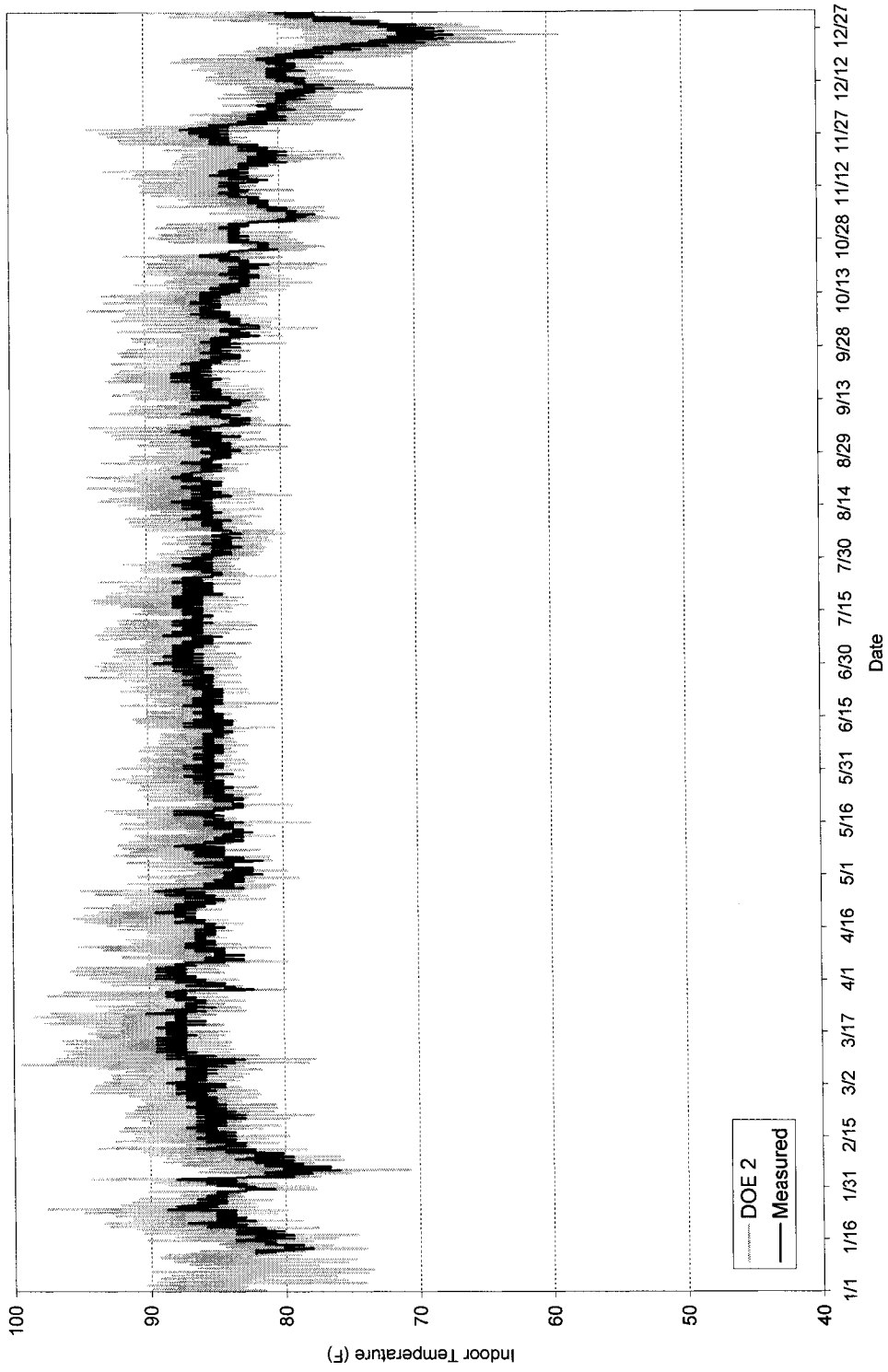


**Figure 5.12** Comparison of the DOE-2 Simulated and Measured Indoor Temperatures: 2<sup>nd</sup> Calibration.

### 5.2.3 Third Calibration

In the third calibration, the major sources of internal heat gains to the temple were reduced. These reductions consisted of the following: a) the maximum numbers of occupants was reduced from 10 to 5; b) The lighting heat gain was reduced from 0.10 to 0.05 Watt/ft<sup>2</sup>; and c) the roof surface absorptance was reduced from 0.90 to 0.75. After these adjustments were made the hourly indoor temperature comparison, as shown in Figure 5.13, demonstrated that there were still significant differences between the simulated and measured indoor temperatures. Namely, the simulated values still had too much fluctuation. The CV-RMSE decreased to 2.07 %, the NMBE increased to – 2.40 %, and the indoor space temperatures were reduced to within 5° to 7 °F of the measured temperatures. This continued to occur during the daytime; therefore, the next calibration attempt focused on how to further reduce daytime heat gain in the indoor space, specifically a reduction of the exterior conduction heat gain and solar heat gain.

### 5.2.4 Fourth Calibration

In the fourth calibration, additional sources of external heat gain were reduced. The ground reflectance was reduced from 0.20 to 0.15. The surrounding shade from trees and adjacent buildings was increased by increasing the height of these objects. In addition, the density of the building materials was increased. The density of the brick walls and concrete floor was increased from 140 to 170 lb/ft<sup>3</sup> in order to enhance the effect of thermal mass. This approach, which adjusted nominal values of known quantities to more effective values was previously used with some success by Manke et al. (1996). After the fourth calibration the hourly indoor temperature comparison improved, as shown in Figure 5.14. However, the simulated indoor temperature still had too much fluctuation. Nonetheless, this fourth calibration improved the calibration, yielding a CV-RMSE of 1.83 %, and the NMBE of – 1.12 %. In this fourth calibration, it was found that DOE-2 calculated the indoor space temperatures to be higher than the measured values by 5 °F during the daytime, but slightly lower at night. These indoor temperature fluctuations seemed to be caused by continuing differences in interior thermal mass; therefore, the next calibration focused on further adjustments to the thermal mass inside the space.

### 5.2.5 Fifth Calibration

In the fifth and final calibration, the interior thermal mass was increased to continue to enhance the effect of thermal inertia on the calculation. In the previous calibrations, the interior columns were not taken into account as a source of the thermal inertia. There are 12 masonry columns in the temple, each with the dimensions of 2.5 ft x 2.5 ft in width, and 26 ft in height. These columns are constructed with bricks, the same kind as was used in the exterior walls. For the DOE-2 input, these columns were assigned as an interior wall, and the wall area was calculated by totaling the surface area of all the columns. After these adjustments were made the hourly indoor temperature comparison, as shown in Figure 5.15, demonstrated that there were now only slight differences between the simulated and the measured indoor temperatures. The CV-RMSE was reduced to 1.59 %, and the NMBE reduced to 0.05 %. These figures are excellent when compared to the ASHRAE-sponsored Predictor Shootouts I and II (Kreider and Haberl.1994; Haberl and Thamilsaran 1996).

Figures 5.16a and 5.16b show detailed comparisons of the simulated and measured indoor temperatures for two-week periods during the summer and winter along with the measured solar radiation. It was found that the simulated temperatures agreed well with the measured temperatures. However, there was a systematic difference in the amplitude of the diurnal temperature swings between the measured and the simulated indoor temperatures. Specifically, the simulated temperature showed a higher sensitivity to the amount of solar radiation. The DOE-2 simulated indoor temperatures seemed to be higher than the measured temperatures on the clear days with a large amount of solar radiation (e.g., during 4/2/99 – 4/4/99 in Figure 5.16a). This might result from an over-estimation of the solar heat gain to the building in DOE-2 due to a presence of actual surrounding shades. It should be noted that the case-study temple is located in the urban area of Bangkok, where high-rise buildings are present in distance locations around the site. This causes a difficulty in accurately simulating the effect of solar heat gain to the building.

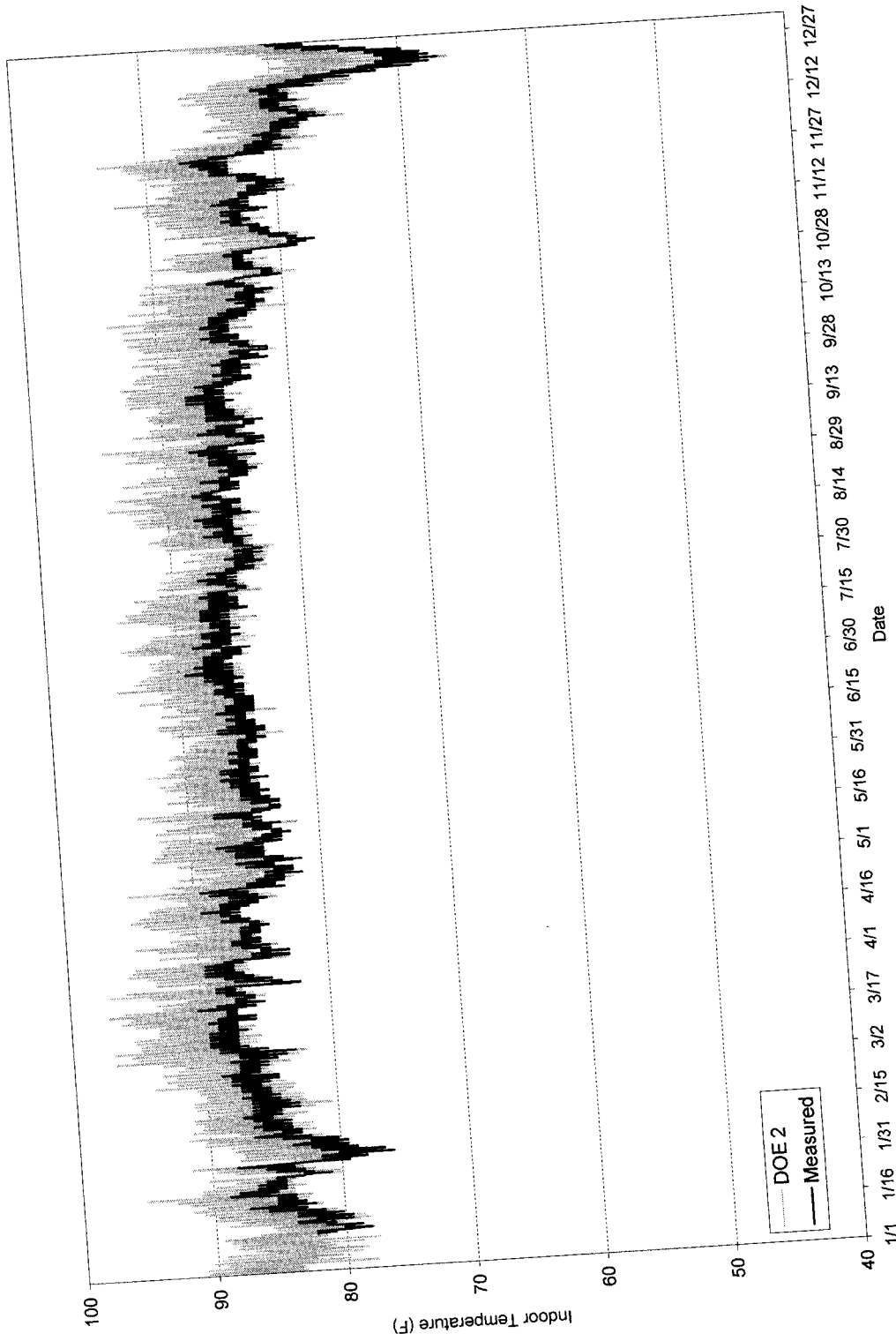


**Figure 5.13** Comparison of the DOE-2 Simulated and Measured Indoor Temperatures: 3<sup>rd</sup> Calibration.

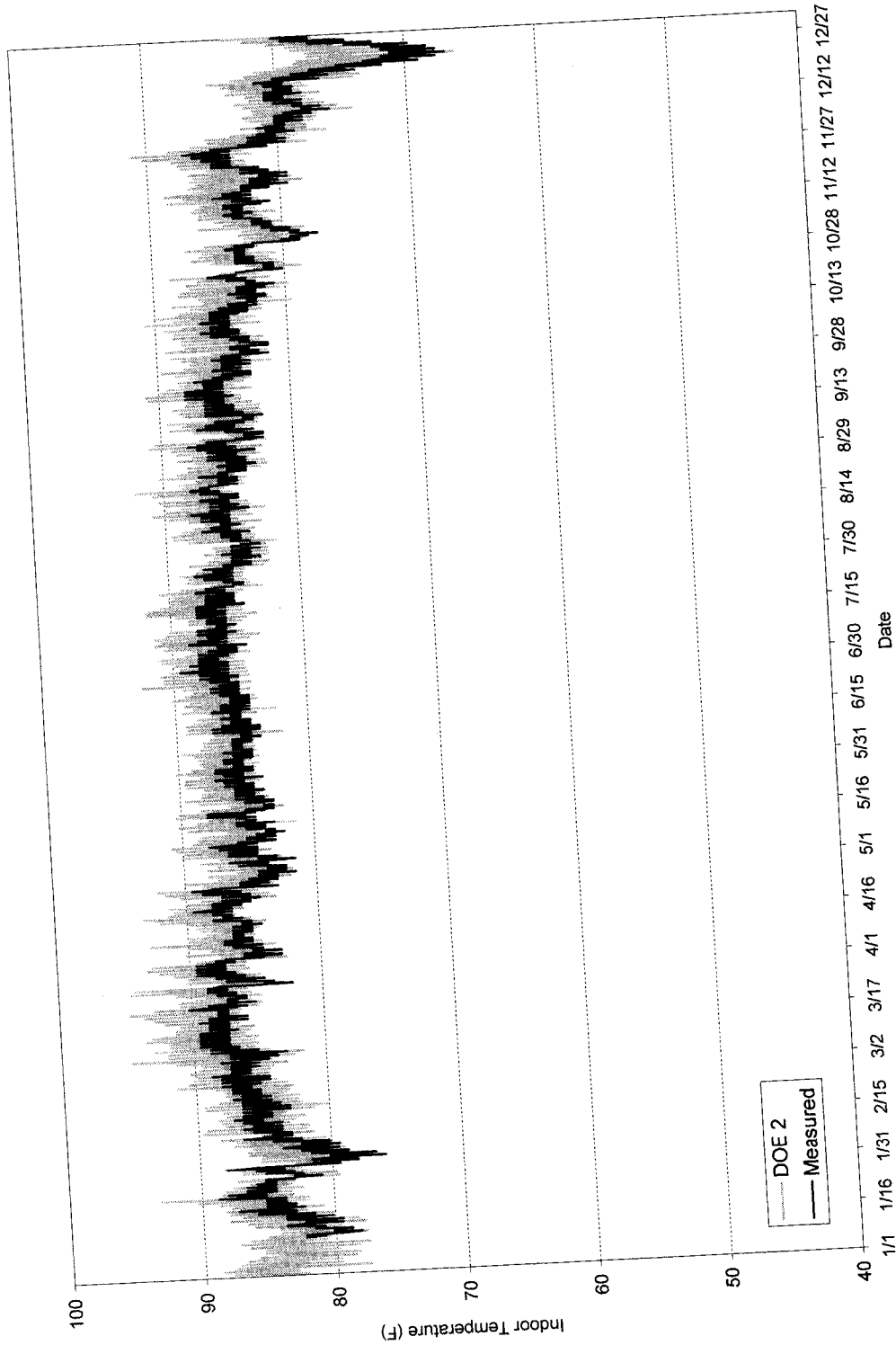


**Figure 5.14** Comparison of the DOE-2 Simulated and Measured Indoor Temperatures: 4<sup>th</sup> Calibration.



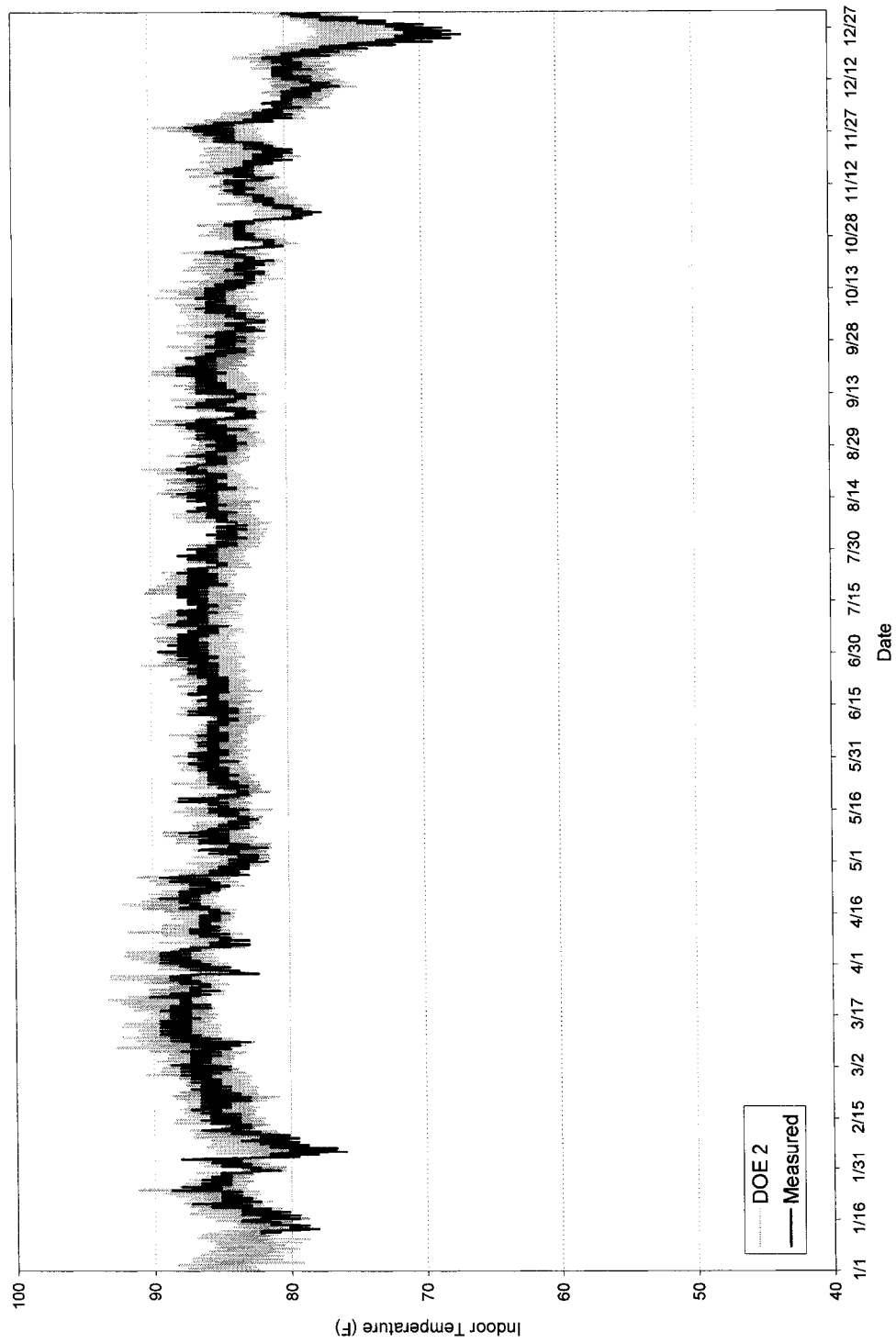


**Figure 5.15** Comparison of the DOE-2 Simulated and Measured Indoor Temperatures: 5<sup>th</sup> Calibration.

In addition, although the ventilation rate assigned in DOE-2 might be appropriate, variations of the daily ventilation schedules of the temple may have caused this error. The ventilation schedule assigned in DOE-2 was obtained from a discussion with the temple maintenance personnel. However, from several site visits made to collect data, it was found that sometimes the temple was closed without reason during the afternoon. This caused the measured indoor temperatures to have less fluctuation when compared to the simulation results. Once a calibrated simulation model was developed, it was used to obtain a better understanding of how the building performed thermally, which is discussed in the next chapter.

Table 5.4 summarizes the results of the entire calibration process from the first run to the final calibration, where the simulated temperatures agreed with the measured temperatures. The major changes made to the DOE-2 input file are listed in the table, along with its resultant CV-RMSE and NMBE. Figure 5.17 demonstrates that as the calibrations proceed, the residuals in terms of the CV-RMSE are gradually reduced and the average deviations from the mean (i.e., NMBE) approaches zero. Runs 1, 2, and 3 reduced the CV-RMSE and forced the NMBE to be negative. Runs 4 and 5 had a small improvement in the CV-RMSE and mostly improved the NMBE.

### **5.3 Analysis and Discussion of Simulation Results**

Once the final calibration was successfully completed, the simulation model was declared calibrated. It was then used to provide more information about how the building performed and reacted to the outside environment. Figures 5.18a and 5.18b show detailed comparisons of the indoor and outdoor conditions during two-week periods during the summer and winter. It is found that what drives the increase in indoor temperatures is not only the outdoor temperature, but also the solar radiation being directly transferred to the attic space, and finally through the indoor space.

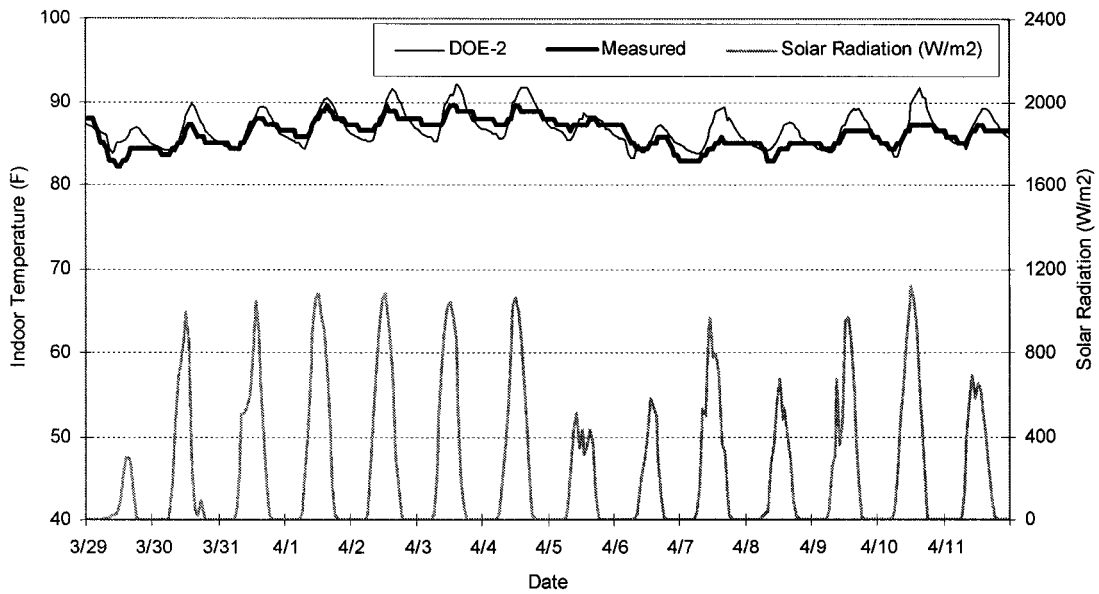


**Figure 5.16a** Comparison of the Simulated and Measured Indoor Air Temperatures During a 2-Week Period of the Summer of 1999.

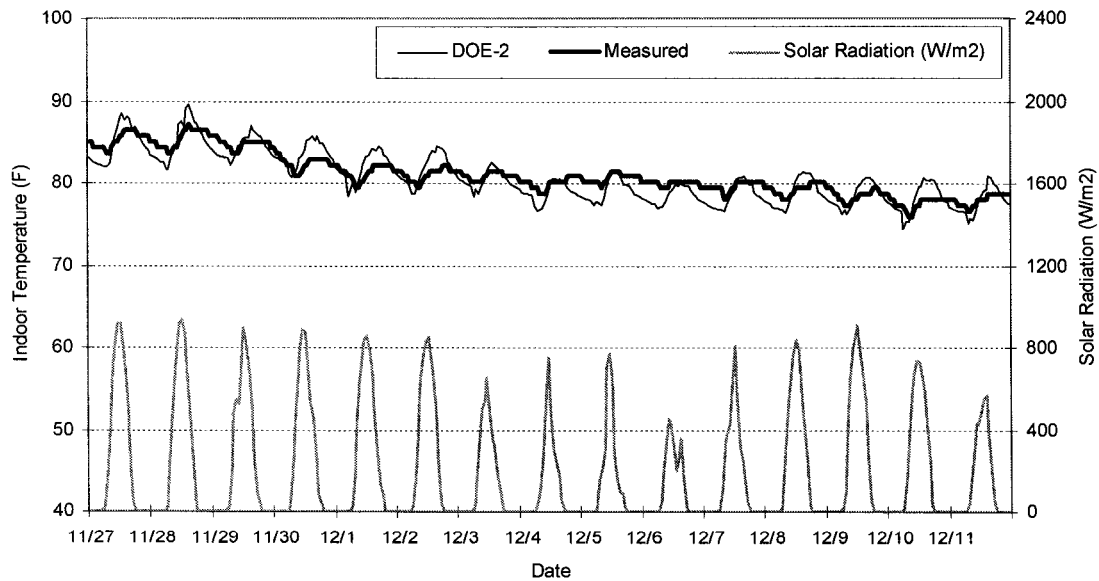


**Figure 5.16b** Comparison of the Simulated and Measured Indoor Air Temperatures During a 2-Week Period of the Winter of 1999.

**TABLE 5.4**  
**Summary of the Calibration Steps**

Run #	Description	CV-RMSE	NMBE
Run 0	<b>Uncalibrated:</b> Two zones (conditioned space & unconditioned attic) with thermostat settings. Space airflow rate = 100 ACH. No CFD applied	6.00%	1.02%
Run 1	<b>1<sup>st</sup> Calibration:</b> Add a small system to the space and set the space to its adjacent unconditioned zone. Space airflow rate = 100 ACH. No CFD applied.	5.53%	-4.56%
Run 2	<b>2<sup>nd</sup> Calibration:</b> Use CFD to calculate airflow rate. 20-Space ACH was used	3.16%	-1.77%
Run 3	<b>3<sup>rd</sup> Calibration:</b> Reduce the number of maximum occupants. Reduce lighting & equipment W/ft <sup>2</sup> . Reduce roof absorptance to 0.75.	2.07%	-2.40%
Run 4	<b>4<sup>th</sup> Calibration:</b> Reduce ground reflectance. Increase building shade from surroundings. Increase the density of walls & floor.	1.83%	-1.12%
Run 5	<b>5<sup>th</sup> Calibration:</b> Add thermal mass to the space by specifying interior walls (colonade).	1.59%	0.05%

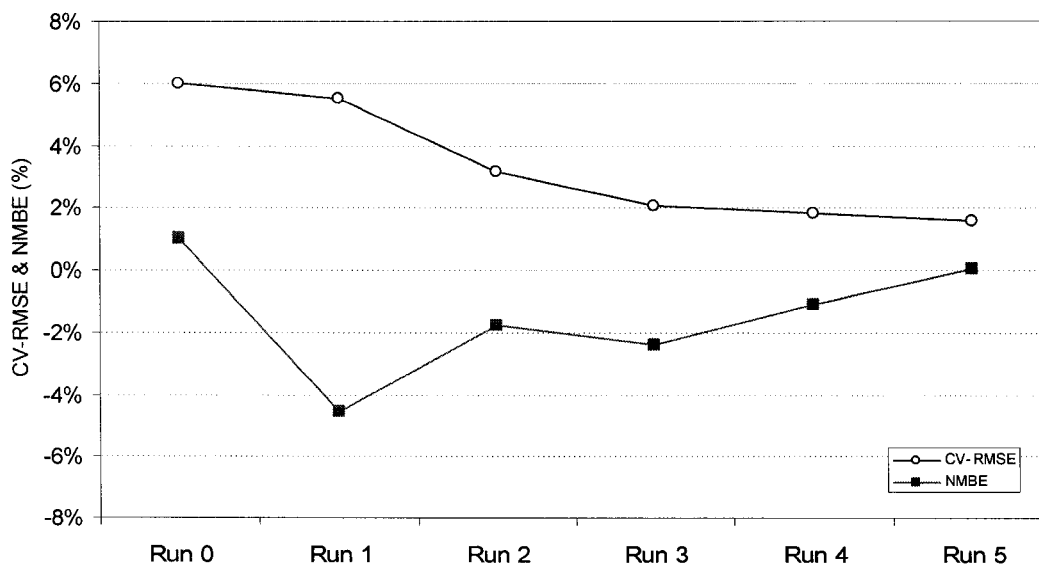


**Figure 5.17** *CV-RMSE and NMBE Comparisons of the Simulated and Measured Indoor Air Temperatures.*

In Figures 5.16a and 5.16b, on clear-sky days, the amount of solar radiation was high, about 1,000 – 1,100 Watt/m<sup>2</sup>, which caused the simulated attic space to be very hot, about 120 ° to 130 °F during the afternoon. The attic then transferred the heat directly to the indoor space below by conduction through the uninsulated ceiling. The indoor temperatures seemed to have less fluctuation, as compared to the outdoors. However, their pattern tends to follow the amount of solar radiation and attic temperatures much closer than that of the outdoor temperatures. This can be observed on the cloudy days of April 5 and 6, where the outdoor temperatures tended to drop below the indoor temperatures. However, the indoors still stayed warm due to the hot attic air. This situation was more noticeable on the winter days from November 27 to December 3. The peak outdoor temperatures dropped by 10 °F, but the peak indoor temperatures dropped only slightly, depending on the attic temperature and the amount of solar radiation.

It can be concluded from these results that the indoor temperatures are predominantly regulated by the heat gain from the attic, and less so from heat conducted through the envelope. Therefore, the proposed design guidelines are focused both on how to prevent heat transfer from the uninsulated attic and ceiling, and how to make the attic cooler during the day. In addition, it was found that the floor temperatures of the temple were relatively constant and usually lower than both the outdoor and the indoor temperatures. The ground could therefore provide a cooling effect on the building, since it could be used as a natural heat sink.

Even though the indoor temperatures are mostly affected by the heat gain from the attic, and not the heat gain from the envelope conduction, it was found that the 2.5 ft-thick brick walls contributed to the building's thermal inertia. Figure 5.18a shows that during the summer days, the high-mass walls helped to reduce the diurnal temperature swings, causing peak indoor temperatures to be maintained at about 90 °F, even though the outdoor and attic temperatures rose to 95 °F and 120 °F, respectively. This condition was most noticeable in the older temple, which was found to be cooler than the new temple during the day. However, the drawbacks occurred at night, when the outdoor temperatures dropped, but the indoor temperatures stayed warmer. This is because the heat stored inside the walls needs time to be released back to the outside. This condition was the most noticeable in the buildings when they were completely closed off from the outside air, such as the old temple.

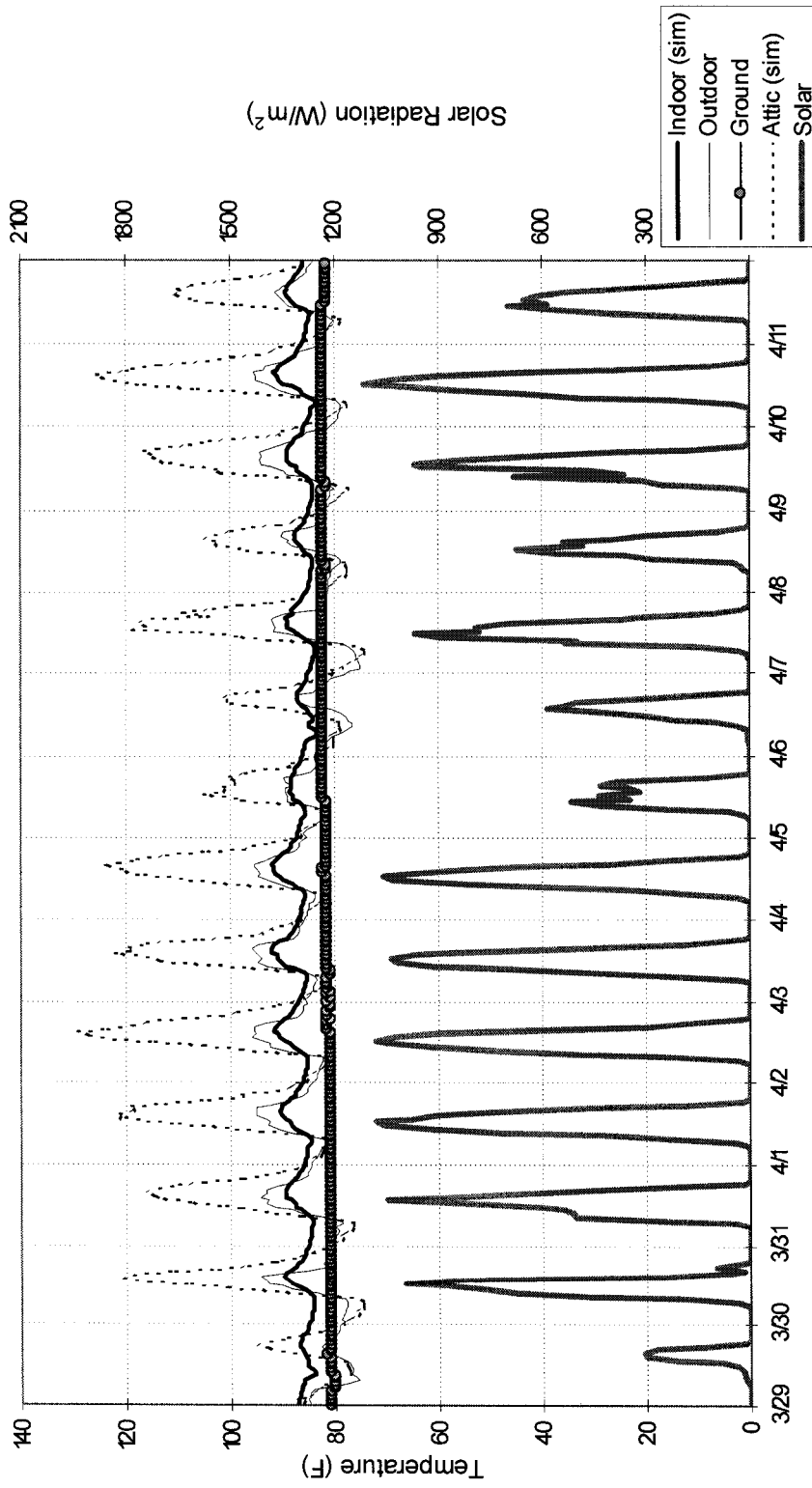
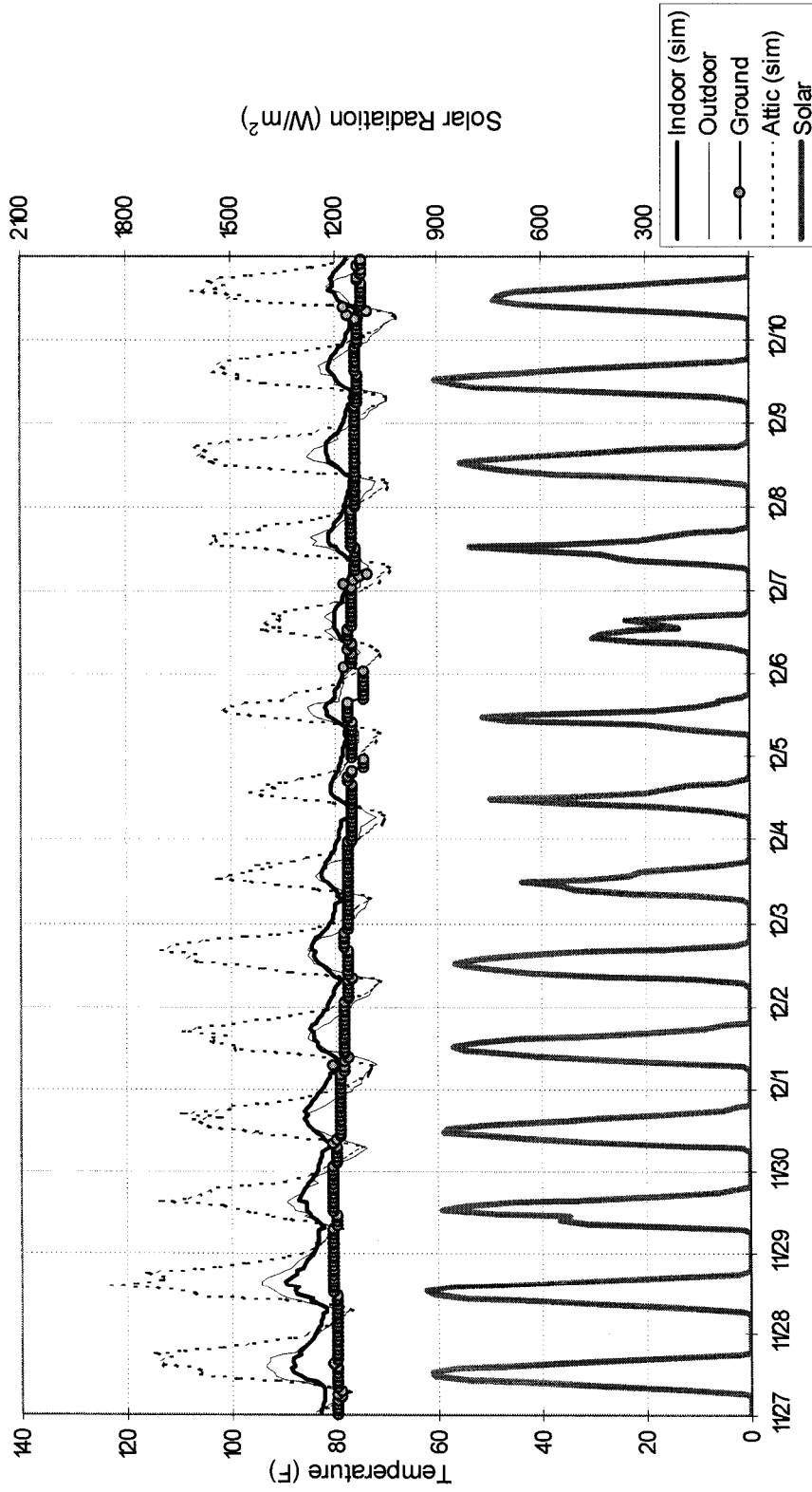


Figure 5.18a DOE-2 Simulated Indoor/Outdoor Conditions of the Old Temple During a 2-Week Period of the Summer: As-Is Condition.



**Figure 5.18b** DOE-2 Simulated Indoor/Outdoor Conditions of the Old Temple During a 2-Week Period of the Winter: As-Is Condition.

## 5.4 Summary of Results

This chapter has presented the results obtained from this investigation, and includes the survey and measurement results, the data gathering results, and the coupled DOE-2/CFD simulation results of the case study temple. The results from the on-site survey of the Thai Buddhist temples provided useful information about the physical condition, operational schedules, and indoor environmental conditions of the case-study temples. The measurement results provided a set of long - term data concerning the indoor and outdoor thermal conditions that is useful for both the comfort analyses and the simulation calibrations. The weather data were collected for climate analyses, and were used to create the weather files for both of the DOE-2 and CFD simulation programs. The calibrated DOE-2/CFD simulations were successfully developed for the older temple, and the output results were used to provide an in-depth thermal analysis that was necessary for further investigations. As part of this investigation, it was found that ASHRAE's recommended convection coefficients were too large when compared to the CFD-derived coefficients.

In terms of the DOE-2 calibration steps, several carefully selected input parameters were tuned in order to obtain a simulation model that accurately represented the case-study temple. Those parameters included the thermal properties of building materials, the convection coefficients, and the zone air flow rate. Table 5.5 summarizes the thermal properties of the exterior walls, the roof, the floor, and the ceiling of the case-study temple once the calibration were completed.

**TABLE 5.5**  
**Thermal Properties of Building Materials**

Building Components	Material Descriptions	Density (lb/ft <sup>3</sup> )	Thermal Conductivity (Btu/h.ft.°F)	Specific Heat (Btu/lb.°F)	Thickness (ft)
Exterior Walls	Brick Walls	140	0.41670	0.2	2.67
Roof	1" Clay Tile	100	0.13125	0.4	0.083
Floor	6" Heavy-Weight Concrete	170	1.04170	0.5	0.5
Ceiling	1" Solid Wood	45	0.04916	0.5	0.083



Based on the results of this research, using the ASHRAE and Givoni comfort zones, both case-study temples were found to be uncomfortable most of the time, especially in the summer when it is usually hot and very humid. Winter is generally more comfortable for short periods. Compared to the new temple, the old temple's high-mass structure, and shading caused it to be more comfortable. Thermal inertia also played an important role in reducing the diurnal temperature swings of the older temple. However, during the evening, the indoor temperatures seem to be warmer than the outdoor temperatures because the heat was stored in the building materials and trapped inside the building. This condition was made worse when the temple is completely closed off from the outside at night. In terms of the building's heat gain, it can be concluded that the major heat gain component is the attic heat and not the heat from the wall conduction. Table 5.6 presents the DOE-2-calculated peak cooling load components of the case-study temple in the afternoon of a summer day (i.e., March 16 at 3 P.M.). It was found that, apart from the ventilation heat gain, 30% of the total building heat gain is resulted from the heat conduction through the roof.

**TABLE 5.6**  
**DOE-2 Calculated Building Peak Cooling**  
**Load Components**

Load Components	Peak Cooling Load	
	kBtu/hr	% of Total
Roof Conduction	143.09	30.05%
Ventilation Load	318.26	66.84%
Wall/Window Conduction	14.41	3.03%
Internal Load	0.42	0.09%
Total	476.18	

## CHAPTER VI

### OPTIONAL DESIGNS AND OPERATIONS

#### 6.1 Introduction

The results presented in Chapter 5 demonstrate that the indoor condition of the case-study temple could be significantly improved by applying an appropriate design and operation modification. As mentioned earlier, the major source of heat gain to the indoor space is the attic. This gain results from solar radiation and poor ceiling insulation. In addition, the heat is trapped inside the building because of the combined effect of limited ventilation in the temple, thermal mass and the temple operation schedule. The closure of doors and openings in the evening increased the trapping of heat inside. As a result, the building is warmer than the outside during the night and remains warm until the next morning. Therefore, new design guidelines will be focused on two important approaches: first, how to avoid attic heat gain, and second, how to remove indoor heat more effectively using only natural means. Each design option must also consider the following two important criteria: 1) only minor changes to the building's footprint are allowed, and 2) no major change in the style of architecture should be proposed.

To avoid attic heat gain, three major design criteria are proposed in this study. First, since solar radiation is a major source of heat gain to the attic, applying a low-absorption roof coating would help reduce the solar heat gain, and thus lower the attic temperature. Second, it was found that no thermal insulation was used on the ceiling of the case study building. Therefore, adding ceiling insulation would be an effective option to block the heat gain from the attic. Third, because of the significant amount of solar radiation in this climate, shading from the sun all year long is necessary. Another option is to increase the sunshade at the building's exterior surfaces, which includes the walls and the roof. In terms of heat removal, it was found that there was a possibility of reducing the peak attic temperature during the daytime by introducing cooler outside air into the attic. A cooler attic would release less heat into the indoor space. It was found from the results shown in Chapter 5 that with the high-thermal mass, various natural ventilation schedules had a significant impact on indoor temperatures. Therefore, it is

important to investigate the effects that various ventilation schedules would have on the case-study building. Table 6.1 summarizes the test results of all selected design and operation options.

**TABLE 6.1**  
**Simulation Results of Design Options with Three Ventilation Modes**

Design options	Space Ventilation Modes		
	As-Is (day only) 20 ACH	Night Only 20 ACH	24-Hour 20 ACH
1 AS-IS (alpha = 0.75)	Peak Indr.temp = <b>93.3 °F</b> Avg Indr. temp = <b>84.2 °F</b> Dev. from grnd = <b>+ 5.3 °F</b> Dev. from outdr.= <b>+ 1.0 °F</b>	Peak Indr.temp = <b>91.4 °F</b> Avg Indr. temp = <b>83.8 °F</b> Dev. from grnd = <b>+ 4.9 °F</b> Dev. from outdr.= <b>+ 0.6 °F</b>	Peak Indr.temp = <b>94.2 °F</b> Avg Indr. temp = <b>84.3 °F</b> Dev. from grnd = <b>+ 5.4 °F</b> Dev. from outdr.= <b>+ 1.1 °F</b>
2 White Roof Only (alpha = 0.22)	Peak Indr.temp = <b>92.5 °F</b> Avg Indr. temp = <b>82.9 °F</b> Dev. from grnd = <b>+ 4.0 °F</b> Dev. from outdr.= <b>- 0.3 °F</b>	Peak Indr.temp = <b>89.5 °F</b> Avg Indr. temp = <b>81.9 °F</b> Dev. from grnd = <b>+ 3.0 °F</b> Dev. from outdr.= <b>- 1.3 °F</b>	Peak Indr.temp = <b>92.4 °F</b> Avg Indr. temp = <b>82.9 °F</b> Dev. from grnd = <b>+ 4.0 °F</b> Dev. from outdr.= <b>- 0.3 °F</b>
3 R-30 Ceiling Insulation Only	Peak Indr.temp = <b>92.2 °F</b> Avg Indr. temp = <b>83.3 °F</b> Dev. from grnd = <b>+ 4.5 °F</b> Dev. from outdr.= <b>+ 0.1 °F</b>	Peak Indr.temp = <b>89.3 °F</b> Avg Indr. temp = <b>82.2 °F</b> Dev. from grnd = <b>+ 3.3 °F</b> Dev. from outdr.= <b>- 1.0 °F</b>	Peak Indr.temp = <b>92.0 °F</b> Avg Indr. temp = <b>83.3 °F</b> Dev. from grnd = <b>+ 4.4 °F</b> Dev. from outdr.= <b>+ 0.1 °F</b>
4 Attic Ventilation (24-hour) Only	Peak Indr.temp = <b>93.1 °F</b> Avg Indr. temp = <b>83.7 °F</b> Dev. from grnd = <b>+ 4.8 °F</b> Dev. from outdr.= <b>+ 0.5 °F</b>	Peak Indr.temp = <b>90.2 °F</b> Avg Indr. temp = <b>82.8 °F</b> Dev. from grnd = <b>+ 4.0 °F</b> Dev. from outdr.= <b>- 0.3 °F</b>	Peak Indr.temp = <b>93.0 °F</b> Avg Indr. temp = <b>83.6 °F</b> Dev. from grnd = <b>+ 4.7 °F</b> Dev. from outdr.= <b>+ 0.4 °F</b>
5 Shading with High Mass Only	Peak Indr.temp = <b>93.4 °F</b> Avg Indr. temp = <b>84.0 °F</b> Dev. from grnd = <b>+ 5.1 °F</b> Dev. from outdr.= <b>+ 0.8 °F</b>	Peak Indr.temp = <b>90.1 °F</b> Avg Indr. temp = <b>83.2 °F</b> Dev. from grnd = <b>+ 4.3 °F</b> Dev. from outdr.= <b>0.0 °F</b>	Peak Indr.temp = <b>93.4 °F</b> Avg Indr. temp = <b>83.8 °F</b> Dev. from grnd = <b>+ 5.0 °F</b> Dev. from outdr.= <b>+ 0.6 °F</b>

In addition to performing the analysis of the base case temple that operates with different ventilation modes, four other design options were proposed: 1) a low solar-absorption roof surface, 2) R-30 ceiling insulation, 3) 24-hour attic ventilation, and 4) shading devices. Each design option was simulated independently using three different space ventilation modes: 1) daytime-only ventilation, 2) nighttime-only ventilation, and 3) 24-hour ventilation. The maximum ventilation rate for all design options was set to 20 ACH, which is the same as that calculated for the base case temple. The simulated indoor temperatures reported by DOE-2 were used as an indicator of how much better each design option performed thermally as compared to the existing temple. To compare all of the results, the following were calculated for each design option: 1) the average indoor temperature, 2) the peak indoor temperature, 3) the average indoor temperature deviation from the ground temperature, and 4) the average indoor temperature deviation from the outdoor temperature. Table 6.1 summarizes the test results of all design and operation options, which will be discussed in detail in the following sections.

## **6.2 Option 1: As-Is Temple with Nighttime-Only Ventilation**

The existing temple normally opens all doors and windows during the daytime from 6 A.M. until 6 P.M. From the measurement and simulation results presented in Chapter 5, it was found that during the night, the indoor temperature was warmer than the outdoor temperatures because hot outdoor air was ventilated into the building during the day, and the heat was stored within the building materials, and trapped inside the temple at night. This condition was made worse because the building was completely closed from the outside during the night. As a result, the average indoor temperature deviation from the outdoor temperature is found to be +1.0 °F, which means that the indoors is regularly warmer than the outdoors. Therefore, it is recommended to ventilate the indoor space with cooler, outdoor air at night. Two simulations were performed to compare the results with those of the existing building. One is the as-is building with nighttime-only ventilation, in which all windows are closed from 6 A.M. to 6 P.M. and opened from 6 P.M. to 6 A.M. The other is the as-is building with 24-hour ventilation. The simulation results are presented in Figures 6.1a, 6.1b, and 6.2.

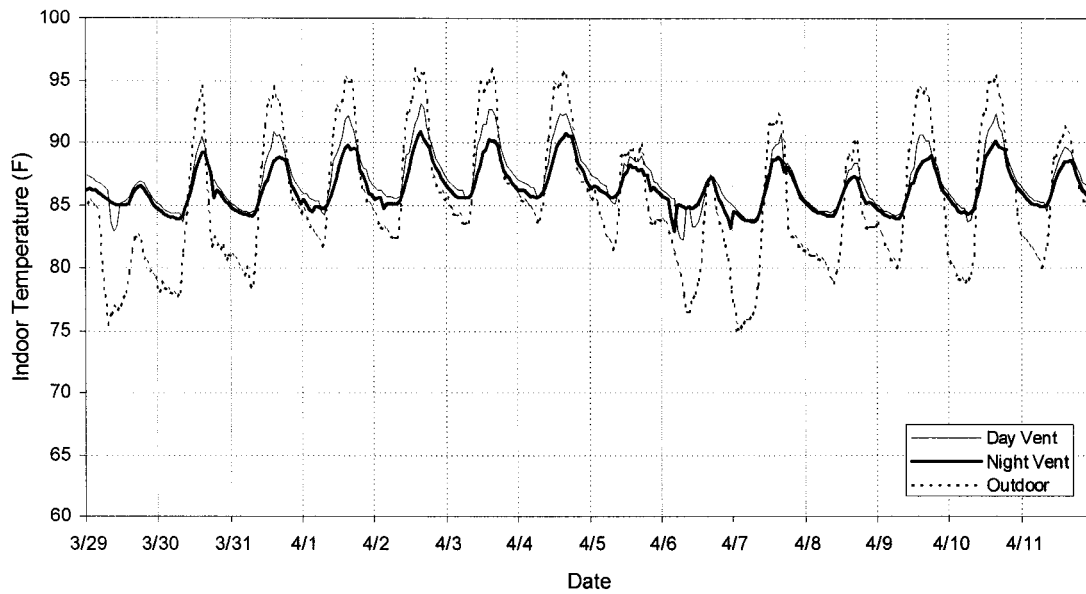


**Figure 6.1a** *DOE-2 Simulated Hourly Indoor Temperatures of the Old Temple for a 2-Week Period of the Summer: As-Is Conditions with Daytime and Nighttime Space Ventilation Modes.*

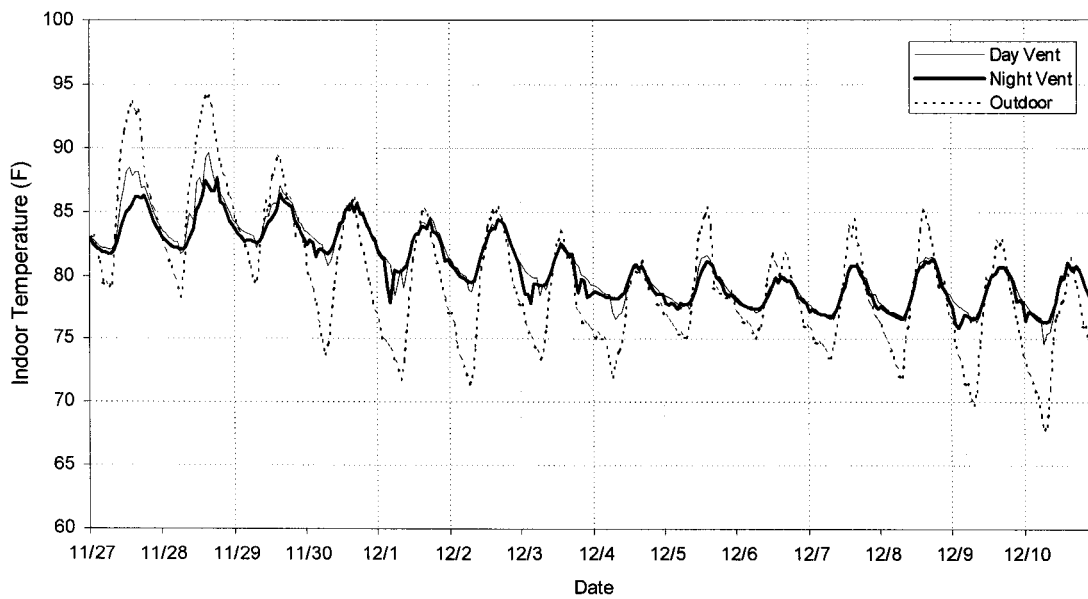


**Figure 6.1b** *DOE-2 Simulated Hourly Indoor Temperatures of the Old Temple for a 2-Week Period of the Winter: As-Is Conditions with Daytime and Nighttime Space Ventilation Modes.*

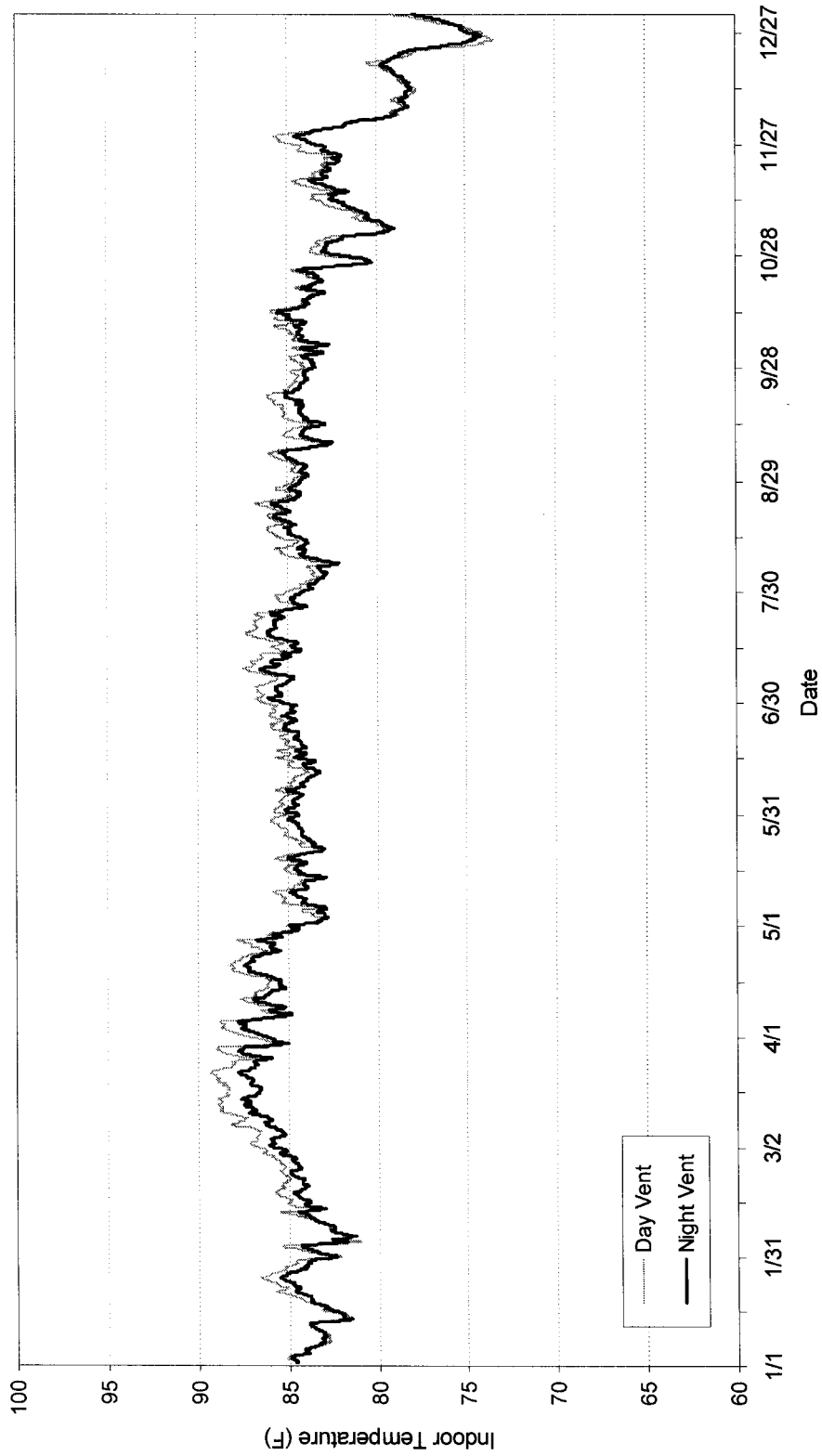


**Figure 6.2** Daily Average DOE-2 Simulated Indoor Temperatures of the Old Temple for One-Year Period: As-Is Conditions with Daytime and Nighttime Space Ventilation Modes.

Figures 6.1a and 6.1b show that the temple performs slightly better in terms of thermal comfort if the nighttime-only ventilation was applied. Nighttime-only ventilation without any changes in building configuration could reduce the peak temperatures in the afternoon by 3-4 °F on summer days. Moreover, this would result in a reduction of the average temperature deviation from the outdoors from +1.0 °F to +0.6 °F, which means that the inside temperatures in the temple would still be warmer than the outside temperature, but not as warm as the inside temperatures in the existing building with daytime-only ventilation. However, if natural ventilation was used for 24 hours, the temple would not perform much differently from the existing temple with daytime-only ventilation. These results indicate that by reducing the building ventilation during the day and increasing the ventilation during the night, the overall comfort conditions could be improved and the peak indoor temperatures reduced.

### **6.3 Option 2: Low Solar-Absorption Roof Surfaces**

To avoid attic heat gain, it is recommended that heat transfer to the roof be prevented at the outside roof surface. A major source of heat gain to the roof is solar radiation. However, the amount of solar heat gain depends greatly upon the thermal characteristics of the roof surface, such as surface roughness and the surface heat absorptance. The roof of the existing temple was built with red clay tiles that have an effective heat absorptance of 0.75, which means that 75% of the solar heat is absorbed on the roof and 25 % is reflected. The surface roughness and solar absorptance of the red clay tiles are high, which causes a significant amount of solar radiation to be absorbed and transmitted to the attic space. This condition is demonstrated in Figure 5.18a, where the simulated attic temperature reaches 130 °F on summer days. Currently, reflective coating materials are available on the market. The absorptance can be as low as 0.22, which could be effectively used to reduce heat gain due to solar radiation for this case-study temple. Simulations were performed using low-absorption coating materials applied on the roof of the base case temple along with three ventilation modes: the daytime-only (i.e., as-is condition), nighttime-only, and 24-hour ventilation. The simulation results are shown in Figures 6.3, 6.4a, 6.4b, 6.5a, and 6.5b.

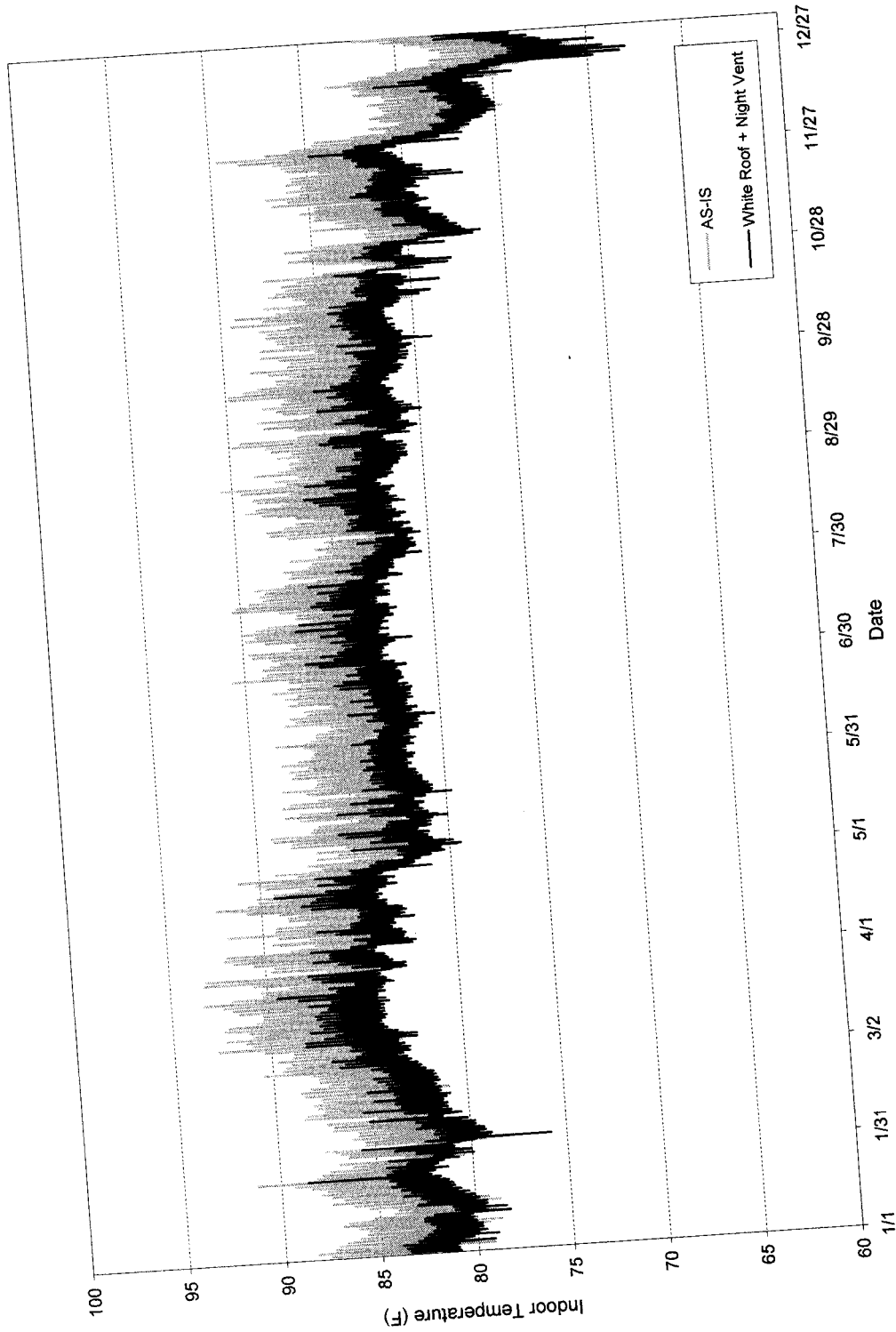


**Figure 6.3** DOE-2 Indoor Temperatures of the Old Temple for a One-Year Period: As-is Condition VS Option 2, Low-Absorption Roof with Nighttime-Only Space Ventilation.



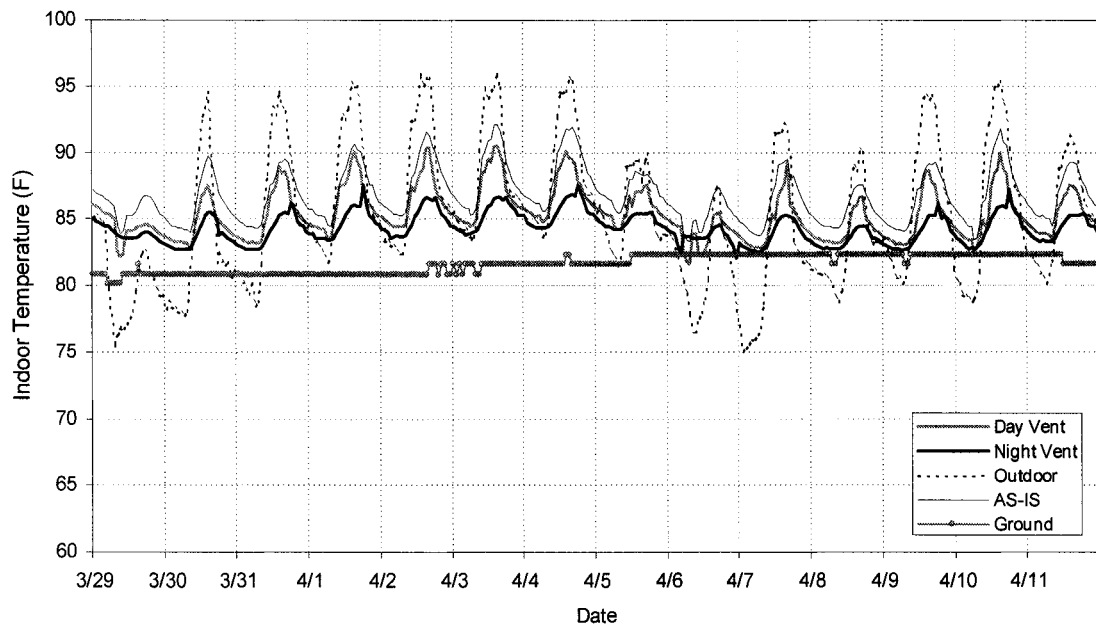


**Figure 6.4a** DOE-2 Simulated and Measured Indoor/Outdoor Conditions of the Old Temple During a 2-week Period of the Summer: Option 2, Low-Absorption Roof.

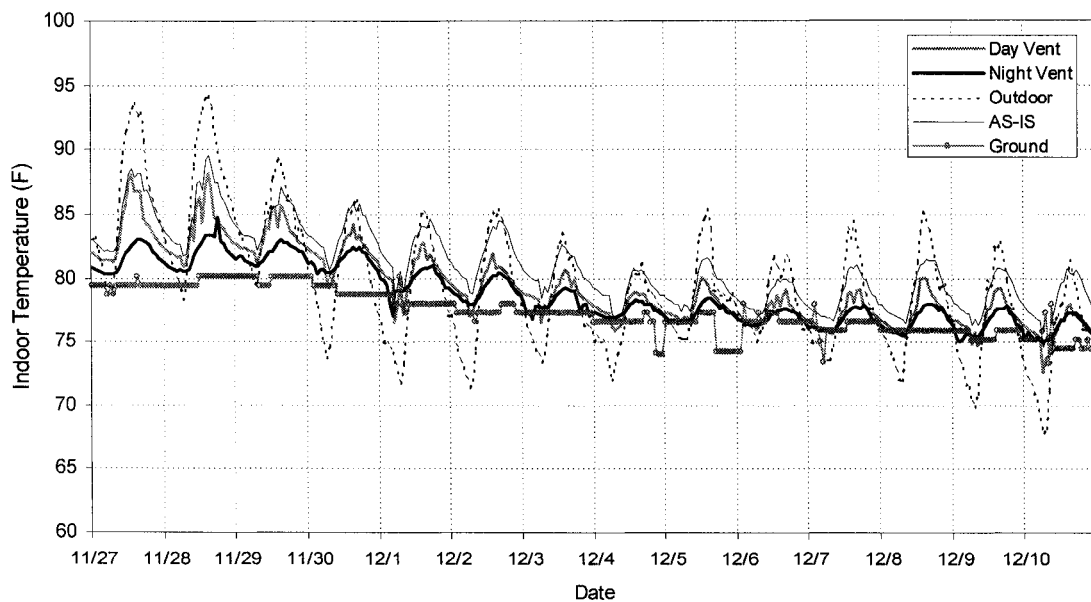


**Figure 6.4b** DOE-2 Simulated and Measured Indoor/Outdoor Conditions of the Old Temple During a 2-week Period of the Winter: Option 2, Low-Absorption Roof.

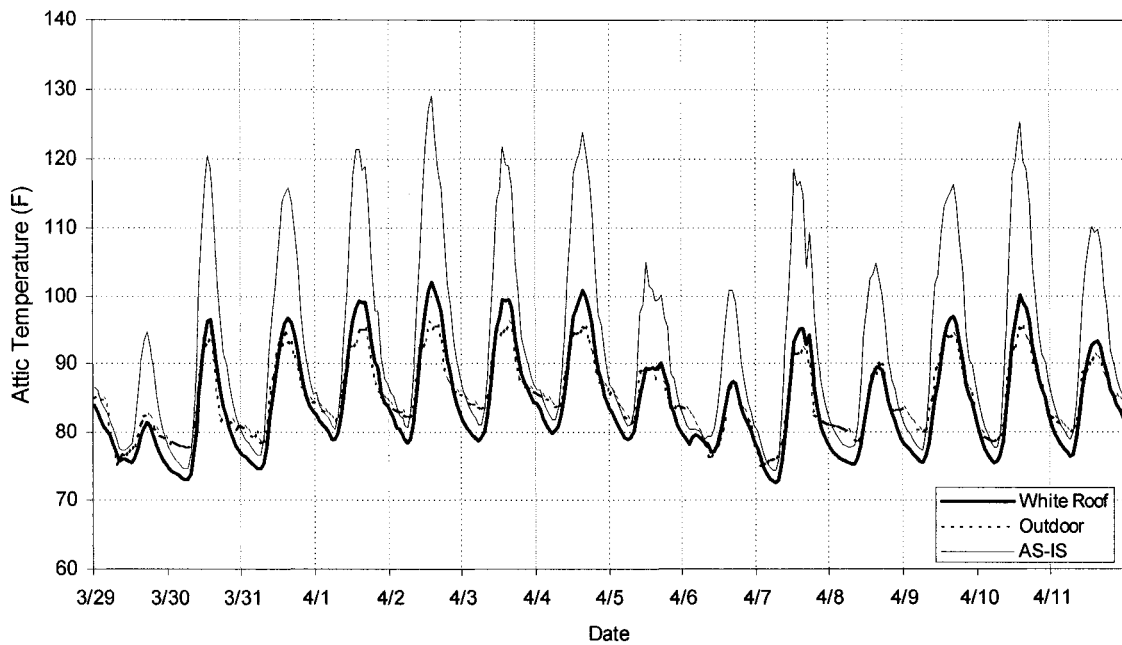


**Figure 6.5a** DOE-2 Simulated Attic Temperature of the Old Temple During a 2-week Period of the Summer: Option 2, Low-Absorption Roof.

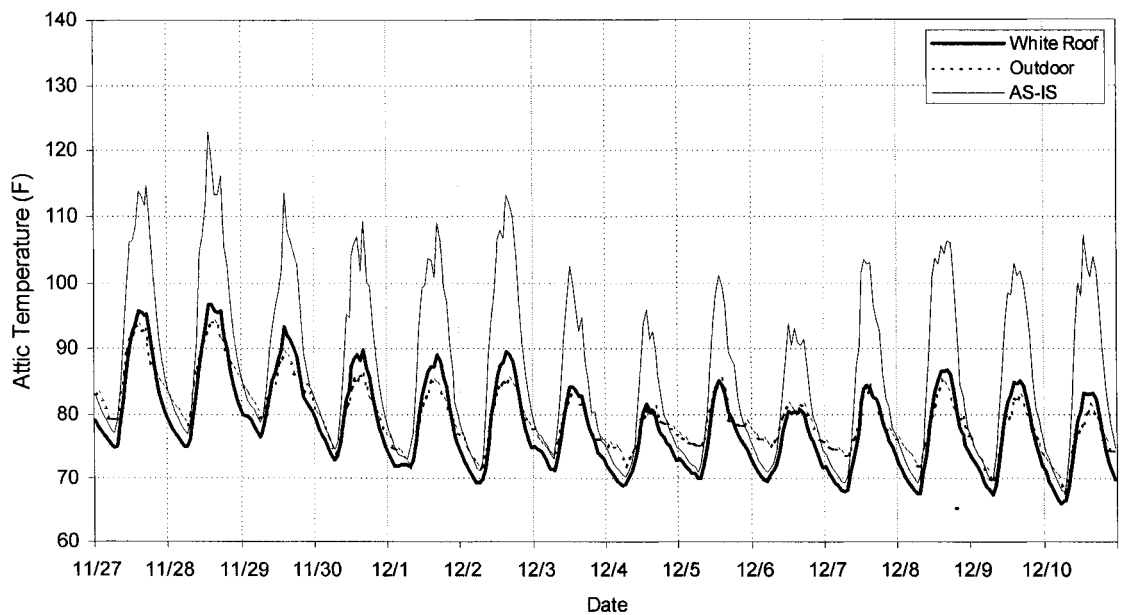


**Figure 6.5b** DOE-2 Simulated Attic Temperature of the Old Temple During a 2-week Period of the Winter: Option 2, Low-Absorption Roof.

The simulation results indicate that the temple performs better in terms of thermal comfort if the low-absorption coating was applied. When compared to the existing temple, Figures 6.3, 6.4a, and 6.4b show that the combination of a low-absorption roof and nighttime-only ventilation would help to reduce peak temperatures in the afternoon by as much as 5 °F all year long. In addition, this would result in a reduction of the average temperature deviation from the outdoors from +1.0 °F to -1.3 °F, which means that on the average, the proposed temple would be cooler than the outside air during certain periods each day. The average temperature deviation from the ground temperature would be +3.0 °F, which is lower than the +5.3 °F of the as-is temple. The indoor temperatures would approach the ground temperature, which is considered the lowest temperatures that the temple could reach under current conditions.

With just the daytime-only or the 24-hour ventilation, the low-absorption roof provides only slightly better indoor conditions. Figures 6.4a and 6.4b indicate that there is only a small reduction in the indoor temperature as compared to the as-is condition if the daytime-only space ventilation is applied. The average temperature deviation from the outdoor temperature is -0.3 °F, which indicates that the indoor temperatures are generally not very different from the outdoor temperatures. This is because of the effect of daytime ventilation. The cooling effect of the thermal storage and thermal insulation of the brick walls and the low-absorption roof would not be effective if too much outdoor air is ventilated into the space. This causes the indoor temperatures to be controlled primarily by the outdoor temperature.

Figures 6.5a and 6.5b show that the peak attic temperatures can be decreased by as much as 30 °F by installing the low-absorption roof. This is to be expected because a smaller amount of heat would be transmitted through the roof. If the attic can be cooled, the thermal condition inside the temple space below will improve.

#### **6.4 Option 3: R-30 Ceiling Insulation**

As mentioned earlier, cooling down the attic significantly would improve the condition inside the temple space. The simulation results from the previous sections demonstrate that with the low-absorption roof, the peak indoor temperatures could be reduced by 5 °F all year round. However, the main objective is to cool down the temple space. Therefore, preventing attic heat

gain to the temple is also important. Aside from the low solar-absorption roof, another option that has the potential to improve indoor comfort is an increase in ceiling insulation on the horizontal surface directly above the temple. It was found that the case-study temple was recently renovated without any kind of ceiling insulation being installed. Therefore, it was necessary to investigate the effects of ceiling insulation in order to compare the results with those of the low-absorption roof for the various ventilation modes (e.g., daytime-only, nighttime-only, and 24-hour).

The simulations were performed using the existing temple configurations, but with the addition of R-30 fiberglass insulation (i.e., 10-inch fiberglass batts with 5.7 lb/ft<sup>3</sup> density, 0.2 Btu/lb·ft·°F specific heat, 0.025 Btu/hr·ft·°F thermal conductivity: ASHRAE 1998; Table 4.3, p. 51) installed on the ceiling of the temple (i.e., the floor of the attic). The results are presented in Figures 6.6, 6.7a, 6.7b, 6.8a, and 6.8b. It was found that the temple performs better in terms of indoor thermal comfort if the R-30 fiberglass insulation was installed. Compared to the condition of the existing temple, Figures 6.6, 6.7a, and 6.7b show that the combination of R-30 ceiling insulation and night ventilation helps to reduce peak temperatures in the afternoon by as much as 5° to 7 °F year around. In addition, this results in the reduction of the average temperature deviation from the outdoors from +1.0 °F to -1.0 °F, which means that on the average, the proposed temple would actually be cooler than the outside. The average temperature deviation from the ground temperature would be +3.3 °F, which is lower than the +5.3 °F of the as-is temple. The indoor temperatures are approaching that of the ground temperature, which is considered the lowest temperature the temple could reach.

With either the daytime-only or 24-hour ventilation, the additional ceiling insulation provides a slightly better indoor conditions. Figures 6.7a and 6.7b indicate that there is a small reduction in the indoor temperature if the daytime-only space ventilation is applied. The average temperature deviation from the outdoor temperature is +0.1 °F, which indicates that the indoor temperature would not be very different from the outdoor temperature. This is because of the effect of daytime ventilation. According to the DOE-2 simulation the cooling effect of thermal storage and thermal insulation in the brick walls and ceiling insulation would deteriorate if too much outdoor air is ventilated into the space. This causes the indoor temperatures to be largely controlled by the outdoor air temperature.

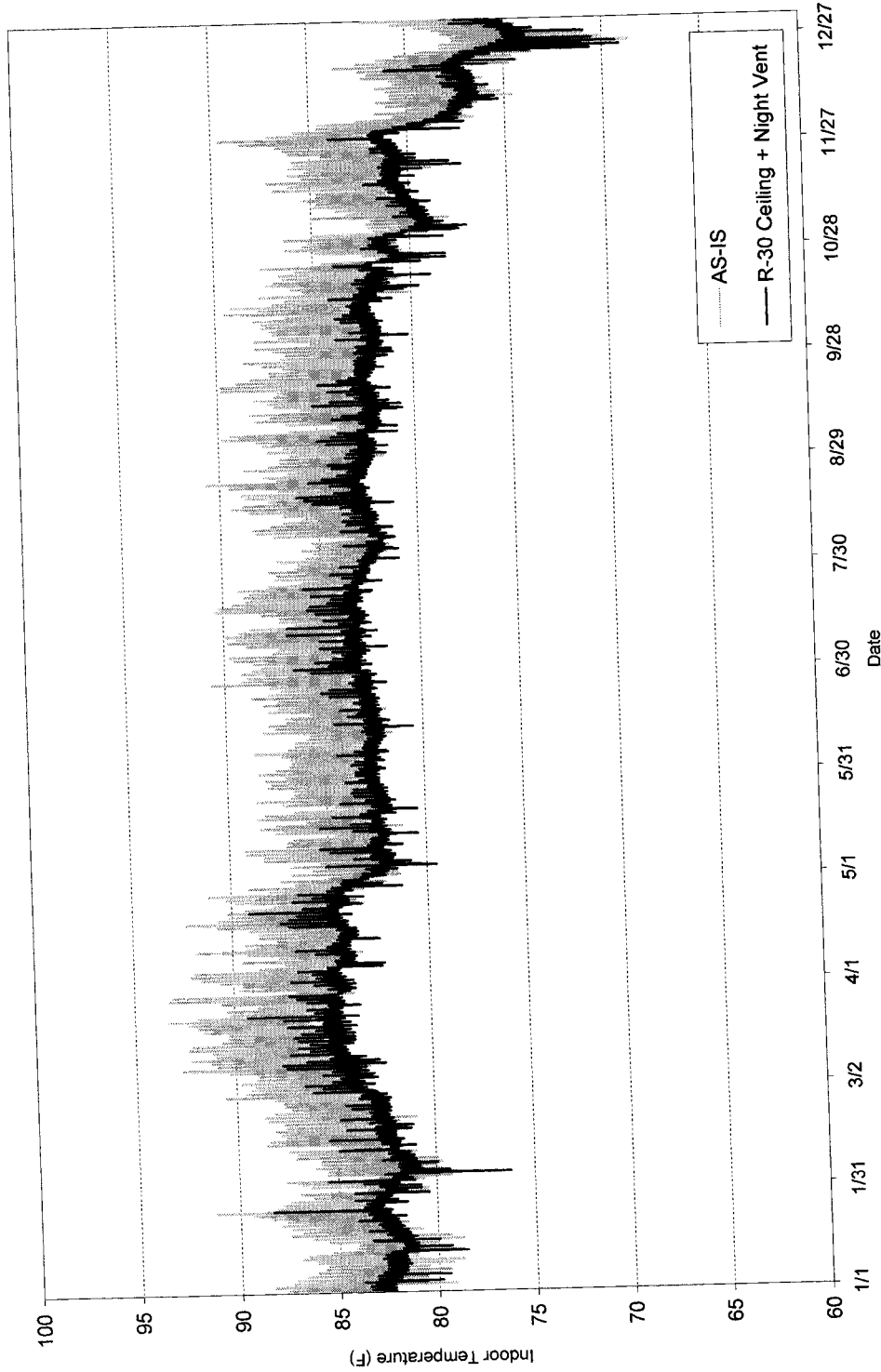


**Figure 6.6** DOE-2 Simulated Indoor Temperatures of the Old Temple for a One-Year Period: As-is Condition VS Option 3, R-30 Ceiling Insulation with Nighttime-Only Space Ventilation.

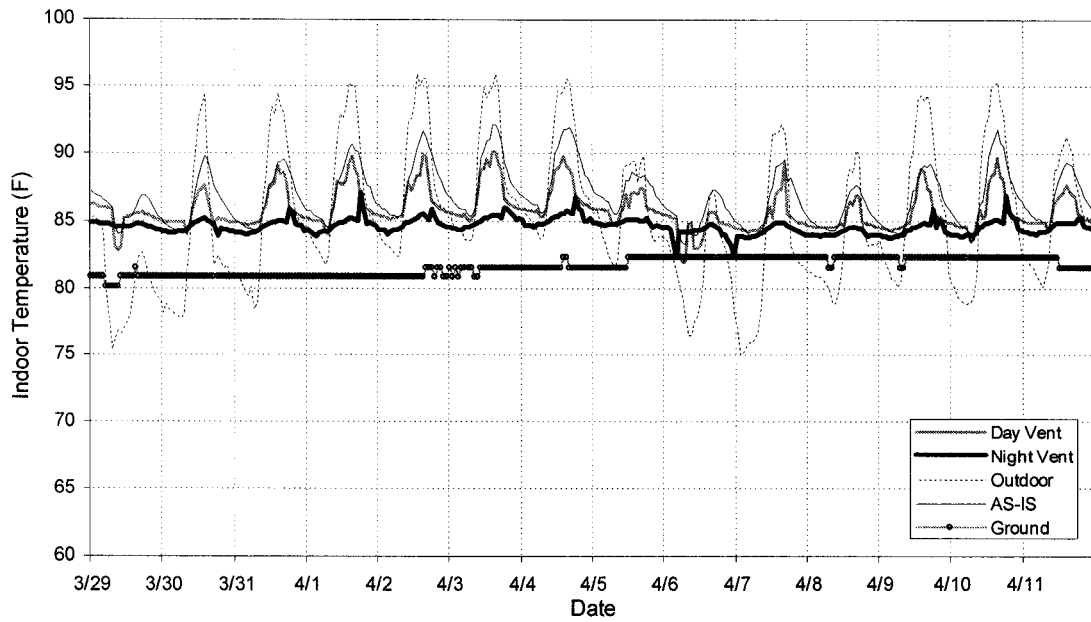


**Figure 6.7a** DOE-2 Simulated and Measured Indoor/Outdoor Conditions of the Old Temple During a 2-week Period of the Summer: Option 3, R-30 Ceiling Insulation.

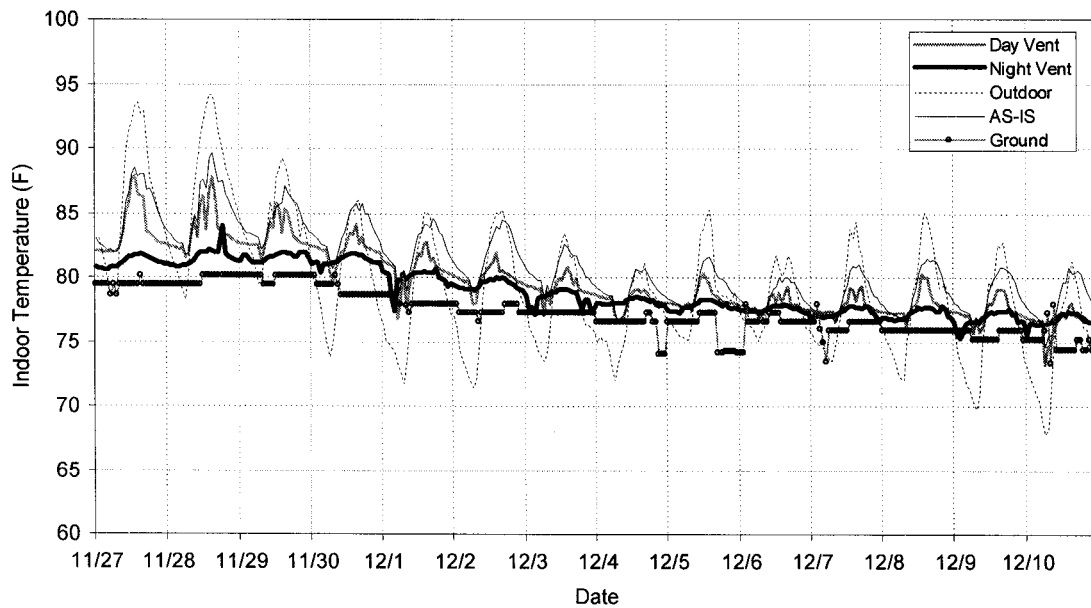


**Figure 6.7b** DOE-2 Simulated and Measured Indoor/Outdoor Conditions of the Old Temple During a 2-week Period of the Winter: Option 3, R-30 Ceiling Insulation.

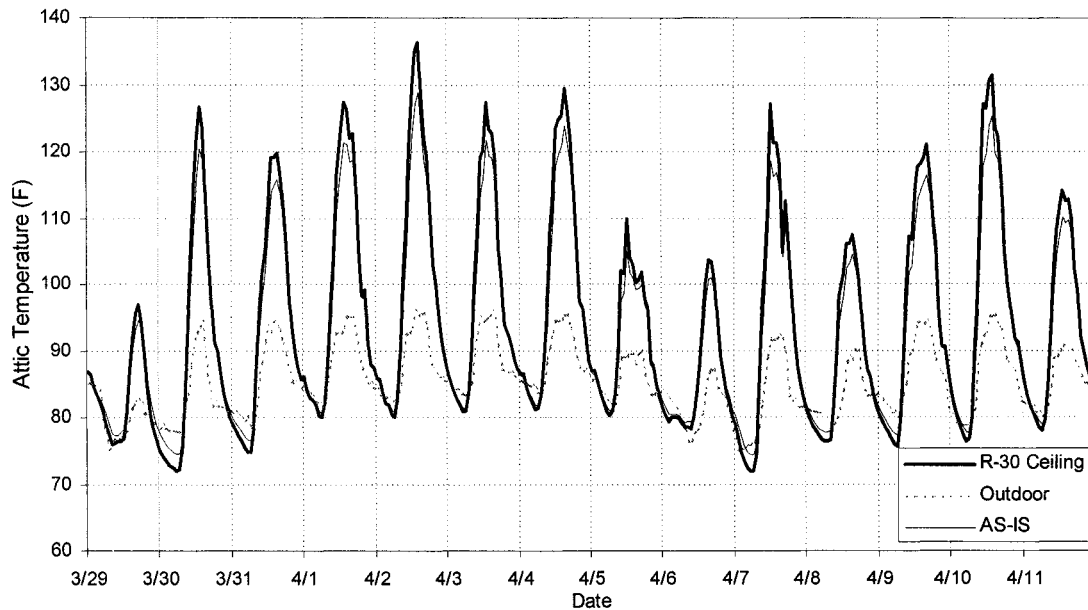


**Figure 6.8a** DOE-2 Simulated Attic Temperature of the Old Temple During a 2-week Period of the Summer: Option 3, R-30 Ceiling Insulation.

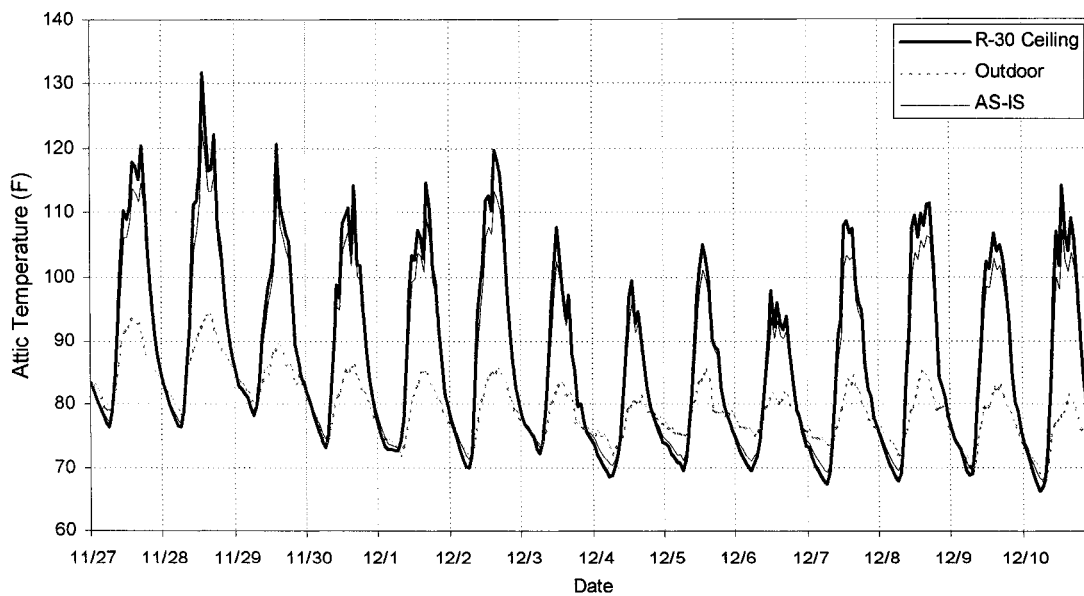


**Figure 6.8b** DOE-2 Simulated Attic Temperature of the Old Temple During a 2-week Period of the Winter: Option 3, R-30 Ceiling Insulation.

In terms of the attic temperature, Figures 6.8a and 6.8b show that the peak attic temperatures would increase by as much as 5 °F if the R-30 ceiling insulation was installed. This is because the same amount of solar heat would transfer into the attic, but a lesser amount could then be transferred into the space through the well-insulated ceiling, leaving heat trapped inside the attic, which raises the temperature.

#### **6.5 Option 4: Shading Devices**

The previous results indicate that a major heat gain to the indoor space is that of the attic. This is due to solar radiation incident upon the roof, and to a lesser extent the conduction heat gain through exterior walls and windows. Thai building designers tend to rely on shading devices as their first and simplest passive cooling method to be used to protect against solar heat gain in the interior space. Even though the exterior walls of the old temple seem to be well-shaded already due to the existence of exterior colonnades, the high exterior walls and the large roof are exposed directly to the sun. Therefore, it is useful to investigate the effects of additional shading devices on the building.

Since the case-study building has only small openings, and parts of these openings are shaded by exterior colonnades, additional shading devices can be designed to shade parts of the exterior walls and roof. Figures 6.9a and 6.9b present a conceptual design of the proposed new shading devices used for these simulations. To protect against direct solar radiation on the sidewalls, a series of overhangs were inserted in between the colonnades on all sides. A small pitched shade was added on top of the existing roof to create the effect of a shaded roof, where the inner layer was shaded from the direct sunlight. Even though the shading devices might not be necessary on the north side of the building, and the design could be different for each direction, the design option demonstrated here applied the same, simple, low profile shading configurations to all sides so that the overall appearance of this traditional architecture could be preserved as much as possible. The simulation results are presented in Figures 6.10, 6.11 a, 6.11b, 6.12a, and 6.12b.



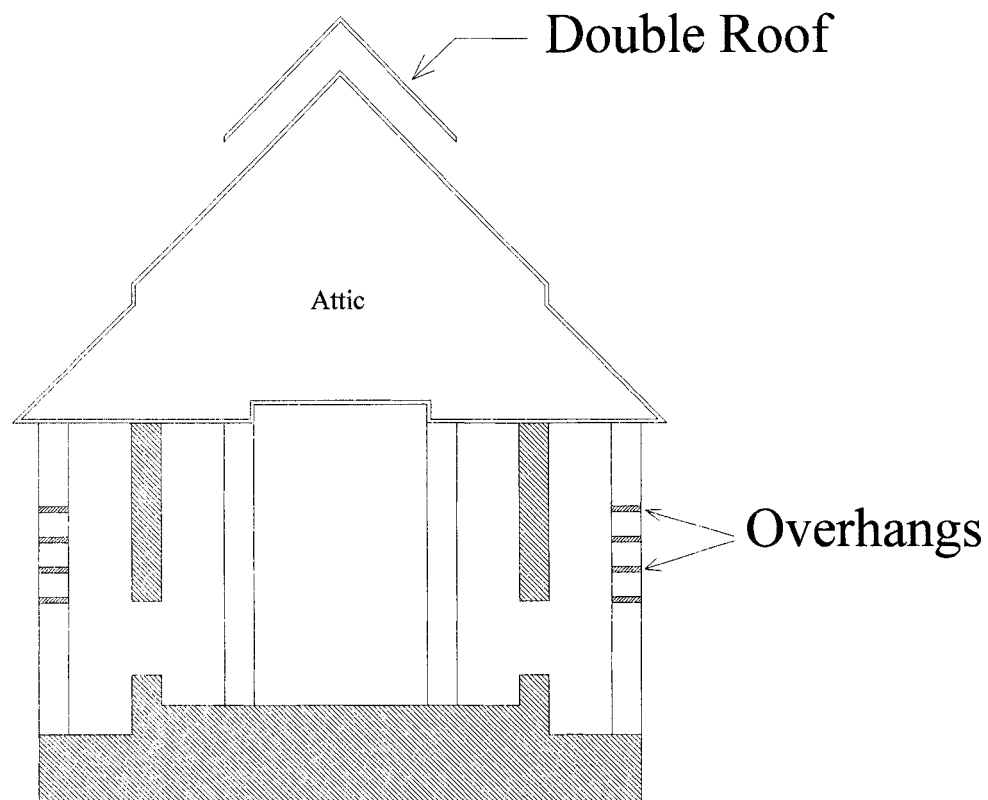


**Figure 6.9a** *Section View of the Old Temple with the Additional Shading Devices. In order to protect against direct solar radiation on the sidewalls, a series of overhangs were inserted in between the colonnades on all sides. A small, pitched shade was added on top of the existing roof to create the effect of a shaded roof, where the inner layer was shaded from the direct sunlight.*

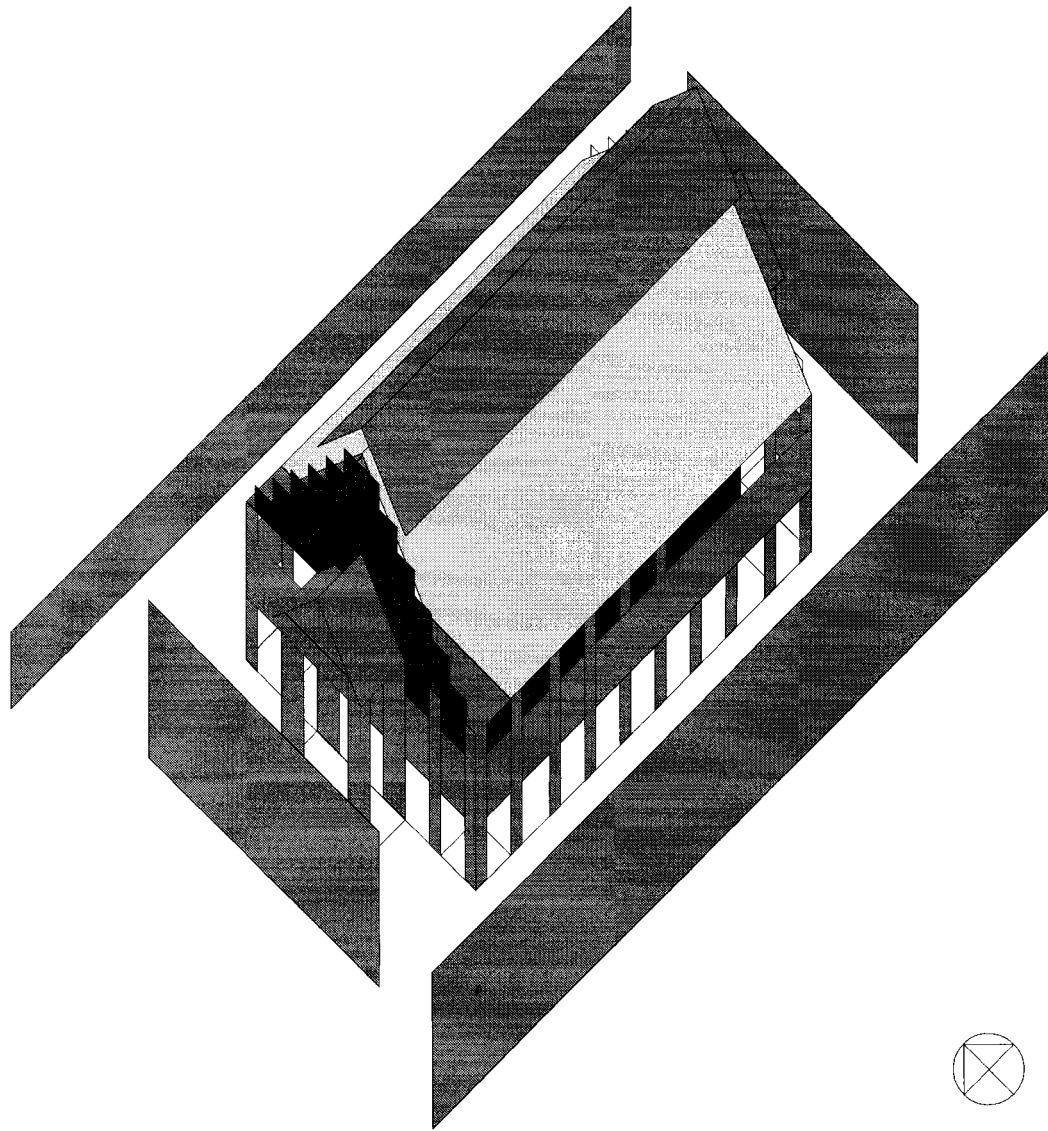


**Figure 6.9b** *DrawBDL Image of the Old Temple with the Additional Shading Devices.*

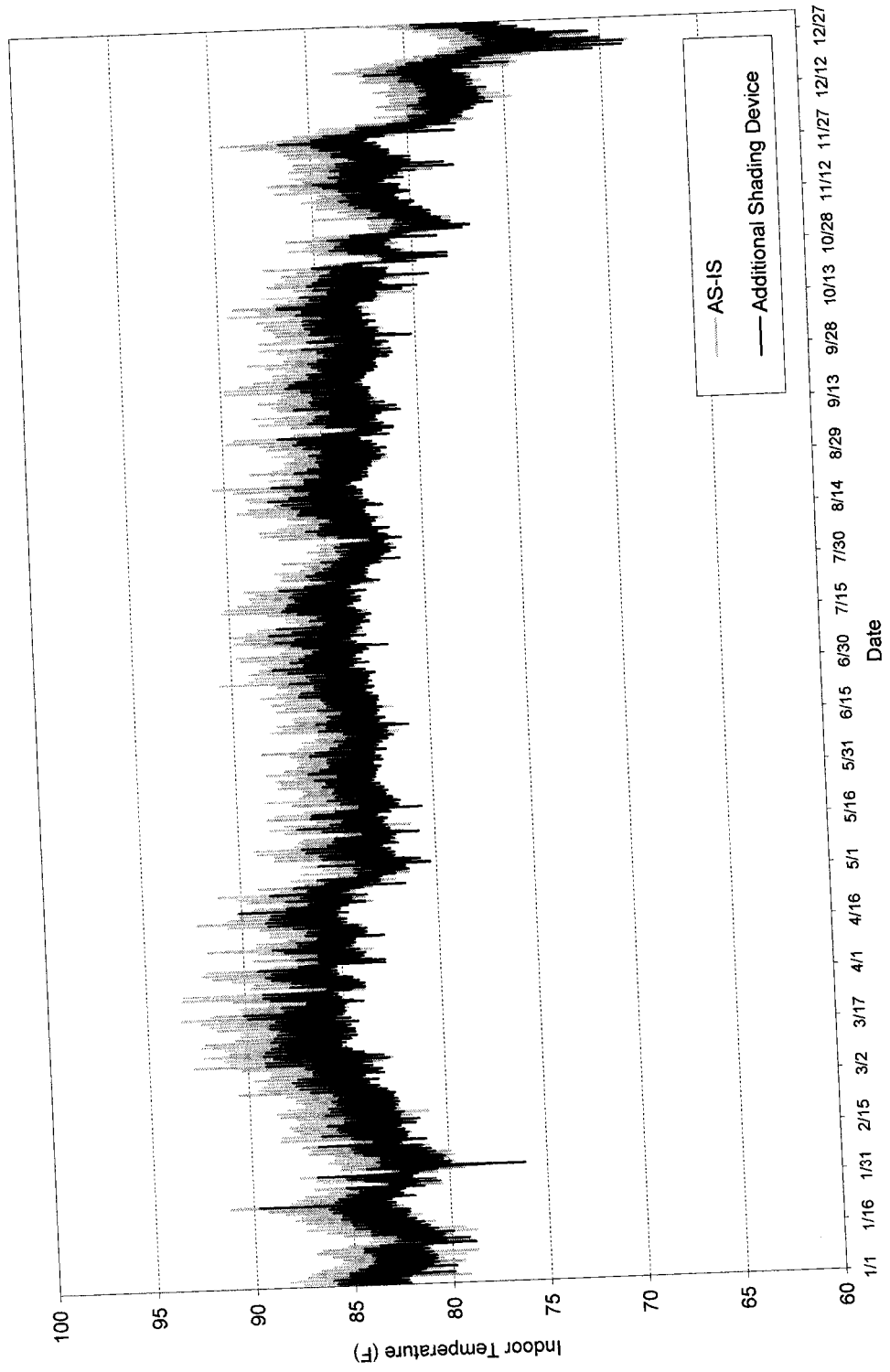


**Figure 6.10** DOE-2 Simulated Indoor Temperatures of the Old Temple for a One-Year Period: As-is Condition VS Option 4, Shading Devices with Nighttime-Only Space Ventilation.

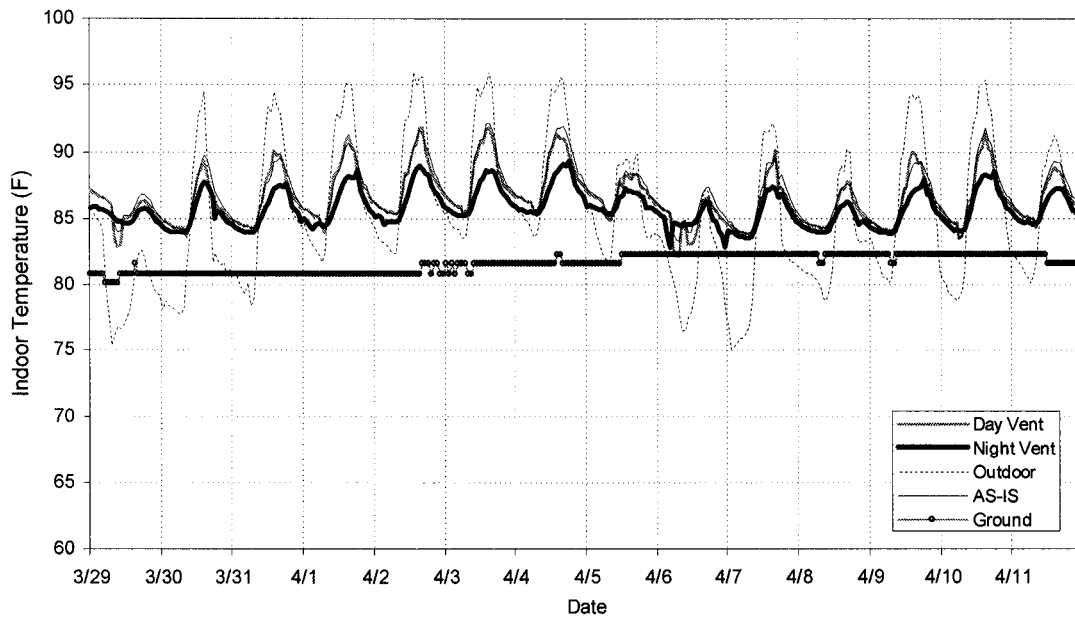


**Figure 6.11a** DOE-2 Simulated and Measured Indoor/Outdoor Conditions of the Old Temple During a 2-week Period of the Summer: Option 4, Shading Devices.

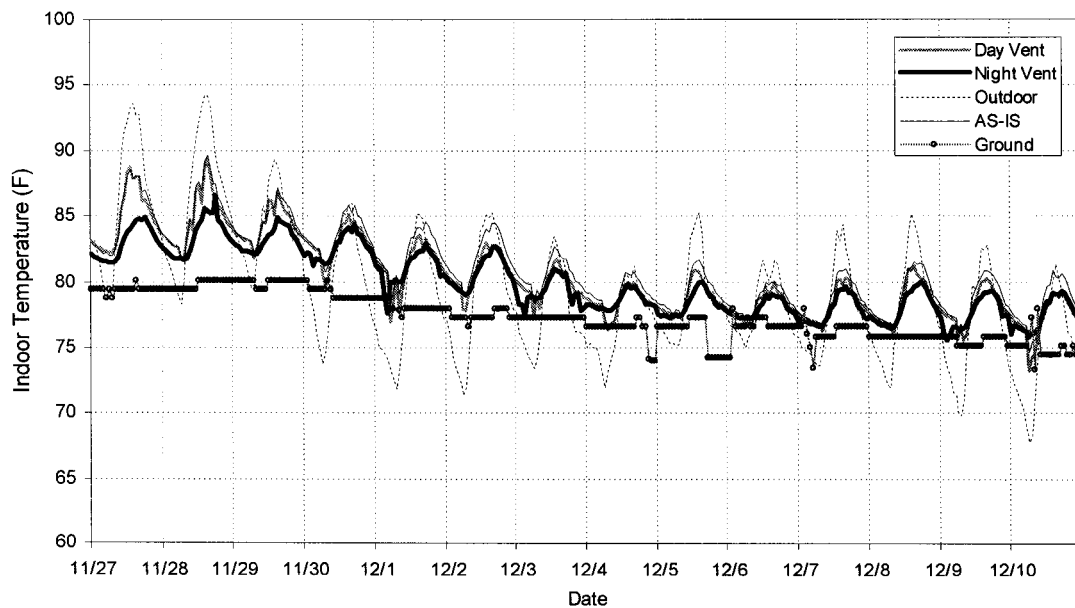


**Figure 6.11b** DOE-2 Simulated and Measured Indoor/Outdoor Conditions of the Old Temple During a 2-week Period of the Winter: Option 4, Shading Devices.

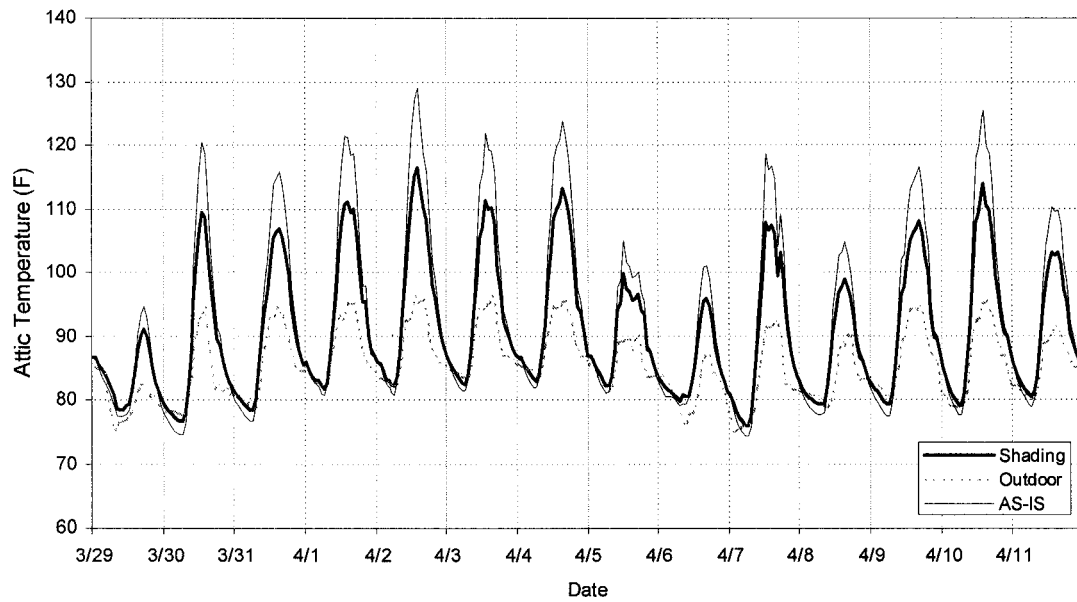


**Figure 6.12a** DOE-2 Simulated Attic Temperature of the Old Temple During a 2-week Period of the Summer: Option 4, Shading Devices.

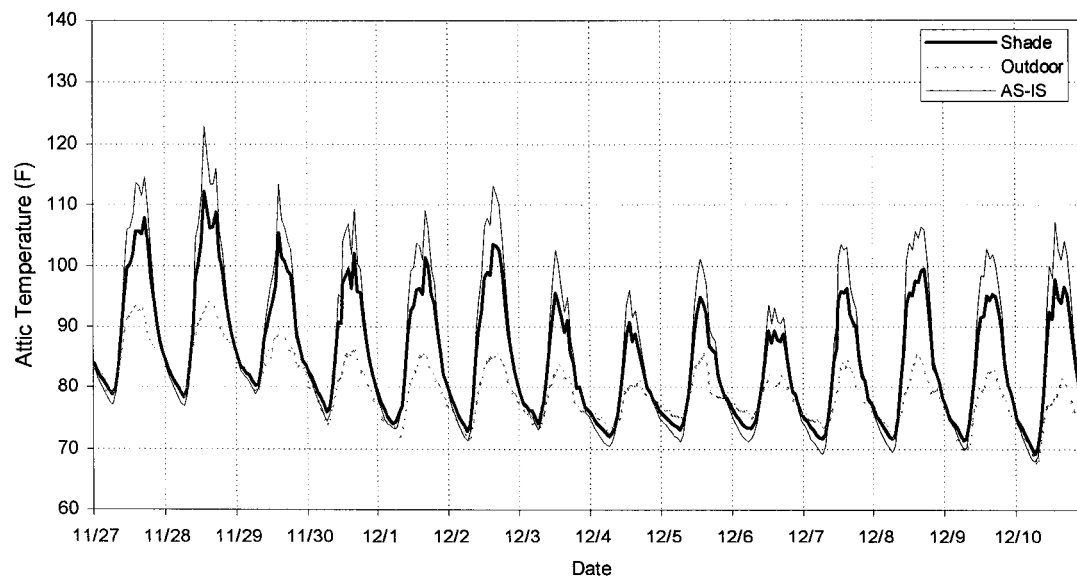


**Figure 6.12b** DOE-2 Simulated Attic Temperature of the Old Temple During a 2-week Period of the Winter: Option 4, Shading Devices.

The simulation results presented in Figures 6.10, 6.11a, and 6.11b indicate that the case-study temple would perform slightly better in terms of indoor thermal comfort if additional shading devices were installed. When compared to the simulation of the existing temple, Figures 6.10, 6.11a, and 6.11b show that a combination of shading devices and night ventilation could help reduce peak temperatures in the temple by as much as 3° to 4 °F on summer days. In addition, this results in a reduction of the average temperature deviation from the outdoor air from +1.0 °F to 0.0 °F, which means that on the average each day, the proposed temple would not be hotter than the outside. The average temperature deviation from the ground temperature is + 4.3 °F, which is lower than the + 5.3 °F of the as-is temple. The indoor temperatures continue to approach the ground temperature, which is considered the lowest temperature the temple could reach during the summer.

With either daytime-only or 24-hour ventilation, the additional shading devices provide only slightly better indoor condition. Figures 6.11a and 6.11b indicate that there are only small reductions in the simulated indoor temperature if the daytime-only space ventilation is applied. The average temperature deviation from the outdoor temperature is + 0.8 °F, which indicates that the indoor temperatures are higher than the outdoor temperature. This is because of the effect of daytime ventilation. When the daytime-only or 24-hour ventilation are used the simulated cooling effects of thermal storage, thermal insulation in the brick walls and the shading devices are not as effective because too much hot outdoor air is drawn into the space. This causes the indoor temperatures to largely be controlled by the outdoor temperature.

In terms of the attic temperature, Figures 6.12a and 6.12b show that the simulated peak attic temperature decreases by as much as 15 °F in the summer, and 10 °F in the winter, if parts of the roof were shaded. This is due to a reduced amount of solar heat gain in the attic. The effects of shading devices would be more noticeable, if the whole roof could be shaded from direct sunlight. However, it would not be economical to build a double-layer roof to cover the entire area. An alternative to this idea would be to have the roof shaded by surrounding structures (e.g., buildings, big trees). This could be possible for temples located in urban areas.

## 6.6 Option 5: Attic Ventilation

As was previously suggested, to avoid attic heat gain the ceiling should be well insulated or the attic cooled by ventilation. One of the methods used that could be used to cool down the attic is the application of a low-absorption coating to the exterior roof surface, as was discussed earlier. Another method would be to use attic ventilation, which would remove heat from the attic as much as possible before it could be transferred to the space below. Attic ventilation can be divided into two types: passive and active. In a passive system, natural ventilation is driven by the buoyancy of the hot air or by the prevailing wind. Therefore, attics need to be designed to take advantage of either condition. For an active system, mechanical equipment (e.g., fans or blowers) would be used to provide the ventilation. However, for Thai-Buddhist temples, the use of mechanical equipment would not be an allowable solution because of the cost of installation and maintenance. Therefore, this proposed design option is concerned only with passive ventilation of the attic. To accomplish this only minor adjustments to the original design of the case-study temple are proposed so that the outside air can be ventilated through the attic driven by natural convection or wind pressure. Figure 6.13a shows a cross section of the proposed design in which inlets and outlets are added to the roof. The DrawBDL output is presented in Figure 6.13b.

From a combined CFD/DOE-2 simulation result, it was found that the average maximum airflow rate in the attic could reach 50 ACH. The hourly simulation results are presented in Figures 6.14, 6.15a, 6.15b, 6.16a, and 6.16b. Unfortunately, it was found that the temple performs only slightly better in terms of simulated indoor thermal comfort if the attic was naturally ventilated with outside air for 24 hours. Compared to the existing temple, Figures 6.14, 6.15a, and 6.15b show that a combination of attic ventilation and nighttime-only space ventilation helps reduce simulated peak temperatures in the afternoon by as much as 3° to 5 °F depending on the season. In addition, this results in the reduction of the average temperature deviation from the outdoors from + 1.0 °F to – 0.3 °F. This means that on the average each day, the proposed temple would be slightly cooler than the outside. The average temperature deviation from the ground temperature is + 4.0 °F, which is lower than the + 5.3 °F of the as-is temple. The simulated indoor temperatures approach the ground temperatures, which are considered the lowest temperature the temple could reach during the summer.

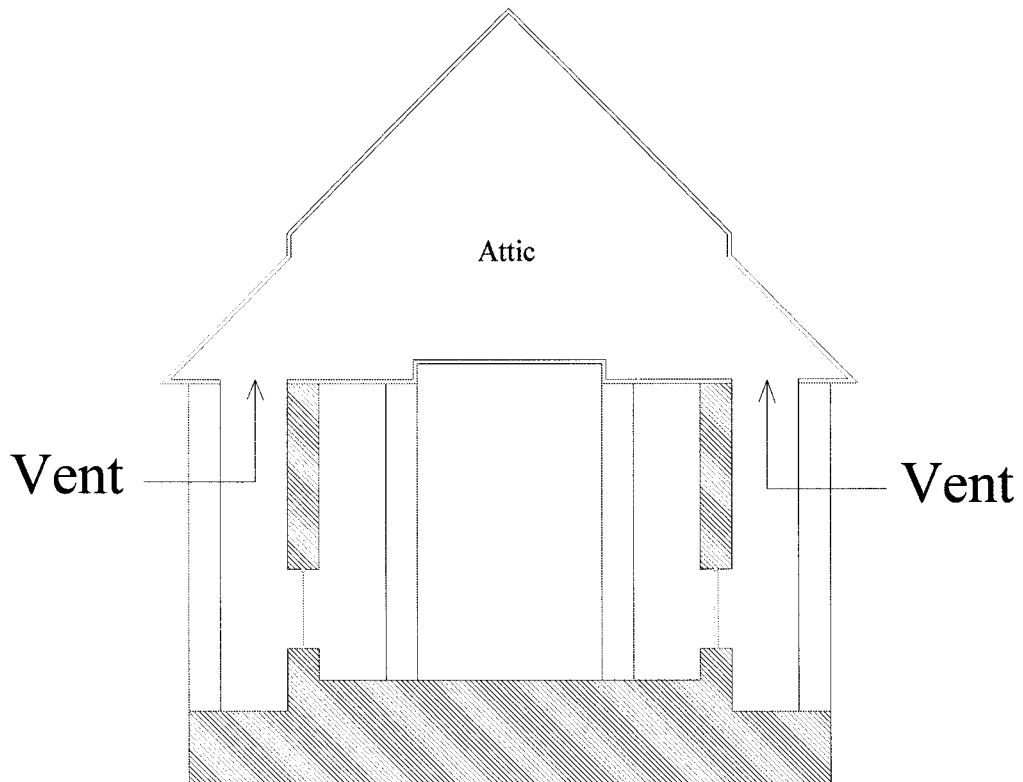


**Figure 6.13a** *Section View of the Old Temple with Attic Ventilation. Using passive ventilation, only minor adjustments to the original building are proposed so that the outside air can be ventilated through the attic driven by wind pressure. The eave area on the north and south sides are open.*



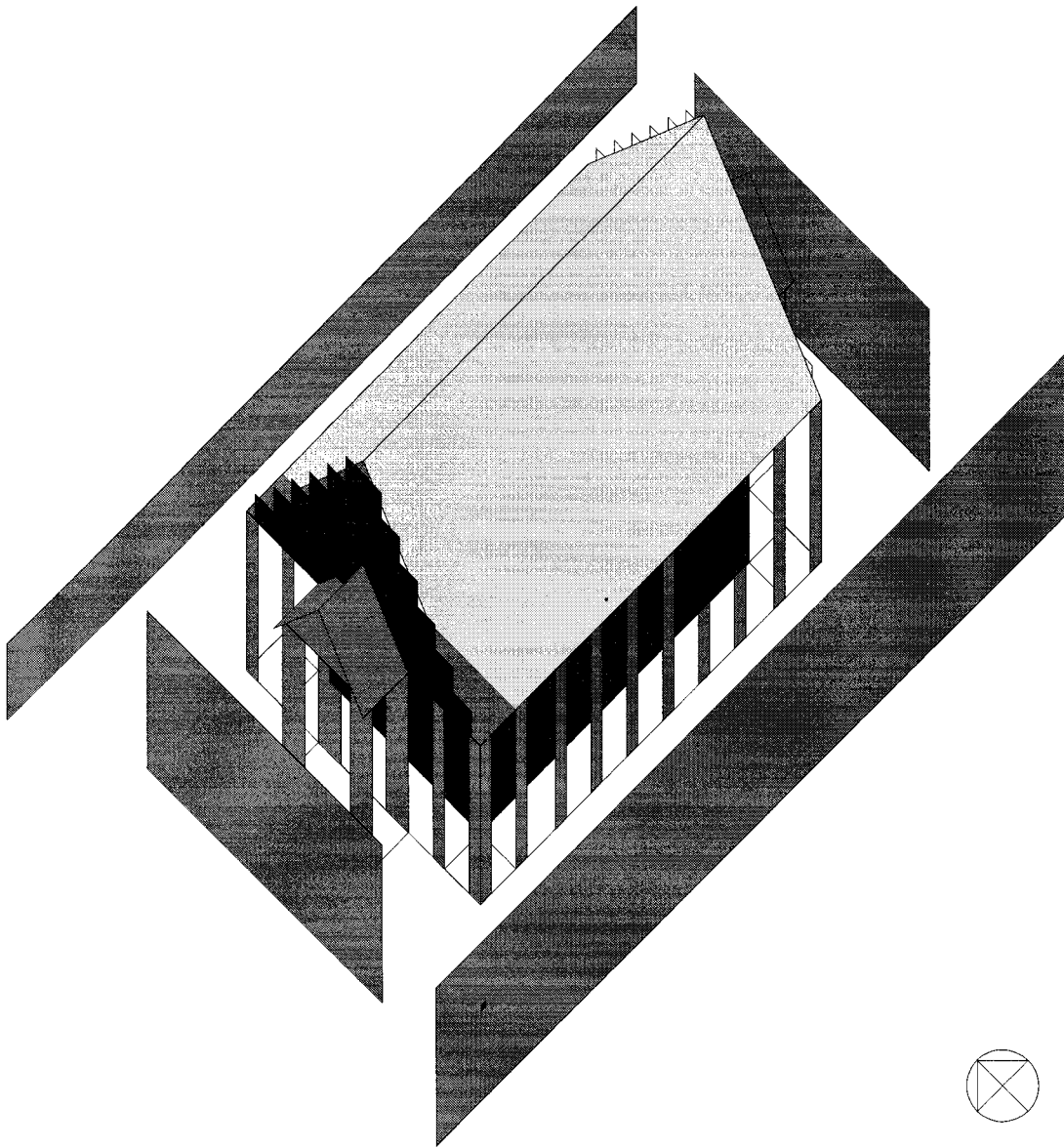


*Figure 6.13b* DrawBDL Image of the Old Temple with Attic Ventilation.

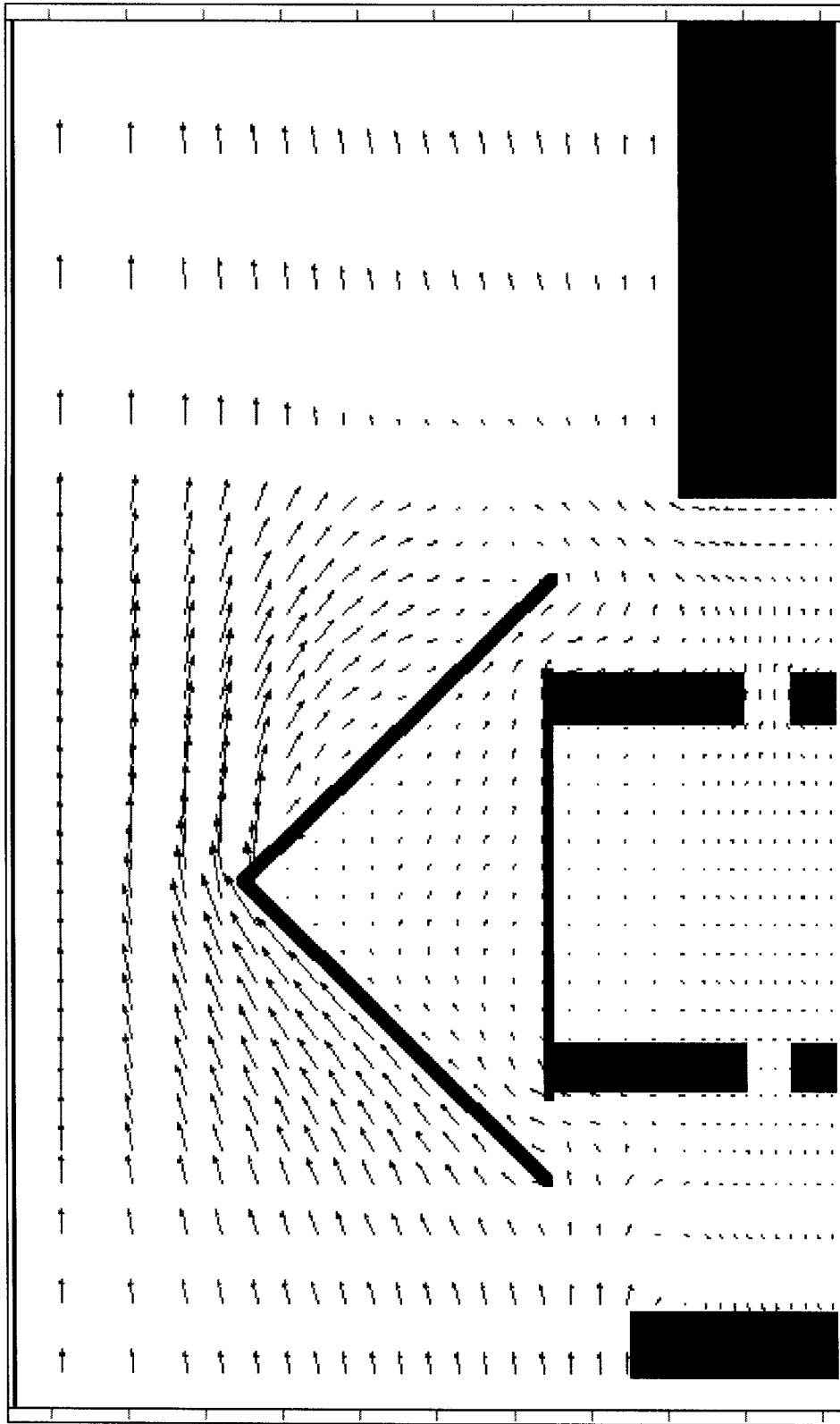


*Figure 6.13c* Vector Plot Showing the Simulated Airflow Through the Building on 04/01/99 at Noon: Option 5, Attic Ventilation.

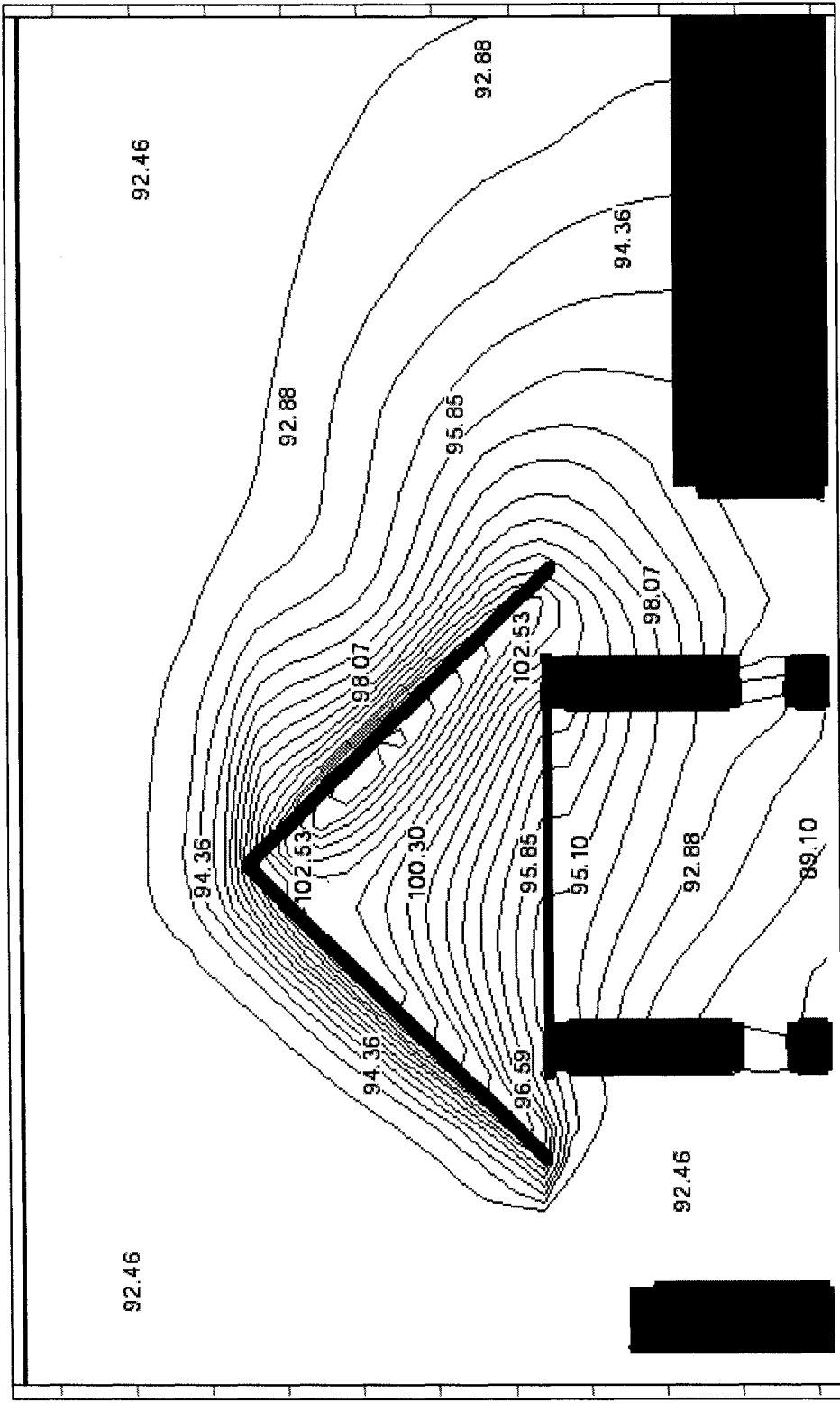


**Figure 6.13d** Contour Plot Showing the Simulated Temperatures of the Air Passing Through the Building on 04/01/99 at Noon: Option 5, Attic Ventilation.

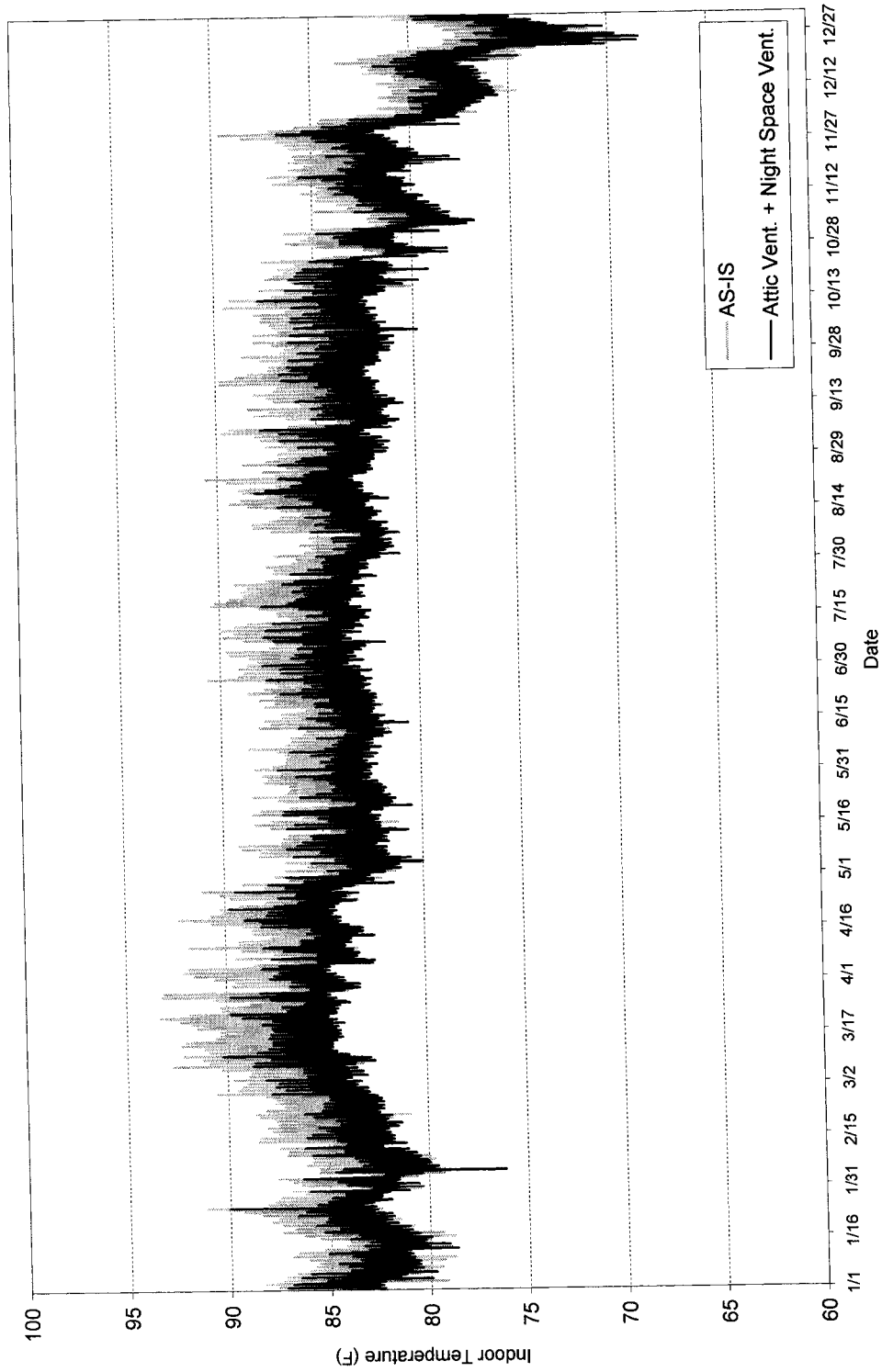


**Figure 6.14** DOE-2 Simulated Indoor Temperatures of the Old Temple for a One-Year Period: As-is Condition VS Option 5, Attic Ventilation with Nighttime-Only Space Ventilation.

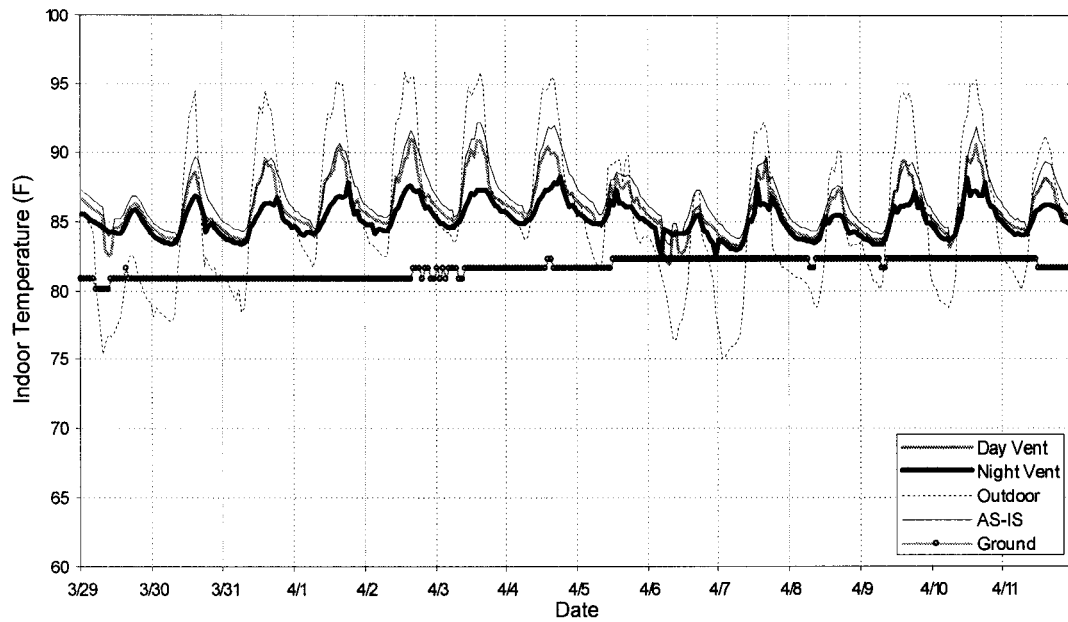


**Figure 6.15a** DOE-2 Simulated and Measured Indoor/Outdoor Conditions of the Old Temple During a 2-week Period of the Summer: Option 5, Attic Ventilation.

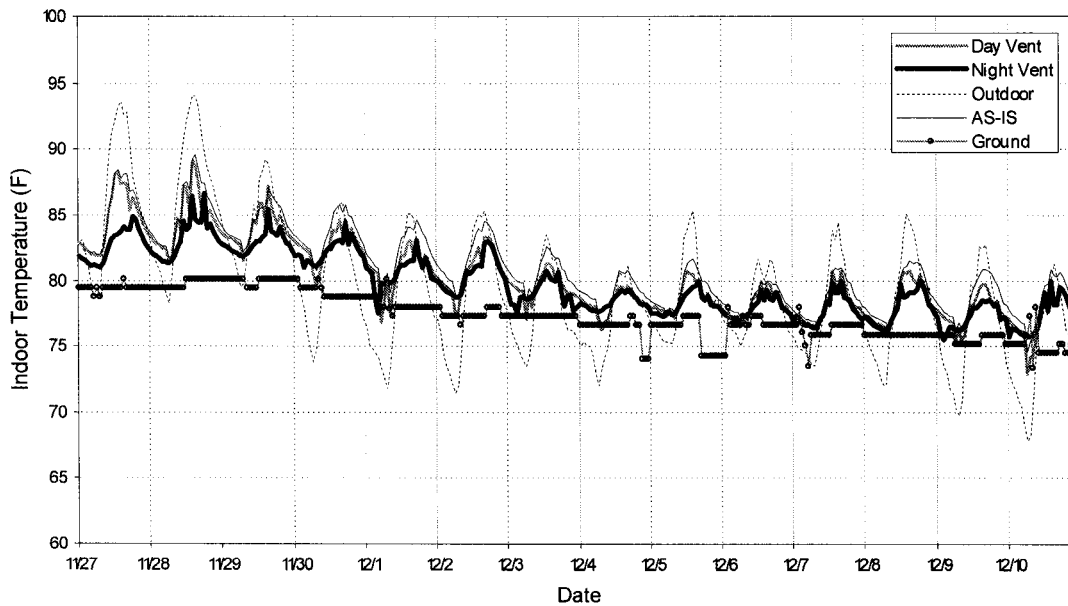


**Figure 6.15b** DOE-2 Simulated and Measured Indoor/Outdoor Conditions of the Old Temple During a 2-week Period of the Winter: Option 5, Attic Ventilation.

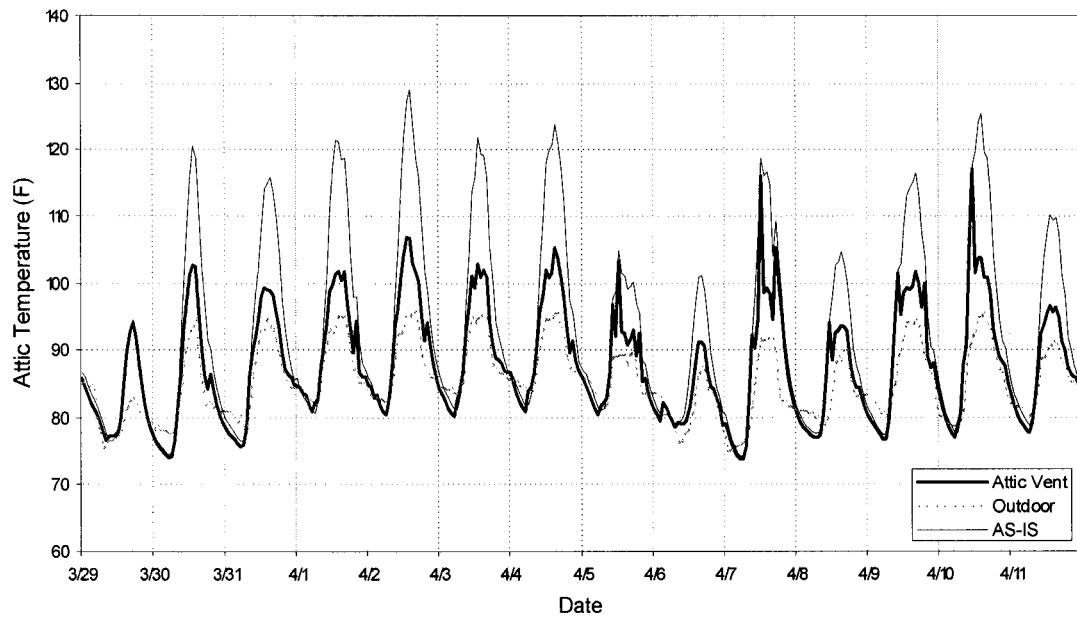


**Figure 6.16a** DOE-2 Simulated Attic Temperature of the Old Temple During a 2-week Period of the Summer: Option 5, Attic Ventilation.

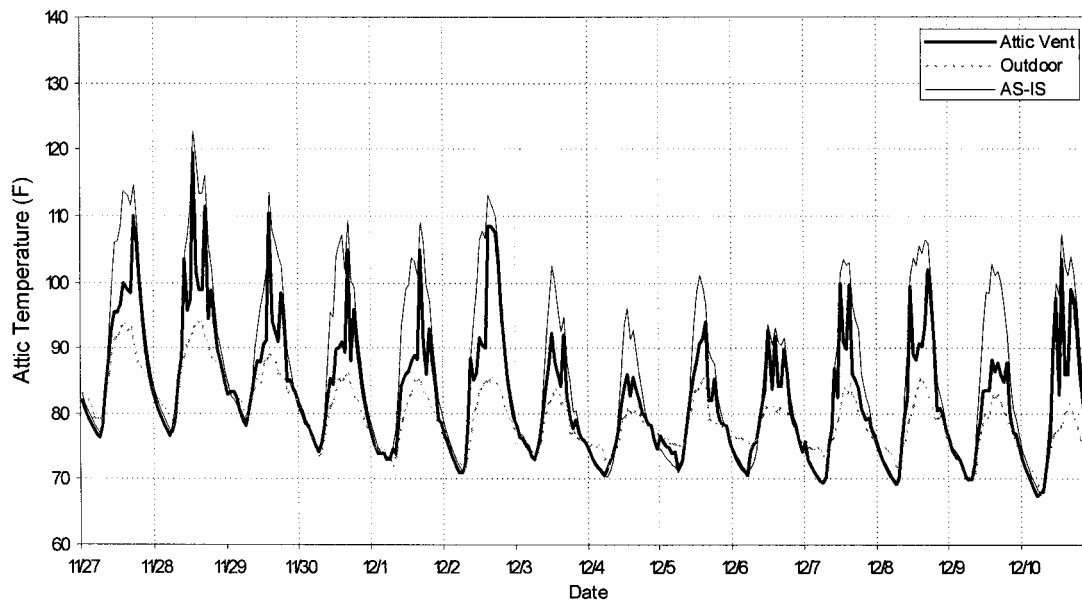


**Figure 6.16b** DOE-2 Simulated Attic Temperature of the Old Temple During a 2-week Period of the Winter: Option 5, Attic Ventilation.

With either the daytime-only or the 24-hour ventilation, the ventilated attic only provides a slightly better simulated indoor condition. Figures 6.15a and 6.15b indicate that there are only small reductions in the simulated indoor temperature if the daytime-only ventilation is applied. The average temperature deviation from the outdoor temperature is + 0.4 °F, which indicates that the indoor air is still slightly warmer than that of the outdoors, most likely due to the effects of the daytime space ventilation. Furthermore, it appears that the cooling effect of thermal storage, insulation in the brick walls, and attic ventilation is not enough to overcome the heat addition from the daytime ventilation, which causes the indoor temperatures to be controlled by the outdoor air temperature.

In terms of simulated attic temperature, Figures 6.16a and 6.16b show that the peak attic temperatures decrease by as much as 25 °F on summer days if the attic was ventilated. However, this effect is not as observable on winter days, which depend on how much warmer the attic is as compared to the outside air. In addition, it should be noted that, in Figures 6.16a and 6.16b, using naturally ventilated attic is effective only when the outdoor wind speeds are high enough to drive the attic ventilation. There were some periods especially in the winter that the wind was calm during the day (i.e., the wind speed data for those hours were 0.0), thus causing the attic to be hot. If the outdoor air was much cooler and mechanical equipment (e.g., whole-house fan) could be used to increase the airflow rate, there is a potential that the attic ventilation could be more effective.

## **6.7 Summary of Optional Designs and Operations**

In the preceding analysis, DOE-2 simulations of four design options with three different ventilation modes were performed, including low solar-absorption roof surfaces, R-30 ceiling insulation, shading devices, and attic ventilation. The objective was to reduce the indoor temperatures to more comfortable levels. Both the peak and annual average indoor temperatures were used to indicate how comfortable the building would be under various designs and ventilation modes. In addition, the average indoor temperature deviations from ground and outdoor temperatures were calculated and used as indicators of how effective each proposed design would be, as compared to the simulated as-is condition. A summary of the results is presented in Table 6.1, Figures 6.17a, 6.17b, Figures 6.18a, 6.18b, Figures 6.19a, and 6.19b.

Figures 6.17 and 6.18 show time-series plots of the simulated indoor temperatures of a building once constructed and operated using these different options, as compared to those of the existing building. Among all the separate design options, it was found that a building constructed with either the white, low-absorption roof or R-30 ceiling insulation have the lowest simulated indoor temperatures. Shading devices and attic ventilation appear to be the least effective options, regardless of which ventilation modes were applied.

In terms of the various ventilation modes, Figures 6.17 and 6.18 demonstrate that nighttime-only ventilation not only reduces peak indoor temperatures, but also the daily indoor temperature fluctuations during the summer. All design options performed much better if the nighttime-only ventilation was used. This is because the outdoors is cooler at night, and ventilating the building with this air helps to remove heat from the building faster, causing the building to be cooler the following morning. If the building is closed during the day, a lesser amount of heat can enter into the building, and the indoor would be cooler. It was also found that the R-30 ceiling insulation option seems to allow the smallest temperature fluctuations, while the white-roof option offers the lowest indoor temperatures, especially at night. However, with the ceiling insulation, it takes longer for the heat in the attic to transfer into the space. With the R-30 fiberglass insulation, the thermal resistance is high enough to delay the heat transfer until the evening when the outside air is cooler, and the attic can lose heat to the ambient.

In terms of the average indoor temperatures presented in Figure 6.19a, the low-absorption roof option seems to perform better than the R-30 ceiling insulation option. However, there is no difference in terms of the peak indoor temperatures between the two options, as shown in Figure 6.19b. It is important to realize that the peak indoor temperatures, which occur in the afternoon, have a direct impact on the thermal comfort of the occupants in the unconditioned buildings. Buildings with low-absorption roofs may be cooler at night, but they are unoccupied during the evening. However, if it turns out that an air-conditioner is installed in the future, the low-absorption roof might be a preferable renovation option because it allows the lowest average indoor temperatures and temperature deviations from the outdoors. Therefore, with a limited construction and maintenance budget, careful decisions regarding both design and renovation must be made based on all possible factors.



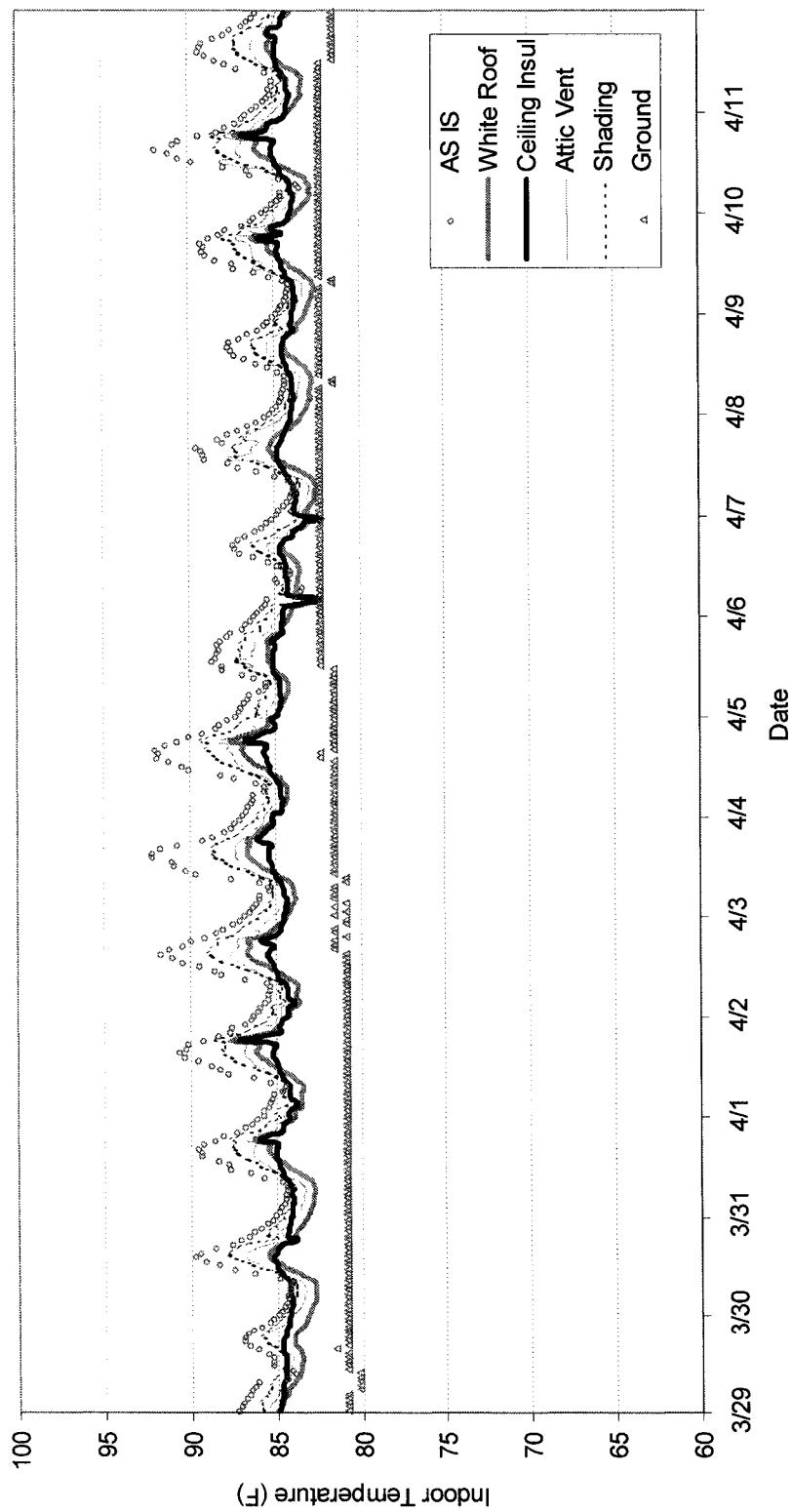


**Figure 6.17a** Comparison of the DOE-2 Simulated Indoor Temperatures of All Design Options with Nighttime-Only Space Ventilation for a 2-Week Period of the Summer.

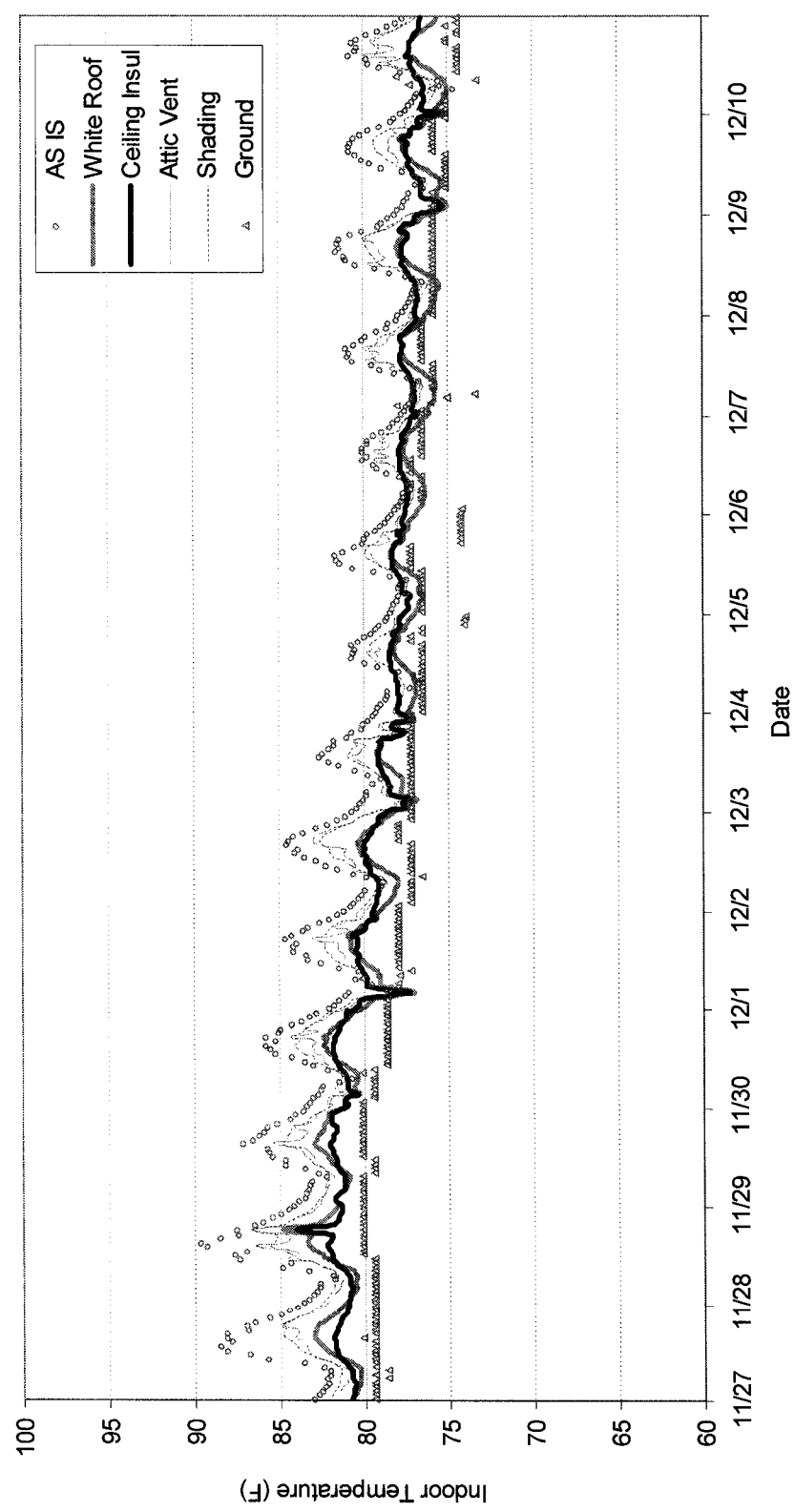


**Figure 6.17b** Comparison of the DOE-2 Simulated Indoor Temperatures of All Design Options with Nighttime-Only Space Ventilation for a 2-Week Period of the Winter.

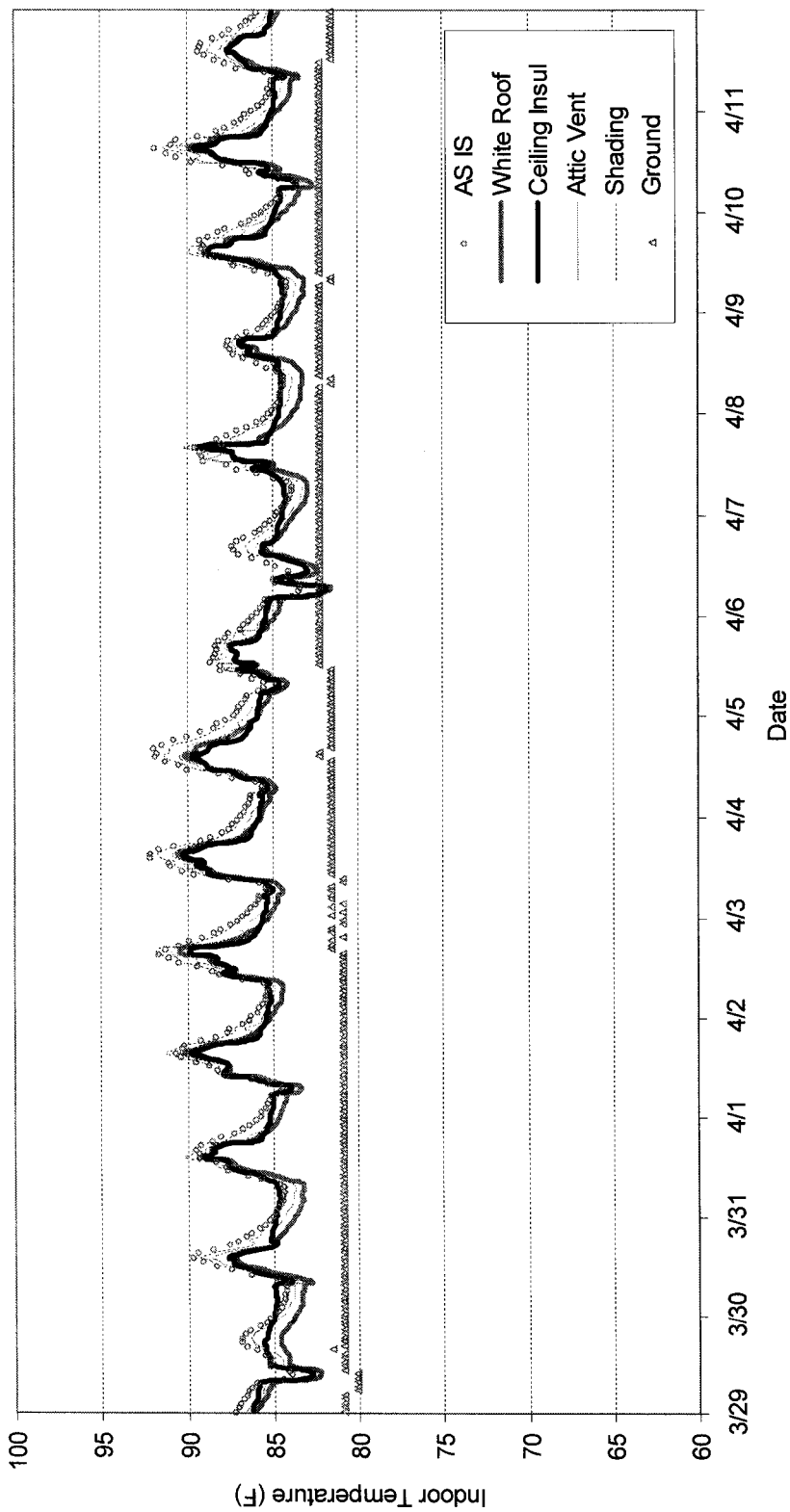


**Figure 6.18a** Comparison of the DOE-2 Simulated Indoor Temperatures of All Design Options with Daytime-Only Space Ventilation for a 2-Week Period of the Summer.

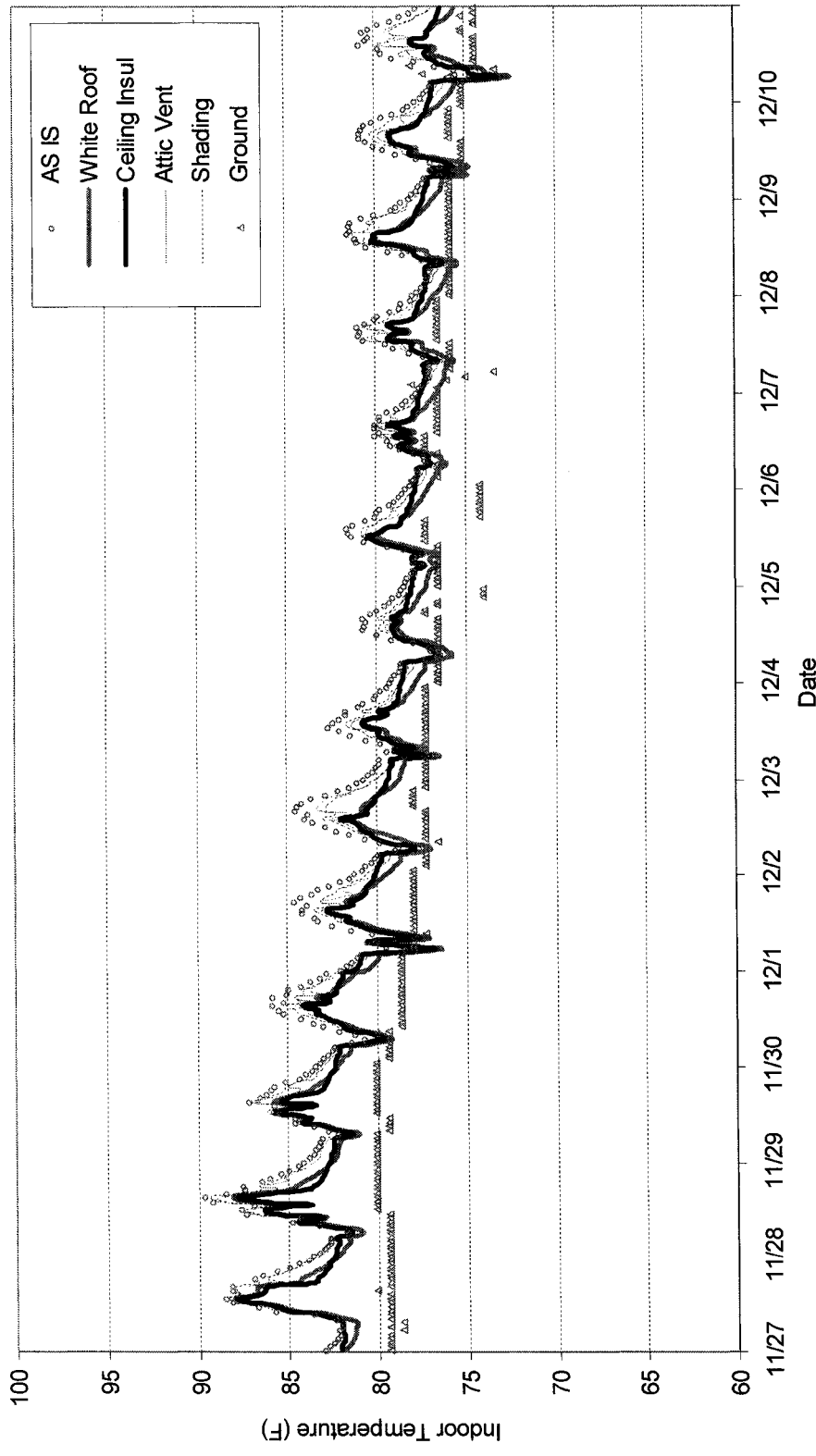


**Figure 6.18b** Comparison of the DOE-2 Simulated Indoor Temperatures of All Design Options with Daytime-Only Space Ventilation for a 2-Week Period of the Winter.

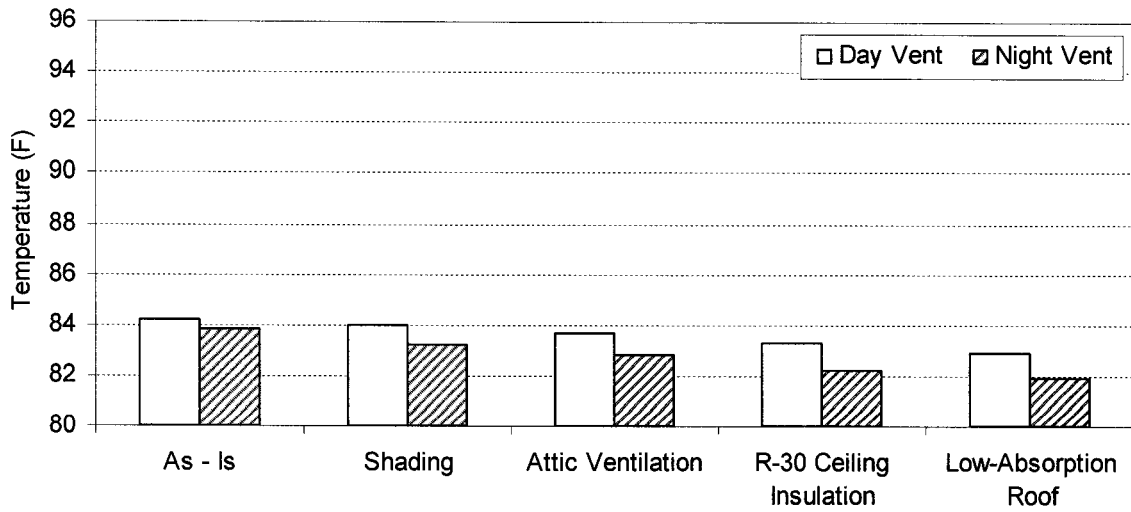


**Figure 6.19a** Annual Average Indoor Temperatures of All Design Options.

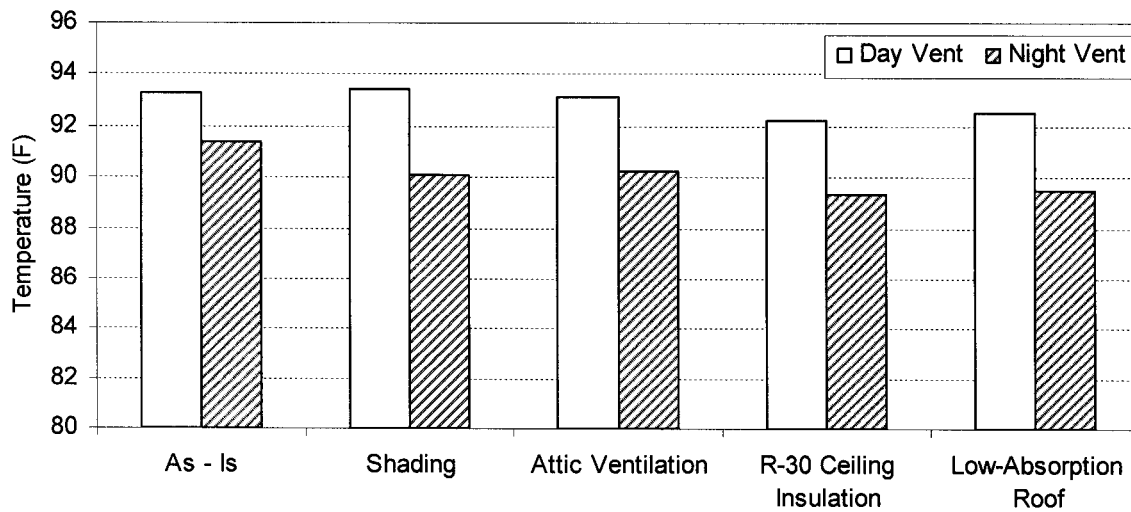


**Figure 6.19b** Annual Maximum Indoor Temperatures of All Design Options.

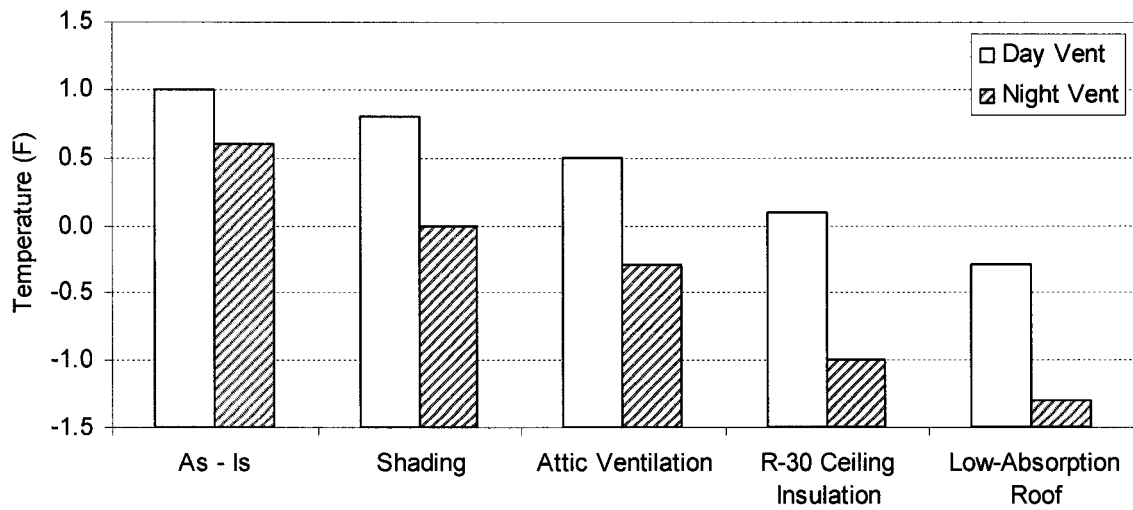


**Figure 6.19c** Annual Average Indoor Temperature Deviations from Outdoor Temperature of All Design Options.

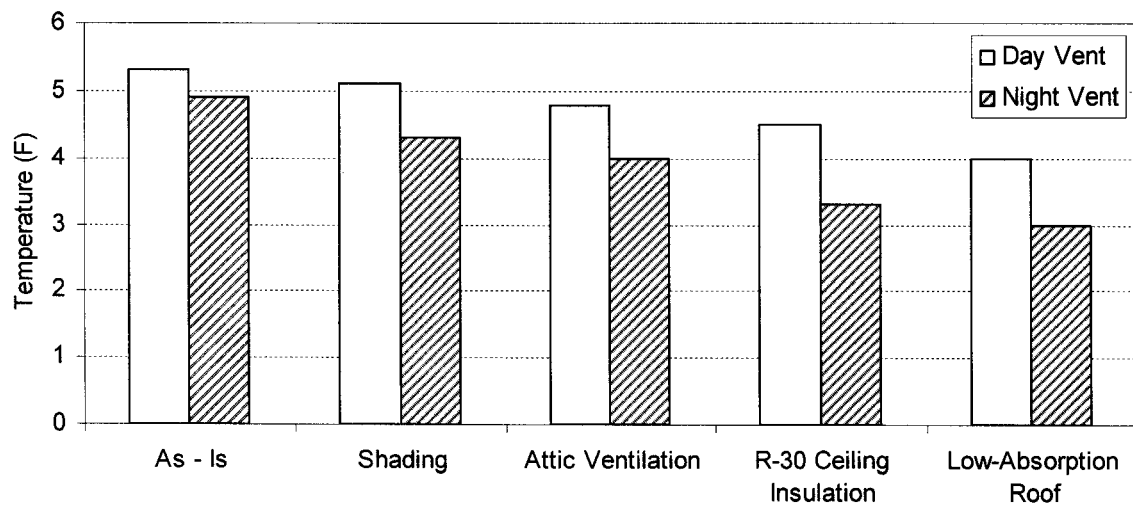


**Figure 6.19d** Annual Average Indoor Temperature Deviations from Ground Temperature of All Design Options.

## CHAPTER VII

### GUIDELINES FOR IMPROVED BUILDING DESIGN AND OPERATION

#### 7.1 Introduction

The preceding chapter has demonstrated the effectiveness of each design and operation option, including its advantages and disadvantages under certain circumstances. The thermal performance of each design option was simulated individually in order to predict what would happen if each was applied to the existing temple. However, to optimize the performance of the building by applying the best possible design and operation, two prototype building designs are proposed here. In this chapter all well-performing options were combined to form the design, construction, and operation of the prototypes, which served as a basis for the guidelines. It is important for this research to realize that thousands of these historic temples are currently preserved in Thailand, and many will be built in the future. Old, historic temples need renovations over time, and future temples will need practical design suggestions to cope with ever-changing construction techniques. Therefore, the guidelines for these prototype buildings need to take into account both new building designs and the possible renovation of older buildings.

The design of the first prototype focuses on how to renovate an existing temple with adjustments that allow for the major building structure and construction materials to be preserved. Almost all of the existing temples in Thailand were constructed with load-bearing masonry walls and columns, framed timber roof structures with red clay-tile roofs, and stone slab-on-ground floors with marble toppings. This construction was used in the old case study temple. Therefore, the first prototype is called the high-mass prototype.

The design of the second prototype focuses on how to design and operate a new temple that will have improved thermal performance, while still conserving the style and functional requirements of this traditional architecture. Presently, new temples in Thailand are constructed with the construction techniques currently found in most commercial and residential buildings. This construction consists of a concrete post-and-beam structure, 4-inch uninsulated masonry

walls, steel roof frames, and sheet metal roof shingles. This construction technique is with that of the newer case study temple, which is a moderately high mass building. In an attempt to reduce embodied energy (Chulsukon 2002) and improve thermal comfort a lightweight or low-mass temple was chosen for the second prototype. The second prototype is called the low-mass prototype.

Both prototypical buildings were designed to have the same architectural footprint as that of the old case-study temple, and to have the same occupancy profile. In the previous chapter, it was shown that the nighttime-only ventilation option tended to create improved thermal performance as compared to both the daytime-only and 24-hour ventilations; therefore, only the nighttime-only ventilation was applied to both prototypes.

## **7.2 Prototype I: High-Mass Temple**

Prototype I is a high-mass temple with nighttime-only ventilation. The proposed construction consists of 2.5-foot-thick load-bearing brick walls and columns, a framed, timber roof structure, a clay-tile roof, and a stone slab-on-grade floor with marble toppings. All major construction techniques are the same as that of the old case-study temple, except that the roof is coated with high reflectance material with a solar absorptance of 0.22. In addition, R-30 fiberglass insulation is added on top of the ceiling, which forms the floor of the attic. A series of overhangs are installed on the colonnades on all sides of the building. In terms of the natural ventilation, all windows are scheduled closed during the day from 6 A.M. to 6 P.M., and open at night from 6 P.M. to 6 A.M. The indoor space is ventilated at night with an estimated maximum airflow rate of 20 ACH. The attic is ventilated 24 hour a day continuously with an estimated maximum airflow rate of 50 ACH. Figure 7.1a shows a cross-section drawing of the first prototype. The CFD results are presented in Figures 7.1b and 7.1c.

The DOE-2/CFD simulation results indicate that the Prototype I temple performs much better in terms of the indoor thermal conditions. Compared to the existing temple, Figures 7.2, 7.3a, and 7.3b show that the afternoon peak temperatures can be reduced by as much as 8 °F for most of the year. The average indoor temperatures are even lower than the lowest indoor temperatures of the existing temple. In addition, it is apparent that the Prototype I building has



fewer indoor temperature fluctuations during the day. The indoor temperatures are maintained closer to the ground temperature, especially during winter days, when they are almost at the same temperature. On the average, Table 7.1 indicates that the Prototype I temple has the average indoor temperature of 81.6 °F, which is 2.6 °F lower than that of the existing temple. The average temperature deviation from the outdoor air is reduced from +1.0 °F to -1.6 °F, which means that on the average, the Prototype I temple is actually cooler than the outside temperatures. The average temperature deviation from the ground temperature is +2.8 °F, which is lower than the +5.3 °F of the existing temple.

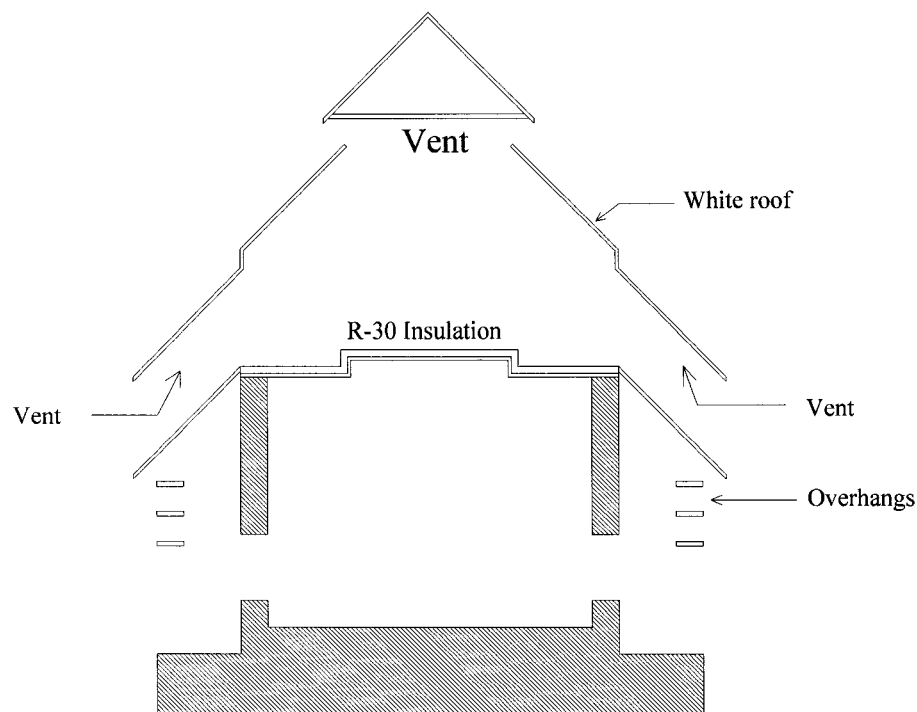


**Figure 7.1a** *Section View of the Prototype I Temple. The proposed construction consists of 2.5-foot-thick load-bearing brick walls and columns, a framed, timber roof structure, a clay-tile roof, and a stone slab-on-grade floor with marble toppings. All major construction techniques are the same as that of the old case-study temple, except that the roof is coated with high reflectance material with a solar absorptance of 0.22. In addition, R-30 fiberglass insulation is added on top of the ceiling, which forms the floor of the attic. A series of overhangs are installed on the colonnades on all sides of the building.*

**TABLE 7.1**  
**Comparisons of Simulation Results of the Prototype I and the As-Is Temple.**

Design options	Space Ventilation Modes		
	As Is (day only) 20 ACH	Night Only 20 ACH	24-Hour 20 ACH
<b>AS - IS Building</b>	Peak Indr.temp = <b>93.3 °F</b> Avg Indr. temp = <b>84.2 °F</b> Dev. from grnd = <b>+ 5.3 °F</b> Dev. from outdr. <b>+ 1.0 °F</b>	Peak Indr.temp = <b>91.4 °F</b> Avg Indr. temp = <b>83.8 °F</b> Dev. from grnd = <b>+ 4.9 °F</b> Dev. from outdr. <b>+ 0.6 °F</b>	Peak Indr.temp = <b>94.2 °F</b> Avg Indr. temp = <b>84.3 °F</b> Dev. from grnd = <b>+ 5.4 °F</b> Dev. from outdr. <b>+ 1.1 °F</b>
<b>Prototype 1: High Mass, White roof, R-30 Ceiling Insulation, Shading</b>	<b>N/A</b>	Peak Indr.temp = <b>89.1 °F</b> Avg Indr. temp = <b>81.6 °F</b> Dev. from grnd = <b>+ 2.8 °F</b> Dev. from outdr. <b>- 1.6 F°</b>	<b>N/A</b>

In terms of the indoor thermal comfort, Figures 7.3c and 7.3d show the psychrometric plots of the simulated indoor conditions of the prototype I temple in the summer and the winter. It was found that the indoor comfort condition of the prototype I temple improves from that of the as-is buildings, as shown in Figures 5.5a and 5.5b. In the summer, the indoor condition is maintained within the Givoni's comfort zone for most of the time. In the winter, the indoor condition is maintained much closer to the ASHRAE's comfort zone. On the average, the hourly indoor temperature appears to be reduced by 5 - 7 °F from that of the as-is building. However, humidity seems to be a problem both in the summer and the winter. Even though the passive cooling techniques used in the prototype I design are successful in preventing heat gain to the building, they do not help remove moisture from the air. The humidity ratios of the indoor air are the same as those outdoors and when the indoor temperature drops by 5 °F, the indoor relative humidity rises by as much as 20 %. Fortunately, this high-humidity condition often occurs in the evening when the building is unoccupied, therefore it has less effect on occupants. Unfortunately, high – humidity conditions can promote the growth of mold and mildew, which can cause rapid deterioration of a building's surface and furnishings. Therefore, further analysis is needed to determine how humidity levels can be reduced.

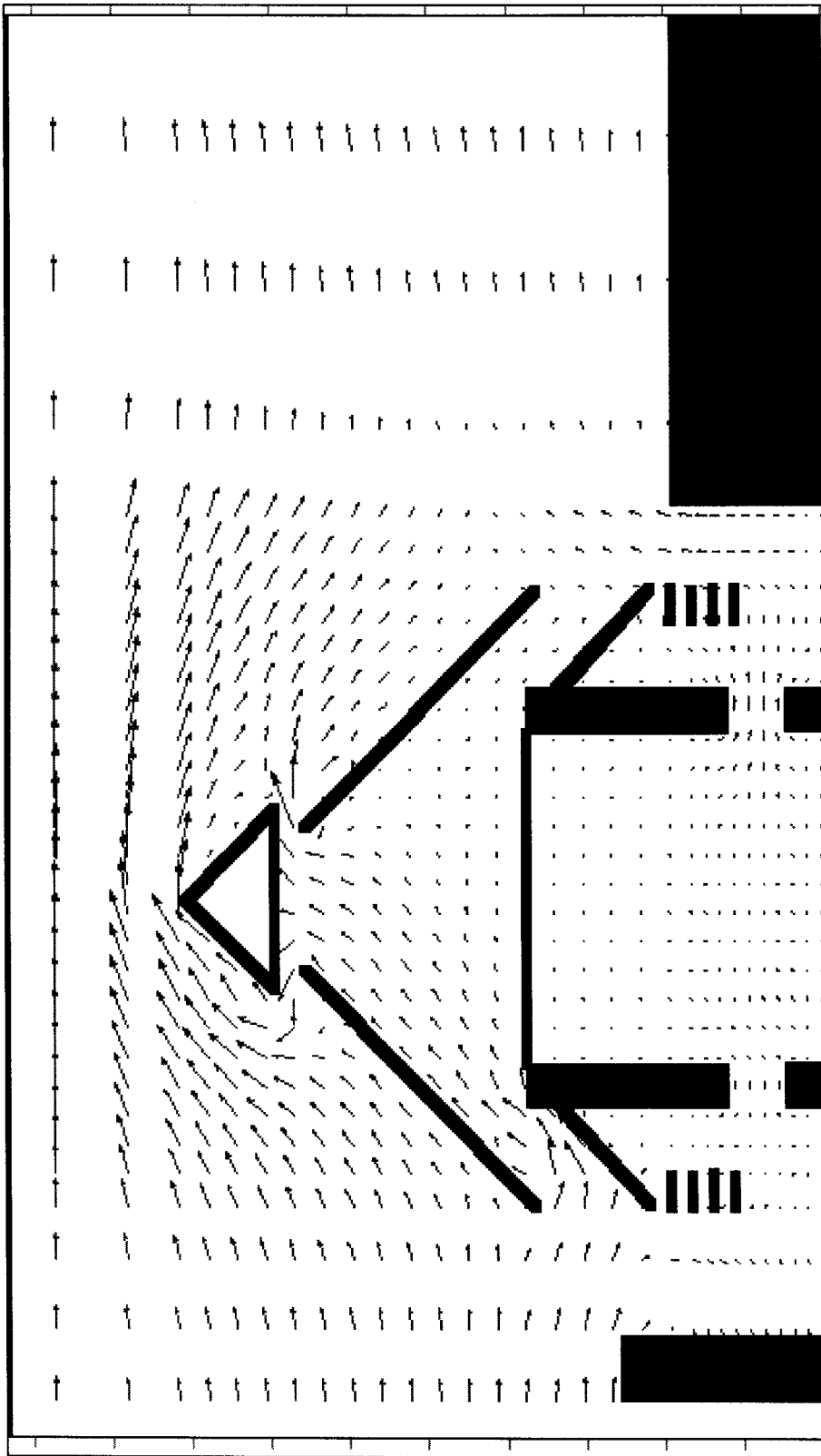


**Figure 7.1b** Vector Plot Showing the Simulated Airflow through the Building on 04/01/99 at Noon: Prototype I, High-Mass Temple.

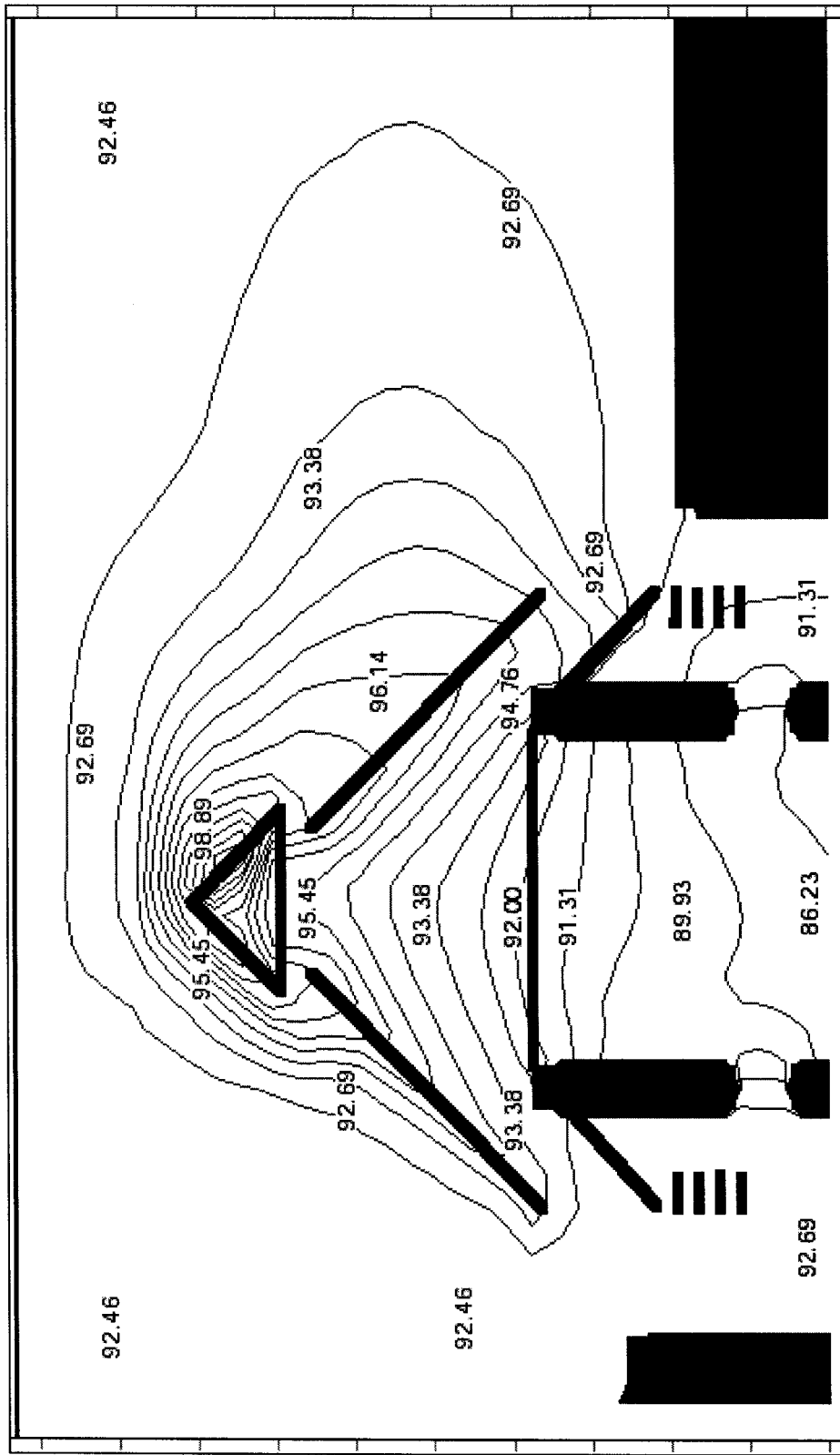


**Figure 7.1c** Contour Plot Showing the Simulated Temperatures of the Air Passing Through the Building on 04/01/99 at Noon: Prototype I, High-Mass Temple.

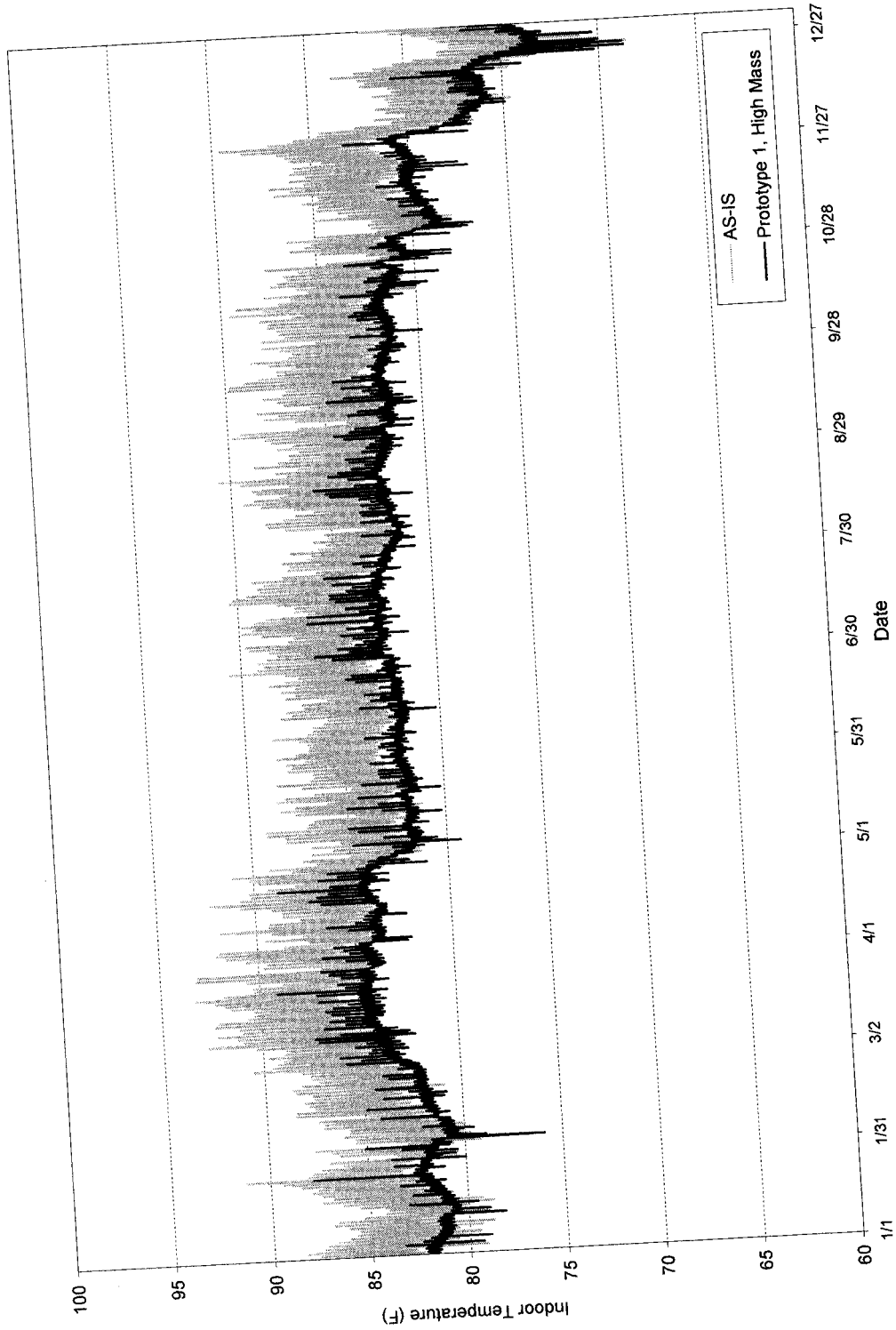


**Figure 7.2** Comparison of the DOE-2 Simulated Indoor Air Temperature of the As-Is Design and Prototype I (High-Mass Design).

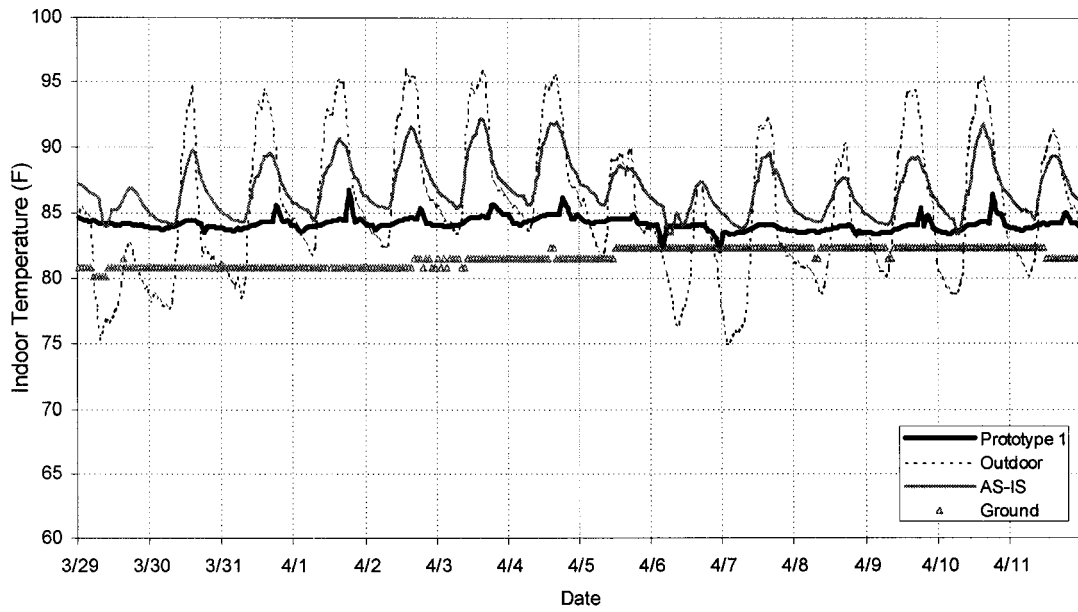


**Figure 7.3a** *DOE-2 Simulated Indoor Temperature of Prototype I (High-Mass Design) for a 2-Week Period of the Summer.*

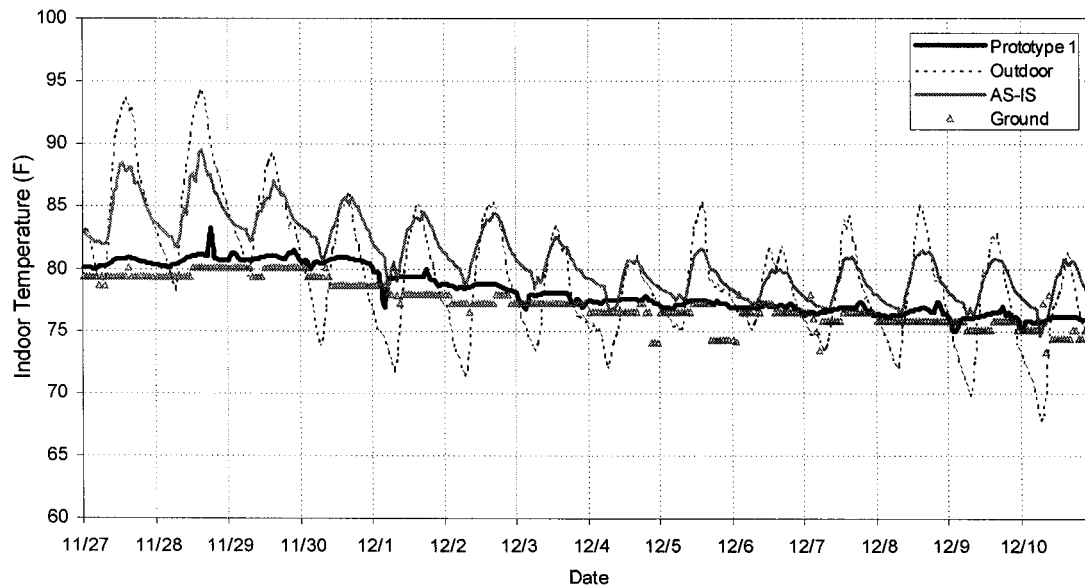


**Figure 7.3b** *DOE-2 Simulated Indoor Temperature of Prototype I (High-Mass Design) for a 2-Week Period of the Winter.*

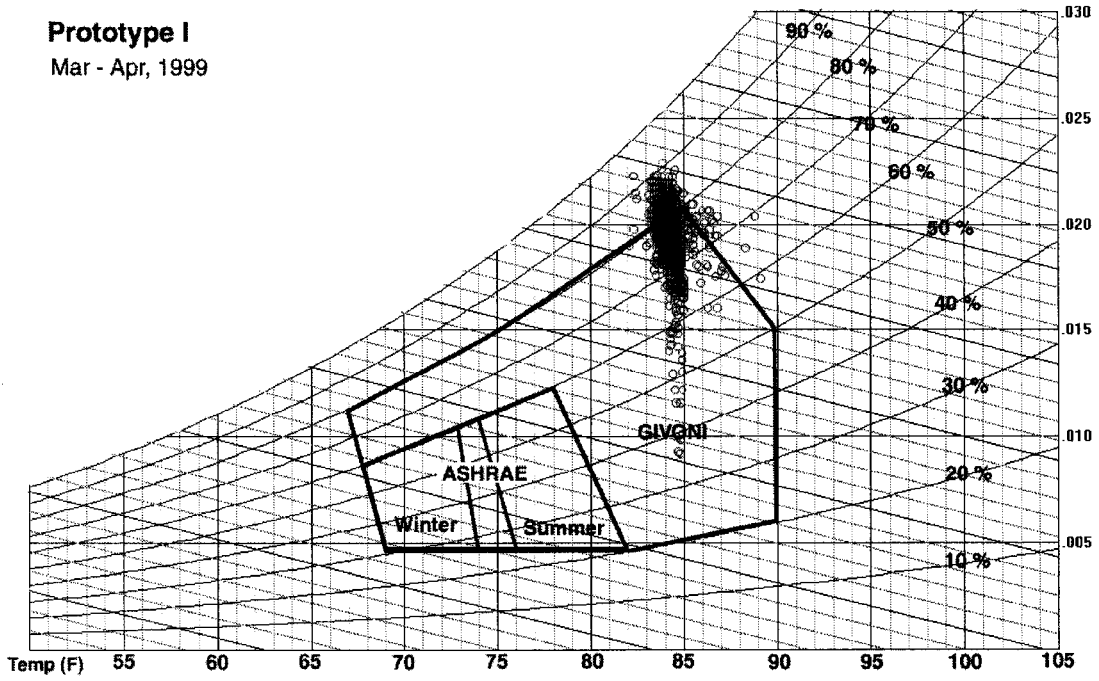


*Figure 7.3c Psychrometric Plot of the Indoor Conditions of the High-Mass Prototype in the Summer.*

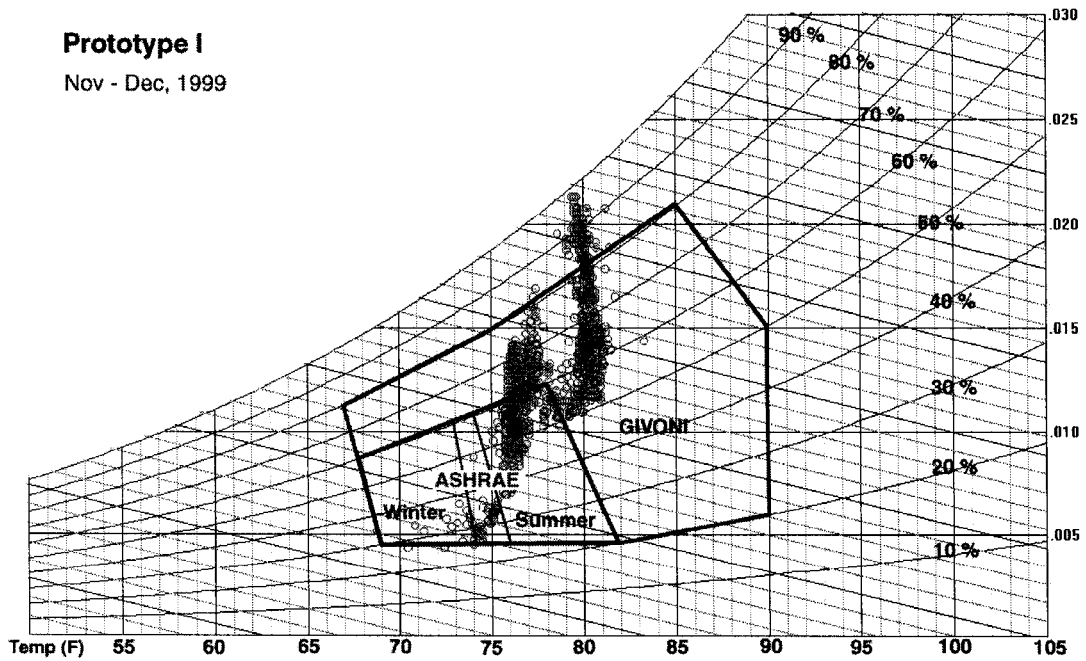


*Figure 7.3d Psychrometric Plot of the Indoor Conditions of the High-Mass Prototype in the Winter.*

### 7.3 Prototype II: Low-Mass Temple

Prototype II is a low-mass temple with nighttime-only ventilation. The proposed construction consists of 4" brick walls with R-11 fiberglass insulation, concrete beams and columns, steel roof frames, a sheet metal roof, and a concrete slab-on-grade floor with marble toppings. The construction is the same as that of the new case study temple, except that the roof is coated with a low-absorption material with a thermal absorptance of 0.22. In addition, R-30 fiberglass insulation is installed on top of the ceiling, which forms the floor of the attic. To provide shades to the sidewalls, a series of overhangs are installed on all sides of the simulated building. In terms of natural ventilation, all windows are closed during the day from 6 A.M. to 6 P.M., and open at night from 6 P.M. to 6 A.M. The indoor space is ventilated at night with an estimated maximum airflow rate of 20 ACH. The attic is ventilated all day with an estimated maximum airflow rate of 50 ACH. Figures 7.4a and 7.4b show a cross-section and an exterior wall detail of the second prototype.

It should be noted that this construction is not really considered low mass if compared to typical low-mass buildings in developed countries, where low - mass buildings are typically built with stucco, metal studs, Styrofoam, and gypsum boards. However, in Thailand, brick masonry wall is still the most widely used construction for small and medium buildings because of its low construction material and labor costs. Exterior insulation and finishing systems (EIFS) have just been introduced to Thailand since the last decade. Unfortunately, this is considered expensive and requires knowledgeable construction labor. However, Boonyatikarn (1999) showed that this system works well in residential buildings in Thailand. Therefore, it is recommended that the performance of this wall system be investigated for use with the Thai Buddhist temples in the future.



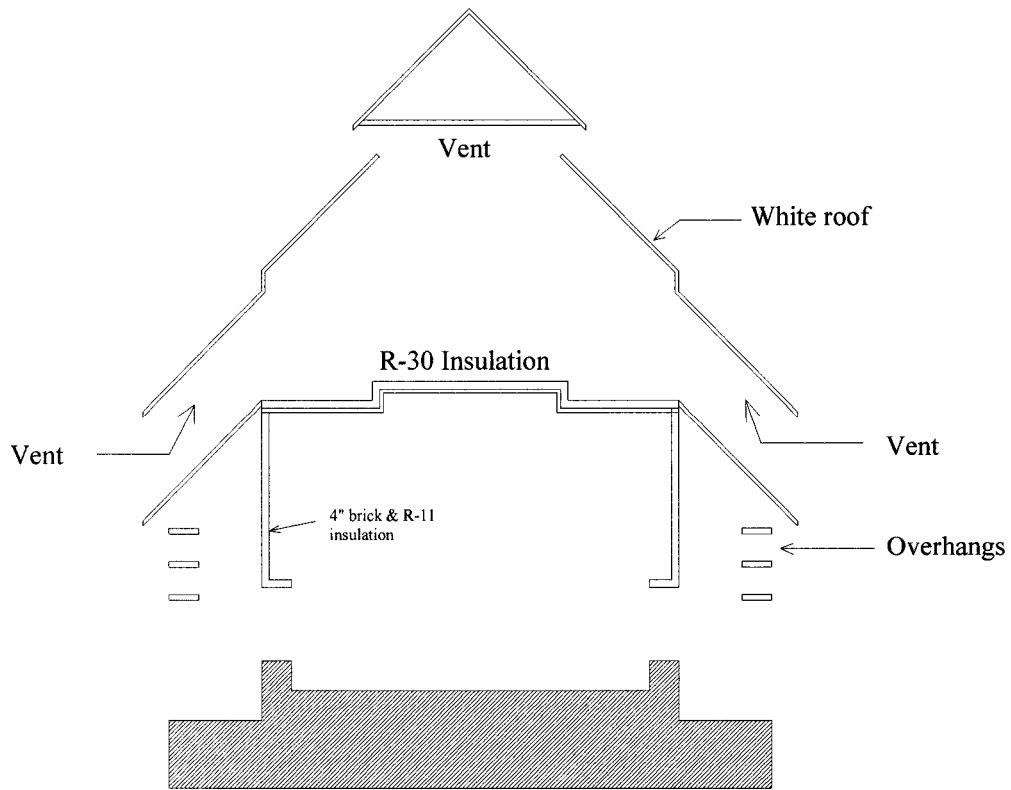


**Figure 7.4a** *Section View of the Prototype II Temple. The construction consists of 4" brick walls with R-11 fiberglass insulation, concrete beams and columns, steel roof frames, a sheet metal roof, and a concrete slab-on-grade floor with marble toppings. The roof is coated with a low-absorption material with a thermal absorptance of 0.22. R-30 fiberglass insulation is installed on top of the ceiling inside the attic, and a series of overhangs are installed on all sides of the building.*

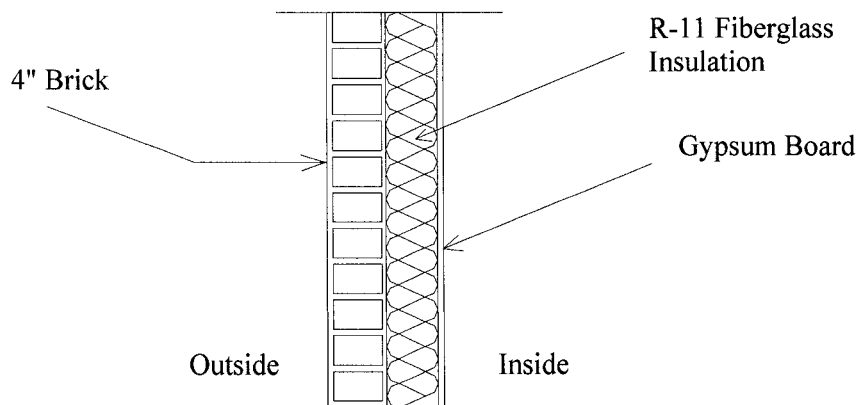


**Figure 7.4b** Exterior Wall Detail of the Prototype II Temple.

The DOE-2 simulation results indicate that the Prototype II temple also has improved performance in terms of indoor thermal conditions. Compared to the existing temple, Figures 7.5, 7.6a, and 7.6b show that the afternoon peak temperatures can be reduced by as much as 8 °F for most of the year. The average indoor temperatures are even lower than the lowest indoor temperatures of the existing temple. In addition, it is apparent that the Prototype II building has fewer indoor temperature fluctuations during the day. The indoor temperatures are maintained closer to the ground temperature, especially during winter days when they are almost at the same temperature. Table 7.2 indicates that the Prototype II temple has an average indoor temperature of 81.0 °F, which is 3.2 °F lower than that of the existing temple. The average temperature deviation from the outdoor air is reduced from +1.0 °F to -2.2 °F, which means that, on the average, the Prototype II temple is actually cooler than the outside air. The average temperature deviation from the ground temperature is +2.1 °F, which is lower than the +5.3 °F of the existing temple.

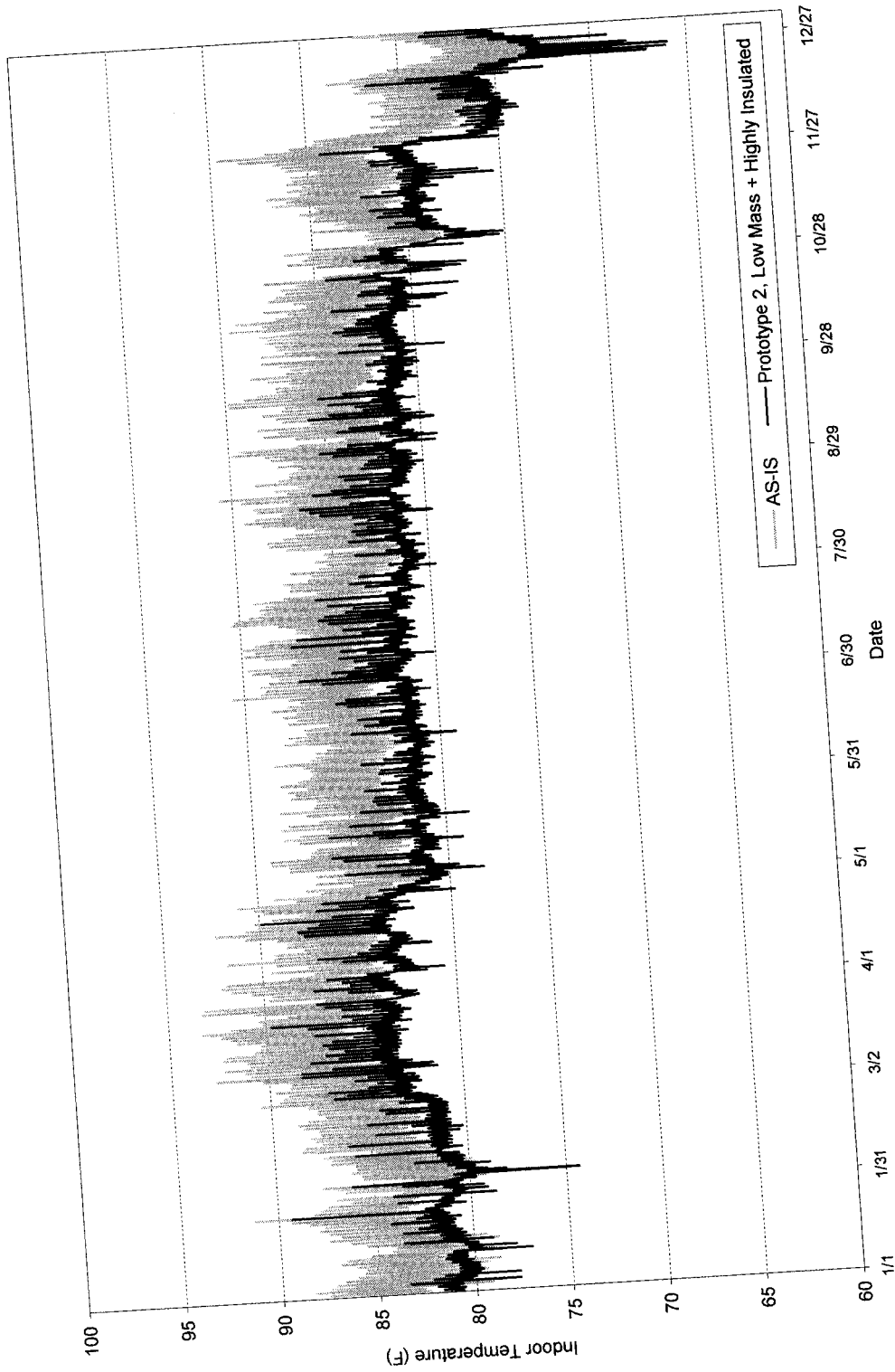


**Figure 7.5** Comparison of the DOE-2 Simulated Indoor Air Temperature of the As-Is Design and Prototype II (Low-Mass Design).

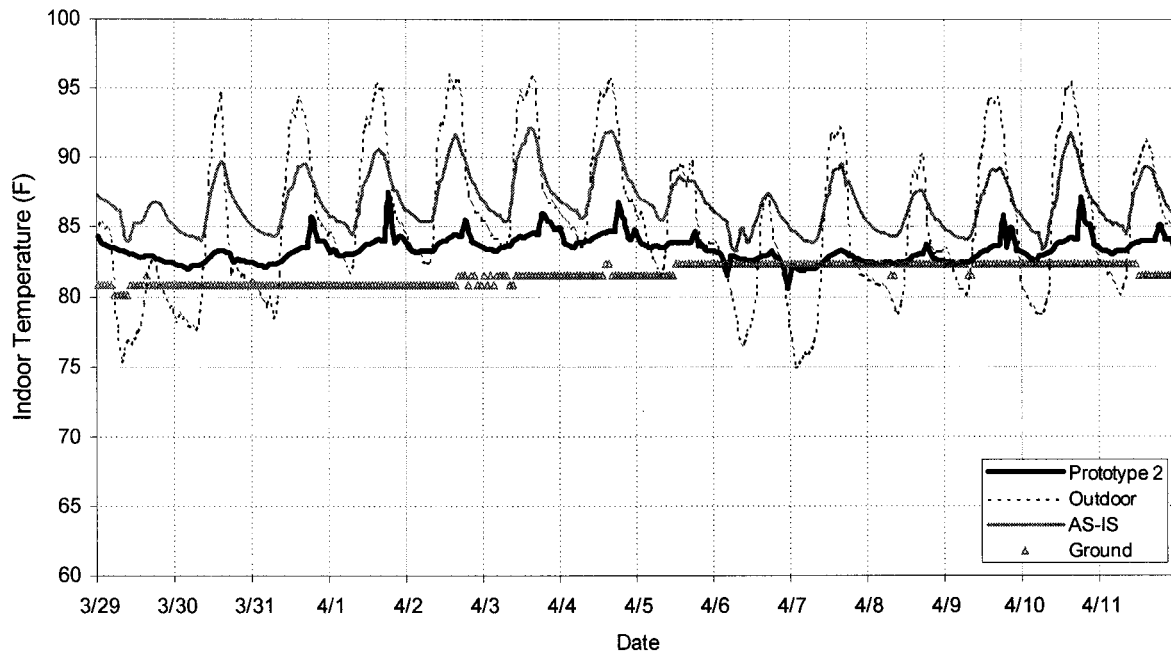


**Figure 7.6a** DOE-2 Simulated Indoor Temperature of Prototype II (Low-Mass Design) for a 2-Week Period of the Summer.

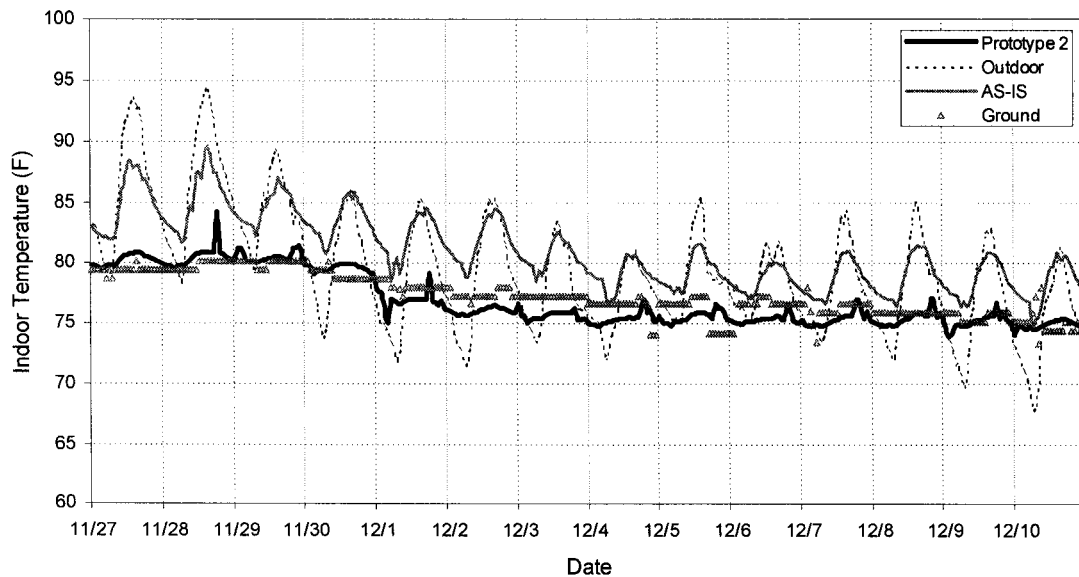


**Figure 7.6b** DOE-2 Simulated Indoor Temperature of Prototype II (Low-Mass Design) for a 2-Week Period of the Winter.

TABLE 7.2

Comparisons of Simulation Results of Prototype I, Prototype II, and the As-Is Temple.

Design options	Space Ventilation Modes		
	As Is (day only) 20 ACH	Night Only 20 ACH	24-Hour 20 ACH
<b>AS - IS Building</b>	Max. Indr.temp = <b>93.3 °F</b> Avg Indr. temp = <b>84.2 °F</b> Dev. from grnd = <b>+ 5.3 °F</b> Dev. from outdr. <b>+ 1.0 °F</b>	Max. Indr.temp = <b>91.4 °F</b> Avg Indr. temp = <b>83.8 °F</b> Dev. from grnd = <b>+ 4.9 °F</b> Dev. from outdr. <b>+ 0.6 °F</b>	Max. Indr.temp = <b>94.2 °F</b> Avg Indr. temp = <b>84.3 °F</b> Dev. from grnd = <b>+ 5.4 °F</b> Dev. from outdr. <b>+ 1.1 °F</b>
<b>Prototype 1:</b> High Mass, White roof, R-30 Ceiling Insulation, Shading	N/A	Max. Indr.temp = <b>89.1 °F</b> Avg Indr. temp = <b>81.6 °F</b> Dev. from grnd = <b>+ 2.8 °F</b> Dev. from outdr. <b>- 1.6 °F</b>	N/A
<b>Prototype 2:</b> Low Mass, White roof, R-11 wall & R-30 ceiling insulation, Shading	N/A	Max. Indr.temp = <b>89.9 °F</b> Avg indr. temp = <b>81.0 °F</b> Dev. from grnd = <b>+ 2.1 °F</b> Dev. from outdr. <b>- 2.2 °F</b>	N/A

#### 7.4 Analysis of the Prototype Buildings

Figures 7.7a and 7.7b show the time - series plots of the hourly indoor temperatures of both prototypes, as compared to those of the existing temple during two-week periods of the summer and the winter. By comparing the results of both prototypes, it was found that the low-mass temple (i.e., Prototype II) performs slightly better than the high-mass temple (i.e., Prototype I) in terms of indoor thermal comfort. The comparison of results are presented in Figures 7.8a, 7.8b, 7.8c, and 7.8d. Figures 7.8a, 7.8c, and 7.8d show that the annual average indoor temperatures, the annual average temperature deviation from the ground temperature, and the annual average temperature deviation from outdoor temperature are lower for the low-mass temple than for the high-mass. However, the peak indoor temperature seems to be slightly higher in the low-mass temple, as indicated in Figure 7.8b. This is because the low-mass temple has higher indoor temperature fluctuations than the high-mass temple, due to the thermal inertia effect normally found in most high-mass buildings.

The effects of thermal inertia on the high-mass building can be seen in Figures 7.9a, 7.9b, 7.9c, 7.10a, 7.10b, and 7.10c, where the data from selected summer and winter days are calculated for the mean, the average maximum, and the average minimum for each hour of the day. It was found that the indoor temperatures of both prototypes were maintained within Givoni's comfort zone with only small daily temperature fluctuations. On an average summer day, the high-mass prototype maintains the indoor temperature at 83° - 85 °F, the low-mass prototype at 81° - 86 °F, and the as-is averages 83° - 92 °F. On an average winter day, the high-mass prototype maintains the indoor temperature at 75° - 81 °F, the low-mass prototype at 74° - 82 °F, and the as-is at 74° - 90 °F. Since the ground serves as a heat sink for the buildings, having an average ground temperature of 81 °F in summer and 74 °F in winter means that both prototypes maintain the indoor temperature at almost as low a level as the ground temperature.

### **7.5 Guidelines for Building Design and Operation**

The preceding analysis provides the basic design and operation guidelines for Thai Buddhist temples. Their thermal performances were estimated using a CFD simulation to confirm airflows, and then a DOE-2 simulation, which used information from the CFD simulations. The simulations were found to be in excellent agreement with the existing temples. Even so, other options concerning changes in space planning, size and position of windows, and building orientation may enhance the performance of the buildings. However, this research only tested selected options involving changes in building materials and ventilation modes. Major architectural changes will be suggested in this chapter, but detailed tests using either simulations or experiments will need to be performed for future research. The proposed building design guidelines for this research are focused on two major issues: first, the guidelines for new temple design and construction, and second, the guidelines for the renovation of existing temples.

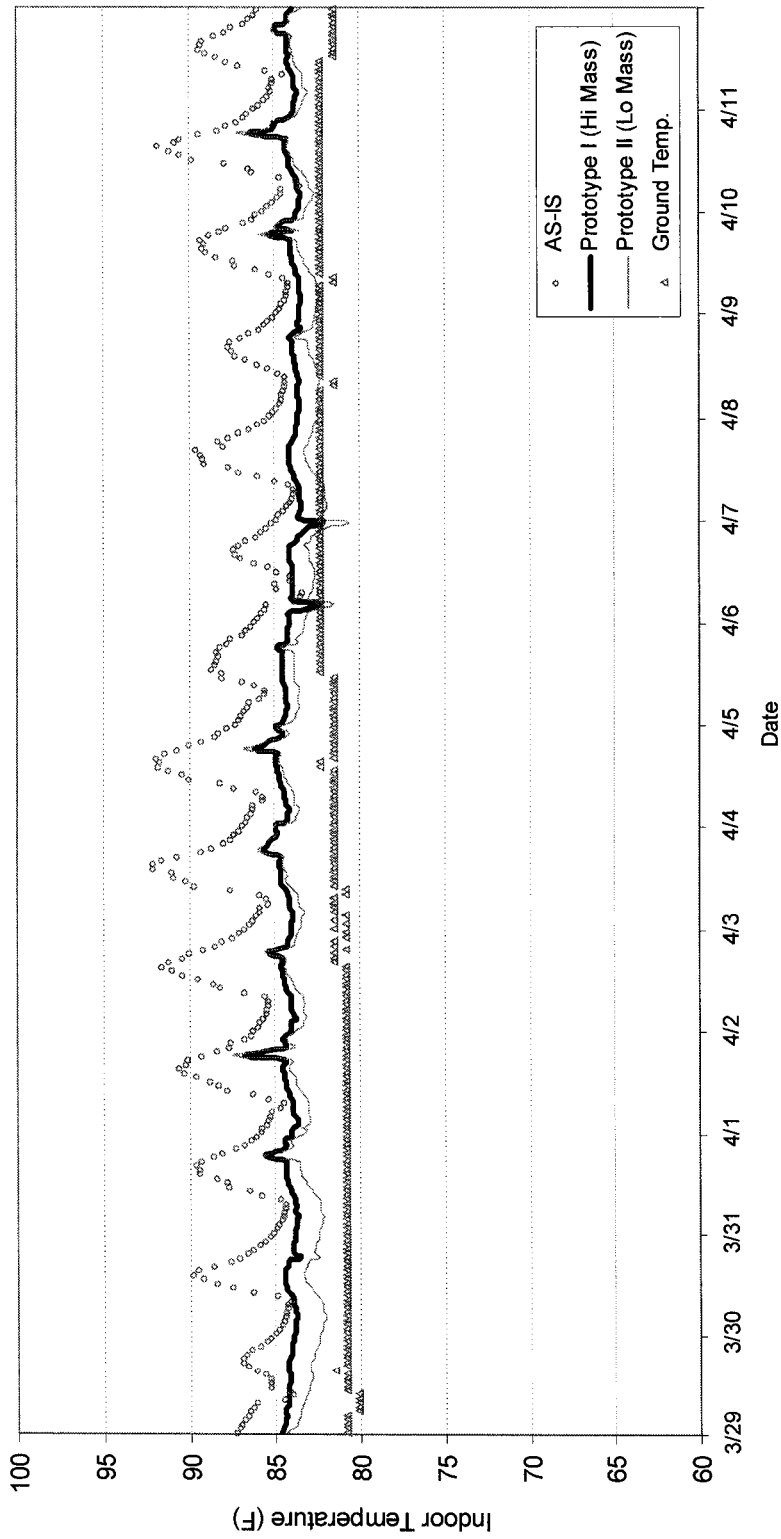


Figure 7.7a Comparison of the DOE-2 Simulated Indoor Temperatures of Both Prototypes for a 2-Week Period of the Summer.

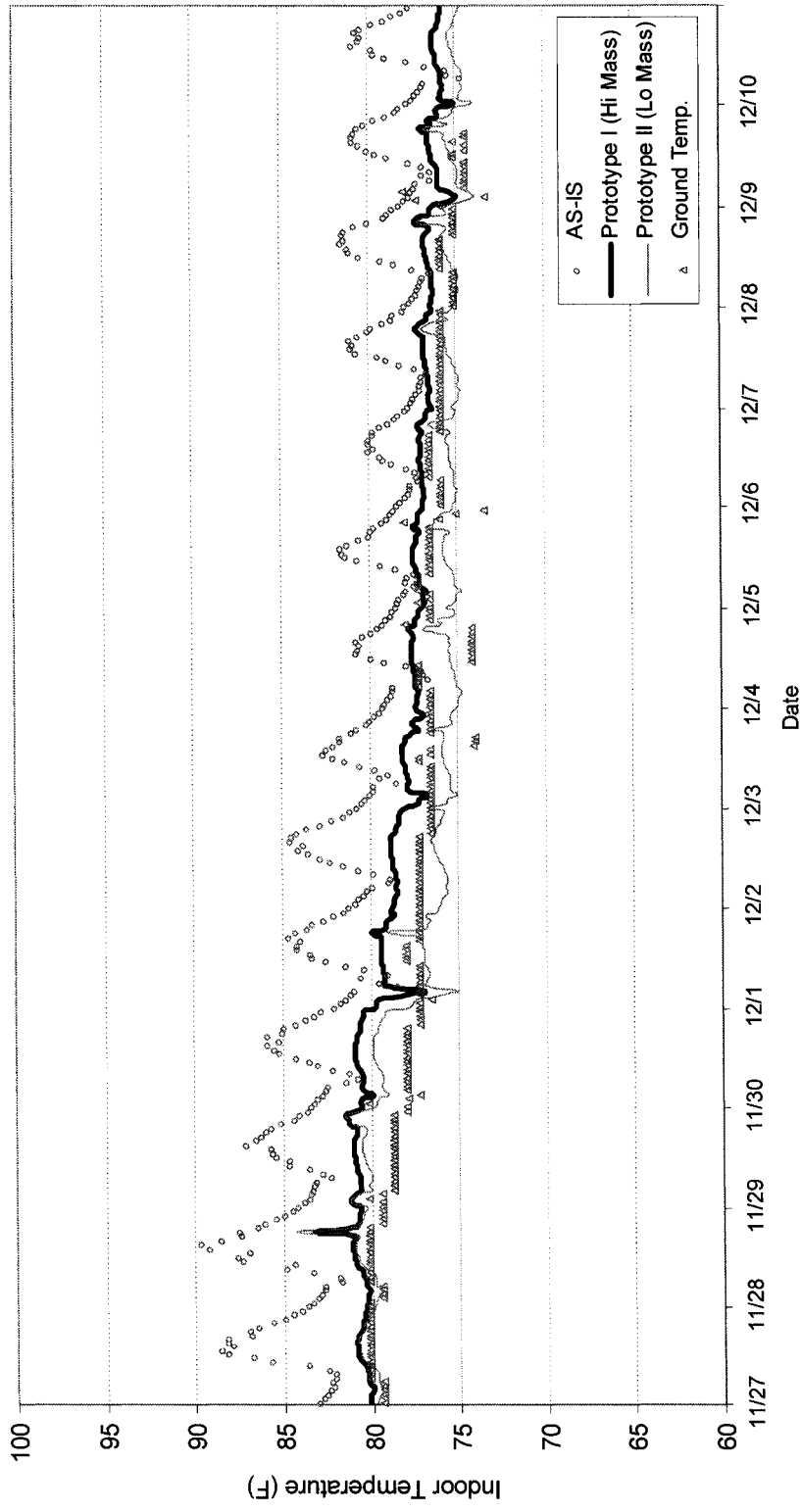
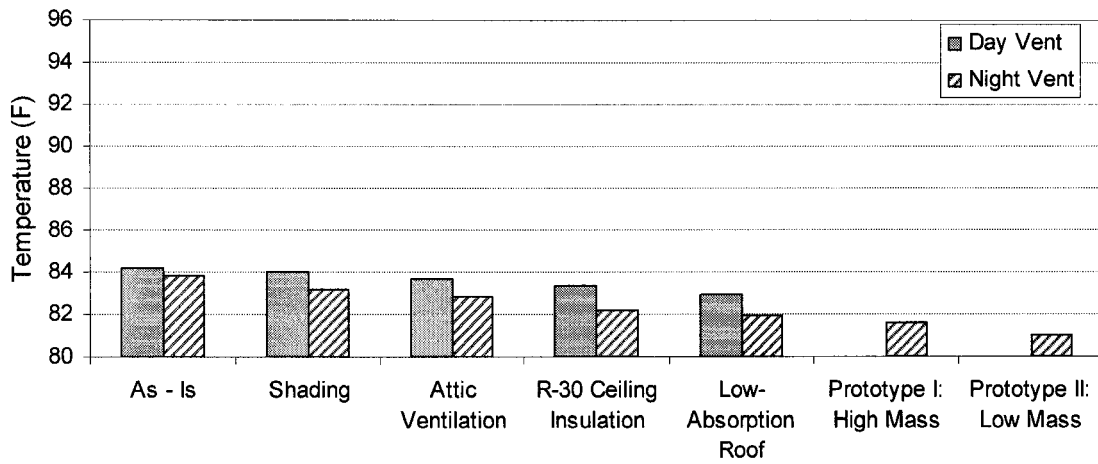
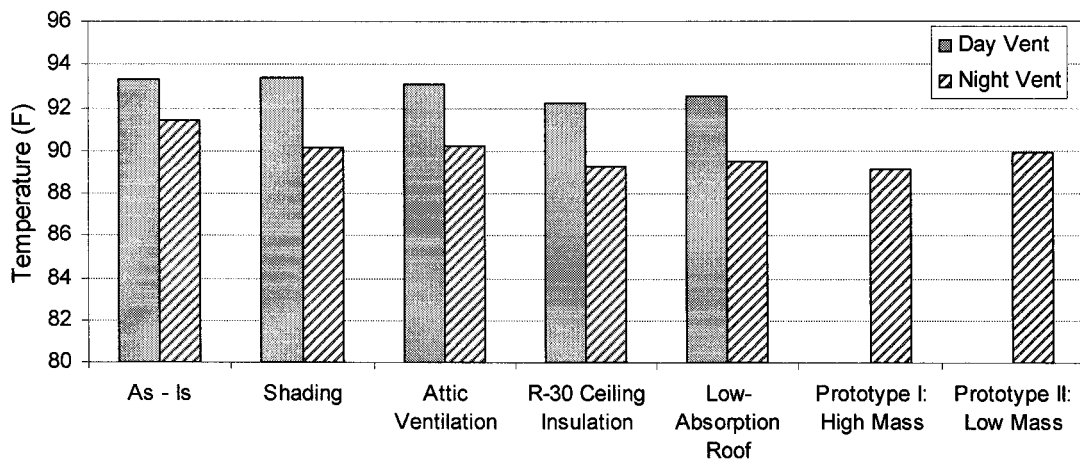


Figure 7.7b Comparison of the DOE-2 Simulated Indoor Temperatures of Both Prototypes for a 2-Week Period of the Winter.





**Figure 7.8a** Annual Average Indoor Temperatures of Individual Options and of Both Prototypes.



**Figure 7.8b** Annual Maximum Indoor Temperatures of Individual Options and of Both Prototypes.

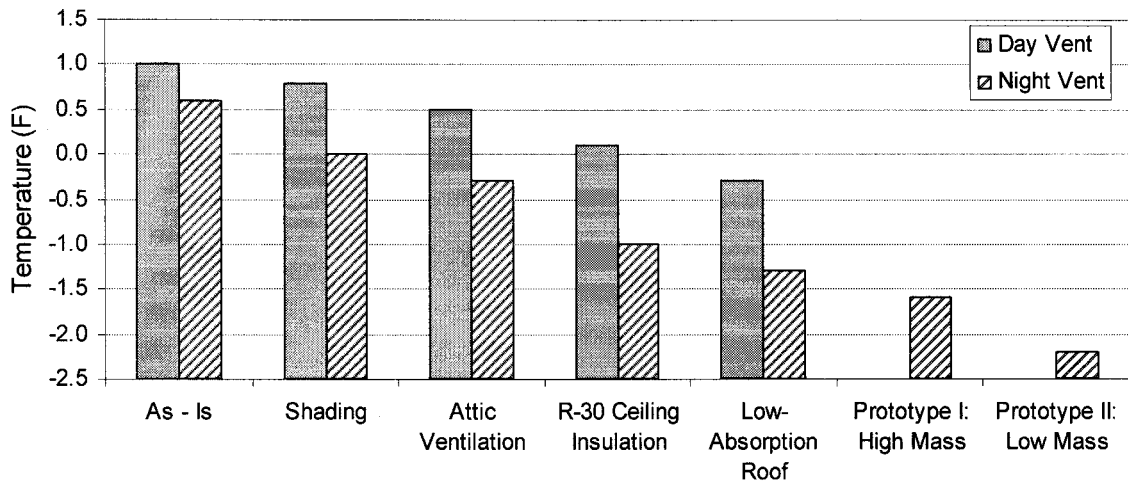


**Figure 7.8c** Annual Average Indoor Temperature Deviations from the Outdoor Temperature of Individual Options and of Both Prototypes.

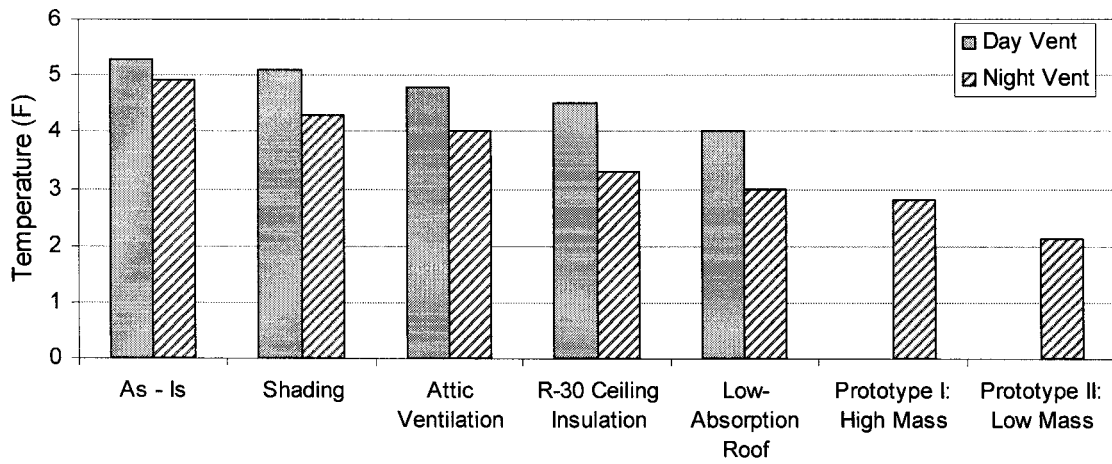


**Figure 7.8d** Annual Average Indoor Temperature Deviations from the Ground Temperature of Individual Options and of Both Prototypes.

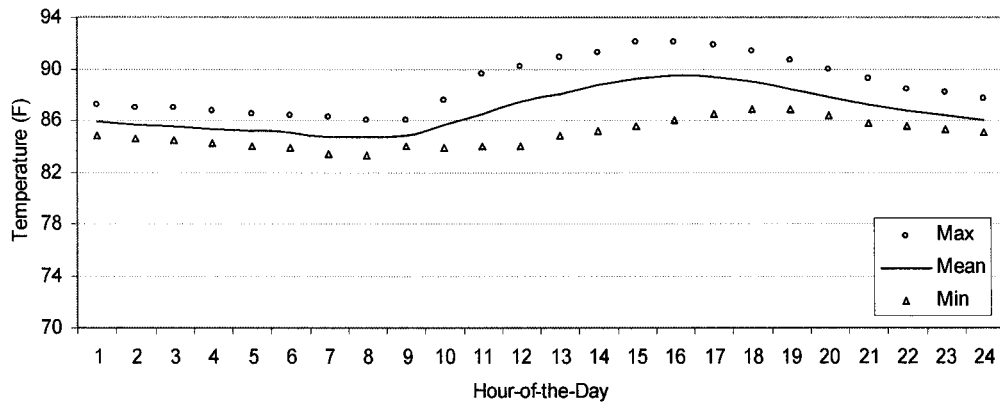


**Figure 7.9a** Average 24-Hour Profile of Indoor Temperatures for the Period of 03/01/99 to 05/30/99 (Summer): As-Is Temple.

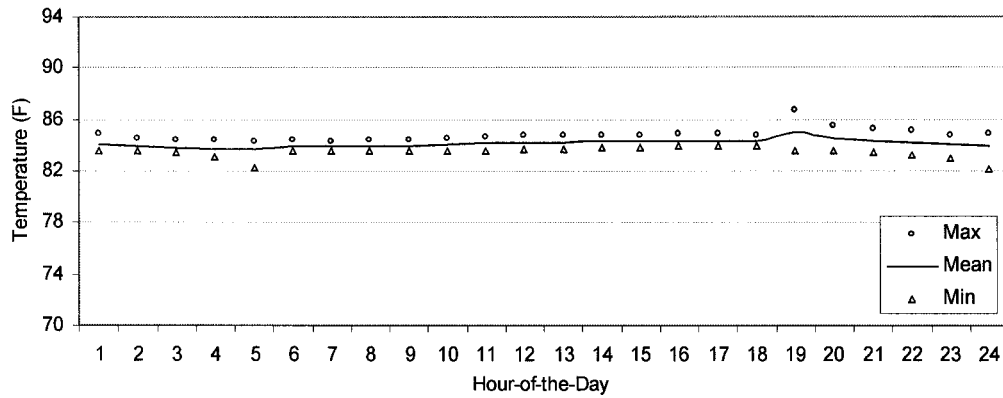


**Figure 7.9b** Average 24-Hour Profile of Indoor Temperatures for the Period of 03/01/99 to 04/30/99 (Summer): Prototype I Temple.

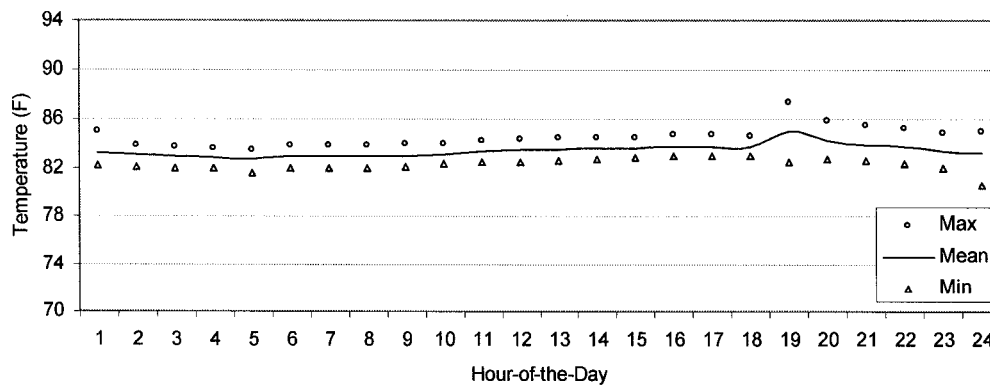


**Figure 7.9c** Average 24-Hour Profile of Indoor Temperatures for the Period of 03/01/99 to 04/30/99 (Summer): Prototype II Temple.

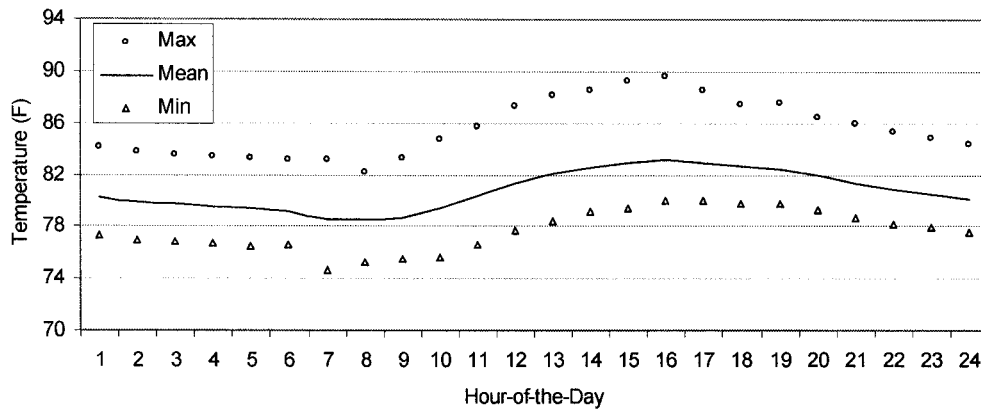


**Figure 7.10a** Average 24-Hour Profile of Indoor Temperatures for the Period of 11/01/99 to 12/31/99 (Winter): As-Is Temple.

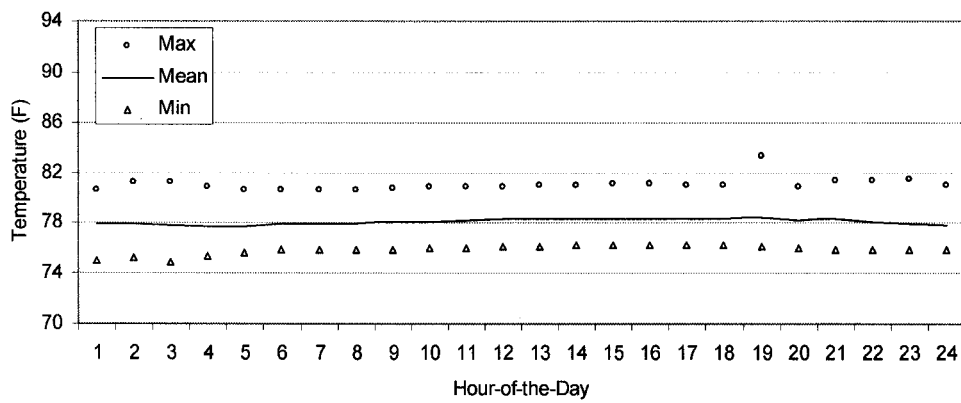


**Figure 7.10b** Average 24-Hour Profile of Indoor Temperatures for the Period of 11/01/99 to 12/31/99 (Winter): Prototype I Temple.

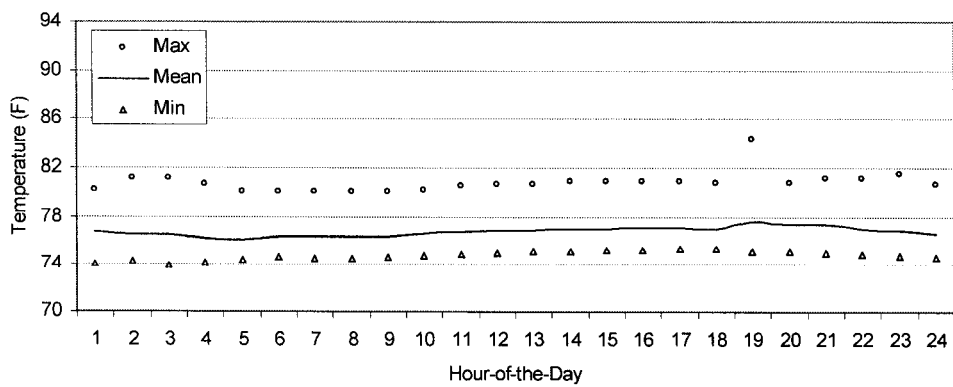


**Figure 7.10c** Average 24-Hour Profile of Indoor Temperatures for the Period of 11/01/99 to 12/31/99 (Winter): Prototype II Temple.

### 7.5.1 Guidelines for New Buildings

1) Use of Wall Insulation. As previously mentioned, new temples in Thailand are constructed using techniques currently found in most commercial and residential buildings. Such construction consists of a concrete post-and-beam structure, concrete masonry walls, steel roof frames, and a sheet metal roof. The construction technique here is the same as that used for the new case-study temple, which is considered moderately lightweight. Therefore, there is a modest thermal mass effect to help keep the building cool during the day. The exterior walls should consist of high thermal resistance materials, fiberglass insulation or Styrofoam, for example. If fiberglass insulation is used, it should be placed at the inside layer of the wall in order to prevent moisture problems. If the Styrofoam is used, the insulation can be placed at the outside layer of the wall. The insulation thickness will depend upon whether or not the walls are shaded from direct sunlight and more importantly, the budget. However, it must be realized that exterior walls receive solar radiation at a high angle due to Thailand's latitude. Super-insulated walls might not be cost-beneficial, as compared to having a highly - insulated roof or ceiling. In the prototype building, 4" thick R-11 fiberglass insulation was used.

2) Use of Slab-on-Grade Floors. Based on the results of the calibrated simulation, a convenient heat sink for the temple is the ground, which is cooler than the outdoor air most of the year. Heat gain to building materials from ambient heat sources can be dampened by the cooler ground, thus reducing the building's indoor air temperature. Unfortunately, many new temples, including the new case-study temple, are constructed without sufficient thermal contact with the ground. Instead, they have ventilated crawl spaces to prevent humidity transfer from the ground. Unfortunately, previous research by Kenneth Labs (1989; ref. Cook 1989, p.197) has shown that the air temperature of an open crawl space is generally higher than that of the floor of the crawl space. Therefore, having ground contacts is preferable for these temples although care should be taken to install an appropriate water vapor barrier to prevent moisture transfer upward.

3) Use of Shading Devices. The shading device is a very important component for buildings in this climate because the solar radiation is so intense. The old case study temple is an example of a building designed with an effective shading devices. Its exterior colonnades not only have a structural purpose (i.e., to support building loads as the load-bearing walls), they also serve as

good shading devices. Unfortunately, many new temples constructed with concrete beams and columns (which can support a wider span) do not need this kind of structure. As a result, new temples are often built today without exterior colonnades, which provide valuable shade. To make matters worse, newer temples usually have glass windows where direct sunlight can penetrate to the interior, as is found in the new case study temple. Therefore, it is recommended that new temples be designed with at least the windows being properly shaded throughout the year. Any glazing should have double pane, low - emissivity windows to help block the heat from incident solar radiation. In addition, shading by surrounding structures and vegetation must be considered. Research by Boonyatikarn (1999) has mentioned that the surrounding trees not only provide shade, but also reduce the local outdoor temperature. The benefit is especially helpful if the roof and walls can be shaded from the sun.

4) Use of Ceiling Insulation. From this investigation, it can be concluded that the major heat gain to the indoor space is heat gain downward from a hot attic due to solar radiation penetrating through the roof. Ceiling insulation on the floor of the attic seems to be the most effective means of reducing indoor temperatures. ASHRAE (2001) also mentioned that hot ceilings have a more significant negative impact on human thermal comfort than do hot walls or floors. Therefore, if the budget allows, highly insulated ceilings should be considered a high priority for improving thermal comfort. In the prototype buildings, 10" thick R-30 fiberglass insulation (i.e., 10-inch fiberglass batts with 5.7 lb/ft<sup>3</sup> density, 0.2 Btu/lb·ft·°F specific heat, 0.025 Btu/hr·ft·°F thermal conductivity: ASHRAE 1998; Table 4.3, p. 51) is used.

5) Use of White, Low-Absorption Walls and Roof. Though the new case study temple was constructed using a white, sheet metal roof, almost 95 % of existing temples still have red clay tile roofs (Kittipunyo 1999). From a discussion with the architect who designed the new case-study temple, white was used because of the architect's personal design concept regarding a religious representation of purity - not actually in response to a heat transfer concern (Ngern-Chooklin 1999). Therefore, it is possible that white roofs might not be used for other temples if this heat transfer benefit is not properly understood. It can be concluded from the simulations that buildings with white, low-absorption roofs have a significant advantage over traditional buildings because only 22 % of solar radiation is absorbed into the roof, thus causing the attic to be cooler than that of the base-case building. Without any special coating, a white colored roof

has a thermal absorptance of 0.30, which is much lower than the 0.80-absorptance of the red, clay-tile roof. Therefore, white colored roofs are highly recommended. However, it should be noted that such roofs should be able to resist the deposition of dirt as well as mold and mildew, which may require periodic washing.

6) Use of Nighttime-Only Ventilation. As was pointed out in the preceding chapters, nighttime-only ventilation is an excellent design and operating option because it helps to remove heat from the building during the night when the outdoor air is cooler. It is therefore recommended that all windows be fully opened after 7 P.M., and closed before 6 A.M. in the morning, allowing in only enough air for ventilation purposes, which is approximately 0.17 ACH based on the 15-CFM/person requirement (ASHRAE 1998, Table 8.2, p.186). This may be in opposition to daily occupancy schedules, and may raise a security concern. However, secure window designs can be applied to solve this problem. In addition to nighttime-only ventilation, opening the windows during the daytime could be made possible during the winter when the outdoor air is cooler than that of the indoors.

7) Use of Attic Ventilation. Ventilating a hot attic during the day at the airflow rate of 50 ACH helps to reduce peak attic temperatures. From the results presented in the previous chapters, it can be concluded that daytime attic ventilation can reduce peak attic temperatures by as much as 25 °F on a hot summer day. However, if the new temple is properly designed with ceiling insulation and a white roof, attic ventilation may not be necessary.

8) Use of Wider Windows, Wing Walls, and Vertical Fins. From the CFD simulations, it was found that the wind normally comes into the building at the corner, either from the northeast or the southwest directions. Therefore, to catch the incoming wind and increase the airflow rate as much as possible, wider windows are highly recommended. In addition, a series of vertical fins on the windows could help direct the incoming wind to the interior. However, this needs to be studied in more detail as it might have a negative impact on the building's appearance.

9) Use of Dehumidification Systems. From the psychrometric charts shown in Figures 7.3c and 7.3d, it was found that although the passive cooling helps improve the thermal comfort condition in the case-study temple, there are potential problems concerning the indoor humidity.

Therefore, the dehumidification systems that use desiccant materials are recommended. Currently, desiccant wheels are designed to take advantage of solar energy in order to heat the desiccant materials and regenerate the dehumidification quality.

### **7.5.2 Guidelines for the Renovation of Old Buildings**

1) Installing Ceiling Insulation. For the old temples, installing at least R-30 ceiling insulation is highly recommended to be a first priority. 10” fiberglass batts could be installed on top of the ceiling without encountering any difficulty in removing the roof shingles or in preparing any on-site concrete work. The existing wood ceiling panels could be preserved, but new ceiling aluminum frames may need to be installed in order to support the additional weight of insulation. The only concern is moisture, which is found to be a major problem in most old buildings in this climate. Moisture, which moves up from the ground through the walls, can degrade the thermal resistance of fiberglass batts. Therefore, building inspections need to be performed before installing any ceiling insulation.

2) Installing White Colored, Low-Absorption Roofs. The most common renovation currently used in old temples concerns the roof shingles replacement (due to rain leakage) (Ngern-Chooklin 1999). Therefore, instead of using the same red, clay tiles, it is recommended that new roofs be white colored sheet metal like that of the new case-study temple. A sheet metal roof is not only lightweight, but also has less thermal capacity. If combined with a low-absorption coating, the thermal performance of the new roof will be better than that of the originally designed temple.

3) Use of Night Ventilation. Unlike new temples that are usually constructed with a more flexible post-and-beam structure, several structural constraints make it impossible for older temples to install larger windows. For this reason, old windows must be open at night and security must be maintained. Therefore, night ventilation for old temples must rely on the performance of existing windows. The size and position of window frames can remain unchanged, but windows need to be redesigned as operable, while still preventing break-ins. Even though all temples are currently closed at night, steel bars are found to be used in many



temples in Thailand because they are inexpensive, which would allow for windows to be open at night while still blocking unauthorized access.

4) Use of Attic Ventilation. If renovating an older temple with a large area of attic vents is not possible, the use of attic fans might provide a good option. However, ventilating the attic with an airflow rate of 50 ACH might require a large fan that would consume a great deal of energy. Unless the eaves around the building can be fully opened to allow natural ventilation like that recommended in the prototype buildings, electric fans are recommended, including electric fans driven by a photovoltaic array.

## 7.6 Summary

In this chapter, to maximize the performance of the building by applying the best possible design and operation, two prototype building designs are proposed. All well-performing options were combined to form the design, construction, and operation of the prototypes, which served as a basis for the guidelines. The guidelines for these prototype buildings take into account both new building designs and the possible renovation of older buildings. The first prototype focused on how to renovate an existing temple with adjustments that allow for the major building structure and construction materials to be preserved. The first prototype is called the high-mass prototype. The second prototype focused on how to design and operate a new temple that will have improved thermal performance, while still conserving the style and functional requirements of this traditional architecture. The second prototype is called the low-mass prototype. Both prototypical buildings were designed to have the same architectural footprint as that of the old case-study temple, and to have the same occupancy profile. Only the nighttime-only ventilation was applied to both prototypes.

By comparing the results of both prototypes, it was found that the low-mass temple (i.e., Prototype II) performs slightly better than the high-mass temple (i.e., Prototype I) in terms of indoor thermal comfort. However, the peak indoor temperature seems to be slightly higher in the low-mass temple. This is because the low-mass temple has higher indoor temperature fluctuations than the high-mass temple, due to the thermal inertia effect normally found in most high-mass buildings.

It was found that the indoor temperatures of both prototypes were maintained within Givoni's comfort zone with only small daily temperature fluctuations. However, humidity seems to be a problem both in the summer and the winter. Even though the passive cooling techniques used in the prototype I design are successful in preventing heat gain to the building, they do not help remove moisture from the air. Fortunately, this high-humidity condition often occurs in the evening when the building is unoccupied, therefore it has less effect on occupants. However, mold and mildew might be the problem in the proposed temple. Moisture removals are then recommended for the future research.

Finally, design and operation guidelines are here proposed. They consist of: 1) increased wall and ceiling insulation, 2) a white-colored, low-absorption roof, 3) a slab-on-ground floor, 4) shading devices, 5) nighttime-only ventilation, 6) attic ventilation, 7) wider windows, wing walls, and vertical fins, and 8) dehumidification system.

## CHAPTER VIII

### SUMMARY AND FUTURE RECOMMENDATIONS

#### 8.1 Summary of Study Objectives

The goal of this research was to develop design and operation guidelines that would lead to an improvement of thermal comfort in unconditioned buildings in a hot and humid climate. To achieve this goal, several tasks had to be accomplished, including: 1) an investigation of the indoor thermal conditions of naturally ventilated buildings in a hot-humid climate using Thai Buddhist temples as a case-study building type, 2) an analysis of the indoor thermal conditions and airflow characteristics of case-study buildings using computer simulations calibrated with data measured from the case-study buildings, 3) the development of improved design guidelines and operation strategies for naturally ventilated buildings in hot-humid regions using Bangkok as a case-study city, and Thai Buddhist Temples as an unconditioned building type, and 4) an evaluation of the effectiveness of these proposed guidelines using computer simulations of the prototype buildings and a comparison of these results with the data measured from the existing buildings.

#### 8.2 Summary of Methodology

A methodology was developed for the purpose of creating a simulation model of a Thai Buddhist temple calibrated with measured data from the case study site. The goal was to obtain a simulation model that correctly represents the real building, and that could be used as a base case for parametric studies. To accomplish this, survey, measurement and data collection procedures were carefully designed along with the use of combined thermal/CFD simulations.

A survey of the Thai Buddhist temples in Bangkok was performed from December to January of 1999. The purpose was to select two case-study buildings that appropriately represent a vast majority of Thai Buddhist temples in terms of architectural style, building design and construction, materials, age, and building use profiles. Two case study buildings, including a new and an old temple, were selected. Measurements of the indoor temperatures, the relative

humidity, and the surface temperatures were performed on both temples in 1999. Bangkok weather data for the same period were also collected. Additional building information was also obtained, which is provided in Appendix A.

To accomplish this, for one 24-hour simulation estimates of air flow rates and convection coefficients were used in the DOE-2 program to produce surface temperatures. These surface temperatures were then passed to the CFD program, which then recalculated the airflow rates and corresponding convection coefficient. This procedure was repeated until an appropriate convergence was produced.

### **8.3 Summary of Results**

The results obtained from this investigation include survey and measurement results, data gathering results, and coupled DOE-2/CFD simulation results. From the survey and measurements, it was found that both of the case-study temples were not comfortable most of the time, especially in the summer when it was hot and humid. The measurements also showed that the old temple was more comfortable than the new temple. Thermal inertia played an important role in reducing the diurnal temperature swings of the older temple. However, during the night, the indoors seemed to be warmer than the outdoors because heat was trapped in the building's materials inside the temple. It was made even worse because the building was completely closed off from the outside at night. In terms of the building's heat gain, the major heat gain component was found to be the attic heat, and to a lesser extent heat from envelope conduction. The results also suggest that the ASHRAE-recommend surface convection coefficients are too large. Smaller values can be obtained using a numerical method. The simulation results agreed with the measurement results, and the simulation model was used as a base-case for the parametric analyses of the different design options.

### **8.4 Summary of Design and Operation Guidelines**

The simulation results demonstrated that the indoor conditions of the case study temple could be remarkably improved by applying the new recommended design and operation instructions. With high-thermal mass, nighttime ventilation schedules greatly reduce the indoor

temperatures. As a result, four design options are recommended from the investigation: 1) a white-colored, low-absorption roof, 2) R-30 ceiling insulation, 3) attic ventilation, and 4) shading devices. Among all of the design options, it was found that a building constructed with either a white, low-absorption roof, or R-30 ceiling insulation would have the lowest indoor temperature, whereas the shading devices and attic ventilation were the least effective options, regardless of which ventilation modes were applied.

In terms of ventilation modes, nighttime-only ventilation not only reduces the peak indoor temperature, but also the daily indoor temperature swings. All design options showed improved indoor comfort if the nighttime-only ventilation was used. Using the nighttime ventilation, it was found that the R-30 ceiling insulation option seemed to allow the smallest temperature fluctuations, while the white-roof option allowed the lowest indoor temperatures, especially at night. For the average indoor temperatures, the low-absorption roof option seemed to perform better than the R-30 ceiling insulation option. However, there was no difference between the two options, in terms of the peak indoor temperature.

Two prototype temples are proposed here based on a combination of the individual features (i.e., 1) nighttime-only space ventilation, 2) low-absorption roof surface, 3) R-30 ceiling insulation, 4) 24-hour attic ventilation, and 5) shading devices). One is a low-mass temple, which is intended for use as the design template for new temples. The other is a high-mass temple, which is intended for use as a renovation guideline for existing temples. It was found that the highly insulated, low mass temple performed slightly better than the high-mass temple in terms of indoor thermal conditions. The indoor temperatures of both the prototype temples were maintained within Givoni's comfort zone, with only very small daily temperature fluctuations. The peak indoor temperature seems to be slightly higher in the low-mass temple. This is because the low-mass temple has higher indoor temperature fluctuations than the high-mass temple, due to the thermal inertia effect normally found in most high-mass buildings.

However, humidity seems to be a problem both in the summer and the winter. Even though the passive cooling techniques used in the prototype I design are successful in preventing heat gain to the building, they do not help remove moisture from the air. Fortunately, this high-humidity condition often occurs in the evening when the building is unoccupied, therefore it has

less effect on occupants. However, mold and mildew might be the problem in the proposed temple.

Finally, design and operation guidelines are here proposed. They consist of: 1) increased wall and ceiling insulation, 2) a white-colored, low-absorption roof, 3) a slab-on-ground floor, 4) shading devices, 5) nighttime-only ventilation, 6) 24-hour attic ventilation, 7) wider windows, wing walls, and vertical fins, and 8) dehumidification system.

### **8.5 Recommendations for Future Research**

1) The proposed guidelines in this research focus on new temple designs that retain the same original footprint as the older case study temple. It does not investigate the effects of different major changes to the building configuration in terms of building shape and form, orientations, and different window sizes and proportions. It was found that the air infiltration rate is a very important variable for the simulation of an unconditioned building, where indoor comfort depends greatly on ventilation to help remove heat from the buildings. With the help of CFD, simulations of airflow across the building, and the indoor thermal performances due to different building shapes, forms, or windows were performed at almost no cost when compared to the use of a wind tunnel or smoke chamber. Therefore, it is here recommended that the coupled thermal/CFD analysis of the Thai Buddhist temples with major changes to architectural design be studied further in the future.

2) The designs proposed here focus on how to enhance the overall thermal performance and comfort condition of the buildings using only passive cooling designs. This research does not investigate the effects of using a hybrid-cooling system, which involves a combination of passive designs and an HVAC system. However, there is the possibility that some temples could install the HVAC systems in the future to alleviate comfort problems. Therefore, future research concerning the use of hybrid cooling for the design and renovation of Thai Buddhist temples is highly recommended.

3) In terms of a thermal comfort assessment, this research uses the comfort zones recommended by ASHRAE and Givoni as indicators of how comfortable an indoor condition is. It does not

investigate the comfort preferences of Thai people in particular. This research assumes that universal human comfort preferences based on worldwide research can be appropriately applied to this group of occupants. Therefore, field studies on the thermal comfort preferences of the occupants in the temples are suggested for future research.

4) Even though the passive cooling techniques used in the prototype building help to prevent heat gain to the building, they do not help remove moisture from the air. The humidity ratios of the indoor air are the same as that outdoors and when the indoor temperature drops, the indoor relative humidity rises. Fortunately, this high-humidity condition often occurs in the evening when the building is unoccupied, therefore it has less effect on occupants. However, mold and mildew might be the problem in the proposed temple. Moisture removals are then recommended for the future research.

5) The night ventilation schedule proposed in this research is based on the activities and the time that the maintenance personnel normally come to open and close the building, which are at 6 A.M. and 7 P.M. If this schedule is set based on the outdoor temperature, the indoor condition will be significantly improved. From the investigation, it was found that in the summer the building should be opened for night ventilation after 8 P.M., and in the winter the building can be left open until late morning. Therefore, there would be a difference in the ventilation schedules of the summer and the winter. It is recommended that the future research perform the study about the ventilation schedule, which is related to the outdoor temperature in more details.

6) It was found that there were some periods of time, especially in the winter, when the outdoor temperature at night was lower than the temperature of the floor of the temple. Since the floor acts as the heat sink for the building, the cooler floor will be beneficial to the passive cooling design here. Therefore, for the future research, it is recommended that the floor be cooled down by the night outdoor air using cool tubes, which are buried beneath the floor of the temple. More detailed studies on the effectiveness of this system are suggested for the future research.

## REFERENCES

- Abouella, N., and M. Milne. 1990. OPAQUE: A microcomputer tool for designing climate responsive opaque building elements. *Proceedings of the Fourth National Conference of Microcomputer Applications in Energy Conservation* (pp. 45-57). Tucson, AZ.
- Abrams, D.W. 1986. *Low-Energy Cooling: A Guide to the Practical Application of Passive Cooling and Cooling Energy Conservation Measures*. New York: Van Nostrand Reinhold Company.
- Alamdari, F. 1991. Microclimate performance of an open atrium office building: A case study in thermo-fluid modeling. In *Computational Fluid Dynamics-Tool or Toy? Proceedings of the 1991 IMechE Conference* (pp. 81-92). London, UK: The Institute of Mechanical Engineers.
- Amtec. 1998. *TECPLOT Version 8.0: User's Manual*. Bellevue, WA: Amtec Engineering, Inc.
- Andrews, M. and M. Prithiviraj. 1997. *HEATX: A 3D CFD Program for Simulation of Flow and Heat Transfer in Shell-and-Tube Heat Exchangers*. Software Manual. College Station, TX: Texas A&M University, Department of Mechanical Engineering.
- Arastech, D.K., E.U. Finlayson, and C. Huizenga. 1994. *Windows 4.1, A PC Program for Analyzing the Thermal Performance of Fenestration Products*. Software Manual. LBL-35298, Berkeley, CA: Lawrence Berkeley Laboratory.
- ASHRAE. 1967. *Handbook of Fundamentals*. Atlanta, GA: American Society of Heating, Refrigerating, and Air-Conditioning Engineers.
- ASHRAE. 1981a. *Handbook of Fundamentals*. Atlanta, GA: American Society of Heating, Refrigerating, and Air-Conditioning Engineers.
- ASHRAE. 1981b. *Thermal Environmental Conditions for Human Occupancy*. Standard 55-1981, Atlanta, GA: American Society of Heating, Refrigerating, and Air-Conditioning Engineers.
- ASHRAE. 1985. *Handbook of Fundamentals*. Atlanta, GA: American Society of Heating, Refrigerating, and Air-Conditioning Engineers.
- ASHRAE. 1992. *Thermal Environmental Conditions for Human Occupancy*. Standard 55-1992. Atlanta, GA: American Society of Heating, Refrigerating, and Air-Conditioning Engineers.
- ASHRAE. 1994a. *Thermal Environmental Conditions for Human Occupancy*. Standard 55-1994. Atlanta, GA: American Society of Heating, Refrigerating, and Air-Conditioning Engineers.



- ASHRAE. 1994b. *Method for Measurement of Moist Air Properties*. Standard 41.6-1994. Atlanta, GA: American Society of Heating, Refrigerating, and Air-Conditioning Engineers.
- ASHRAE. 1998. *Cooling and Heating Load Calculation Principles*. Atlanta, GA: American Society of Heating, Refrigerating, and Air-Conditioning Engineers.
- ASHRAE. 2001. *Handbook of Fundamentals*. Atlanta, GA: American Society of Heating, Refrigerating, and Air-Conditioning Engineers.
- ASTM. 2001a. Standard practice for preparation and use of an ice-point bath as a reference temperature. *ASTM Standard E 563-97*. West Conshohocken, PA: American Society of Testing and Materials.
- ASTM. 2001b. Standard guide for use of freezing-point cells for reference temperatures. *ASTM Standard E 1502-98*. West Conshohocken, PA: American Society of Testing and Materials.
- ASTM. 2001c. Standard guide for use of water triple point cells. *ASTM Standard E 1750-95*. West Conshohocken, PA: American Society of Testing and Materials.
- ASTM. 2001d. Standard test method for calibration of thermocouples by comparison techniques. *ASTM Standard E 220-86* (Reapproved 1996). West Conshohocken, PA: American Society of Testing and Materials.
- ASTM. 2001e. Standard guide for testing sheathed thermocouples prior to, during, and after installation. *ASTM Standard E 1350-97*. West Conshohocken, PA: American Society of Testing and Materials.
- ASTM. 2001f. Standard practice for maintaining constant relative humidity by means of aqueous solutions. *ASTM Standard E 104-85* (Reapproved 1996). West Conshohocken, PA: American Society of Testing and Materials.
- ASTM. 2001g. Standard test methods for radiation thermometers (single waveband type). *ASTM Standard E 1256-95*. West Conshohocken, PA: American Society of Testing and Materials.
- ASTM. 2001h. Standard test method for calibration of a pyranometer using a pyrhelimeter. *ASTM Standard G167-00*. West Conshohocken, PA: American Society of Testing and Materials.
- Awbi, H.B. 1991a. *Ventilation of Buildings*. London: E&FN Spon.
- Awbi, H.B. 1991b. Computational fluid dynamics in ventilation. In *Computational Fluid Dynamic-Tool or Toy? Proceedings of the 1991 IMechE Conference* (pp. 67-79). London, UK: The Institute of Mechanical Engineers.

- Awolesi, S.T., H.W. Awbi, M.J. Seymour, and R.A. Hiley. 1991. The use of CFD techniques for the assessment and improvement of a workshop ventilation system. In *Computational Fluid Dynamic-Tool or Toy? Proceedings of the 1991 IMechE Conference* (pp. 39-46). London, UK: The Institute of Mechanical Engineers.
- Baer, S. 1983. Raising the open U value by passive means. *Proceedings of the Eighth National Passive Solar Conference* (pp. 839-842). Boulder, CO: The American Solar Energy Society.
- Baer, S. 1984. *Cooling with Night Air*. Albuquerque, NM: Zomeworks.
- Baillie, A.P., I.D. Griffith, and J.W. Huber. 1987. *Thermal Comfort Assessment*. Report ETSU-S-1177, Surrey, UK: University of Surrey, Department of Psychology.
- Balaras, C. 1996. Cooling in buildings. In Santamouris, M. and D. Asimakopoulos, ed. *Passive Cooling of Buildings*. London, UK: James & James (Science Publishers) Ltd.
- Balcomb, D., ed. 1988. *Passive Solar Buildings*. Cambridge, MA: MIT Press.
- Benedict, R.P. 1984. *Fundamentals of Temperature, Pressure, and Flow Measurements*. 3<sup>rd</sup> edition. New York: John Wiley & Son, Inc.
- Bliss, S. 1984. Detailing for roof ventilation. *Solar Age* 9(1), 39-42.
- Boonyatikarn, S. 1999. *Design Techniques for Energy Efficient Residential*. Bangkok, Thailand: Chulalongkorn University Press.
- Bou-Saada, T. E. 1994. An improved procedure for developing calibrated hourly simulation models of an electrically heated and cooled commercial building. M.S. Thesis, Texas A&M University, College Station, Texas. (Also available Energy Systems Laboratory Report No. ESL-TH-94/12-01).
- Bou-Saada, T., and J. Haberl. 1995. An improved procedure for developing calibrated hourly simulation models. *Proceedings of Building Simulation '95* (pp. 99-113). Madison, Wisconsin: International Building Performance Simulation Association.
- Boutet, T.S. 1987. *Controlling Air Movement: A Manual for Architects and Builders*. New York: McGraw-Hill.
- Boyer, H., F. Garde, J.C. Gatina, and J. Brau. 1998. A multimodel approach to building thermal simulation for design and research purposes. *Energy and Buildings* 28(1): 71-78.
- Bronson, D. 1992. Calibrating DOE-2 to weather and non-weather-dependent loads for a commercial building: Data processing routines to calibrate a DOE-2 model, volume II. *Energy Systems Laboratory Technical Report* No. ESL-TR-92/04-02. Texas A&M University, College Station.

- Bronson, D., S. Hinchey, J. Haberl, and D. O'Neal. 1992. A procedure for calibrating the DOE-2 simulation program to non-weather dependent loads. *ASHRAE Transactions* 98(1):636-652.
- BSO. 1993. *BLAST User Reference*. Urban-Champaign, IL: University of Illinois at Urbana-Champaign, Department of Mechanical and Industrial Engineering, Blast Support Office.
- Busch, J. 1990. Thermal responses to the Thai office environment. *ASHRAE Transactions* 96(1): 859-872.
- Chandra, S. 1989. Ventilative cooling. In Cook, J., ed. *Passive Cooling: Fundamentals and Applications*. Cambridge, MA: MIT Press.
- Chandra, S., P. Farley, and M. Houston. 1983. *A Handbook for Designing Ventilated Buildings*. FSEC-CR-93-83. Cape Canaveral, FL: Florida Solar Energy Center.
- Chandra, S., and A.A. Kerestecioglu. 1984. Heat transfer in naturally ventilated rooms data from full-scale measurements. *ASHRAE Transactions* 90: 211-224.
- Chen, Q., and J.V.D. Kooi. 1988. ACCURACY: A computer program for combined problems of energy analysis, indoor airflow, and air quality. *ASHRAE Transactions* 94(2): 196-214.
- Chulsukon, P. 2002. Development and analysis of a sustainable, low energy house in a hot and humid climate. M.S. Thesis, Texas A&M University, College Station, Texas.
- Clarke, J. P., J. Hand, J. Hensen, C. Pernot, and E. Aasem. 1993. *ESP-r, A Program for Building Energy Simulation Version 8 Series*. Glasgow, Scotland: University of Strathclyde, Energy Simulation Research Unit (ESRU).
- Cleary, P. 1985. Moisture control by attic ventilation--an in situ study. *ASHRAE Transactions* 91(1A): 227-239.
- Cook, J., ed. 1989. *Passive Cooling: Fundamentals and Applications*. Cambridge, MA: MIT Press.
- Corson, G.C. 1992. Input-output sensitivity of building energy simulations. *ASHRAE Transactions* 98(1): 618-633.
- deDear, R. J., and A. Auliciems. 1985. Validation of the predicted mean vote model of thermal comfort in six Australian field studies. *ASHRAE Transactions* 91(2): 452-468.
- Degelman, L., and V. Soebarto. 1995. Software description of ENER-WIN: A visual interface model for hourly energy simulation in buildings. *Proceedings of Building Simulation '95*. IBPSA. (pp. 692-696). Madison, WI: International Building Performance Simulation Association.

- DOAA. 1998a. *As-built drawings of the Pathum-wanaram temple*. Department of Art and Architecture. The Ministry of Education of Thailand.
- DOAA. 1998b. *As-built drawings of the Rama IX temple*. Department of Art and Architecture. The Ministry of Education of Thailand.
- DOE. 2002. Getting started with EnergyPlus. *EnergyPlus Program Documentation*. Washington, DC: U.S. Department of Energy.
- Erbs, D.G., S.A. Klein, and J.A. Duffie. 1982. Estimation of the diffuse radiation fraction for hourly, daily, and monthly-average global radiation. *Solar Energy* 28(1): 293-314.
- ESRU. 1997. The ESP-r system for building energy simulations: User Guide Version 9 Series. *ESRU Manual U96/1*. University of Strathclyde. Glasgow, UK.
- Fairey, P., and W. Battencourt. 1981. La-Sucka--a wind driven ventilation augmentation and control device. *Proceedings of the International Passive and Hybrid Cooling Conference* (pp. 196-200). Boulder, CO: AS/ISES.
- Fairey, P. 1984. *Radiant Energy Transfer and Radiant Barrier Systems in Buildings-DN-6 and Designing and Installing Radiant Barrier Systems-DN-7*. Cape Canaveral, FL: Florida Solar Energy Center.
- Fanger, P.O. 1972. *Thermal Comfort*. Copenhagen: Danish Technical Press.
- Fawcett, N.S.J. 1991. Getting started with CFD. In *Computational Fluid Dynamic-Tool or Toy?*. *Proceedings of the 1991 IMechE Conference* (pp. 1-4). London, UK: The Institute of Mechanical Engineers.
- Givoni, B. 1976. *Man, Climate, and Architecture*. 2<sup>nd</sup> edition. London: Applied Science Publishers.
- Givoni, B. 1998. *Climate Considerations in Building and Urban Design*. New York: Van Nostrand Reinhold.
- Graca, G.C., Q. Chen, L.R. Glicksman, and L.K. Norford. 2002. Simulation of wind-driven ventilative cooling systems for an apartment building in Beijing and Shanghai. *Energy and Buildings* 34(2002): 1-11.
- Greenspan, L. 1977. Humidity fixed points of binary saturated aqueous solutions. *Journal of Research of the National Bureau of Standards: Physics and Chemistry* 81A(1).
- Griffiths, I. 1990. *Thermal Comfort in Buildings with Passive Solar Features*. Report ENS-090-uk, Surrey, UK: University of Surrey, Department of Psychology.
- Haberl, J., R. Lopez, and R. Sparks. 1992. Building energy monitoring workbook. *ESL Technical Report*. ESL-TR-92/06-02. College Station, TX: Texas A&M University, Energy Systems Laboratory.

- Haberl, J., and S. Thamilseran. 1996. Predicting hourly building energy use: The great energy predictor shootout II: Measuring retrofit savings --Overview and discussion of results, *ASHRAE Transactions* 102(2): 324-340.
- Haberl, J.S., and T.E. Bou-Saada. 1998. Procedure for calibrating hourly simulation models to measured building energy and environmental data. *ASME Journal of Solar Energy Engineering* 120(August):193-213.
- Haberl, J., T. Bou-Saada, V. Soebarto, and A. Reddy. 1998. Use of calibrated simulation for the evaluation of residential energy conservation options of two Habitat for Humanity houses in Houston, Texas. *The Eleventh Symposium on Improving Building Systems in Hot and Humid Climates Proceedings* (pp. 359-369). June 1-2, 1998. Radisson Plaza Hotel, Forth Worth, Texas.
- Holleman, T. 1951. Airflow through conventional window openings. *Research Report*. RR-33, College Station, TX: Texas A&M University, Texas Engineering Experiment Station.
- Huang, J. 1994. *DrawBDL Version 2.02*. El Cerrito, CA: Joe Huang and Associates.
- Humphreys, M. 1975. Field studies of thermal comfort compared and applied. *Current Paper*. CP 76/75, Watford, UK: Building Research Establishment.
- Humphreys, M. 1992. Thermal comfort requirements, climate and energy. *Proceedings of the Second World Renewable Energy Congress* (pp. 1725-1734). Reading, UK: Second World Renewable Energy Congress.
- Hunt, G. R., P.F. Linden, M. Kolokotroni, and E. Perera. 1997. Salt-bath modeling of airflows. *Building Services Journal* 1997: 43-44.
- Incropera, F. P., and D.P. De Witt. 1990. *Fundamentals of Heat and Mass Transfer*. New York: John Wiley & Son, Inc.
- ISO. 1984. *International Standard 7730, Moderate Thermal Environment – Determination of the PMV and PPD Indices and Specification of the Conditions for Thermal Comfort*. Geneva, Switzerland: International Standard Organization.
- Jitkhajornwanich, K., A.C. Pitts, A. Malama, and S. Sharples. 1998. Thermal comfort in transitional spaces in the cool season of Bangkok. In *Field Studies of Thermal Comfort and Adaptation*. *ASHRAE Technical Data Bulletin*. Vol. 14. No. 1. Atlanta, GA: American Society of Heating, Refrigerating, and Air-Conditioning Engineers.
- Jones, P., D.K. Alexander, and R.M. Rahman. 1993. Evaluation of the thermal performance of low-cost tropical housing. *Proceedings of the Third IBPSA Conference* (pp. 137-143). Adelaide, Australia: International Building Performance Simulation Association.
- Kammerud, R., E. Ceballos, B. Curtis, W. Place, and B. Anderson. 1984. Ventilation cooling of residential buildings. *ASHRAE Transactions* 95(2): 226-251.

- Kittipunyo, P. 1999. Telephone Communication. January. Pathum Wanaram Temple, Bangkok, Thailand.
- Krarti, M. 2000. *Energy Audit of Building Systems: An Engineering Approach*. New York: CRC Press.
- Kreider, J., and J. Haberl. 1994. Predicting hourly building energy usage: The great energy predictor shootout: Overview and discussion of results. *ASHRAE Transactions Technical Paper* 100(2): 56-70.
- Kreider, J.F., and A. Rabl. 1994. *Heating and Cooling of Buildings: Design for Efficiency*. New York: McGraw-Hill.
- Labs, K. 1989. Earth coupling. In Cook, J., ed. *Passive Cooling: Fundamentals and Applications*. Cambridge, MA: MIT Press.
- Lauder, E., and D.B. Spalding. 1974. The numerical computation of turbulent flows. *Computer Methods in Applied Mechanics and Engineering* 3(1): 269-289.
- LBNL. 1982. *The DOE-2.1A Reference Manual*. Berkeley, CA: Lawrence Berkeley National Laboratory.
- LBNL. 1994. *The DOE-2.1E Supplement*. Berkeley, CA: Lawrence Berkeley National Laboratory.
- LBNL. 2001. *The DOE-2.1E Documentation Update Package #4*. Berkeley, CA: Lawrence Berkeley National Laboratory.
- Lewis, P., and D. Alexander. 1990. HTB2: A flexible model for dynamic building simulation. *Building and Environment* 25(1): 7-16.
- Manke, J.M., D.C. Hittle, and C.E. Hancock. 1996. Calibrating building energy analysis models using short term test data. *Proceedings of the 1996 International ASME Solar Energy Conference* (p.369-378). San Antonio, TX.
- Martin, M. 1989. Radiative cooling. In Cook, J., ed. *Passive Cooling: Fundamentals and Applications*. Cambridge, MA: MIT Press.
- McGee, T. 1988. *Principles and Methods of Temperature Measurement*. New York: John Wiley & Son, Inc.
- McQuiston, F., S.L. Der, and S.B. Sandoval. 1984. Thermal simulation of attic and ceiling spaces. *ASHRAE Transactions* 90(1): 859-872.
- Mease, N. E., W.G. Cleveland, G.E. Mattingly, and J.M. Hall. 1992. *Air Speeds Calibration at the National Institute of Standards and Technology*. Gaithersburg, MD: U.S. Department of Commerce, National Institute of Standards and Technology.

- Medina, M., D. O'Neal, and D. Turner. 1992. Effects of radiant barrier systems on ventilated attics in a hot and humid climate. *Proceedings of the Eighth Symposium on Improving Building Systems in Hot and Humid Climates* (pp. 47-52). Dallas, TX: Texas A&M University, Energy Systems Laboratory.
- Milne, M., M. Vasser, and V. Sehgal. 1988. SOLAR-5 update: Work in progress for the new release. *Proceedings of the Third National Conference of Microcomputer Applications in Energy Conservation*. Tucson, AZ.
- Nagrao, C.O.R. 1995. Conflation of computational fluid dynamics and building thermal simulation. Ph.D. Thesis, University of Strathclyde, Glasgow, UK.
- Ngern-Chooklin, A. 1999. Telephone Communication. February. Department of Art and Architecture. The Ministry of Education, Thailand
- Nicol, F., J.N. Jamy, O. Sykes, M.A. Humphreys, S. Roaf, and M. Hancock. 1994. *Thermal Comfort in Pakistan*. UK: Oxford Brookes University, School of Architecture.
- Niles, P.W.B. 1989. Simulation analysis. In Balcomb, D., ed. *Passive Solar Buildings*. Cambridge, MA: MIT Press.
- NIST. 1991. NIST Calibration services for humidity measurement. NISTIR 4677. Gaithersburg, MD: U.S. Department of Commerce, National Institute of Standards and Technology.
- Oh, J. K. 2000. Development and validation of a computer model for energy-efficient shaded fenestration design. Ph.D. Dissertation, Texas A&M University, College Station, Texas.
- Olgay, V. 1963. *Design with Climate: A Bioclimatic Approach to Architectural Regionalism*. Princeton: Princeton University Press.
- Onset. 2002. *HOBO Data-logger User Manual*. Bourne, MA: Onset Computer Corporation.
- Patankar, V.S. 1980. *Numerical Heat Transfer and Fluid Flow*. USA: Hemisphere Publishing Corp.
- Prithviraj, M., and M.J. Andrews. 1998a. Three-dimensional numerical simulation of shell-and-tube heat exchangers part 1: Foundation and fluid mechanics. *Numerical Heat Transfer Part A: Applications* 33(8): 799-816.
- Prithviraj, M., and M.J. Andrews. 1998b. Three-dimensional numerical simulation of shell-and-tube heat exchangers part 2: Heat transfer. *Numerical Heat Transfer Part A: Applications* 33(8): 817-828.
- Raytek. 1999. *The Raytek Raynger ST6 Infrared Thermometer: User Manual*. Santa Cruz, CA: Raytek Corporation.
- Rose, W.B., and A. TenWolde. 2002. Venting of attics and cathedral ceilings. *ASHRAE Journal* October 2002. p. 26-33.

- RTMD. 1995. *The Typical Weather of Bangkok During 1985-1995*. Bangkok, Thailand: The Royal Thai Meteorological Department.
- RTMD. 2000. *The Hourly Weather Data of Bangkok Station*. Bangkok, Thailand: The Royal Thai Meteorological Department.
- Schiller, G. 1990. A comparison of measured and predicted comfort in office buildings. *ASHRAE Transactions* 96(1): 215-230.
- SEL. 1995. *TRNSYS Manual Version 14.1*. Madison, WI: University of Wisconsin-Madison.
- Smith, E. 1951. The feasibility of using models for predetermining natural ventilation. *Research Report*. RR-26, College Station, TX: Texas A&M University, Texas Engineering Experiment Station.
- Snider, D.M., and M.J. Andrews. 1996. The simulation of mixing layers driven by compound buoyancy and shear. *ASME Journal of Fluids Engineering* 118(2): 370-376.
- Sobin, H. 1983. Analysis of wind tunnel data on naturally ventilated models. *Appendix A: Test Data Catalog*. Tucson, AZ: H. Sobin Associate.
- Srebric, J., Q. Chen, and L.R. Glicksman. 2000. A coupled airflow-and-energy simulation program for indoor thermal environment studies. *ASHRAE Transactions* 105(2): 414-427.
- Tanabe, S. 1988. *Thermal Comfort Requirement in Japan*. Tokyo, Japan: Waseda University.
- Tantasawasdi, C., J. Srebric, and Q. Chen. 2001. Natural ventilation design for houses in Thailand. *Energy and Buildings* 33(8): 815-824.
- Vazquez, B., M. Samano, and M. Yianneskis. 1991. The effect of air inlet location on the ventilation of an auditorium. In *Computational Fluid Dynamic-Tool or Toy? Proceedings of the 1991 IMechE Conference* (pp. 56-66). London, UK: The Institute of Mechanical Engineers.
- Wu, H. 1988. The potential use & application of oscillating fans in extending the summer comfort envelope. *Research Report*, Tempe, AZ: Arizona State University, Environmental Testing Laboratory.
- Yau, R.M.H., and G.E. Whittle. 1991. Air flow analysis for large spaces in an airport terminal building: Computational fluid dynamics and reduced-scale physical model test. In *Computational Fluid Dynamic-Tool or Toy? Proceedings of the 1991 IMechE Conference* (pp. 47-55). London, UK: The Institute of Mechanical Engineers.
- Yellott, J. 1989. Evaporative Cooling. In Cook, J., ed. *Passive Cooling: Fundamentals and Applications*. Cambridge, MA: MIT Press.



## APPENDIX A

### DETAILS OF THE CASE-STUDY TEMPLES

#### A.1 The Old Temple

The old case-study temple is named “Pathum Wanaram Temple.” It was constructed during the early 1900’s. This temple is located in the urban area of Bangkok and it has been considered to be under Royal Patronage, since it was built by the Kings of Thailand (King Rama IV) and preserved by the Royal Thai Government. The construction mainly consists of load-bearing brick masonry walls and columns, timber roof frames, a red clay-tile roof, one-inch thick wood ceiling boards, and a stone slab-on-grade floor with marble topping. Windows and doors are made of one-inch thick solid wood. The building’s main structure is a load bearing wall system with 2.5-foot (0.80 m) thick walls that results in a limited size and number of openings. The walls and ceiling are insulated. No attic ventilation is used.

Figure A.1 shows the exterior wall on the north side of the building. All windows on the side walls are made of solid wood, and they are normally closed at night due to security reasons. Steel bars were installed on all windows. This figure also shows that the windows are relatively small comparing with the side walls. This is because of the construction techniques commonly found in old buildings. The building’s load-bearing wall structure limits the size of the windows; therefore, the architect applied decorations to make the windows seem to be larger (Ngern-Chooklin 1999; telephone communication).

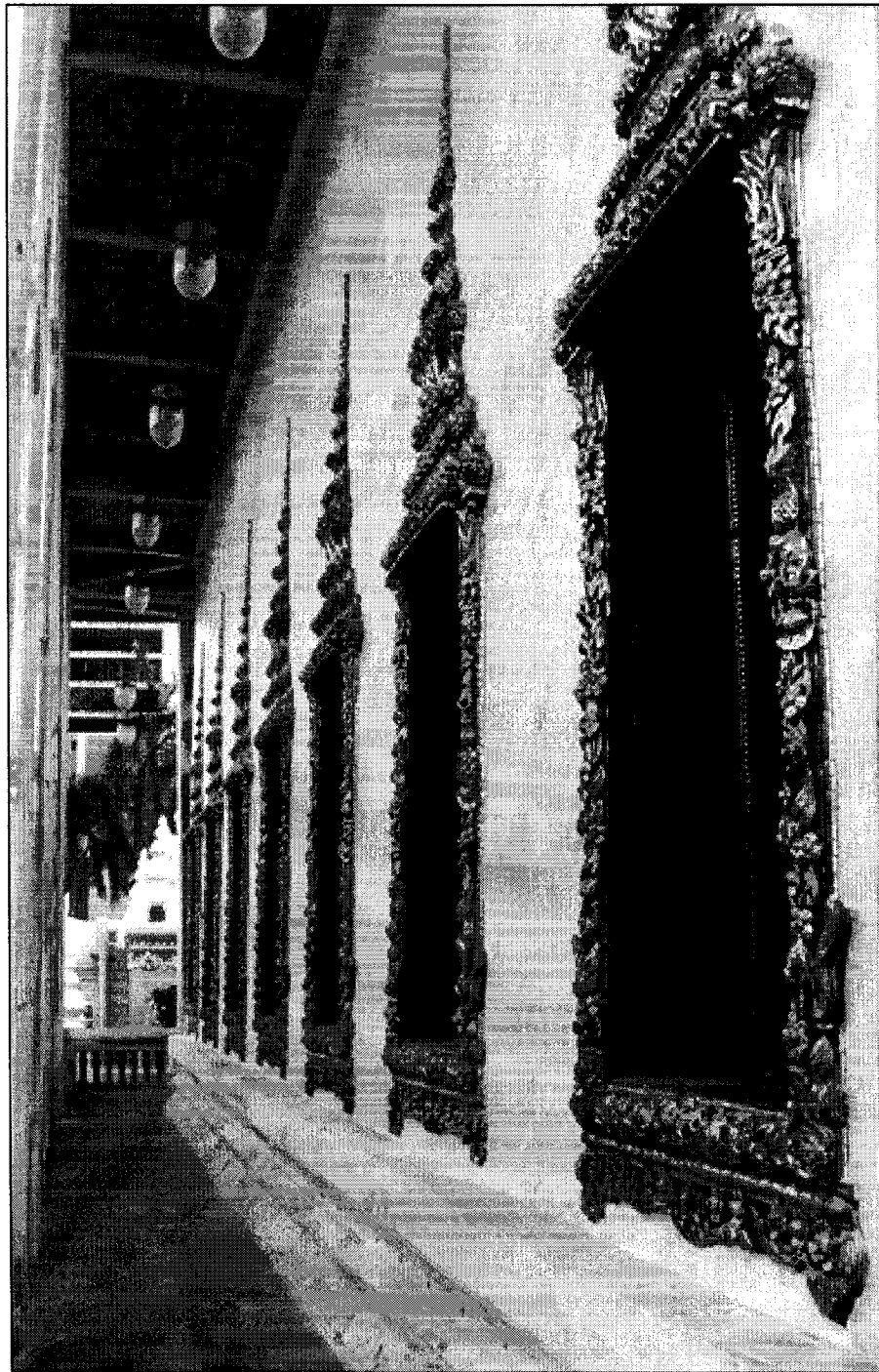
The interior view in Figure A.2 shows the wooden ceiling, a chandelier, a series of ceiling lamps, and a ceiling fan. The ceiling fan and the chandelier were found to be broken, and it is difficult to replace the incandescent lamps because of the height of the ceiling. Figure A.3 shows the interior corridor on the north side of the building. Thanks to the exterior colonnades, the interior is well-shaded from the sun at all times. This causes the interior to be dim because of the lack of daylight. However, this is not a major issue for a religious building, where activities does not require a high level of illumination except that daily maintenance might be difficult. It should be noted that several portable fans were found used to provide comfort for occupants.

Figure A.4 shows a surface of an interior column where mold and mildew grew and destroyed wall paintings. This indicates a serious moisture problem found in most old buildings in the tropics. From the discussion with the monk (Kittipunyo 1999; telephone communication), the roof shingles were replaced in 1997. To prevent rain leakage, a plastic membrane was installed beneath the clay-tile roof shingles, which causes the moisture in the attic to be trapped inside. Even though, there is no proof that attic ventilation helps to remove the moisture from the attic (Rose and TenWolde 2002), it was found from this building that the moisture problem occurred more seriously after the attic was sealed.

## **A.2 The New Temple**

The new case-study temple is named “King Rama IX Temple.” It was constructed in 1995. This temple is located in the urban area of Bangkok and it is also under Royal Patronage. This temple was designed by the Department of Art and Architecture at the Ministry of Education by a group of architects who were appointed in 1995 to work for King Rama IX of Thailand. The primary design was intended to be the prototype for contemporary Thai Buddhist temples built in the future. The temple was mainly constructed with four-inch thick brick masonry exterior walls, steel roof frames, a sheet metal roof, one-inch thick wood ceiling, and has a slab-on-beam concrete floor with granite topping and a ventilated crawl space beneath the floor. The exterior walls and roof are painted white. Windows and doors are single-pane clear glass on aluminum frames. The building’s main structural system is concrete post-and-beam. The walls and ceiling are insulated. No attic ventilation is used.

Figure A.5 shows the front entrance on the east side of the temple. In contrast to the north and the south sides, which are not well-shaded as shown in Figure A.6, the east and the west sides have colonnades that provide shading to the front and the rear entrances. The effect of no shading is shown in Figure A.7, where the windows on the south side are not properly shaded from the direct sun, thus causing the interior space to be hot for most of the year. Figures A.7 and A.8 show that the portable fans are very necessary to provide comfort for occupants, since there were at least six portable fans found in this temple. They consume a major part of electricity in this temple.



*Figure A.1* Exterior View of the Old Temple Showing a Series of Windows on the North Side of the Building. This picture shows the exterior window decorations and the outside corridor. Steel bars were installed on all windows for security.



**Figure A.2** *Interior View of the Old Temple Showing the Wooden Ceiling, a Chandelier, Ceiling Lamps, and a Ceiling Fan. The ceiling fan and the chandelier were found to be broken. It is difficult to replace the lamps because of the height of the ceiling.*



**Figure A.3** *Interior View of the Old Temple Showing the Interior Corridor. This picture shows that a portable fan was used to provide comfort to occupants. It was found that the indoor was dark during the day because of insufficient daylight.*



*Figure A.4* Moisture Problem in the Old Temple. This picture shows a surface of an interior column where mold and mildew grew and destroyed wall paintings.

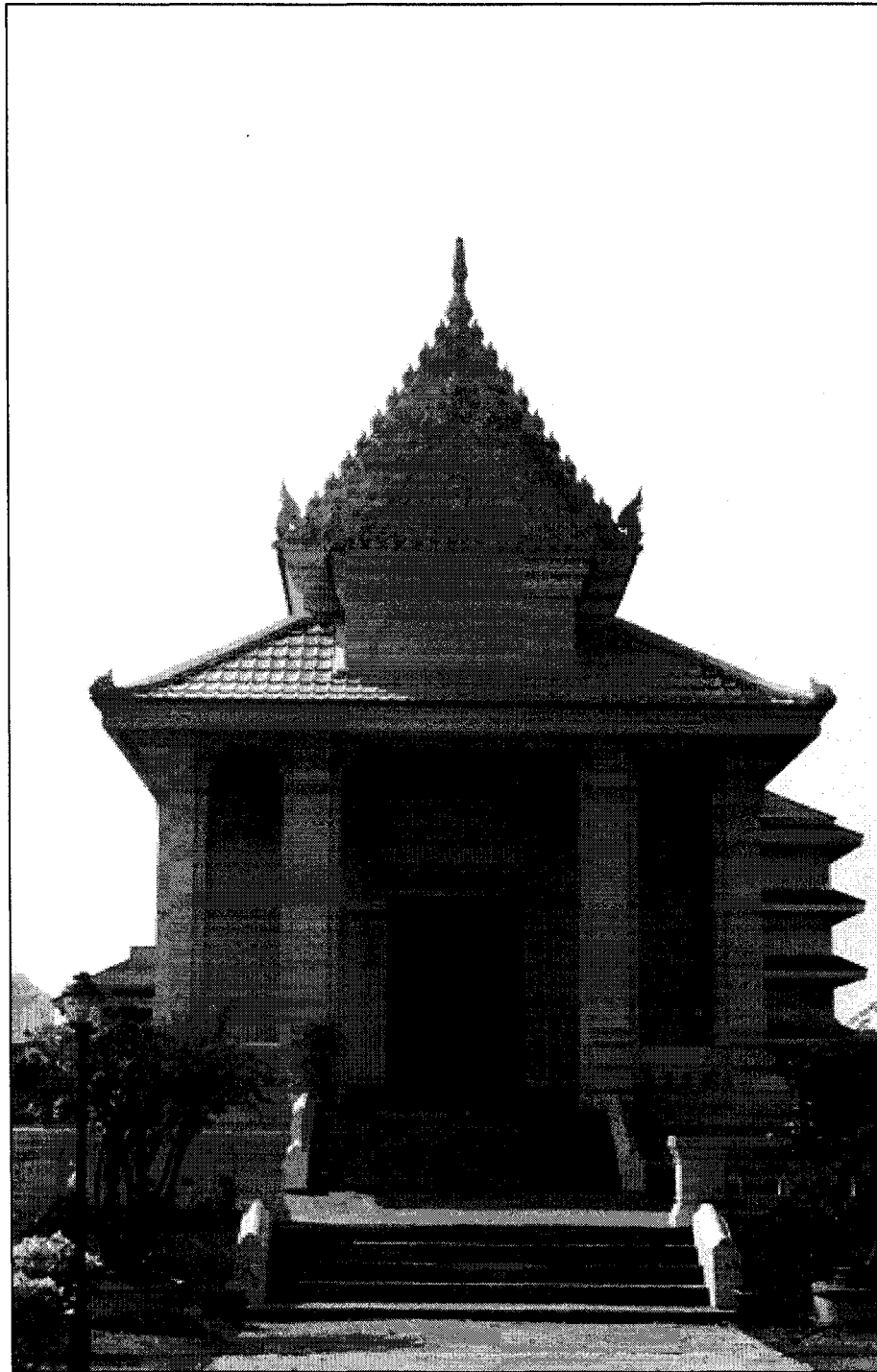


*Figure A.5* Exterior View of the New Temple Showing the Front Entrance. This picture was taken from the east side of the building at noon on January 6, 1999.

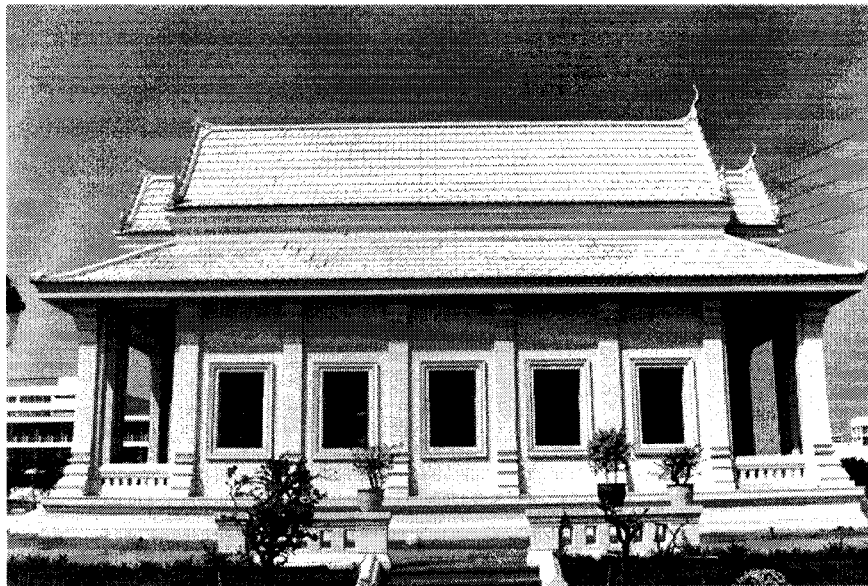


**Figure A.6** *Exterior View of the New Temple Showing the South Side of the Building. This picture was taken at noon on January 6, 1999. It shows that the exterior wall on this side, including its windows were not shaded from the direct sunlight. Only the east and the west side have colonnade.*



**Figure A.7** *Interior View of the New Temple Showing the Interior Wall at the South Side of the Building. This picture shows that the windows were not properly shaded from the direct sunlight. This caused the space to be hot for most of the year.*



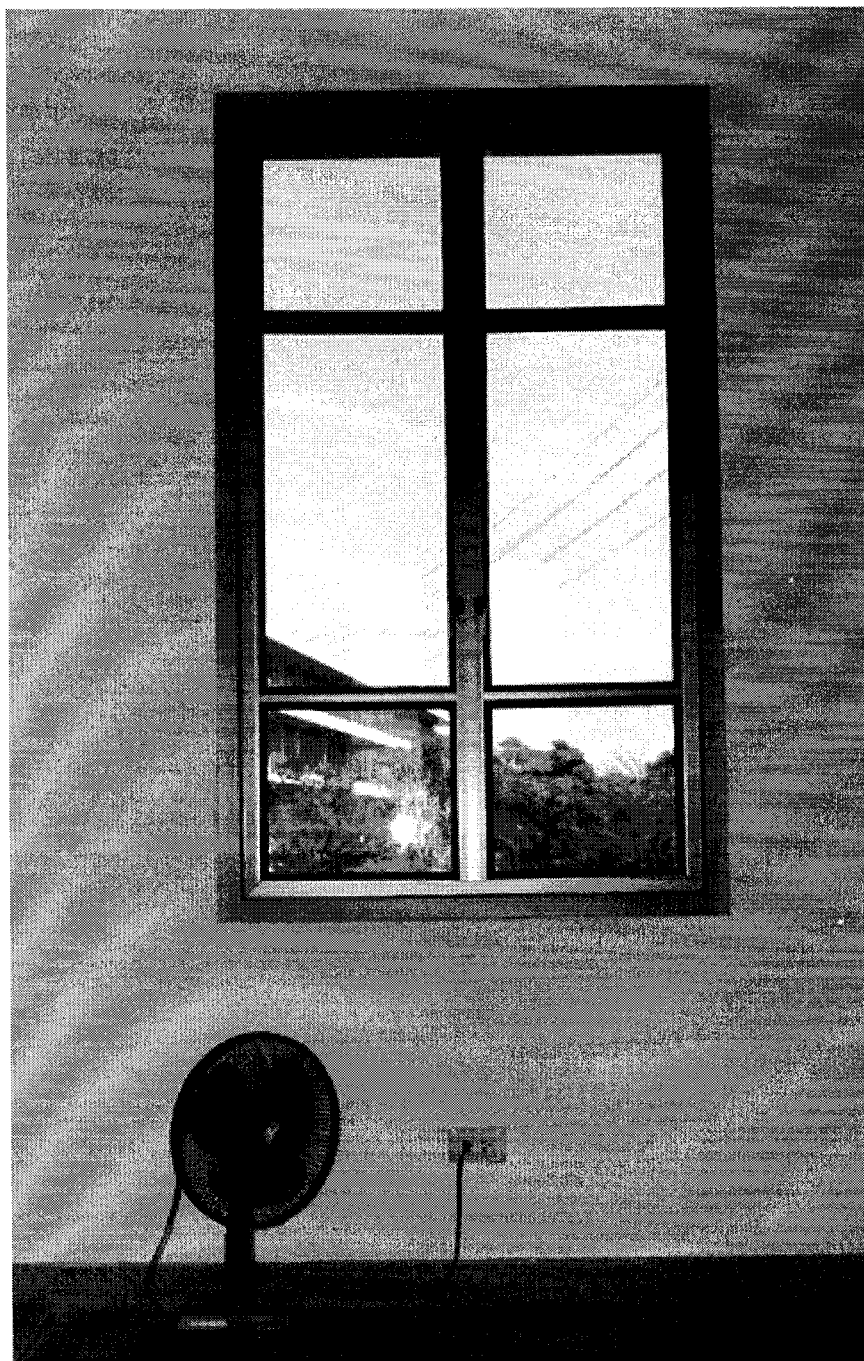


**Figure A.8** *A Window on the North Side Wall of the New Temple. This picture shows a single-pane clear glass window with aluminum frames used in the New Temple.*

## APPENDIX B

### CLIMATE CHARACTERISTICS OF BANGKOK

#### B.1 Typical Climate Characteristic of Bangkok

Bangkok is the capital city of Thailand. It is located on 13°45'N latitude and 100°28'E longitude. As described by Jitkhajornwanich (1998), this part of the country is hot and humid all year round. Generally, the climate is classified as tropical with three seasons per year. The winter occurs from November to January, the summer occurs from February to May, and May to October is considered the rainy season. An extremely hot period usually occurs in April. From the weather data obtained from the Royal Thai Meteorological Department (RTMD 1995), the typical climate characteristics of Bangkok are as follows:

1.Dry-bulb temperature (Figure B.1.1). The annual average dry-bulb temperature is 28 °C (82.4 °F). The average maximum air temperatures are between 31°–35 °C (87.8–95.0 °F) and the average minimum air temperature is 20 °C – 25 °C (68–77°F). The diurnal temperature range is approximately 7°–11° C (12.6–19.8 °F).

2.Relative humidity (Figure B.1.2). The annual average relative humidity (RH) is 74%. The average maximum RH ranges from 90 % - 94 %. The average minimum RH is 53 % - 70 %.

3.Solar radiation. The monthly average daily solar radiation on the horizontal surface for April can be as much as 2,000 Btu/ft<sup>2</sup> per day, causing this period to be the hottest summer month (Jitkhajornwanich 1998).

4.Precipitation. Thailand is located in a very wet climate. The annual average precipitation is approximately 1,500–1,600 mm (60-64 inches). In August and September, the amount of rainfall may exceed 400 mm (16 inches) per month.

5. Wind speed & direction. During the winter, the wind blows from the northeast (i.e., from Southern China), and in the summer, the wind blows from the southwest (i.e., from the Indian Ocean).

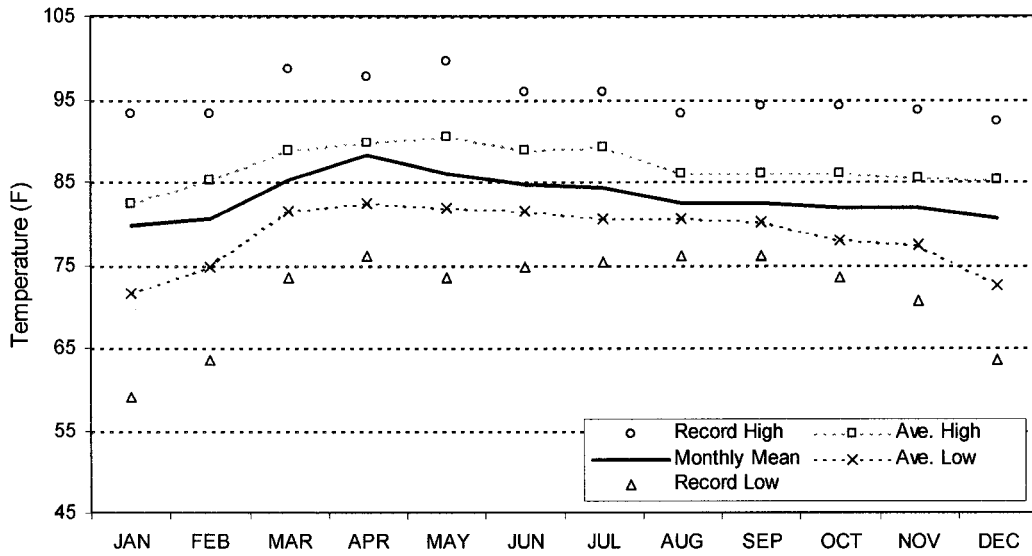


**Figure B.1.1** Monthly Average Dry-Bulb Temperature of Bangkok During 1985-1995.

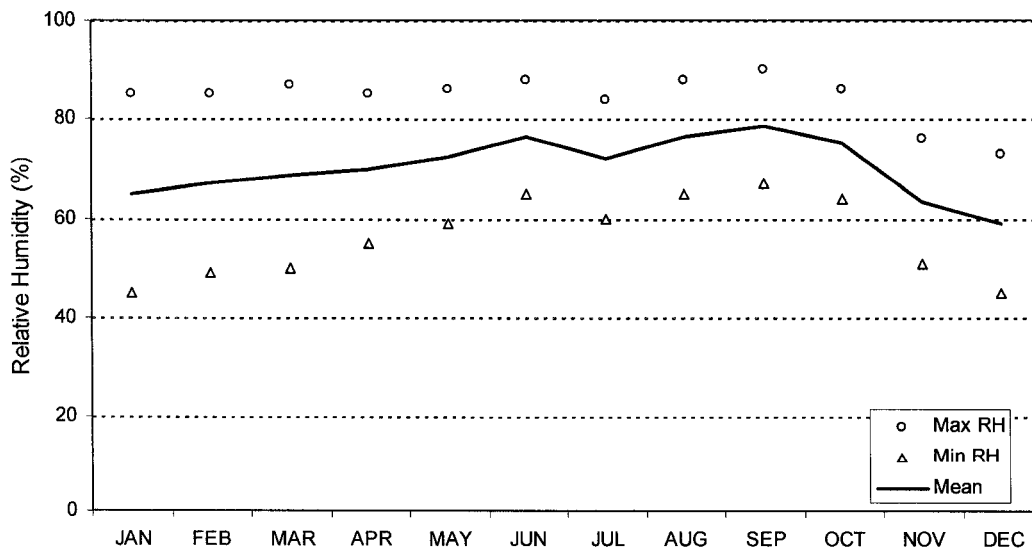


**Figure B.1.2** Monthly Average Relative Humidity of Bangkok During 1985-1995.

## **B.2 The 1999 Bangkok Weather Data**

The 1999 weather data from Bangkok, Thailand can be obtained from two sources: the Royal Thai Meteorological Department (RMTD) and the U.S. National Climatic Data Center (NCDC). The latter provides on-line access to the daily-average weather data of all stations in countries that are members of the World Meteorological Organization (WMO). This is done to comply with an international agreement. The daily weather data can be downloaded from the NCDC's FTP server at <http://ftp.ncdc.noaa.gov>. However, these data come from only one station - the Don Muang International Airport in Bangkok. The measurements generally include the daily dry-bulb temperature, dew point temperature, relative humidity, precipitation, wind speed, wind direction, cloudiness, visibility, atmospheric pressure, and various types of weather occurrences such as hail, fog, thunder, glaze, etc.

The weather data available from the RMTD basically include hourly: 1) barometric pressure, 2) dry-bulb temperature, 3) wet-bulb temperature, 4) relative humidity, 5) wind speed, 6) wind direction, 7) rainfall, 8) global horizontal solar radiation, and 9) the sky conditions. The data collected from these measurements were taken at 11 sub-stations around Bangkok and averaged into one set of data by the RMTD for distributions. All measurements except that of the wind speed were taken manually. These hourly data were collected by one snapshot measurement for each hour.

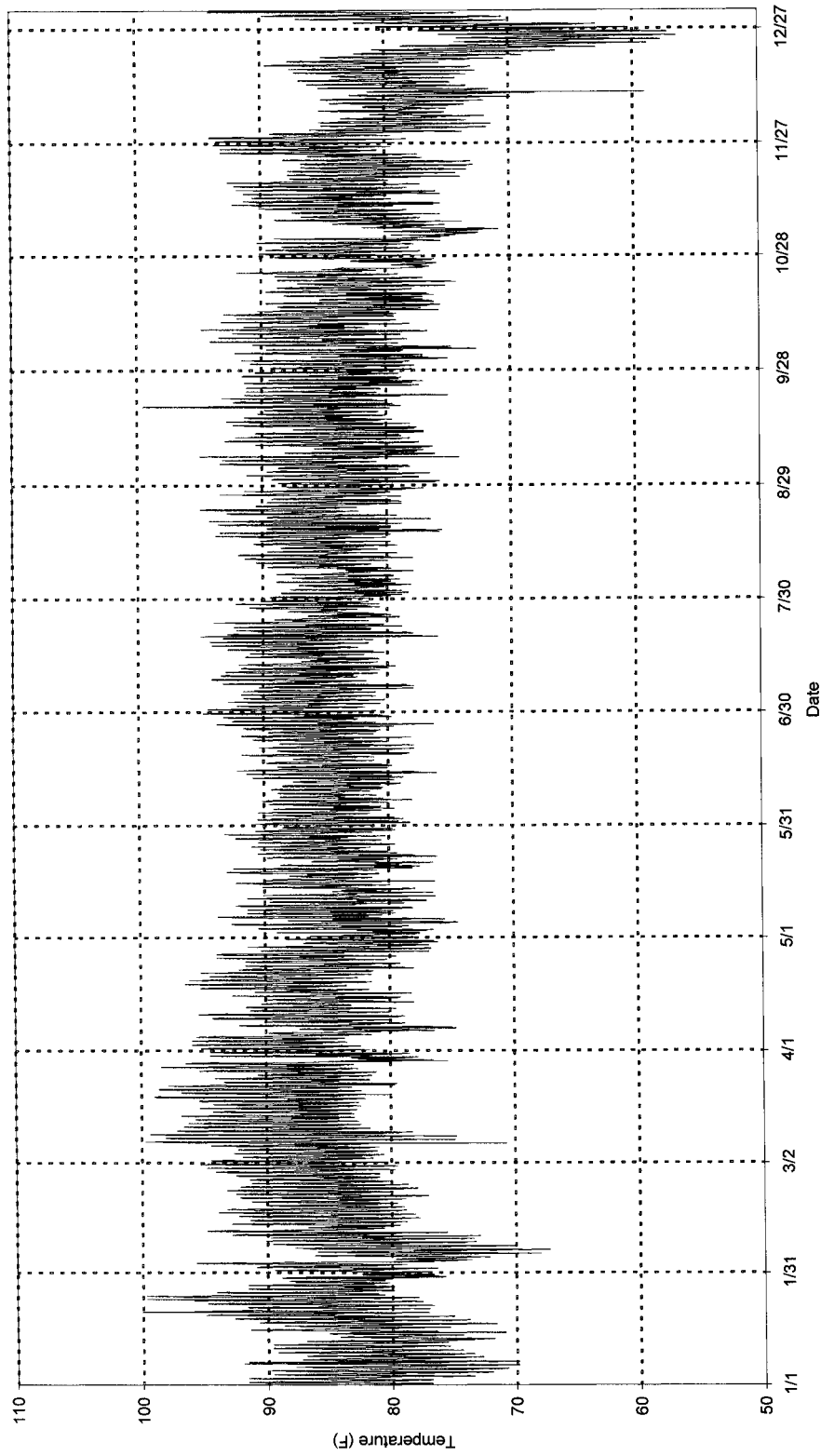


**Figure B.2.1** Outdoor Dry-Bulb Temperature in Bangkok in 1999.

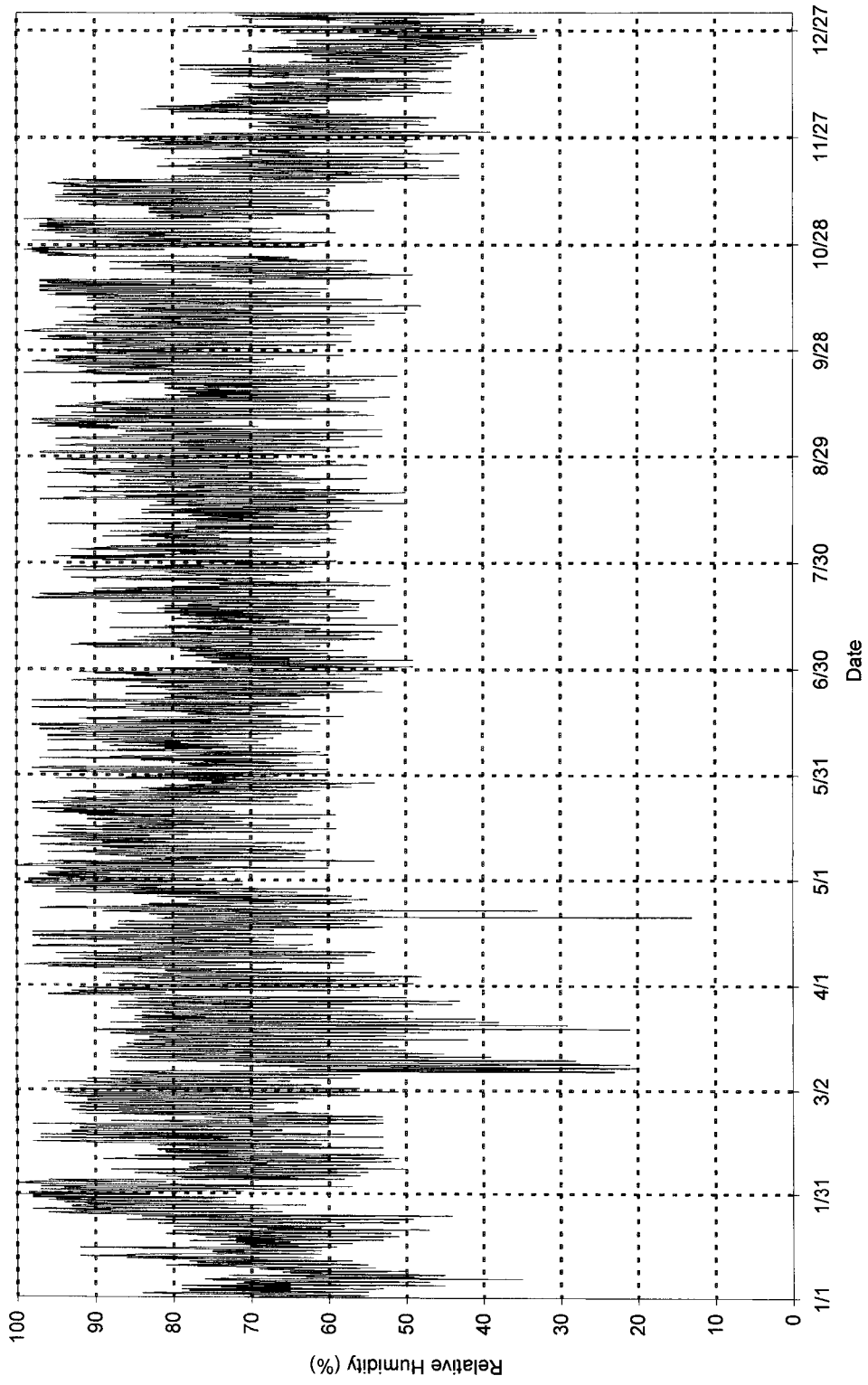


**Figure B.2.2** Outdoor Relative Humidity in Bangkok in 1999.

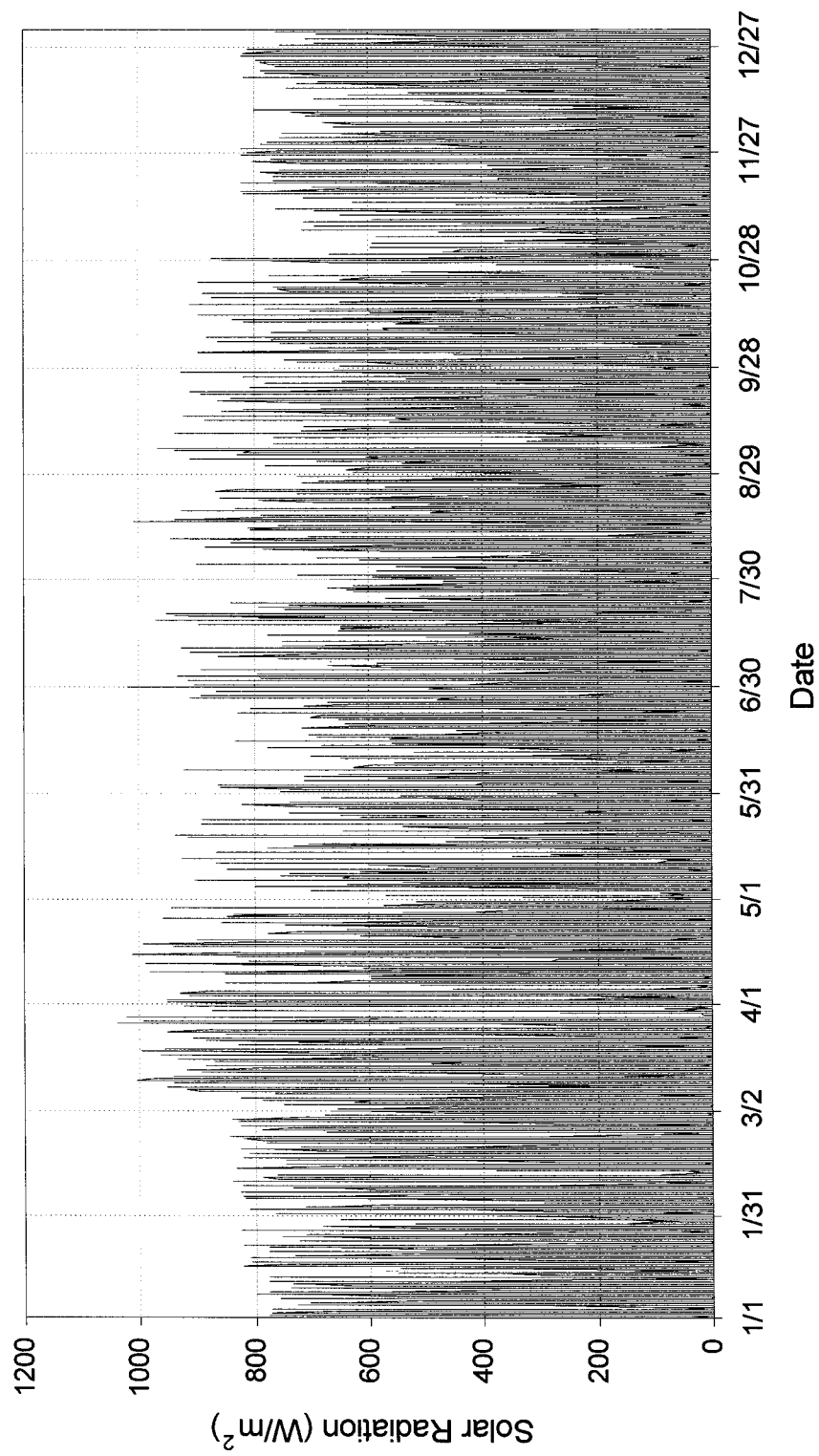


**Figure B.2.3** Global Horizontal Solar Radiation in Bangkok in 1999.

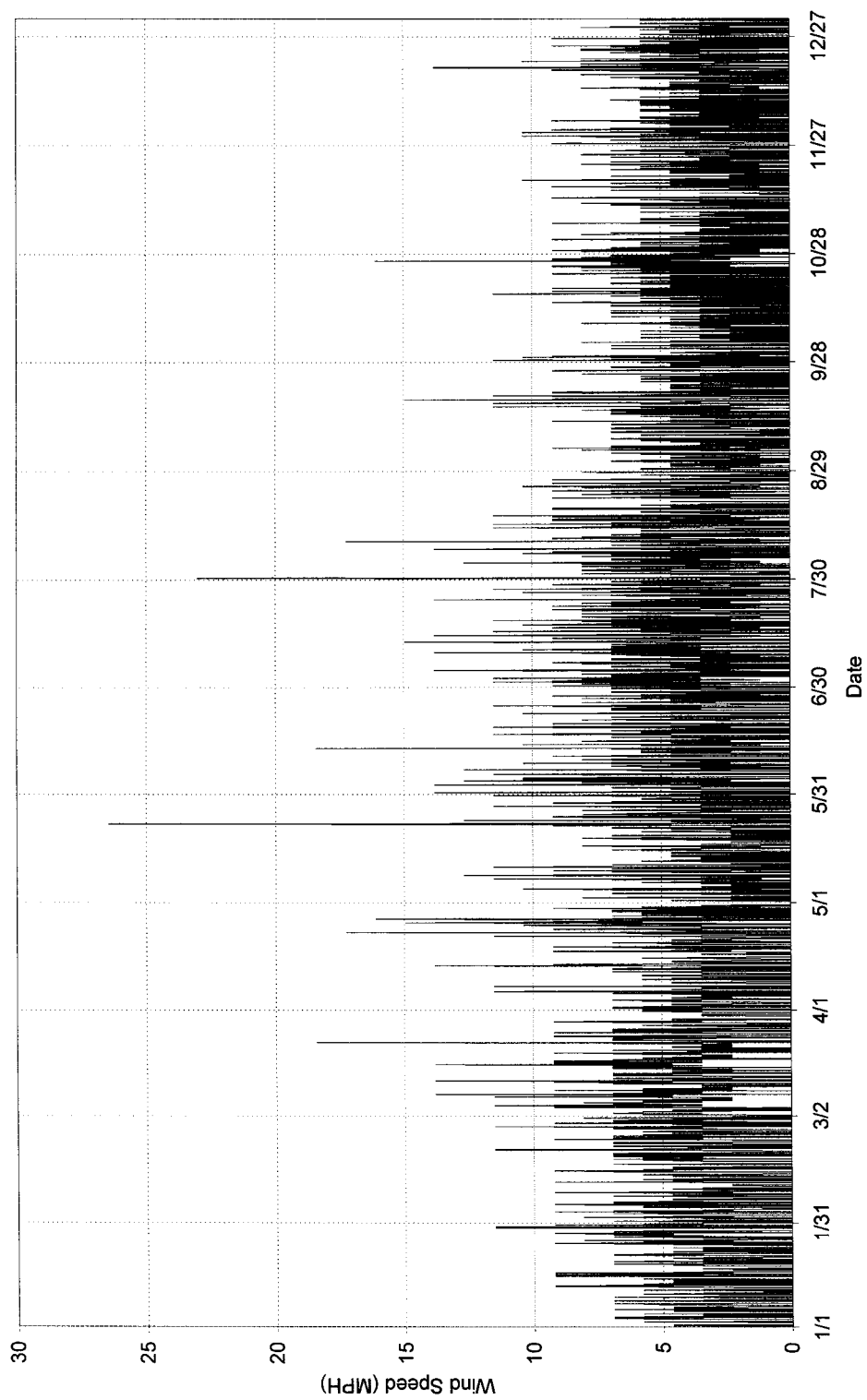
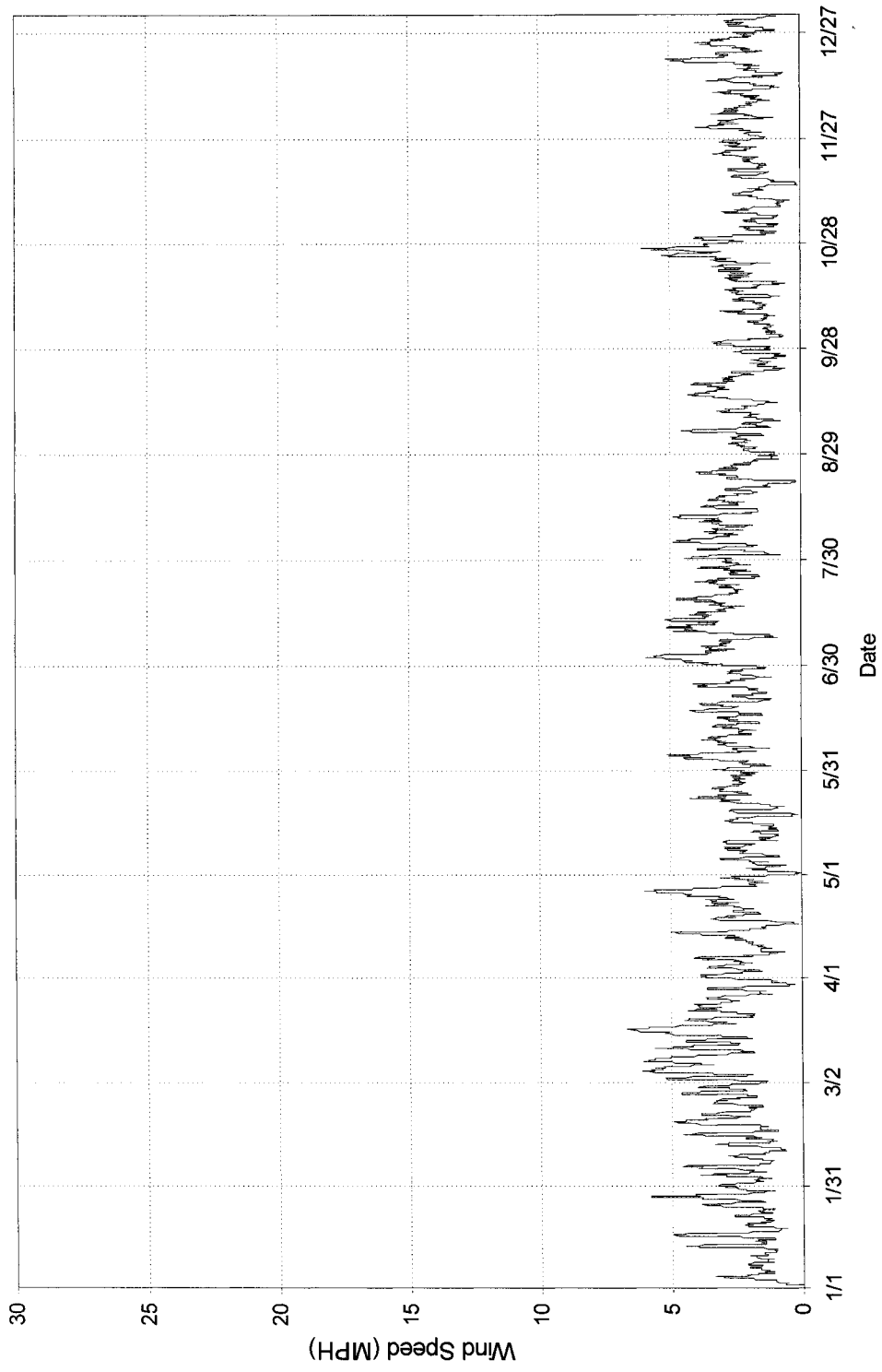


Figure B.2.4a Bangkok's Hourly Wind Speed in 1999.





**Figure B.2.4b** Bangkok's 12-Hour Running Average Wind Speed in 1999

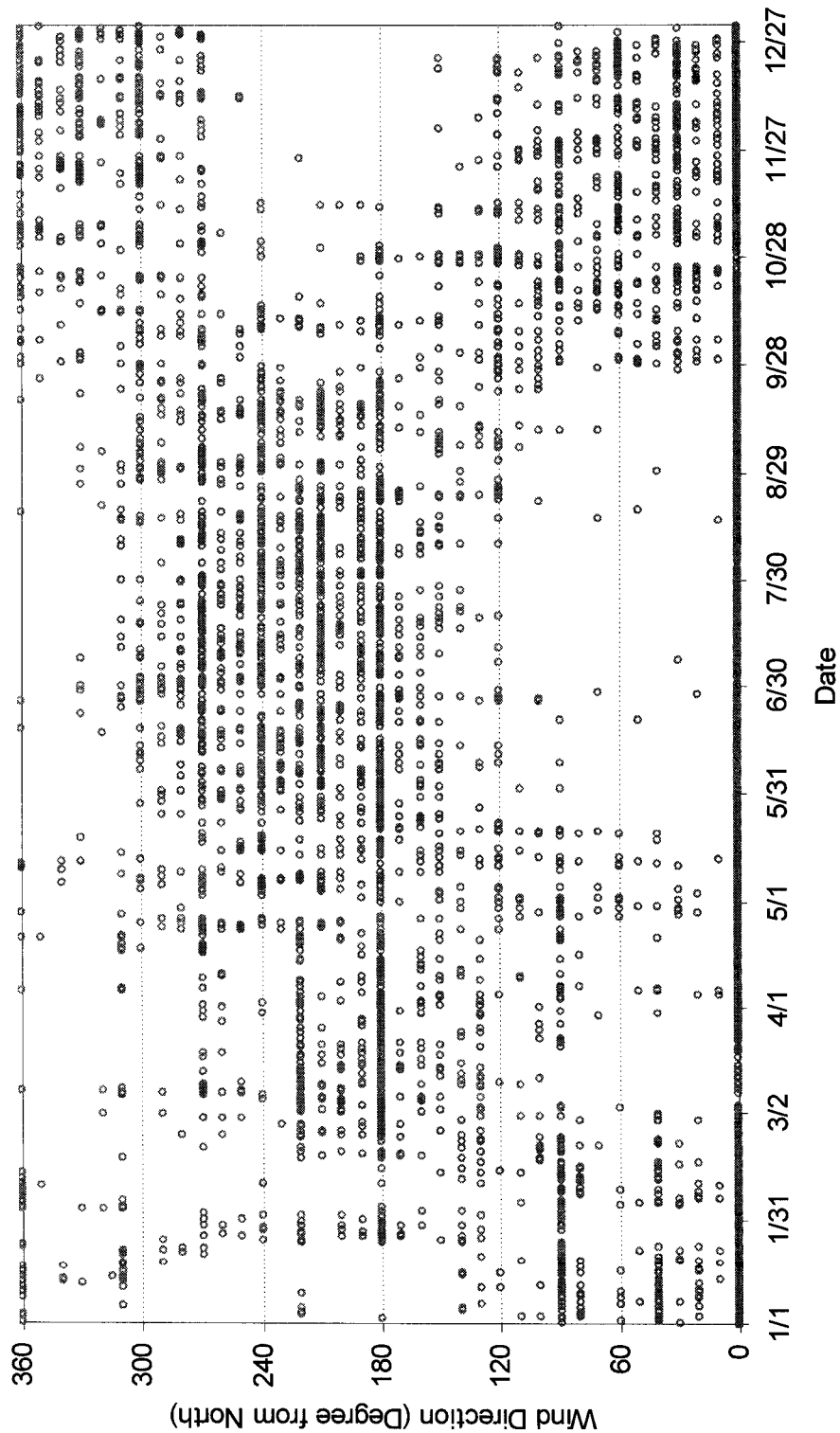


Figure B.2.5 Bangkok's Hourly Wind Direction in 1999.

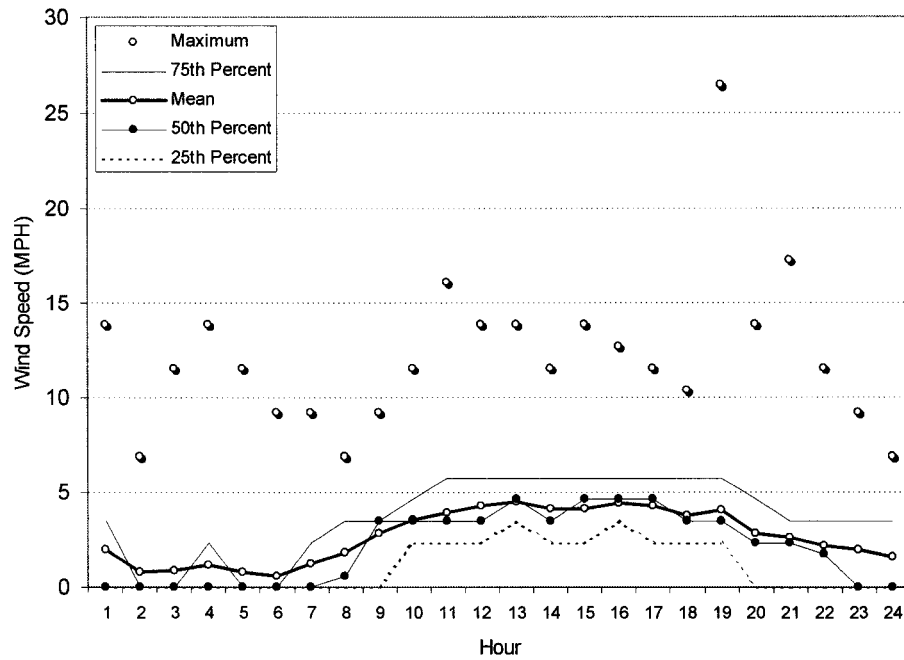


Figure B.2.6a Hourly Average Daily Wind Speed in the Summer of 1999.

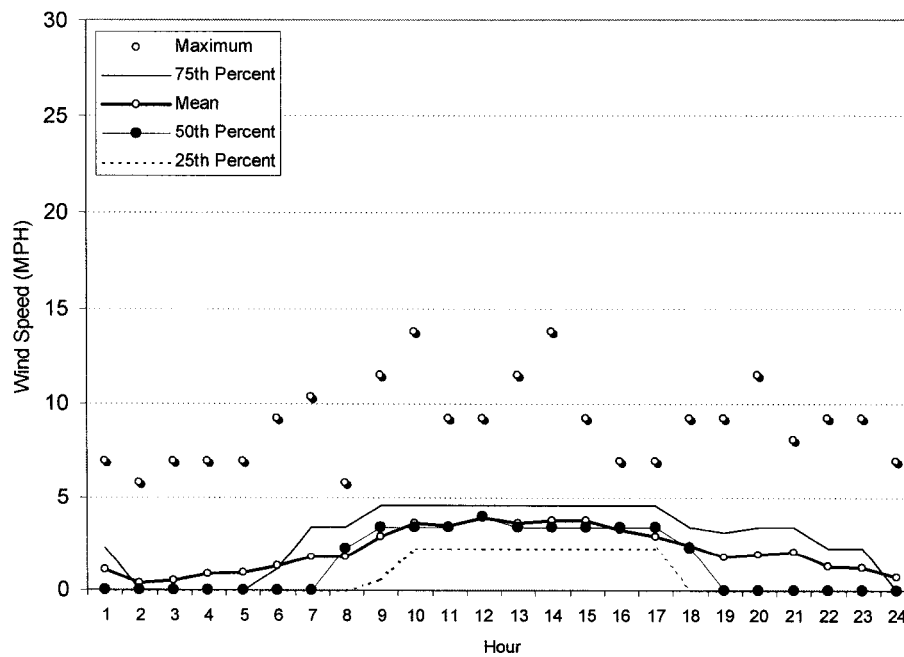


Figure B.2.6b Hourly Average Daily Wind Speed in the Winter of 1999.

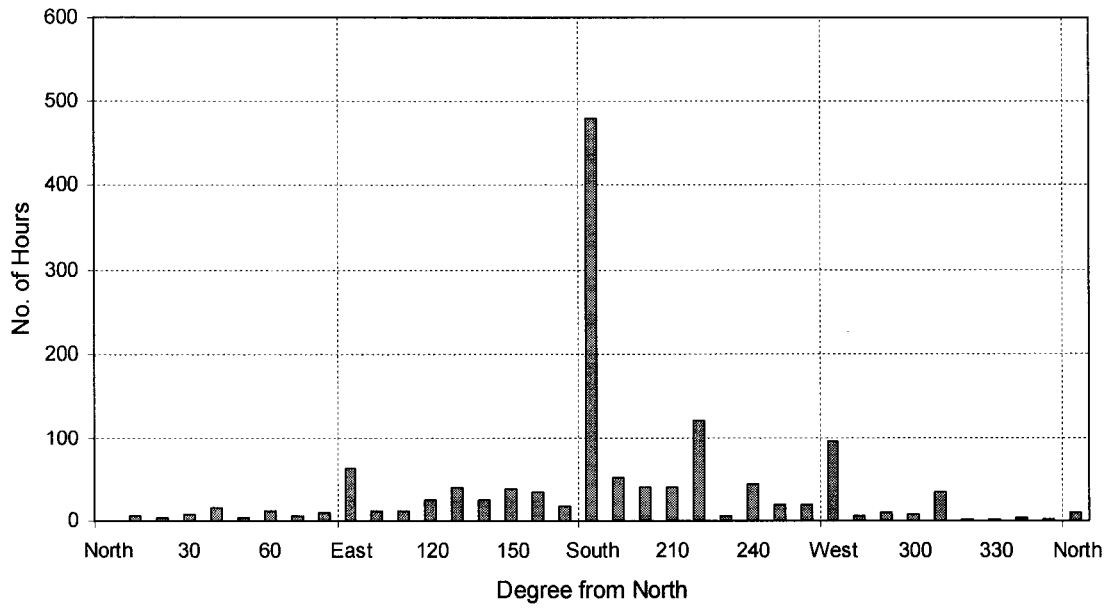


Figure B.2.7a Summer Wind Direction (March-April).

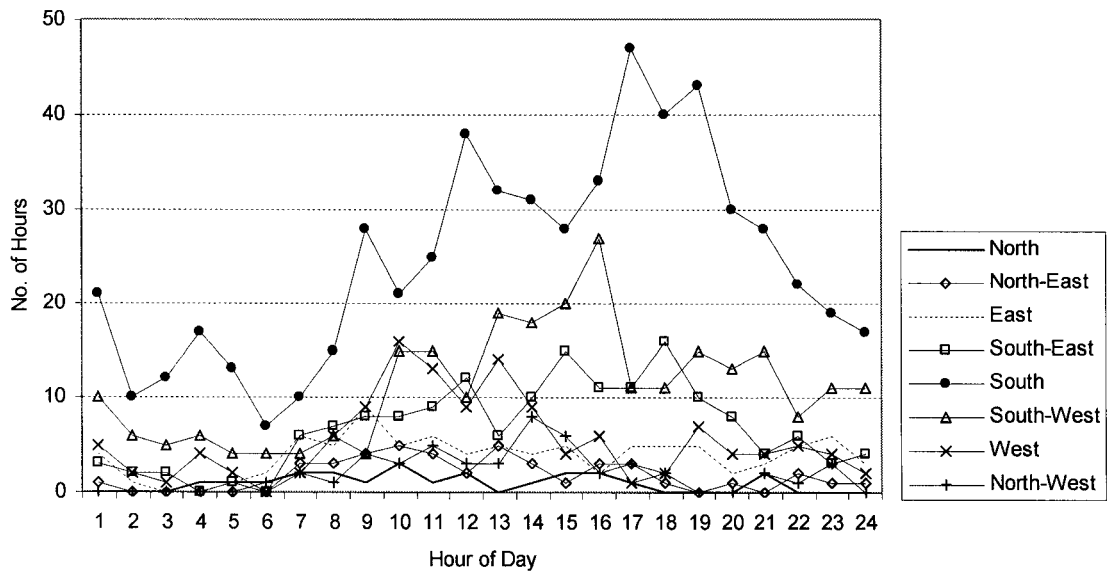


Figure B.2.7b Hourly Wind Direction Frequency During the Summer of 1999.

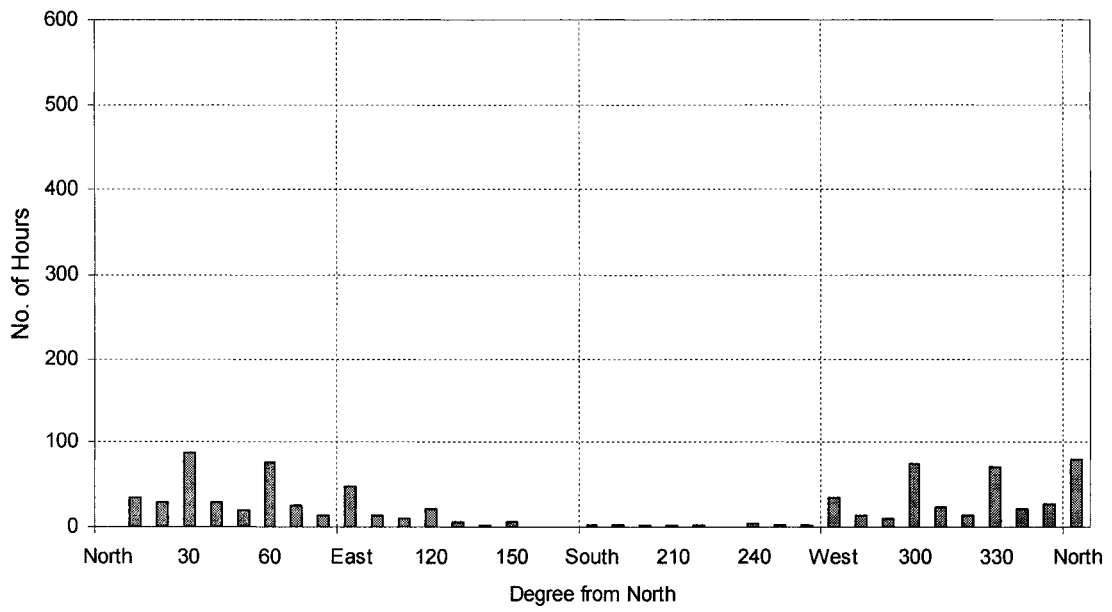


Figure B.2.8a Winter Wind Direction (November-December).

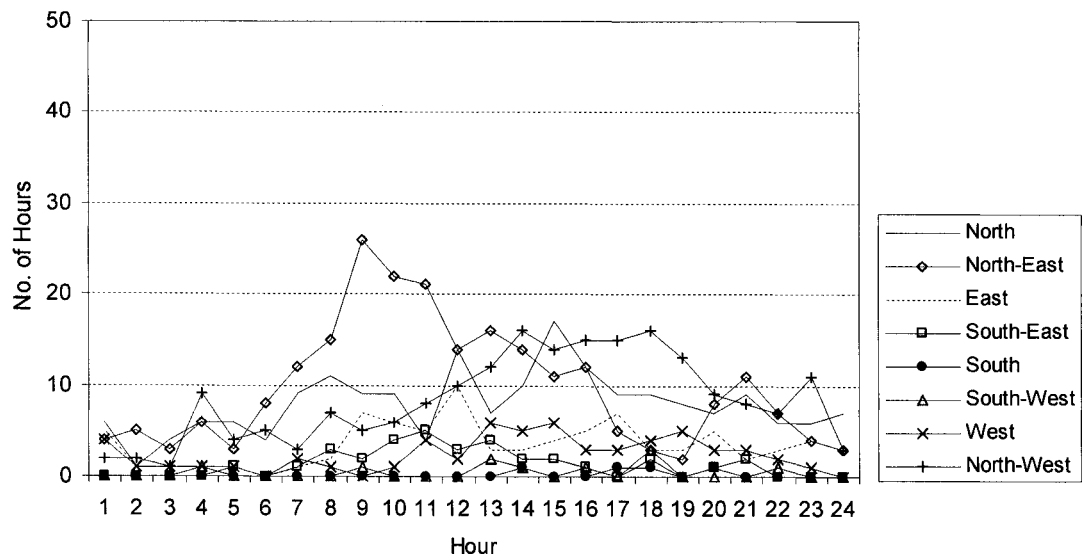


Figure B.2.8b Hourly Wind Direction Frequency During the Winter of 1999.

### **B.3 Instruments Used by the Bangkok Meteorological Department**

Regarding the instruments used to obtain the 1999 hourly weather data, dry-bulb temperatures were measured with a mercury-in-glass thermometer that was protected from solar radiation by a radiation shield. The wet-bulb temperatures were measured with a radiation-shielded wet-bulb thermometer with aspiration. The dew-point temperatures were then calculated from the dry-bulb and wet-bulb temperatures. The instrument used for relative humidity was a thin-film electrical conductivity hygrometer. For the wind data, at each station an anemometer (3-cup w/vane type) was used to take hourly measurements of the wind speeds and direction. The rainfall data were measured with a tray-type rain collector that can measure hourly amounts and the total accumulated amount of rainfall.

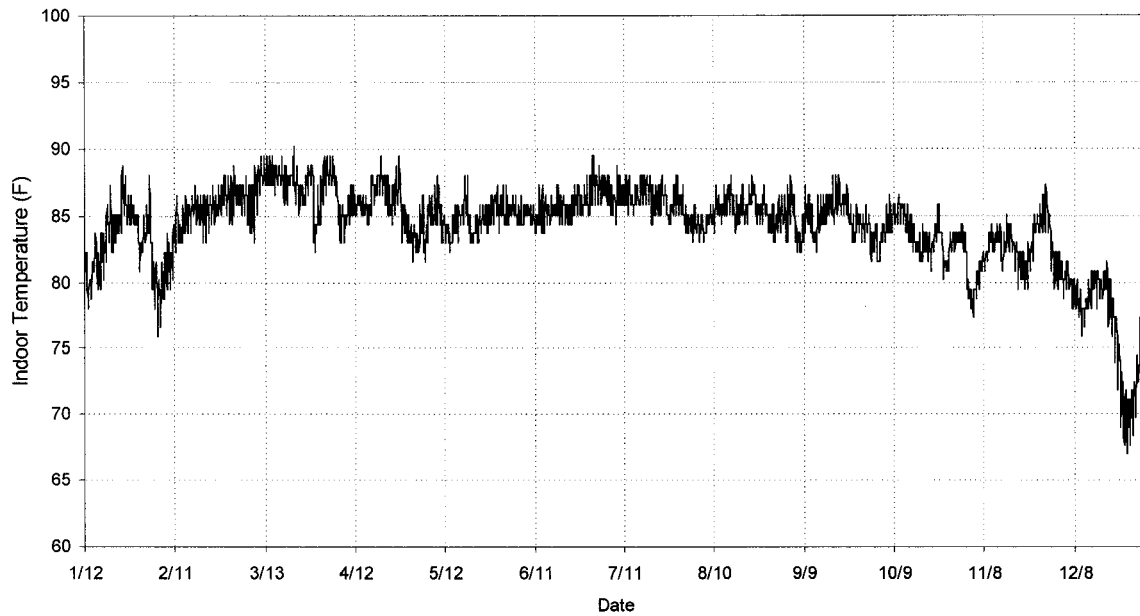
Regarding the solar radiation measurements, the global horizontal solar radiation was measured with an Eppley 180° pyranometer. There was no other equipment used to measure the beam or diffuse-only solar radiation. Also, the cloudiness was rated manually by an observer on a 0-10 scale in which 0-3 meant a clear sky, 4-6 meant a partly cloudy sky, and 7-10 meant a cloudy sky.

The measurements mentioned above are for the surface data only. The upper air data are obtained by the use of buoys, and the marine data can be obtained from the Royal Thai Navy.

## **APPENDIX C**

### **MEASUREMENT RESULTS OF THE CASE-STUDY TEMPLES**

This Appendix contains the measurement results of the case-study temples. The indoor air temperature, relative humidity, and floor surface temperature of each case study temple were measured using micro data-loggers installed in secured boxes (Onset 2002). Six data-loggers were used to measure room and floor temperatures using a surface-mounted external sensor. For each temple, the measurements included: 1) indoor air temperature and relative humidity at the floor level, 2) indoor air temperature and relative humidity at the ceiling level, and 3) the indoor floor surface temperature. The hourly data were retrieved once a month, beginning in February of 1999 and the data files emailed to the U.S. The wall surface temperatures were measured using a handheld infrared thermometer (Raytek 1999) from October of 1999 through January of 2000.

**C.1 Measurement Results of the Old Temple.**

*Figure C.1.1 Indoor Temperature of the Old Temple During Jan 1- Dec 31, 1999.*

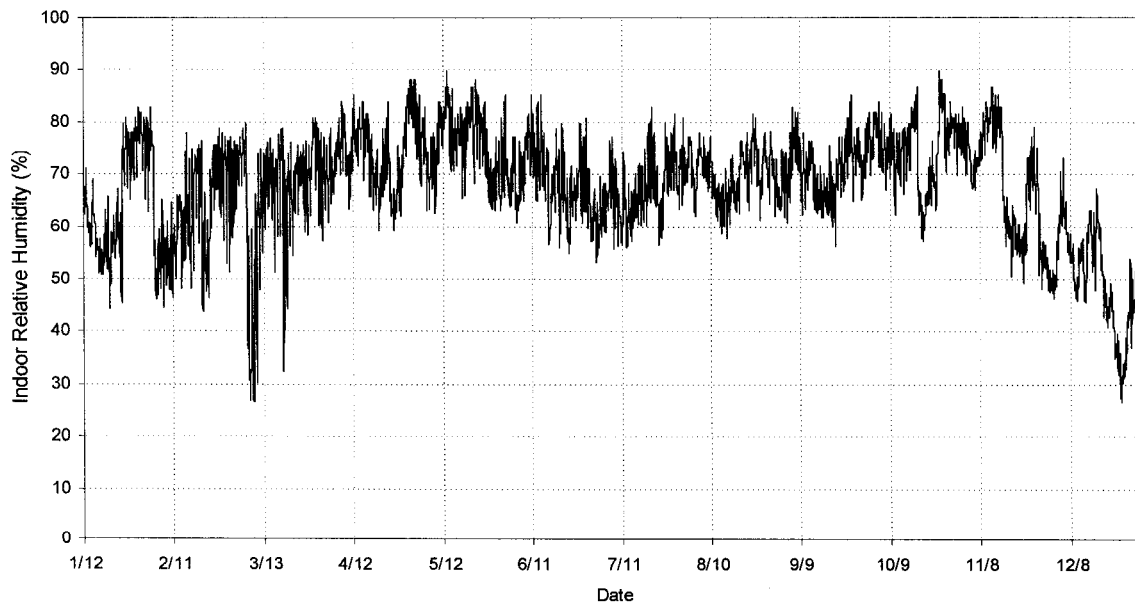


*Figure C.1.2 Indoor Relative Humidity of the Old Temple During Jan 12-Dec 31, 1999.*



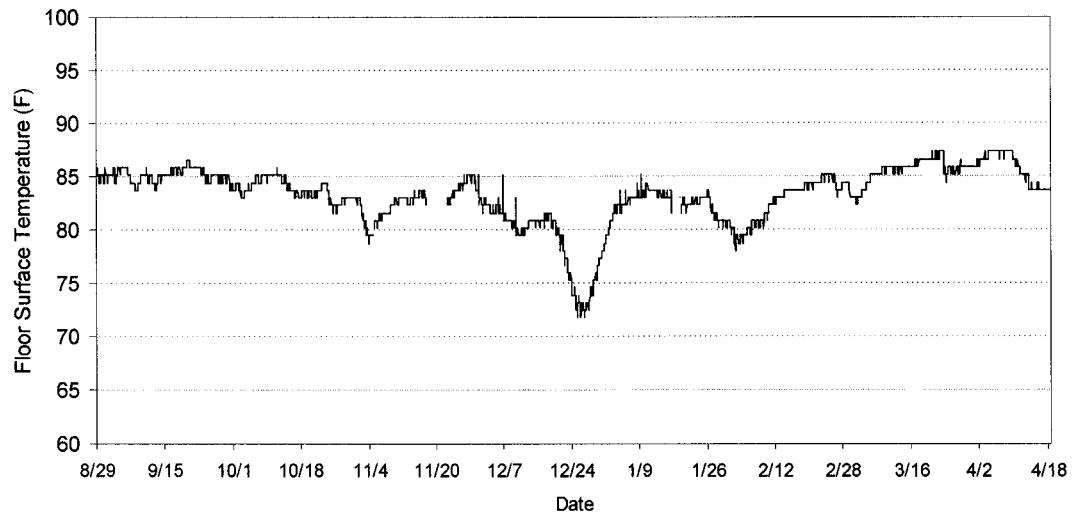


Figure C.1.3 Floor Surface Temperature of the Old Temple During August 1999-May 2000.

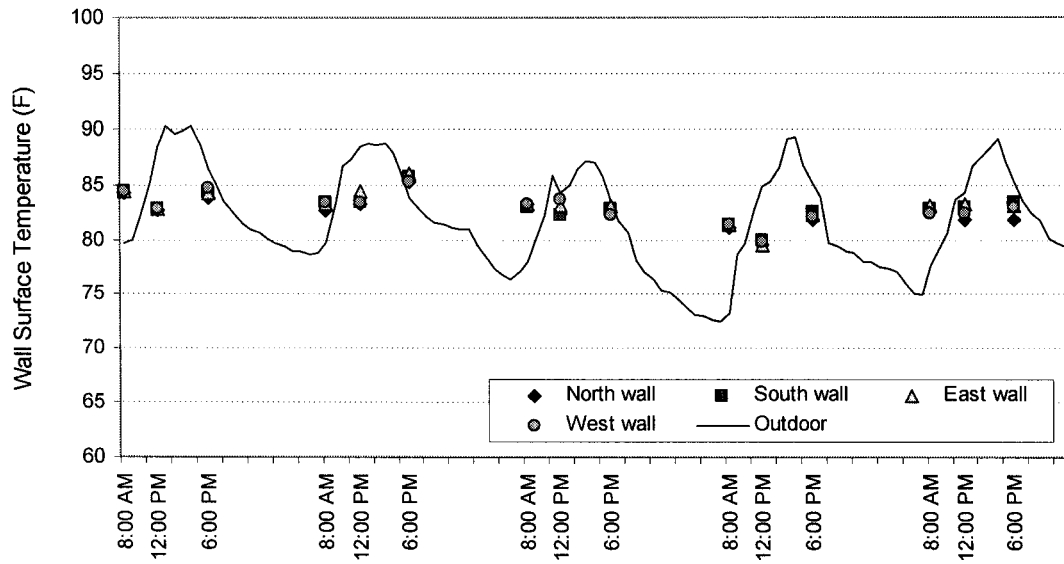
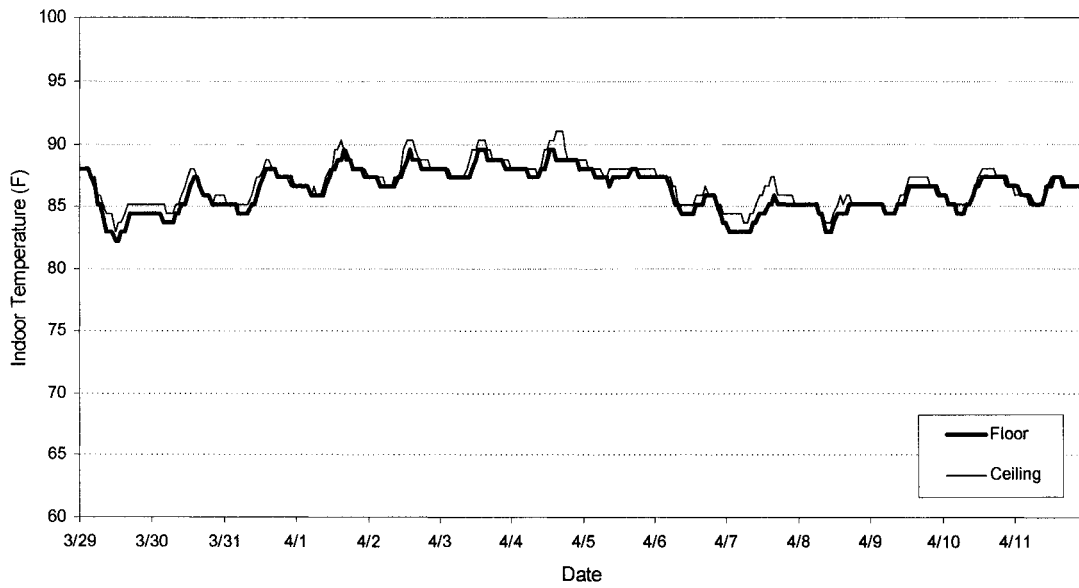
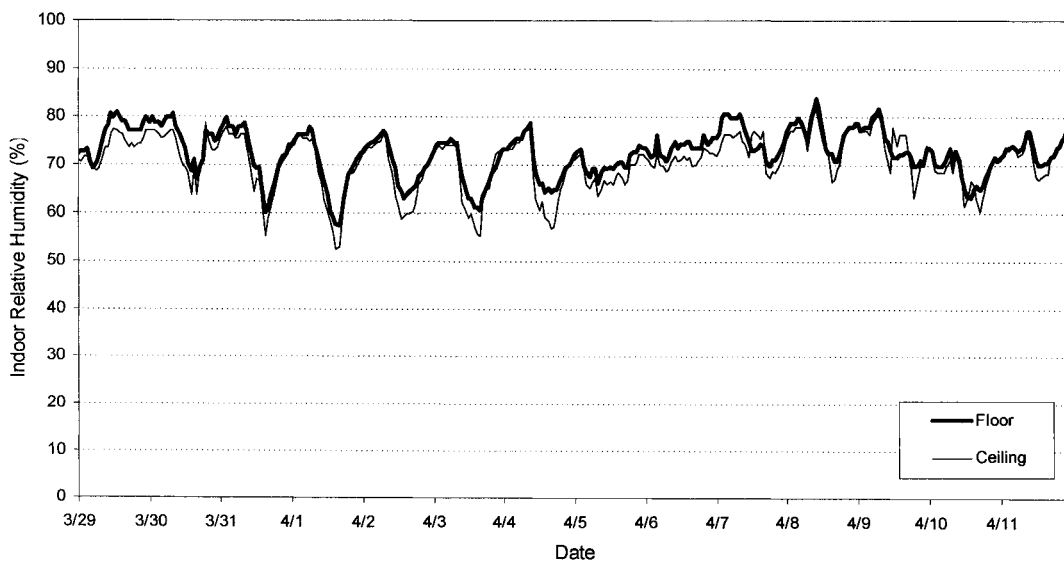


Figure C.1.4 Wall Surface Temperatures of the Old Temple During January 17-21, 1999.



**Figure C.1.5** *Indoor Temperatures of the Old Temple at the Floor and Ceiling Levels During the Summer.*



**Figure C.1.6** *Indoor Relative Humidity of the Old Temple at the Floor and Ceiling Levels During the Summer.*

## C.2 Measurement Results of the New Temple

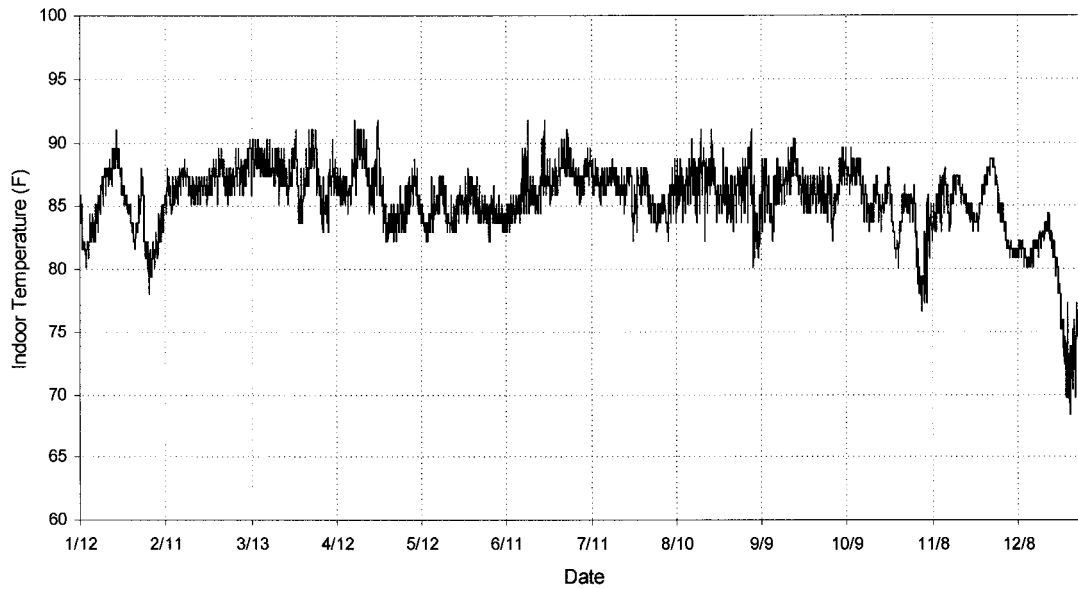


*Figure C.2.1 Indoor Temperature of the New Temple During Jan 12-Dec 31, 1999.*

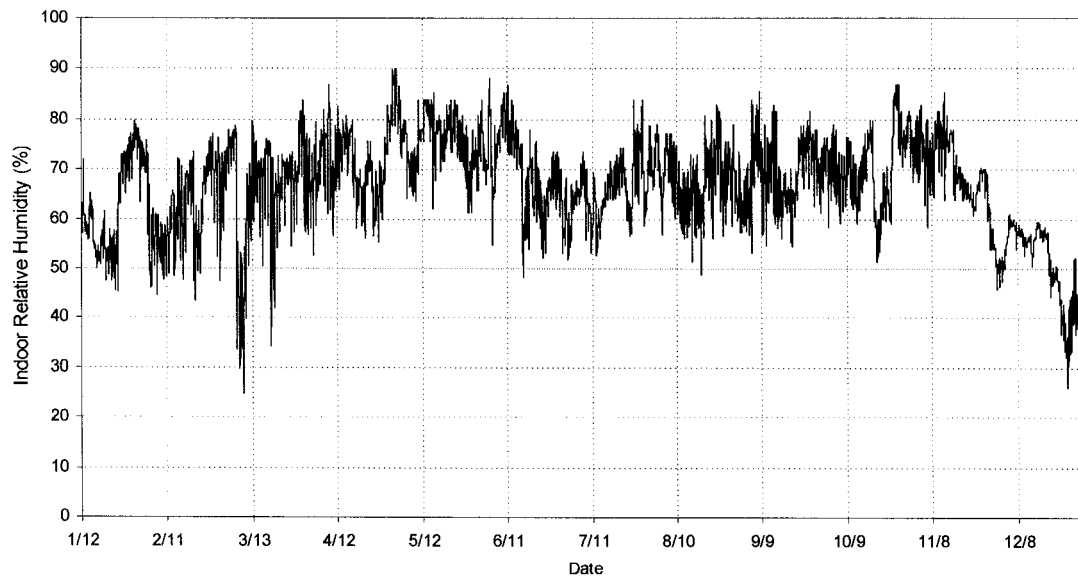


*Figure C.2.2 Indoor Relative Humidity of the New Temple During Jan 12-Dec 31, 1999.*

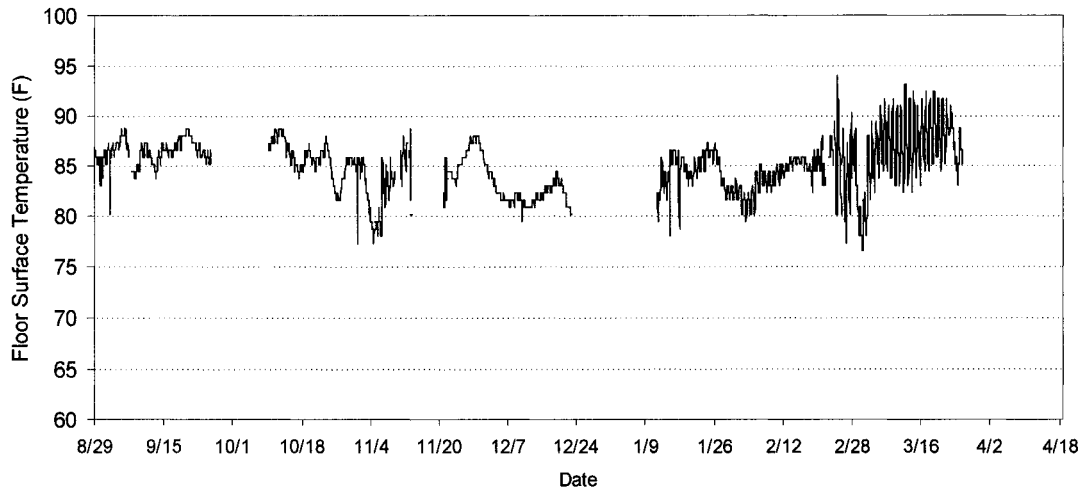


Figure C.2.3 Floor Surface Temperature of the New Temple During August 1999-May 2000.

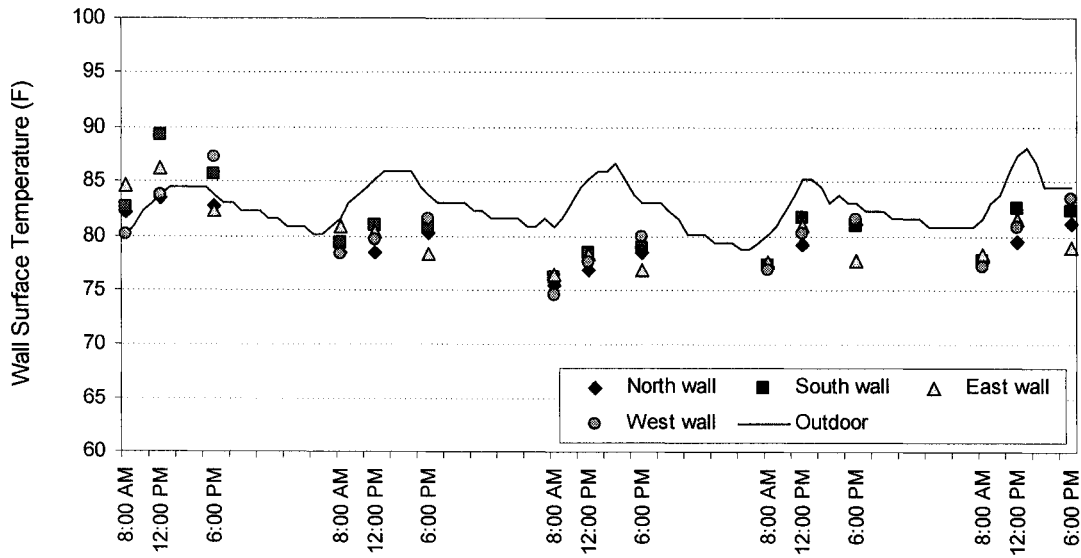
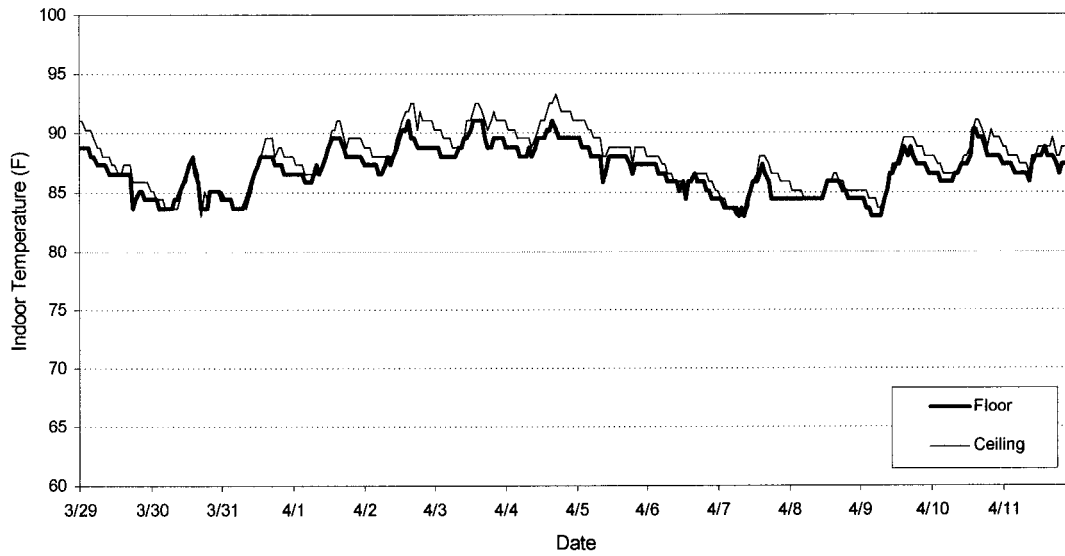
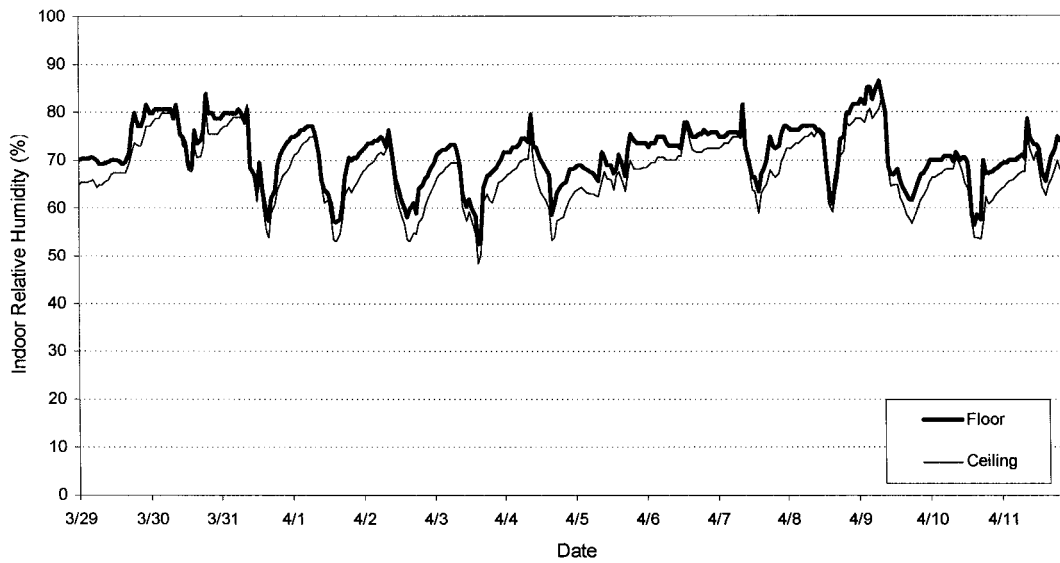


Figure C.2.4 Wall Surface Temperatures of the New Temple During November 8-12, 1999.



**Figure C.2.5** *Indoor Temperatures of the New Temple at the Floor and Ceiling Levels During the Summer.*



**Figure C.2.6** *Indoor Relative Humidity of the New Temple at the Floor and Ceiling Levels During the Summer.*

## APPENDIX D

### DOE-2 SIMULATION

#### D.1 DOE-2 Input File of the Base-Case Temple

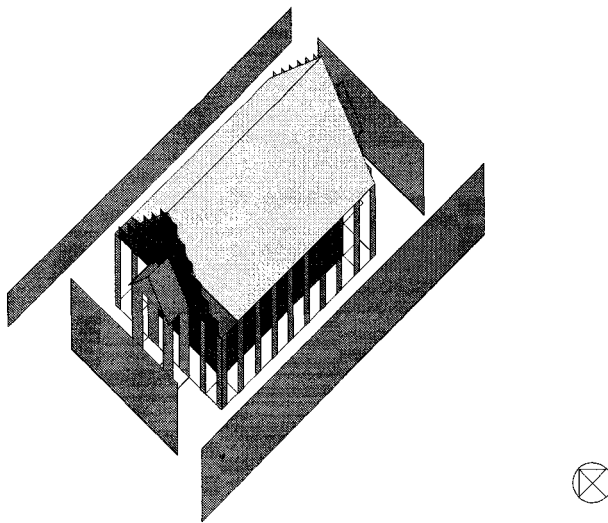


*Figure D.1.1 DrawBDL Output of the Base-Case Temple.*

```

INPUT  LOADS  ..
TITLE  LINE-1 *ATCH SRESHTHAPUTRA*
        LINE-2 *COPYRIGHT 2002*
        LINE-2 *OLD TEMPLE: ORIGINAL DESIGN, AUGUST 2000*
        LINE-3 *BANGKOK, THAILAND*  ..

RUN-PERIOD      JAN 1 1999 THRU DEC 31 1999  ..
ABORT           ERRORS  ..
DIAGNOSTIC      WARNINGS ..
LOADS-REPORT    SUMMARY= (ALL-SUMMARY)
                VERIFICATION= (ALL-VERIFICATION) ..

BUILDING-LOCATION  LATITUDE= 13.9      LONGITUDE= -100.6
                 ALTITUDE= 39       TIME-ZONE= -7
                 HOLIDAY= NO
                 GROSS-AREA= 2160    AZIMUTH= 0.0
                 DAYLIGHT-SAVINGS= NO
                 GROUND-T = (80,80,82,82,80,80
                             ,80,80,80,80,78,74)
                 SURF-TEMP-CALC = YES ..

$ CONSTRUCTION

$ WALLS: 30-INCH BRICK WALLS & CEMENT MORTAR SURFACE
$ ROOF : 3/8-INCH RED CLAY TILE WITH 0.75 ABSORPTANCE
$ FLOOR: 8-INCH HEAVY WEIGHT CONCRETE SLAB-ON-GRADE & MARBLE TOP
$ CEILING: 3/4-INCH SOFT WOOD
$ DOORS & WINDOWS: SOLID WOOD (U=0.5)

BRICK-WALL      =MATERIAL
                 THICKNESS = 2.67
                 CONDUCTIVITY = 0.4167
                 DENSITY = 140.0
                 SPECIFIC-HEAT= 0.2  ..

```

```

CLAY-TILE      =MATERIAL
                THICKNESS = 0.083
                CONDUCTIVITY = 0.13125
                DENSITY = 100
                SPECIFIC-HEAT= 0.4  ..

CONCRETE-FLOOR =MATERIAL
                THICKNESS = 0.5
                CONDUCTIVITY = 1.0417
                DENSITY = 170.0
                SPECIFIC-HEAT= 0.5  ..

WOOD-PANEL     =MATERIAL
                THICKNESS = 0.0833
                CONDUCTIVITY = 0.04916
                DENSITY = 45
                SPECIFIC-HEAT= 0.5  ..

WA-1 = LAYERS  MATERIAL= (BRICK-WALL)
                INSIDE-FILM-RES = 0.80  ..

RF-1 = LAYERS  MATERIAL= (CLAY-TILE)
                INSIDE-FILM-RES = 0.71  ..

FL-1 = LAYERS  MATERIAL= (CONCRETE-FLOOR)
                INSIDE-FILM-RES = 0.93  ..

CL-1 = LAYERS  MATERIAL= (WOOD-PANEL)
                INSIDE-FILM-RES = 0.86  ..

WALL-1         =CONSTRUCTION  LAYERS=WA-1
                ABSORPTANCE=0.85  ..
WALL-2         =CONSTRUCTION  LAYERS=WA-1
                ABSORPTANCE=0.85  ..
ROOF-1        =CONSTRUCTION  LAYERS=RF-1
                ABSORPTANCE=0.75  ..
FLOOR-1       =CONSTRUCTION  LAYERS=FL-1
                ABSORPTANCE=0.90  ..
CEIL-1        =CONSTRUCTION  LAYERS=CL-1
                ABSORPTANCE=0.85  ..
DR-1          =CONSTRUCTION  U=0.5  ..

$ OCCUPANCY SCHEDULE
OC-1          =DAY-SCHEDULE  (1,5) (0.0) (6,12) (0.5)
                (13,18) (0.2) (19,24) (0.0) ..
OC-2          =DAY-SCHEDULE  (1,5) (0.0) (6,12) (1.0)
                (13,18) (0.5) (19,24) (0.0) ..
OC-WEEK       =WEEK-SCHEDULE (WD) OC-1 (WEH) OC-2  ..
OCCUPY-1     =SCHEDULE      THRU DEC 31 OC-WEEK  ..

$ LIGHTING SCHEDULE
LT-1          =DAY-SCHEDULE  (1,5) (0.0) (6,18) (1.0)
                (19,24) (0.0)  ..
LT-WEEK       =WEEK-SCHEDULE (WD) LT-1 (WEH) LT-1  ..
LIGHTS-1     =SCHEDULE      THRU DEC 31 LT-WEEK  ..

$ EQUIPMENT SCHEDULE
EQ-1          =DAY-SCHEDULE  (1,5) (0.0) (6,12) (0.5)
                (13,18) (0.2) (19,24) (0.0) ..
EQ-2          =DAY-SCHEDULE  (1,5) (0.0) (6,12) (1.0)
                (13,18) (0.5) (19,24) (0.0) ..
EQ-WEEK       =WEEK-SCHEDULE (WD) EQ-1 (WEH) EQ-2  ..
EQUIP-1      =SCHEDULE      THRU DEC 31 EQ-WEEK  ..

$ INFILTRATION SCHEDULE
ALLVENT-T     =SCHEDULE      THRU DEC 31 (ALL) (1,24) (1)  ..
NOVENT-T      =SCHEDULE      THRU DEC 31 (ALL) (1,24) (0)  ..
DAY-WD        =DAY-SCHEDULE  (1,5) (0.0) (6,12) (1.0)
                (13,18) (1.0) (19,24) (0.0) ..
DAY-WE        =DAY-SCHEDULE  (1,5) (0.0) (6,12) (1.0)
                (13,18) (1.0) (19,24) (0.0) ..
DAY-WK        =WEEK-SCHEDULE (WD) DAY-WD (WEH) DAY-WE ..
DAYVENT-T     =SCHEDULE      THRU DEC 31 DAY-WK  ..
NIGHTVENT-T   =SCHEDULE      THRU DEC 31 (ALL) (1,5) (1)
                (6,18) (0) (19,24) (1)  ..

$ SET DEFAULT VALUES
SET-DEFAULT FOR SPACE FLOOR-WEIGHT=0  ..
SET-DEFAULT FOR DOOR CONSTRUCTION=DR-1 ..

```

§ GENERAL SPACE DEFINITION

TEMPLE =SPACE-CONDITIONS  
 TEMPERATURE =(84)  
 PEOPLE-SCHEDULE =OCCUPY-1  
 NUMBER-OF-PEOPLE =5  
 PEOPLE-HEAT-GAIN =350  
 LIGHTING-SCHEDULE =LIGHTS-1  
 LIGHTING-TYPE =INCAND  
 LIGHT-TO-SPACE =0.5  
 LIGHTING-W/SQFT =0.05  
 EQUIP-SCHEDULE =EQUIP-1  
 EQUIPMENT-W/SQFT =0.1  
 INF-METHOD =AIR-CHANGE  
 INF-SCHEDULE =DAYVENT-T  
 AIR-CHANGES/HR =20.0 ..

§ SPECIFIC SPACE DETAILS

ATTIC-1 =SPACE ZONE-TYPE=UNCONDITIONED  
 VOLUME=51376  
 AREA=3952  
 INF-METHOD = AIR-CHANGE  
 INF-SCHEDULE = ALLVENT-T  
 AIR-CHANGES/HR = 5.0 ..

FRONT-RF=ROOF AZIMUTH=180 TILT=45  
 HEIGHT=36.7 WIDTH=76 X=12 Y=12 Z=25  
 CONSTRUCTION=ROOF-1  
 GND-REFLECTANCE=0.15  
 SHADING-DIVISION = 40  
 INSIDE-SURF-TEMP = YES ..

BACK-RF =ROOF AZIMUTH=0 TILT=45  
 HEIGHT=36.7 WIDTH=76 X=88 Y=64 Z=25  
 CONSTRUCTION=ROOF-1  
 GND-REFLECTANCE=0.15  
 SHADING-DIVISION = 40  
 INSIDE-SURF-TEMP = YES ..

RIGHT-RF1=EXTERIOR-WALL AZIMUTH=90  
 HEIGHT=4 WIDTH=48 X=88 Y=14 Z=25  
 CONSTRUCTION=WALL-1  
 GND-REFLECTANCE=0.15  
 SHADING-DIVISION = 20  
 INSIDE-SURF-TEMP = YES ..

RIGHT-RF2=EXTERIOR-WALL AZIMUTH=90  
 HEIGHT=4 WIDTH=40 X=88 Y=18 Z=29  
 CONSTRUCTION=WALL-1  
 GND-REFLECTANCE=0.15  
 SHADING-DIVISION = 20  
 INSIDE-SURF-TEMP = YES ..

RIGHT-RF3=EXTERIOR-WALL AZIMUTH=90  
 HEIGHT=4 WIDTH=32 X=88 Y=22 Z=33  
 CONSTRUCTION=WALL-1  
 GND-REFLECTANCE=0.15  
 SHADING-DIVISION = 20  
 INSIDE-SURF-TEMP = YES ..

RIGHT-RF4=EXTERIOR-WALL AZIMUTH=90  
 HEIGHT=4 WIDTH=24 X=88 Y=26 Z=37  
 CONSTRUCTION=WALL-1  
 GND-REFLECTANCE=0.15  
 SHADING-DIVISION = 20  
 INSIDE-SURF-TEMP = YES ..

RIGHT-RF5=EXTERIOR-WALL AZIMUTH=90  
 HEIGHT=4 WIDTH=16 X=88 Y=30 Z=41  
 CONSTRUCTION=WALL-1  
 GND-REFLECTANCE=0.15  
 SHADING-DIVISION = 20  
 INSIDE-SURF-TEMP = YES ..

RIGHT-RF6=EXTERIOR-WALL AZIMUTH=90  
 HEIGHT=4 WIDTH=8 X=88 Y=34 Z=45  
 CONSTRUCTION=WALL-1  
 GND-REFLECTANCE=0.15  
 SHADING-DIVISION = 20  
 INSIDE-SURF-TEMP = YES ..

LEFT-RF1=EXTERIOR-WALL AZIMUTH=270  
 HEIGHT=4 WIDTH=48 X=12 Y=62 Z=25  
 CONSTRUCTION=WALL-1  
 GND-REFLECTANCE=0.15  
 SHADING-DIVISION = 20



```

INSIDE-SURF-TEMP = YES ..

LEFT-RF2=EXTERIOR-WALL AZIMUTH=270
HEIGHT=4 WIDTH=40 X=12 Y=58 Z=29
CONSTRUCTION=WALL-1
GND-REFLECTANCE=0.15
SHADING-DIVISION = 20
INSIDE-SURF-TEMP = YES ..

LEFT-RF3=EXTERIOR-WALL AZIMUTH=270
HEIGHT=4 WIDTH=32 X=12 Y=54 Z=33
CONSTRUCTION=WALL-1
GND-REFLECTANCE=0.15
SHADING-DIVISION = 20
INSIDE-SURF-TEMP = YES ..

LEFT-RF4=EXTERIOR-WALL AZIMUTH=270
HEIGHT=4 WIDTH=24 X=12 Y=50 Z=37
CONSTRUCTION=WALL-1
GND-REFLECTANCE=0.15
SHADING-DIVISION = 20
INSIDE-SURF-TEMP = YES ..

LEFT-RF5=EXTERIOR-WALL AZIMUTH=270
HEIGHT=4 WIDTH=16 X=12 Y=46 Z=41
CONSTRUCTION=WALL-1
GND-REFLECTANCE=0.15
SHADING-DIVISION = 20
INSIDE-SURF-TEMP = YES ..

LEFT-RF6=EXTERIOR-WALL AZIMUTH=270
HEIGHT=4 WIDTH=8 X=12 Y=42 Z=45
CONSTRUCTION=WALL-1
GND-REFLECTANCE=0.15
SHADING-DIVISION = 20
INSIDE-SURF-TEMP = YES ..

CEILING-A=INTERIOR-WALL AREA=1722
INT-WALL-TYPE=STANDARD
NEXT-TO SPACE-1
CONSTRUCTION=CEIL-1
INSIDE-SURF-TEMP = YES ..

SPACE-1 =SPACE SPACE-CONDITIONS= TEMPLE
AREA=2160 VOLUME=54000
SHAPE=BOX HEIGHT=25
WIDTH=60 DEPTH=36
NUMBER-OF-PEOPLE=5 ..

FRONT-1 =EXTERIOR-WALL AZIMUTH=180
HEIGHT=25 WIDTH=60 X=20 Y=20 Z=0
CONSTRUCTION=WALL-1
GND-REFLECTANCE=0.15
SHADING-DIVISION = 40
INSIDE-SURF-TEMP = YES ..

WF-1 =DOOR WIDTH=4 HEIGHT=6.7
X=4 Y=4 SETBACK=1.2
INSIDE-SURF-TEMP = NO ..

WF-2 =DOOR WIDTH=4 HEIGHT=6.7
X=12 Y=4 SETBACK=1.2
INSIDE-SURF-TEMP = NO ..

WF-3 =DOOR WIDTH=4 HEIGHT=6.7
X=20 Y=4 SETBACK=1.2
INSIDE-SURF-TEMP = NO ..

WF-4 =DOOR WIDTH=4 HEIGHT=6.7
X=28 Y=4 SETBACK=1.2
INSIDE-SURF-TEMP = NO ..

WF-5 =DOOR WIDTH=4 HEIGHT=6.7
X=36 Y=4 SETBACK=1.2
INSIDE-SURF-TEMP = NO ..

WF-6 =DOOR WIDTH=4 HEIGHT=6.7
X=44 Y=4 SETBACK=1.2
INSIDE-SURF-TEMP = NO ..

WF-7 =DOOR WIDTH=4 HEIGHT=6.7
X=52 Y=4 SETBACK=1.2
INSIDE-SURF-TEMP = NO ..

RIGHT-1 =EXTERIOR-WALL AZIMUTH=90
HEIGHT=25 WIDTH=36 X=80 Y=20 Z=0
CONSTRUCTION=WALL-1
GND-REFLECTANCE=0.15
SHADING-DIVISION = 40
INSIDE-SURF-TEMP = YES ..

WR-1 =DOOR WIDTH=5.5 HEIGHT=10
X=2.5 Y=0 SETBACK=1.2
INSIDE-SURF-TEMP = NO ..

WR-2 =DOOR WIDTH=8.0 HEIGHT=10

```

```

X=14.0 Y=0 SETBACK=1.2
INSIDE-SURF-TEMP = NO ..
WR-3 =DOOR WIDTH=5.5 HEIGHT=10
X=28.0 Y=0 SETBACK=1.2
INSIDE-SURF-TEMP = NO ..

BACK-1 =EXTERIOR-WALL AZIMUTH=0
HEIGHT=25 WIDTH=60 X=80 Y=56 Z=0
CONSTRUCTION=WALL-1
GND-REFLECTANCE=0.15
SHADING-DIVISION = 40
INSIDE-SURF-TEMP = YES ..

WB-1 =DOOR WIDTH=4 HEIGHT=6.7
X=4 Y=4 SETBACK=1.2
INSIDE-SURF-TEMP = NO ..
WB-2 =DOOR WIDTH=4 HEIGHT=6.7
X=12 Y=4 SETBACK=1.2
INSIDE-SURF-TEMP = NO ..
WB-3 =DOOR WIDTH=4 HEIGHT=6.7
X=20 Y=4 SETBACK=1.2
INSIDE-SURF-TEMP = NO ..
WB-4 =DOOR WIDTH=4 HEIGHT=6.7
X=28 Y=4 SETBACK=1.2
INSIDE-SURF-TEMP = NO ..
WB-5 =DOOR WIDTH=4 HEIGHT=6.7
X=36 Y=4 SETBACK=1.2
INSIDE-SURF-TEMP = NO ..
WB-6 =DOOR WIDTH=4 HEIGHT=6.7
X=44 Y=4 SETBACK=1.2
INSIDE-SURF-TEMP = NO ..
WB-7 =DOOR WIDTH=4 HEIGHT=6.7
X=52 Y=4 SETBACK=1.2
INSIDE-SURF-TEMP = NO ..

LEFT-1 =EXTERIOR-WALL AZIMUTH=270
HEIGHT=25 WIDTH=36 X=20 Y=56 Z=0
CONSTRUCTION=WALL-1
GND-REFLECTANCE=0.15
SHADING-DIVISION = 40
INSIDE-SURF-TEMP = YES ..

WL-1 =DOOR WIDTH=5.5 HEIGHT=10
X=2.5 Y=0 SETBACK=1.2
INSIDE-SURF-TEMP = NO ..
WL-2 =DOOR WIDTH=5.5 HEIGHT=10
X=28.0 Y=0 SETBACK=1.2
INSIDE-SURF-TEMP = NO ..

CEILING-S=INTERIOR-WALL AREA=2160
X=20 Y=20 Z=25 TILT=0
INT-WALL-TYPE=STANDARD
NEXT-TO ATTIC-1
CONSTRUCTION=CEIL-1
INSIDE-SURF-TEMP = YES ..

FLOOR=UNDERGROUND-FLOOR AREA=4160 CONSTRUCTION=FLOOR-1
INSIDE-SURF-TEMP = YES ..

COLONADE =INTERIOR-WALL AREA=8000
X=12 Y=12 Z=0 TILT=0
INT-WALL-TYPE=INTERNAL
CONSTRUCTION=WALL-2
INSIDE-SURF-TEMP = NO ..

BOX-1 =SPACE SPACE-CONDITIONS= TEMPLE
AREA=1 VOLUME=1
SHAPE=BOX HEIGHT=1
WIDTH=1 DEPTH=1
NUMBER-OF-PEOPLE=1 ..

FRONT-B =EXTERIOR-WALL AZIMUTH=180
HEIGHT=1 WIDTH=1
CONSTRUCTION=WALL-1 ..

RIGHT-B =EXTERIOR-WALL AZIMUTH=90
HEIGHT=1 WIDTH=1
CONSTRUCTION=WALL-1 ..

LEFT-B =INTERIOR-WALL AREA=1
INT-WALL-TYPE=ADIABATIC
NEXT-TO SPACE-1
CONSTRUCTION=WALL-1 ..

BACK-B =INTERIOR-WALL AREA=1
INT-WALL-TYPE=ADIABATIC
NEXT-TO SPACE-1

```

```

CONSTRUCTION=WALL-1 ..

CEILING-B=INTERIOR-WALL AREA=1
TILT=0
INT-WALL-TYPE=ADIABATIC
NEXT-TO SPACE-1
CONSTRUCTION=CEIL-1 ..

FLOOR-B=UNDERGROUND-FLOOR AREA=1 CONSTRUCTION=FLOOR-1 ..

$ BUILDING SHADE: OVERHANGS

FRONT-OH =BUILDING-SHADE X=12 Y=12 Z=25
HEIGHT=8 WIDTH=76 TILT=0
AZIMUTH=180 ..

BACK-OH =BUILDING-SHADE X=88 Y=64 Z=25
HEIGHT=8 WIDTH=76 TILT=0
AZIMUTH=0 ..

LEFT-OH =BUILDING-SHADE X=12 Y=64 Z=25
HEIGHT=8 WIDTH=52 TILT=0
AZIMUTH=270 ..

RIGHT-OH =BUILDING-SHADE X=88 Y=12 Z=25
HEIGHT=8 WIDTH=52 TILT=0
AZIMUTH=90 ..

$ BUILDING SHADE: LEFT PORCH (WEST)

L-PO-OH =BUILDING-SHADE X= 4 Y=48 Z=25
HEIGHT=8 WIDTH=20 TILT=0
AZIMUTH=270 ..

L-PO-BK =BUILDING-SHADE X=12 Y=48 Z=25
HEIGHT=14.2 WIDTH=10 TILT=45
AZIMUTH=0 ..

L-PO-FR =BUILDING-SHADE X=2 Y=28 Z=25
HEIGHT=14.2 WIDTH=10 TILT=45
AZIMUTH=180 ..

L-PO-C1 =BUILDING-SHADE X=4 Y=48 Z=0
HEIGHT=25 WIDTH=5 TILT=90
AZIMUTH=270 ..

L-PO-C2 =BUILDING-SHADE X=4 Y=33 Z=0
HEIGHT=25 WIDTH=5 TILT=90
AZIMUTH=270 ..

$ BUILDING SHADE: RIGHT PORCH (EAST)

R-PO-OH =BUILDING-SHADE X=96 Y=28 Z=25
HEIGHT=8 WIDTH=20 TILT=0
AZIMUTH=90 ..

R-PO-BK =BUILDING-SHADE X=98 Y=48 Z=25
HEIGHT=14.2 WIDTH=10 TILT=45
AZIMUTH=0 ..

R-PO-FR =BUILDING-SHADE X=88 Y=28 Z=25
HEIGHT=14.2 WIDTH=10 TILT=45
AZIMUTH=180 ..

R-PO-C1 =BUILDING-SHADE X=96 Y=43 Z=0
HEIGHT=25 WIDTH=5 TILT=90
AZIMUTH=90 ..

R-PO-C2 =BUILDING-SHADE X=96 Y=28 Z=0
HEIGHT=25 WIDTH=5 TILT=90
AZIMUTH=90 ..

$ BUILDING SHADE: COLONADES

$ FRONT COLONADES

FRONT-C1 =BUILDING-SHADE X=12 Y=12 Z=0
HEIGHT=25 WIDTH=2.5 TILT=90
AZIMUTH=180 ..

FRONT-C2 =BUILDING-SHADE X=20 Y=12 Z=0
HEIGHT=25 WIDTH=2.5 TILT=90
AZIMUTH=180 ..

FRONT-C3 =BUILDING-SHADE X=28.75 Y=12 Z=0
HEIGHT=25 WIDTH=2.5 TILT=90
AZIMUTH=180 ..

FRONT-C4 =BUILDING-SHADE X=36.75 Y=12 Z=0

```

HEIGHT=25 WIDTH=2.5 TILT=90  
 AZIMUTH=180 ..  
 FRONT-C5 =BUILDING-SHADE X=44.75 Y=12 Z=0  
 HEIGHT=25 WIDTH=2.5 TILT=90  
 AZIMUTH=180 ..  
 FRONT-C6 =BUILDING-SHADE X=52.75 Y=12 Z=0  
 HEIGHT=25 WIDTH=2.5 TILT=90  
 AZIMUTH=180 ..  
 FRONT-C7 =BUILDING-SHADE X=60.75 Y=12 Z=0  
 HEIGHT=25 WIDTH=2.5 TILT=90  
 AZIMUTH=180 ..  
 FRONT-C8 =BUILDING-SHADE X=68.75 Y=12 Z=0  
 HEIGHT=25 WIDTH=2.5 TILT=90  
 AZIMUTH=180 ..  
 FRONT-C9 =BUILDING-SHADE X=77.5 Y=12 Z=0  
 HEIGHT=25 WIDTH=2.5 TILT=90  
 AZIMUTH=180 ..  
 FRONT-C10=BUILDING-SHADE X=85.5 Y=12 Z=0  
 HEIGHT=25 WIDTH=2.5 TILT=90  
 AZIMUTH=180 ..

§ BACK COLONADES

BACK-C1 =BUILDING-SHADE X=88 Y=64 Z=0  
 HEIGHT=25 WIDTH=2.5 TILT=90  
 AZIMUTH=0 ..  
 BACK-C2 =BUILDING-SHADE X=80 Y=64 Z=0  
 HEIGHT=25 WIDTH=2.5 TILT=90  
 AZIMUTH=0 ..  
 BACK-C3 =BUILDING-SHADE X=71.25 Y=64 Z=0  
 HEIGHT=25 WIDTH=2.5 TILT=90  
 AZIMUTH=0 ..  
 BACK-C4 =BUILDING-SHADE X=63.25 Y=64 Z=0  
 HEIGHT=25 WIDTH=2.5 TILT=90  
 AZIMUTH=0 ..  
 BACK-C5 =BUILDING-SHADE X=55.25 Y=64 Z=0  
 HEIGHT=25 WIDTH=2.5 TILT=90  
 AZIMUTH=0 ..  
 BACK-C6 =BUILDING-SHADE X=47.25 Y=64 Z=0  
 HEIGHT=25 WIDTH=2.5 TILT=90  
 AZIMUTH=0 ..  
 BACK-C7 =BUILDING-SHADE X=39.25 Y=64 Z=0  
 HEIGHT=25 WIDTH=2.5 TILT=90  
 AZIMUTH=0 ..  
 BACK-C8 =BUILDING-SHADE X=31.25 Y=64 Z=0  
 HEIGHT=25 WIDTH=2.5 TILT=90  
 AZIMUTH=0 ..  
 BACK-C9 =BUILDING-SHADE X=22.5 Y=64 Z=0  
 HEIGHT=25 WIDTH=2.5 TILT=90  
 AZIMUTH=0 ..  
 BACK-C10 =BUILDING-SHADE X=14.5 Y=64 Z=0  
 HEIGHT=25 WIDTH=2.5 TILT=90  
 AZIMUTH=0 ..

§ LEFT COLONADES

LEFT-C1 =BUILDING-SHADE X=12 Y=64 Z=0  
 HEIGHT=25 WIDTH=2.5 TILT=90  
 AZIMUTH=270 ..  
 LEFT-C2 =BUILDING-SHADE X=12 Y=56 Z=0  
 HEIGHT=25 WIDTH=2.5 TILT=90  
 AZIMUTH=270 ..  
 LEFT-C3 =BUILDING-SHADE X=12 Y=48 Z=0  
 HEIGHT=25 WIDTH=5.0 TILT=90  
 AZIMUTH=270 ..  
 LEFT-C4 =BUILDING-SHADE X=12 Y=33 Z=0  
 HEIGHT=25 WIDTH=5.0 TILT=90  
 AZIMUTH=270 ..  
 LEFT-C5 =BUILDING-SHADE X=12 Y=22.5 Z=0  
 HEIGHT=25 WIDTH=2.5 TILT=90  
 AZIMUTH=270 ..

```
LEFT-C6 =BUILDING-SHADE X=12      Y=14.5 Z=0
          HEIGHT=25 WIDTH=2.5 TILT=90
          AZIMUTH=270      ..
```

#### \$ RIGHT COLONADES

```
RIGHT-C1 =BUILDING-SHADE X=88      Y=12 Z=0
          HEIGHT=25 WIDTH=2.5 TILT=90
          AZIMUTH=90      ..

RIGHT-C2 =BUILDING-SHADE X=88      Y=20 Z=0
          HEIGHT=25 WIDTH=2.5 TILT=90
          AZIMUTH=90      ..

RIGHT-C3 =BUILDING-SHADE X=88      Y=28 Z=0
          HEIGHT=25 WIDTH=5.0 TILT=90
          AZIMUTH=90      ..

RIGHT-C4 =BUILDING-SHADE X=88      Y=43 Z=0
          HEIGHT=25 WIDTH=5.0 TILT=90
          AZIMUTH=90      ..

RIGHT-C5 =BUILDING-SHADE X=88      Y=53.5 Z=0
          HEIGHT=25 WIDTH=2.5 TILT=90
          AZIMUTH=90      ..

RIGHT-C6 =BUILDING-SHADE X=88      Y=61.5 Z=0
          HEIGHT=25 WIDTH=2.5 TILT=90
          AZIMUTH=90      ..
```

#### \$ SHADE FROM SURROUNDINGS

```
NORTH-SHADE= BUILDING-SHADE X=120   Y=85 Z=0
              HEIGHT=12 WIDTH=140 TILT=90
              AZIMUTH=0      ..

SOUTH-SHADE= BUILDING-SHADE X=-20    Y=-10 Z=0
              HEIGHT=25 WIDTH=140 TILT=90
              AZIMUTH=180    ..

EAST-SHADE = BUILDING-SHADE X=110    Y= 10 Z=0
              HEIGHT=25 WIDTH=52  TILT=90
              AZIMUTH=90      ..

WEST-SHADE = BUILDING-SHADE X=-10    Y=64 Z=0
              HEIGHT=25 WIDTH=52  TILT=90
              AZIMUTH=270    ..
```

#### \$ LOADS HOURLY REPORT

```
HR-SCH-1 =SCHEDULE THRU DEC 31 (ALL) (1,24) (1) ..

LRB-1 =REPORT-BLOCK VARIABLE-TYPE= GLOBAL
      VARIABLE-LIST=(3,4,13,14,15,17,19) ..
      $ wbt3, dbt4, solar131415, wind speed17 & direction19 $

LRB-2 =REPORT-BLOCK VARIABLE-TYPE= GLOBAL
      VARIABLE-LIST=(50,51,36,37) ..
      $ sol altitude50, azimuth51, beam36, diffuse rad37 $

LRB-3 =REPORT-BLOCK VARIABLE-TYPE= SPACE-1
      VARIABLE-LIST=(4,9,10,11,12,13) ..
      $ delayed wall gain4, door conduction gain9 $
      $ equipment sensible gain10 $
      $ source11, people12, light sensible gain13 $

LRB-4 =REPORT-BLOCK VARIABLE-TYPE= ATTIC-1
      VARIABLE-LIST=(4,5,9,10,11,12,13) ..
      $ delayed wall14, roof gain5, door conduction gain9 $
      $ equipment sensible gain10 $
      $ source11, people12, light sensible gain13 $

LRB-5 =REPORT-BLOCK VARIABLE-TYPE= FRONT-1
      VARIABLE-LIST=(1,2,3,4,5,6,16,17,18) ..
      $ total solar on wall1, fraction of wall shaded2 $
      $ outside air film U value3, P. diff across wall4 $
      $ heat transfer from wall to zone5 $
      $ outside surface T6, solrad reflected from ground16 $
      $ direct solrad intensity on surface before shaded17 $
      $ diffuse solrad intensity on surface after shaded18 $

LRB-6 =REPORT-BLOCK VARIABLE-TYPE= RIGHT-1
      VARIABLE-LIST=(1,2,3,4,5,6,16,17,18) ..
      $ total solar on wall1, fraction of wall shaded2 $
      $ outside air film U value3, P. diff across wall4 $
      $ heat transfer from wall to zone5 $
      $ outside surface T6, solrad reflected from ground16 $
      $ direct solrad intensity on surface before shaded17 $
      $ diffuse solrad intensity on surface after shaded18 $
```

```

LRB-7  =REPORT-BLOCK      VARIABLE-TYPE= BACK-1
        VARIABLE-LIST=(1,2,3,4,5,6,16,17,18) ..
        $ total solar on wall1, fraction of wall shaded2 $
        $ outside air film U value3, P. diff across wall4 $
        $ heat transfer from wall to zone5 $
        $ outside surface T6, solrad reflected from ground16 $
        $ direct solrad intensity on surface before shaded17 $
        $ diffuse solrad intensity on surface after shaded18 $

LRB-8  =REPORT-BLOCK      VARIABLE-TYPE= LEFT-1
        VARIABLE-LIST=(1,2,3,4,5,6,16,17,18) ..
        $ total solar on wall1, fraction of wall shaded2 $
        $ outside air film U value3, P. diff across wall4 $
        $ heat transfer from wall to zone5 $
        $ outside surface T6, solrad reflected from ground16 $
        $ direct solrad intensity on surface before shaded17 $
        $ diffuse solrad intensity on surface after shaded18 $

LRB-9  =REPORT-BLOCK      VARIABLE-TYPE= FRONT-RF
        VARIABLE-LIST=(1,2,3,4,5,6,16,17,18) ..
        $ total solar on wall1, fraction of wall shaded2 $
        $ outside air film U value3, P. diff across wall4 $
        $ heat transfer from wall to zone5 $
        $ outside surface T6, solrad reflected from ground16 $
        $ direct solrad intensity on surface before shaded17 $
        $ diffuse solrad intensity on surface after shaded18 $

LRB-10 =REPORT-BLOCK      VARIABLE-TYPE= BACK-RF
        VARIABLE-LIST=(1,2,3,4,5,6,16,17,18) ..
        $ total solar on wall1, fraction of wall shaded2 $
        $ outside air film U value3, P. diff across wall4 $
        $ heat transfer from wall to zone5 $
        $ outside surface T6, solrad reflected from ground16 $
        $ direct solrad intensity on surface before shaded17 $
        $ diffuse solrad intensity on surface after shaded18 $

LRB-11 =REPORT-BLOCK      VARIABLE-TYPE= RIGHT-RF5
        VARIABLE-LIST=(1,2,3,4,5,6,16,17,18) ..
        $ total solar on wall1, fraction of wall shaded2 $
        $ outside air film U value3, P. diff across wall4 $
        $ heat transfer from wall to zone5 $
        $ outside surface T6, solrad reflected from ground16 $
        $ direct solrad intensity on surface before shaded17 $
        $ diffuse solrad intensity on surface after shaded18 $

LRB-12 =REPORT-BLOCK      VARIABLE-TYPE= LEFT-RF5
        VARIABLE-LIST=(1,2,3,4,5,6,16,17,18) ..
        $ total solar on wall1, fraction of wall shaded2 $
        $ outside air film U value3, P. diff across wall4 $
        $ heat transfer from wall to zone5 $
        $ outside surface T6, solrad reflected from ground16 $
        $ direct solrad intensity on surface before shaded17 $
        $ diffuse solrad intensity on surface after shaded18 $

$     LDS-REP-1  =HOURLY-REPORT      REPORT-SCHEDULE=HR-SCH-1
$
END      ..
COMPUTE LOADS ..

INPUT SYSTEMS ..

        SYSTEMS-REPORT      SUMMARY=(SS-A) ..

$ SCHEDULES

HEAT-1   =SCHEDULE      THRU DEC 31 (ALL) (1,24) (45) ..
COOL-1   =SCHEDULE      THRU DEC 31 (ALL) (1,24) (120) ..
NOVENT-1=SCHEDULE      THRU DEC 31 (ALL) (1,24) (0) ..
DAYVENT-1=SCHEDULE      THRU DEC 31 (ALL) (1,5) (0)
        (6,18) (1) (19,24) (0) ..
NIGHTVENT-2=SCHEDULE    THRU DEC 31 (ALL) (1,5) (1)
        (6,18) (0) (19,24) (1) ..

$ ZONE DATA

BOX-1    =ZONE          DESIGN-HEAT-T=50
        DESIGN-COOL-T=100
        ZONE-TYPE=CONDITIONED
        THERMOSTAT-TYPE=TWO-POSITION
        HEAT-TEMP-SCH=HEAT-1

```

```

                                COOL-TEMP-SCH=COOL-1  ..
SPACE-1      =ZONE              ZONE-TYPE = UNCONDITIONED  ..
ATTIC-1      =ZONE              ZONE-TYPE = UNCONDITIONED  ..

$ AIR CONDITIONER
SYS-1        =SYSTEM            SYSTEM-TYPE=RESYS
                                ZONE-NAMES=(BOX-1,SPACE-1,ATTIC-1)
                                MAX-SUPPLY-T=140  MIN-SUPPLY-T=50
                                NATURAL-VENT-AC=20
                                NATURAL-VENT-SCH=DAYVENT-1 ..

PLANT-1     =PLANT-ASSIGNMENT  SYSTEM-NAMES={SYS-1}  ..

$ SYSTEM HOURLY REPORT
HR-SCH-1    =SCHEDULE          THRU DEC 31 (ALL) (1,24) (1) ..
HR-SCH-2    =SCHEDULE          THRU JAN 16 (ALL) (1,24) (0)
                                THRU JAN 22 (ALL) (1,24) (1)
                                THRU DEC 31 (ALL) (1,24) (0) ..
SRB-1       =REPORT-BLOCK      VARIABLE-TYPE= SPACE-1
                                VARIABLE-LIST=(6,9,31,8,91,92) ..
                                $ zone temp, thermal conductance
                                $ avg temp, total zone cooling energy input
                                $ MRT, OT
SRB-2       =REPORT-BLOCK      VARIABLE-TYPE= ATTIC-1
                                VARIABLE-LIST=(6,9,31,8,91,92) ..
                                $ zone temp, thermal conductance
                                $ avg temp, total zone cooling energy input
                                $ MRT, OT
SRB-3       =REPORT-BLOCK      VARIABLE-TYPE= BOX-1
                                VARIABLE-LIST=(6,9,31,8,91,92) ..
                                $ zone temp, thermal conductance
                                $ avg temp, total zone cooling energy input
                                $ MRT, OT
$           SYS-REP-1          =HOURLY-REPORT      REPORT-SCHEDULE=HR-SCH-1
$           REPORT-BLOCK=(SRB-1) ..

END ..
COMPUTE SYSTEMS ..
STOP ..

```

## D.2 DOE-2 Output File of the Base-Case Temple

ATCH SRESHTHAPUTRA  
 BANGKOK, THAILAND  
 REPORT- LS-A SPACE PEAK LOADS SUMMARY  
 OLD TEMPLE: ORIGINAL DESIGN, AUGUST 2000 DOE-2.1E-110 Tue Sep 10 01:09:46 2002LDL RUN 1  
 WEATHER FILE- BANGKOK 1999

SPACE NAME	MULTIPLIER	COOLING LOAD (KBTU/HR)	TIME OF PEAK	DRY- BULB	WET- BULB	HEATING LOAD (KBTU/HR)	TIME OF PEAK	DRY- BULB	WET- BULB
ATTIC-1	1.	259.314	MAR 16 3 PM	94.F	76.F	-43.673	DEC 23 6 AM	60.F	53.F
SPACE-1	1.	202.810	MAR 16 3 PM	94.F	76.F	-326.417	DEC 23 6 AM	60.F	53.F
BOX-1	1.	0.128	MAR 7 12 NOON	93.F	66.F	0.000		0.F	0.F
SUM		462.251				-370.090			
BUILDING PEAK		202.853	MAR 16 3 PM	94.F	76.F	-326.417	DEC 23 6 AM	60.F	53.F

ATCH SRESHTHAPUTRA  
 BANGKOK, THAILAND  
 REPORT- LS-B SPACE PEAK LOAD COMPONENTS  
 OLD TEMPLE: ORIGINAL DESIGN, AUGUST 2000 DOE-2.1E-110 Tue Sep 10 01:09:46 2002LDL RUN 1  
 WEATHER FILE- BANGKOK 1999

SPACE	ATTIC-1	SPACE TEMPERATURE USED FOR THE LOADS CALCULATION IS	70 F / 21 C
MULTIPLIER	1.0	FLOOR MULTIPLIER	1.0
FLOOR AREA	3952 SQFT		
VOLUME	51376 CUFT		
COOLING LOAD		HEATING LOAD	
MAR 16 3PM		DEC 23 6AM	
94 F	34 C	60 F	16 C
76 F	24 C	53 F	12 C
276 BTU/H.SQFT	870 W/M2	0 BTU/H.SQFT	0 W/M2
8.5 KTS	4.4 M/S	4.9 KTS	2.5 M/S
0		0	
SENSIBLE (KBTU/H) ( KW )	LATENT (KBTU/H) ( KW )	SENSIBLE (KBTU/H) ( KW )	





ATCH SRESHTAPUTRA OLD TEMPLE: ORIGINAL DESIGN, AUGUST 2000 DOB-2.1B-110 Tue Sep 10 01:09:46 2002LDL RUN 1  
 BANGKOK, THAILAND WEATHER FILE- BANGKOK 1999  
 REPORT- 1S-B SPACE PEAK LOAD COMPONENTS SPACE-1

SPACE SPACE-1 SPACE TEMPERATURE USED FOR THE LOADS CALCULATION IS 84 F / 29 C

MULTIPLIER	1.0	FLOOR MULTIPLIER	1.0	COOLING LOAD	HEATING LOAD
FLOOR AREA	2160 SQFT	201 M2			
VOLUME	54000 CUFT	1529 M3			
=====					
TIME	MAR 16 3PM		DEC 23 6AM		
DRY-BULB TEMP	94 F	34 C	60 F	16 C	
WET-BULB TEMP	76 F	24 C	53 F	12 C	
TOT HORIZONTAL SOLAR RAD	276 BTU/H.SQFT	870 W/M2	0 BTU/H.SQFT	0 W/M2	
WINDSPEED AT SPACE	9.7 KTS	5.0 M/S	5.6 KTS	2.9 M/S	
CLOUD AMOUNT 0(CLEAR)-10	0		0		

	SENSIBLE (KBTU/H) ( KW )	LATENT (KBTU/H) ( KW )	SENSIBLE (KBTU/H) ( KW )
WALL CONDUCTION	2.449	0.717	0.000
ROOF CONDUCTION	0.000	0.000	0.000
WINDOW GLASS+FRM COND	0.000	0.000	0.000
WINDOW GLASS SOLAR	0.000	0.000	0.000
DOOR CONDUCTION	1.945	0.570	0.000
INTERNAL SURFACE COND	-11.014	-3.227	0.000
UNDERGROUND SURF COND	-3.046	-0.893	0.000
OCCUPANTS TO SPACE	0.194	0.057	0.082
LIGHT TO SPACE	0.108	0.032	0.000
EQUIPMENT TO SPACE	0.121	0.035	0.000
PROCESS TO SPACE	0.000	0.000	0.000
INFILTRATION	212.053	62.132	552.674
TOTAL	202.810	59.423	552.756
TOTAL / AREA	0.094	0.296	0.256
TOTAL LOAD	755.565 KBTU/H	221.381 KW	-326.417 KBTU/H
TOTAL LOAD / AREA	349.80 BTU/H.SQFT	1103.205 W/M2	151.119 BTU/H.SQFT

\*\*\*\*\*  
 \* NOTE 1) THE ABOVE LOADS EXCLUDE OUTSIDE VENTILATION AIR \*  
 \* LOADS \*  
 \* 2) TIMES GIVEN IN STANDARD TIME FOR THE LOCATION \*  
 \* IN CONSIDERATION \*  
 \* 3) THE ABOVE LOADS ARE CALCULATED ASSUMING A \*  
 \* CONSTANT INDOOR SPACE TEMPERATURE \*\*\*\*\*

ATCH SRSHHAPUTRA OLD TEMPLE: ORIGINAL DESIGN, AUGUST 2000 DOE-2.1E-110 Tue Sep 10 01:09:46 2002IDL RUN 1  
 BANGKOK, THAILAND  
 REPORT- LS-B SPACE PEAK LOAD COMPONENTS BOX-1 WEATHER FILE- BANGKOK 1999

SPACE BOX-1  
 SPACE TEMPERATURE USED FOR THE LOADS CALCULATION IS 84 F / 29 C

MULTIPLIER 1.0 FLOOR MULTIPLIER 1.0  
 FLOOR AREA 1 SQFT 0 M2  
 VOLUME 1 CUFT 0 M3

COOLING LOAD HEATING LOAD  
 MAR 7 12NOON

93 F 34 C  
 66 F 19 C  
 321 BTU/H.SQFT 1011 W/M2  
 4.2 KTS 2.2 M/S  
 0

	SENSIBLE (KBTU/H)	LATENT (KSTU/H)	SENSIBLE (KBTU/H)
WALL CONDUCTION	0.002	0.000	0.000
ROOF CONDUCTION	0.000	0.000	0.000
WINDOW GLASS+FRM COND	0.000	0.000	0.000
WINDOW GLASS SOLAR	0.000	0.000	0.000
DOOR CONDUCTION	0.000	0.000	0.000
INTERNAL SURFACE COND	0.000	0.000	0.000
UNDERGROUND SURF COND	-0.001	0.000	0.000
OCCUPANTS TO SPACE	0.125	0.037	0.024
LIGHT TO SPACE	0.000	0.000	0.000
EQUIPMENT TO SPACE	0.000	0.000	0.000
PROCESS TO SPACE	0.000	0.000	0.000
INFILTRATION	0.002	0.000	0.000
TOTAL	0.128	0.037	0.000
TOTAL / AREA	0.128	0.404	0.000
TOTAL LOAD	0.210 KBTU/H	0.061 KW	0.000 KBTU/H
TOTAL LOAD / AREA	209.89 BTU/H.SQFT	661.957 W/M2	0.000 BTU/H.SQFT

\*\*\*\*\*  
 \* NOTE 1) THE ABOVE LOADS EXCLUDE OUTSIDE VENTILATION AIR \*  
 \* --- LOADS \*  
 \* 2) TIMES GIVEN IN STANDARD TIME FOR THE LOCATION \*  
 \* IN CONSIDERATION \*  
 \* 3) THE ABOVE LOADS ARE CALCULATED ASSUMING A \*  
 \* CONSTANT INDOOR SPACE TEMPERATURE \*  
 \*\*\*\*\*

ATCH SRESHTHAFUTRA OLD TEMPLE: ORIGINAL DESIGN, AUGUST 2000 DOE-2.1E-110 Tue Sep 10 01:09:46 2002LDL RUN 1  
 BANGKOK, THAILAND  
 REPORT- LS-C BUILDING PEAK LOAD COMPONENTS WEATHER FILE- BANGKOK 1999

\*\*\* BUILDING \*\*\*

FLOOR AREA	2161 SQFT	201 M2		
VOLUME	54001 CUFT	1529 M3		
=====				
	COOLING LOAD		HEATING LOAD	
	MAR 16 3PM		DEC 23 6AM	
DRY-BULB TEMP	94 F	34 C	60 F	16 C
WET-BULB TEMP	76 F	24 C	53 F	12 C
TOT HORIZONTAL SOLAR RAD	276 BTU/H.SQFT	870 W/M2	0 BTU/H.SQFT	0 W/M2
WINDSPEED AT SPACE	8.5 KTS	4.4 M/S	4.9 KTS	2.5 M/S
CLOUD AMOUNT 0(CLEAR)-10	0		0	

	SENSIBLE (KBTU/H)	LATENT (KBTU/H)	SENSIBLE (KBTU/H)	SENSIBLE (KW)
WALL CONDUCTION	2.451	0.718	0.000	0.000
ROOF CONDUCTION	0.000	0.000	0.000	0.000
WINDOW GLASS+FRM COND	0.000	0.000	0.000	0.000
WINDOW GLASS SOLAR	0.000	0.000	0.000	0.000
DOOR CONDUCTION	1.945	0.570	0.000	0.000
INTERNAL SURFACE COND	-11.014	-3.227	0.000	0.000
UNDERGROUND SURF COND	-3.047	-0.893	0.000	0.000
OCCUPANTS TO SPACE	0.233	0.068	0.029	0.029
LIGHT TO SPACE	0.109	0.032	0.000	0.000
EQUIPMENT TO SPACE	0.121	0.035	0.000	0.000
PROCESS TO SPACE	0.000	0.000	0.000	0.000
INFILTRATION	212.055	62.132	552.679	161.935
TOTAL	202.853	59.436	552.777	161.964
TOTAL / AREA	0.094	0.296	0.256	0.807
TOTAL LOAD	755.630 KBTU/H	221.400 KW	-326.417 KBTU/H	-95.640 KW
TOTAL LOAD / AREA	349.67 BTU/H.SQFT	1102.789 W/M2	151.049 BTU/H.SQFT	476.383 W/M2

\*\*\*\*\*  
 \* \* NOTE 1) THE ABOVE LOADS EXCLUDE OUTSIDE VENTILATION AIR \*  
 \* \* LOADS \*  
 \* \*-----\*  
 \* \* 2) TIMES GIVEN IN STANDARD TIME FOR THE LOCATION \*  
 \* \* IN CONSIDERATION \*  
 \* \* 3) THE ABOVE LOADS ARE CALCULATED ASSUMING A \*  
 \* \* CONSTANT INDOOR SPACE TEMPERATURE \*  
 \* \* \*\*\*\*\*

ATCH SRESHTHAFUTRA OLD TEMPLE: ORIGINAL DESIGN, AUGUST 2000 DOB-2.1B-110 Tue Sep 10 01:09:46 2002LIDL RUN 1  
 BANGKOK, THAILAND  
 REPORT- LS-D BUILDING MONTHLY LOADS SUMMARY WEATHER FILE- BANGKOK 1999

MONTH	C O O L I N G				H E A T I N G				E L E C			
	COOLING ENERGY (MBTU)	TIME OF MAX DY HR	DRY- BULB TEMP	WET- BULB TEMP	MAXIMUM COOLING LOAD (KBTU/HR)	HEATING ENERGY (MBTU)	TIME OF MAX DY HR	DRY- BULB TEMP	WET- BULB TEMP	MAXIMUM HEATING LOAD (KBTU/HR)	ELEC- TRICAL ENERGY (KWH)	MAXIMUM ELEC LOAD (KW)
JAN	3.47517	24 15	98.F	78.F	136.985	-12.911	16 10	76.F	67.F	-129.367	86.	0.324
FEB	4.89142	11 15	95.F	79.F	102.561	-11.052	5 8	68.F	63.F	-159.215	77.	0.324
MAR	14.26425	16 15	94.F	76.F	202.853	-6.643	9 9	78.F	59.F	-96.731	84.	0.324
APR	8.55546	26 11	91.F	78.F	163.071	-6.764	6 7	79.F	77.F	-82.412	82.	0.324
MAY	4.76105	8 15	91.F	80.F	121.703	-9.883	21 6	76.F	75.F	-58.824	86.	0.324
JUN	5.64083	18 16	92.F	81.F	127.390	-8.214	12 7	80.F	76.F	-50.805	82.	0.324
JUL	9.08756	9 17	93.F	78.F	177.747	-7.872	25 8	79.F	74.F	-40.815	85.	0.324
AUG	5.03894	9 18	91.F	82.F	170.708	-9.867	2 18	80.F	77.F	-65.404	85.	0.324
SEP	5.03208	18 17	92.F	84.F	127.690	-9.671	29 7	78.F	74.F	-69.563	82.	0.324
OCT	2.35235	8 16	95.F	78.F	121.874	-13.284	26 8	76.F	75.F	-130.509	86.	0.324
NOV	2.62195	27 13	92.F	74.F	97.169	-13.950	2 9	76.F	74.F	-118.991	82.	0.324
DEC	0.16137	31 16	90.F	72.F	26.451	-32.280	23 6	60.F	53.F	-326.417	84.	0.324
TOTAL	65.882				-142.390						1003.	
MAX					202.853					-326.417		0.324



ATCH SRESHTHAPUTRA  
 BANGKOK, THAILAND  
 REPORT- IS-E SPACE MONTHLY LOAD COMPONENTS IN MBTU FOR SPACE-1 WEATHER FILE- BANGKOK 1999

OLD TEMPLE: ORIGINAL DESIGN, AUGUST 2000 DOE-2.1E-110 Tue Sep 10 01:09:46 2002LDR RUN 1

(UNIT=MBTU)	WALLS	ROOFS	INT SUR	UND SUR	INFIL	WIN CON	WIN SOL	OCCUP	LIGHTS	EQUIP	SOURCE	TOTAL
HEATING	0.622	0.000	-6.708	-3.710	-3.358	0.000	0.000	0.127	0.038	0.079	0.000	-12.911
JAN SEN CL	0.394	0.000	-1.487	-0.822	5.282	0.000	0.000	0.038	0.015	0.024	0.000	3.443
LAT CL					33.424			0.019		0.000	0.000	33.444
HEATING	0.396	0.000	-5.650	-3.125	-2.864	0.000	0.000	0.100	0.030	0.062	0.000	-11.052
FEB SEN CL	0.416	0.000	-1.751	-0.969	7.076	0.000	0.000	0.045	0.017	0.028	0.000	4.863
LAT CL					47.009			0.023		0.000	0.000	47.032
HEATING	1.195	0.000	-5.463	-1.535	-1.004	0.000	0.000	0.085	0.026	0.053	0.000	-6.643
MAR SEN CL	0.960	0.000	-2.732	-0.763	16.620	0.000	0.000	0.074	0.027	0.046	0.000	14.231
LAT CL					62.732			0.039		0.000	0.000	62.771
HEATING	0.956	0.000	-5.639	-1.560	-0.694	0.000	0.000	0.089	0.028	0.056	0.000	-6.764
APR SEN CL	0.665	0.000	-2.291	-0.634	10.657	0.000	0.000	0.064	0.022	0.040	0.000	8.524
LAT CL					68.544			0.035		0.000	0.000	68.579
HEATING	0.497	0.000	-6.531	-3.582	-0.493	0.000	0.000	0.117	0.036	0.073	0.000	-9.882
MAY SEN CL	0.315	0.000	-1.663	-0.919	6.901	0.000	0.000	0.048	0.016	0.030	0.000	4.728
LAT CL					57.249			0.026		0.000	0.000	57.274
HEATING	0.778	0.000	-5.826	-3.223	-0.131	0.000	0.000	0.098	0.030	0.061	0.000	-8.214
JUN SEN CL	0.485	0.000	-2.104	-1.164	8.281	0.000	0.000	0.056	0.021	0.035	0.000	5.610
LAT CL					71.908			0.030		0.000	0.000	71.938
HEATING	1.097	0.000	-5.716	-3.162	-0.274	0.000	0.000	0.095	0.028	0.059	0.000	-7.872
JUL SEN CL	0.726	0.000	-2.478	-1.371	12.048	0.000	0.000	0.065	0.024	0.041	0.000	9.055
LAT CL					80.515			0.035		0.000	0.000	80.550
HEATING	0.678	0.000	-6.355	-3.515	-0.889	0.000	0.000	0.111	0.034	0.069	0.000	-9.867
AUG SEN CL	0.385	0.000	-1.839	-1.017	7.376	0.000	0.000	0.052	0.018	0.032	0.000	5.006
LAT CL					56.379			0.027		0.000	0.000	56.406
HEATING	0.493	0.000	-6.212	-3.436	-0.726	0.000	0.000	0.109	0.034	0.068	0.000	-9.671
SEP SEN CL	0.332	0.000	-1.718	-0.950	7.249	0.000	0.000	0.045	0.017	0.028	0.000	5.001
LAT CL					51.925			0.024		0.000	0.000	51.948
HEATING	0.171	0.000	-6.950	-3.844	-2.916	0.000	0.000	0.132	0.040	0.082	0.000	-13.284
OCT SEN CL	0.172	0.000	-1.245	-0.688	4.015	0.000	0.000	0.032	0.012	0.020	0.000	2.319
LAT CL					31.282			0.017		0.000	0.000	31.299
HEATING	0.223	0.000	-6.972	-5.753	-1.700	0.000	0.000	0.130	0.041	0.081	0.000	-13.950
NOV SEN CL	0.208	0.000	-0.956	-0.794	4.087	0.000	0.000	0.025	0.009	0.015	0.000	2.592
LAT CL					21.110			0.013		0.000	0.000	21.123
HEATING	-1.025	0.000	-8.084	-11.115	-12.359	0.000	0.000	0.155	0.051	0.097	0.000	-32.280
DEC SEN CL	0.003	0.000	-0.110	-0.152	0.387	0.000	0.000	0.002	0.001	0.001	0.000	0.133
LAT CL					1.434			0.001		0.000	0.000	1.435
HEATING	6.082	0.000	-76.115	-47.561	-27.408	0.000	0.000	1.349	0.416	0.841	0.000	-142.396
TOT SEN CL	5.060	0.000	-20.376	-10.244	89.978	0.000	0.000	0.547	0.199	0.341	0.000	65.505
LAT CL					583.512			0.289		0.000	0.000	583.801







## APPENDIX E

### CFD SIMULATION

The 3-D CFD program used in this research is the 1998 version of HEATX, which was written by Andrews and reported in Prithiviraj and Andrews (1998a, 1998b). Copies of the software can be obtained from Dr. Malcolm Andrews, Department of Mechanical Engineering, Texas A&M University. Phone: 979-877-8843. Email: mandrews@mengr.tamu.edu.

#### E.1 HEATX Input File

```

title=Temple 082902
# note: Copyright 2002. Atch Sreshthaputra
# note: Original Temple.
# note: Southwest Flow, with Surroundings
# note: Added Heat Transfer Coefficient @ roof/ceiling
# note: With Buoyancy only in the attic, 24-Hour Transient Run, Coarse Grids
# note: Wall surface temperature, Interior Column, Floor Temp Assigned
idbg=0
#

steady = false
buoy = true
nstep = 4320
epsmas = 5.0e+0
dt=20.0

restrt=off
dump=on
nx=79; ny=37; nz=30
#xlast=76.0;ylast=64.0;zlast=23.0

grid(x, 1,2,pow,0.0,4.0)
grid(x, 3,5,pow,0.0,3.0)
grid(x, 6,65,pow,0.0,24.0)
grid(x, 66,68,pow,0.0,3.0)
grid(x, 69,79,pow,0.0,42.0)

grid(y, 1,3,pow,0.0,6.0)
grid(y, 4,4,pow,0.0,1.0)
grid(y, 5,24,pow,0.0,16.0)
grid(y, 25,27,pow,0.0,3.0)
grid(y, 28,37,pow,0.0,38.0)

grid(z, 1,10,pow,0.0,4.0)
grid(z, 11,25,pow,0.0,12.0)
grid(z, 26,28,pow,0.0,3.0)
grid(z, 29,30,pow,0.0,4.0)

# EQUATIONS TO SOLVE
turbke=true      # turbulent flow problem
solve(p,u,v,w,ke,ep,h)=true

# PRINT OUT
iprtmn=1; iprtmx=nx      # i cell range for printing
jprtmn=1; jprtmx=ny      # j cell range for printing
kprtmn=1; kprtmx=nz      # k cell range for printing

```

```

icol=5                # number of columns
ndtprt=1
iniprt=false         # do not print initial field values

neqprt=1;nmoprt=1;print(p,u,v,ke,ep,h)=1

# RELAXATION
relaxln(p)=0.05
relaxdt(u,v,w)=5.0e-2
relaxdt(ke,ep)=5.0e-2
#relaxdt(h)=0.05

# ITERATION COUNTS
nitphi(p)=10
nitphi(u,v,w)=1
nitphi(ke,ep)=1
nitphi(h,ht1)=1
# epsphi(h)=1.0e+5
nitall=3000

# INITIAL CONDITIONS

# INITIAL ke and ep
bdyc(1,ke,set,cell,0.0,0.00132,1,nx,1,ny,1,nz,0,0)
bdyc(1,ep,set,cell,0.0,0.000003,1,nx,1,ny,1,nz,0,0)

# EXTERIOR WALLS
bdyc(1,por,set,cell,0.0,0.0,12,14, 8, 8,1,15,0,0) # South wall 1
bdyc(1,por,set,cell,0.0,0.0,15,17, 8, 8,1, 3,0,0) # South wall 1A
bdyc(1,por,set,cell,0.0,0.0,15,17, 8, 8,8,15,0,0) # South wall 1B
bdyc(2,por,set,cell,0.0,0.0,12,14,21,21,1,15,0,0) # North wall 2
bdyc(2,por,set,cell,0.0,0.0,15,17,21,21,1, 3,0,0) # North wall 2A
bdyc(2,por,set,cell,0.0,0.0,15,17,21,21,8,15,0,0) # North wall 2B
bdyc(3,por,set,cell,0.0,0.0,18,20, 8, 8,1,15,0,0) # South wall 3
bdyc(3,por,set,cell,0.0,0.0,21,23, 8, 8,1, 3,0,0) # South wall 3A
bdyc(3,por,set,cell,0.0,0.0,21,23, 8, 8,8,15,0,0) # South wall 3B
bdyc(4,por,set,cell,0.0,0.0,18,20,21,21,1,15,0,0) # North wall 4
bdyc(4,por,set,cell,0.0,0.0,21,23,21,21,1, 3,0,0) # North wall 4A
bdyc(4,por,set,cell,0.0,0.0,21,23,21,21,8,15,0,0) # North wall 4B
bdyc(5,por,set,cell,0.0,0.0,24,26, 8, 8,1,15,0,0) # South wall 5
bdyc(5,por,set,cell,0.0,0.0,27,29, 8, 8,1, 3,0,0) # South wall 5A
bdyc(5,por,set,cell,0.0,0.0,27,29, 8, 8,8,15,0,0) # South wall 5B
bdyc(6,por,set,cell,0.0,0.0,24,26,21,21,1,15,0,0) # North wall 6
bdyc(6,por,set,cell,0.0,0.0,27,29,21,21,1, 3,0,0) # North wall 6A
bdyc(6,por,set,cell,0.0,0.0,27,29,21,21,8,15,0,0) # North wall 6B
bdyc(7,por,set,cell,0.0,0.0,30,31, 8, 8,1,15,0,0) # South wall 7
bdyc(7,por,set,cell,0.0,0.0,32,35, 8, 8,1, 3,0,0) # South wall 7A
bdyc(7,por,set,cell,0.0,0.0,32,35, 8, 8,8,15,0,0) # South wall 7B
bdyc(8,por,set,cell,0.0,0.0,30,31,21,21,1,15,0,0) # North wall 8
bdyc(8,por,set,cell,0.0,0.0,32,35,21,21,1, 3,0,0) # North wall 8A
bdyc(8,por,set,cell,0.0,0.0,32,35,21,21,8,15,0,0) # North wall 8B
bdyc(9,por,set,cell,0.0,0.0,36,37, 8, 8,1,15,0,0) # South wall 9
bdyc(9,por,set,cell,0.0,0.0,38,40, 8, 8,1, 3,0,0) # South wall 9A
bdyc(9,por,set,cell,0.0,0.0,38,40, 8, 8, 8,15,0,0) # South wall 9B
bdyc(10,por,set,cell,0.0,0.0,36,37,21,21,1,15,0,0) # North wall 10
bdyc(10,por,set,cell,0.0,0.0,38,40,21,21,1, 3,0,0) # North wall 10A
bdyc(10,por,set,cell,0.0,0.0,38,40,21,21,8,15,0,0) # North wall 10B
bdyc(11,por,set,cell,0.0,0.0,41,43, 8, 8,1,15,0,0) # South wall 11
bdyc(11,por,set,cell,0.0,0.0,44,46, 8, 8,1, 3,0,0) # South wall 11A
bdyc(11,por,set,cell,0.0,0.0,44,46, 8, 8,8,15,0,0) # South wall 11B
bdyc(12,por,set,cell,0.0,0.0,41,43,21,21,1,15,0,0) # North wall 12
bdyc(12,por,set,cell,0.0,0.0,44,46,21,21,1, 3,0,0) # North wall 12A
bdyc(12,por,set,cell,0.0,0.0,44,46,21,21,8,15,0,0) # North wall 12B
bdyc(13,por,set,cell,0.0,0.0,47,49, 8, 8,1,15,0,0) # South wall 13
bdyc(13,por,set,cell,0.0,0.0,50,52, 8, 8,1, 3,0,0) # South wall 13A
bdyc(13,por,set,cell,0.0,0.0,50,52, 8, 8,8,15,0,0) # South wall 13B
bdyc(14,por,set,cell,0.0,0.0,47,49,21,21,1,15,0,0) # North wall 14
bdyc(14,por,set,cell,0.0,0.0,50,52,21,21,1, 3,0,0) # North wall 14A
bdyc(14,por,set,cell,0.0,0.0,50,52,21,21,8,15,0,0) # North wall 14B
bdyc(15,por,set,cell,0.0,0.0,53,55, 8, 8,1,15,0,0) # South wall 15
bdyc(16,por,set,cell,0.0,0.0,53,55,21,21,1,15,0,0) # North wall 16
bdyc(17,por,set,cell,0.0,0.0,12,13,11,13,1,15,0,0) # West wall 17
bdyc(18,por,set,cell,0.0,0.0,12,13,16,18,1,15,0,0) # West wall 18
bdyc(15,por,set,cell,0.0,0.0,12,13, 9,10,8,15,0,0) # West wall 15A

```

```

bdyc(16,por,set,cell,0.0,0.0,12,13,14,15,8,15,0,0) # West wall 16A
bdyc(17,por,set,cell,0.0,0.0,12,13,19,20,8,15,0,0) # West wall 17A
bdyc(19,por,set,cell,0.0,0.0,54,55,11,18,1,15,0,0) # East wall 19
bdyc(18,por,set,cell,0.0,0.0,54,55, 9,10,8,15,0,0) # East wall 18A
bdyc(19,por,set,cell,0.0,0.0,54,55,19,20,8,15,0,0) # East wall 19A

```

#### # INTERIOR COLUMNS

```

bdyc(51,por,set,cell,0.0,0.0,18,19,11,11,1,15,0,0) # Ins Col 1
bdyc(52,por,set,cell,0.0,0.0,24,25,11,11,1,15,0,0) # Ins Col 2
bdyc(53,por,set,cell,0.0,0.0,30,31,11,11,1,15,0,0) # Ins Col 3
bdyc(54,por,set,cell,0.0,0.0,36,37,11,11,1,15,0,0) # Ins Col 4
bdyc(55,por,set,cell,0.0,0.0,42,43,11,11,1,15,0,0) # Ins Col 5
bdyc(56,por,set,cell,0.0,0.0,48,49,11,11,1,15,0,0) # Ins Col 6
bdyc(57,por,set,cell,0.0,0.0,18,19,18,18,1,15,0,0) # Ins Col 7
bdyc(58,por,set,cell,0.0,0.0,24,25,18,18,1,15,0,0) # Ins Col 8
bdyc(59,por,set,cell,0.0,0.0,30,31,18,18,1,15,0,0) # Ins Col 9
bdyc(60,por,set,cell,0.0,0.0,36,37,18,18,1,15,0,0) # Ins Col 10
bdyc(61,por,set,cell,0.0,0.0,42,43,18,18,1,15,0,0) # Ins Col 11
bdyc(62,por,set,cell,0.0,0.0,48,49,18,18,1,15,0,0) # Ins Col 12

```

#### # EXTERIOR COLUMNS

```

bdyc(63,por,set,cell,0.0,0.0, 6, 7,5,5,1,15,0,0) # Ext Col 1
bdyc(64,por,set,cell,0.0,0.0,12,13,5,5,1,15,0,0) # Ext Col 2
bdyc(65,por,set,cell,0.0,0.0,18,19,5,5,1,15,0,0) # Ext Col 3
bdyc(66,por,set,cell,0.0,0.0,24,25,5,5,1,15,0,0) # Ext Col 4
bdyc(67,por,set,cell,0.0,0.0,30,31,5,5,1,15,0,0) # Ext Col 5
bdyc(68,por,set,cell,0.0,0.0,36,37,5,5,1,15,0,0) # Ext Col 6
bdyc(69,por,set,cell,0.0,0.0,42,43,5,5,1,15,0,0) # Ext Col 7
bdyc(70,por,set,cell,0.0,0.0,48,49,5,5,1,15,0,0) # Ext Col 8
bdyc(71,por,set,cell,0.0,0.0,54,55,5,5,1,15,0,0) # Ext Col 9
bdyc(72,por,set,cell,0.0,0.0,60,61,5,5,1,15,0,0) # Ext Col 10
bdyc(73,por,set,cell,0.0,0.0, 6, 7,24,24,1,15,0,0) # Ext Col 11
bdyc(74,por,set,cell,0.0,0.0,12,13,24,24,1,15,0,0) # Ext Col 12
bdyc(75,por,set,cell,0.0,0.0,18,19,24,24,1,15,0,0) # Ext Col 13
bdyc(76,por,set,cell,0.0,0.0,24,25,24,24,1,15,0,0) # Ext Col 14
bdyc(77,por,set,cell,0.0,0.0,30,31,24,24,1,15,0,0) # Ext Col 15
bdyc(78,por,set,cell,0.0,0.0,36,37,24,24,1,15,0,0) # Ext Col 16
bdyc(79,por,set,cell,0.0,0.0,42,43,24,24,1,15,0,0) # Ext Col 17
bdyc(80,por,set,cell,0.0,0.0,48,49,24,24,1,15,0,0) # Ext Col 18
bdyc(81,por,set,cell,0.0,0.0,54,55,24,24,1,15,0,0) # Ext Col 19
bdyc(82,por,set,cell,0.0,0.0,60,61,24,24,1,15,0,0) # Ext Col 20
bdyc(83,por,set,cell,0.0,0.0, 6, 7, 8, 8,1,15,0,0) # Ext Col 21
bdyc(84,por,set,cell,0.0,0.0, 6, 7,11,12,1,15,0,0) # Ext Col 22
bdyc(85,por,set,cell,0.0,0.0, 6, 7,17,18,1,15,0,0) # Ext Col 23
bdyc(86,por,set,cell,0.0,0.0, 6, 7,21,21,1,15,0,0) # Ext Col 24
bdyc(87,por,set,cell,0.0,0.0,60,61, 8, 8,1,15,0,0) # Ext Col 25
bdyc(88,por,set,cell,0.0,0.0,60,61,11,12,1,15,0,0) # Ext Col 26
bdyc(89,por,set,cell,0.0,0.0,60,61,17,18,1,15,0,0) # Ext Col 27
bdyc(90,por,set,cell,0.0,0.0,60,61,21,21,1,15,0,0) # Ext Col 28
bdyc(91,por,set,cell,0.0,0.0,64,65,11,12,1,15,0,0) # Ext Col 29
bdyc(92,por,set,cell,0.0,0.0,64,65,17,18,1,15,0,0) # Ext Col 30
bdyc(93,por,set,cell,0.0,0.0, 4, 4,11,12,1,15,0,0) # Ext Col 31
bdyc(94,por,set,cell,0.0,0.0, 4, 4,17,18,1,15,0,0) # Ext Col 32

```

#### # SURROUNDINGS

```

bdyc(95,por,set,cell,0.0,0.0, 6,61,28,30,1,10,0,0) # Surround 1
bdyc(96,por,set,cell,0.0,0.0,70,72,28,30,1,10,0,0) # Surround 2
bdyc(97,por,set,cell,0.0,0.0,70,72, 5,24,1,10,0,0) # Surround 3
bdyc(98,por,set,cell,0.0,0.0, 6,72, 1, 1,1,12,0,0) # Surround 4

```

#### # CEILING

```

bdyc(33,port,set,cell,0.0,0.0,6,61,5,24,15,15,0,0) # Ceiling port=0.0

```

#### # FLOOR SURFACE TEMPERATURE SETTINGS

```

bdyc(100,h,walfn,bot,0.0,27000,12,55, 9,10,1,1,1,2340) # Floor h
bdyc(100,h,walfn,bot,0.0,27000,14,53,12,17,1,1,1,2340) # Floor h
bdyc(100,h,walfn,bot,0.0,27000,12,55,19,20,1,1,1,2340) # Floor h
bdyc(101,h,walfn,bot,0.0,27500,12,55, 9,10,1,1,2341,4320) # Floor h
bdyc(101,h,walfn,bot,0.0,27500,14,53,12,17,1,1,2341,4320) # Floor h
bdyc(101,h,walfn,bot,0.0,27500,12,55,19,20,1,1,2341,4320) # Floor h

```

```

bdyc(102,u,walfn,bot,0.0,0.0,12,55,9,20,1,1,1,nstep) # Floor u =0
bdyc(102,v,walfn,bot,0.0,0.0,12,55,9,20,1,1,1,nstep) # Floor v =0

```

#### # WALL SURFACE TEMPERATURE SETTINGS

1

```

bdyc(100,h,walfn,south,0.0,28000,14,53, 9, 9,1, 3,1,1980) # South wall h
bdyc(100,h,walfn,south,0.0,28000,14,53, 9, 9,8,15,1,1980) # South wall h

```

```

bdyc(100,h,walfn,south,0.0,28000,18,20,9,9,4,7,1,1980) # South wall h
bdyc(100,h,walfn,south,0.0,28000,24,26,9,9,4,7,1,1980) # South wall h
bdyc(100,h,walfn,south,0.0,28000,30,31,9,9,4,7,1,1980) # South wall h
bdyc(100,h,walfn,south,0.0,28000,36,37,9,9,4,7,1,1980) # South wall h
bdyc(100,h,walfn,south,0.0,28000,41,43,9,9,4,7,1,1980) # South wall h
bdyc(100,h,walfn,south,0.0,28000,47,49,9,9,4,7,1,1980) # South wall h

bdyc(100,h,walfn,north,0.0,28000,14,53,20,20,1,3,1,1980) # North wall h
bdyc(100,h,walfn,north,0.0,28000,14,53,20,20,8,15,1,1980) # North wall h
bdyc(100,h,walfn,north,0.0,28000,18,20,20,20,4,7,1,1980) # North wall h
bdyc(100,h,walfn,north,0.0,28000,24,26,20,20,4,7,1,1980) # North wall h
bdyc(100,h,walfn,north,0.0,28000,30,31,20,20,4,7,1,1980) # North wall h
bdyc(100,h,walfn,north,0.0,28000,36,37,20,20,4,7,1,1980) # North wall h
bdyc(100,h,walfn,north,0.0,28000,41,43,20,20,4,7,1,1980) # North wall h
bdyc(100,h,walfn,north,0.0,28000,47,49,20,20,4,7,1,1980) # North wall h

bdyc(100,h,walfn, east,0.0,28000,53,53,11,18,1,7,1,1980) # East wall h
bdyc(100,h,walfn, east,0.0,28000,53,53,9,20,8,15,1,1980) # East wall h
bdyc(100,h,walfn, west,0.0,28000,14,14,11,13,1,7,1,1980) # West wall h
bdyc(100,h,walfn, west,0.0,28000,14,14,16,18,1,7,1,1980) # West wall h
bdyc(100,h,walfn, west,0.0,28000,14,14,9,20,8,15,1,1980) # West wall h

# WALL SURFACE TEMPERATURE SETTINGS 2
bdyc(100,h,walfn,south,0.0,29000,14,53,9,9,1,3,1981,4320) # South wall h
bdyc(100,h,walfn,south,0.0,29000,14,53,9,9,8,15,1981,4320) # South wall h
bdyc(100,h,walfn,south,0.0,29000,18,20,9,9,4,7,1981,4320) # South wall h
bdyc(100,h,walfn,south,0.0,29000,24,26,9,9,4,7,1981,4320) # South wall h
bdyc(100,h,walfn,south,0.0,29000,30,31,9,9,4,7,1981,4320) # South wall h
bdyc(100,h,walfn,south,0.0,29000,36,37,9,9,4,7,1981,4320) # South wall h
bdyc(100,h,walfn,south,0.0,29000,41,43,9,9,4,7,1981,4320) # South wall h
bdyc(100,h,walfn,south,0.0,29000,47,49,9,9,4,7,1981,4320) # South wall h

bdyc(100,h,walfn,north,0.0,29000,14,53,20,20,1,3,1981,4320) # North wall h
bdyc(100,h,walfn,north,0.0,29000,14,53,20,20,8,15,1981,4320) # North wall h
bdyc(100,h,walfn,north,0.0,29000,18,20,20,20,4,7,1981,4320) # North wall h
bdyc(100,h,walfn,north,0.0,29000,24,26,20,20,4,7,1981,4320) # North wall h
bdyc(100,h,walfn,north,0.0,29000,30,31,20,20,4,7,1981,4320) # North wall h
bdyc(100,h,walfn,north,0.0,29000,36,37,20,20,4,7,1981,4320) # North wall h
bdyc(100,h,walfn,north,0.0,29000,41,43,20,20,4,7,1981,4320) # North wall h
bdyc(100,h,walfn,north,0.0,29000,47,49,20,20,4,7,1981,4320) # North wall h

bdyc(100,h,walfn, east,0.0,29000,53,53,11,18,1,7,1981,4320) # East wall h
bdyc(100,h,walfn, east,0.0,29000,53,53,9,20,8,15,1981,4320) # East wall h
bdyc(100,h,walfn, west,0.0,29000,14,14,11,13,1,7,1981,4320) # West wall h
bdyc(100,h,walfn, west,0.0,29000,14,14,16,18,1,7,1981,4320) # West wall h
bdyc(100,h,walfn, west,0.0,29000,14,14,9,20,8,15,1981,4320) # West wall h

# INTERIOR COLUMN SURFACE TEMPERATURE
bdyc(101,h,walfn,north,0.0,28000.0,18,19,10,10,1,15,1,nstep) # column C1
bdyc(101,h,walfn,south,0.0,28000.0,18,19,12,12,1,15,1,nstep) # column C1
bdyc(101,h,walfn, west,0.0,28000.0,20,20,11,11,1,15,1,nstep) # column C1
bdyc(101,h,walfn, east,0.0,28000.0,17,17,11,11,1,15,1,nstep) # column C1

bdyc(102,h,walfn,north,0.0,28000.0,24,25,10,10,1,15,1,nstep) # column C2
bdyc(102,h,walfn,south,0.0,28000.0,24,25,12,12,1,15,1,nstep) # column C2
bdyc(102,h,walfn, west,0.0,28000.0,26,26,11,11,1,15,1,nstep) # column C2
bdyc(102,h,walfn, east,0.0,28000.0,23,23,11,11,1,15,1,nstep) # column C2

bdyc(103,h,walfn,north,0.0,28000.0,30,31,10,10,1,15,1,nstep) # column C3
bdyc(103,h,walfn,south,0.0,28000.0,30,31,12,12,1,15,1,nstep) # column C3
bdyc(103,h,walfn, west,0.0,28000.0,32,32,11,11,1,15,1,nstep) # column C3
bdyc(103,h,walfn, east,0.0,28000.0,29,29,11,11,1,15,1,nstep) # column C3

bdyc(104,h,walfn,north,0.0,28000.0,36,37,10,10,1,15,1,nstep) # column C4
bdyc(104,h,walfn,south,0.0,28000.0,36,37,12,12,1,15,1,nstep) # column C4
bdyc(104,h,walfn, west,0.0,28000.0,38,38,11,11,1,15,1,nstep) # column C4
bdyc(104,h,walfn, east,0.0,28000.0,35,35,11,11,1,15,1,nstep) # column C4

bdyc(105,h,walfn,north,0.0,28000.0,42,43,10,10,1,15,1,nstep) # column C5
bdyc(105,h,walfn,south,0.0,28000.0,42,43,12,12,1,15,1,nstep) # column C5
bdyc(105,h,walfn, west,0.0,28000.0,44,44,11,11,1,15,1,nstep) # column C5
bdyc(105,h,walfn, east,0.0,28000.0,41,41,11,11,1,15,1,nstep) # column C5

bdyc(106,h,walfn,north,0.0,28000.0,48,49,10,10,1,15,1,nstep) # column C6
bdyc(106,h,walfn,south,0.0,28000.0,48,49,12,12,1,15,1,nstep) # column C6
bdyc(106,h,walfn, west,0.0,28000.0,50,50,11,11,1,15,1,nstep) # column C6
bdyc(106,h,walfn, east,0.0,28000.0,47,47,11,11,1,15,1,nstep) # column C6

```

```

bdyc(107,h,walfn,north,0.0,28000.0,18,19,17,17,1,15,1,nstep) # column C7
bdyc(107,h,walfn,south,0.0,28000.0,18,19,19,19,1,15,1,nstep) # column C7
bdyc(107,h,walfn,west,0.0,28000.0,20,20,18,18,1,15,1,nstep) # column C7
bdyc(107,h,walfn,east,0.0,28000.0,17,17,18,18,1,15,1,nstep) # column C7

bdyc(108,h,walfn,north,0.0,28000.0,24,25,17,17,1,15,1,nstep) # column C8
bdyc(108,h,walfn,south,0.0,28000.0,24,25,19,19,1,15,1,nstep) # column C8
bdyc(108,h,walfn,west,0.0,28000.0,26,26,18,18,1,15,1,nstep) # column C8
bdyc(108,h,walfn,east,0.0,28000.0,23,23,18,18,1,15,1,nstep) # column C8

bdyc(109,h,walfn,north,0.0,28000.0,30,31,17,17,1,15,1,nstep) # column C9
bdyc(109,h,walfn,south,0.0,28000.0,30,31,19,19,1,15,1,nstep) # column C9
bdyc(109,h,walfn,west,0.0,28000.0,32,32,18,18,1,15,1,nstep) # column C9
bdyc(109,h,walfn,east,0.0,28000.0,29,29,18,18,1,15,1,nstep) # column C9

bdyc(110,h,walfn,north,0.0,28000.0,36,37,17,17,1,15,1,nstep) # column C10
bdyc(110,h,walfn,south,0.0,28000.0,36,37,19,19,1,15,1,nstep) # column C10
bdyc(110,h,walfn,west,0.0,28000.0,38,38,18,18,1,15,1,nstep) # column C10
bdyc(110,h,walfn,east,0.0,28000.0,35,35,18,18,1,15,1,nstep) # column C10

bdyc(111,h,walfn,north,0.0,28000.0,42,43,17,17,1,15,1,nstep) # column C11
bdyc(111,h,walfn,south,0.0,28000.0,42,43,19,19,1,15,1,nstep) # column C11
bdyc(111,h,walfn,west,0.0,28000.0,44,44,18,18,1,15,1,nstep) # column C11
bdyc(111,h,walfn,east,0.0,28000.0,41,41,18,18,1,15,1,nstep) # column C11

bdyc(112,h,walfn,north,0.0,28000.0,48,49,17,17,1,15,1,nstep) # column C12
bdyc(112,h,walfn,south,0.0,28000.0,48,49,19,19,1,15,1,nstep) # column C12
bdyc(112,h,walfn,west,0.0,28000.0,50,50,18,18,1,15,1,nstep) # column C12
bdyc(112,h,walfn,east,0.0,28000.0,47,47,18,18,1,15,1,nstep) # column C12

rho = 1.0
gravz = -9.81

# BOUNDARY CONDITIONS

bdyc(10,p,inflow,south,0.73,1,1,5,1,1,1,12,1,1260)
bdyc(10,p,inflow,south,0.73,1,73,nx,1,1,1,12,1,1260)
bdyc(10,p,inflow,south,0.73,1,1,nx,1,1,13,nz,1,1260)
bdyc(10,p,inflow,south,1.09,1,1,5,1,1,1,12,1261,1440)
bdyc(10,p,inflow,south,1.09,1,73,nx,1,1,1,12,1261,1440)
bdyc(10,p,inflow,south,1.09,1,1,nx,1,1,13,nz,1261,1440)
bdyc(10,p,inflow,south,1.45,1,1,5,1,1,1,12,1441,1620)
bdyc(10,p,inflow,south,1.45,1,73,nx,1,1,1,12,1441,1620)
bdyc(10,p,inflow,south,1.45,1,1,nx,1,1,13,nz,1441,1620)
bdyc(10,p,inflow,south,1.45,1,1,5,1,1,1,12,1621,1800)
bdyc(10,p,inflow,south,1.45,1,73,nx,1,1,1,12,1621,1800)
bdyc(10,p,inflow,south,1.45,1,1,nx,1,1,13,nz,1621,1800)
bdyc(10,p,inflow,south,1.39,1,1,5,1,1,1,12,1801,2880)
bdyc(10,p,inflow,south,1.39,1,73,nx,1,1,1,12,1801,2880)
bdyc(10,p,inflow,south,1.39,1,1,nx,1,1,13,nz,1801,2880)
bdyc(10,p,inflow,south,1.82,1,1,5,1,1,1,12,2881,3060)
bdyc(10,p,inflow,south,1.82,1,73,nx,1,1,1,12,2881,3060)
bdyc(10,p,inflow,south,1.82,1,1,nx,1,1,13,nz,2881,3060)
bdyc(10,p,inflow,south,1.09,1,1,5,1,1,1,12,3061,3240)
bdyc(10,p,inflow,south,1.09,1,73,nx,1,1,1,12,3061,3240)
bdyc(10,p,inflow,south,1.09,1,1,nx,1,1,13,nz,3061,3240)
bdyc(10,p,inflow,south,1.45,1,1,5,1,1,1,12,3241,3420)
bdyc(10,p,inflow,south,1.45,1,73,nx,1,1,1,12,3241,3420)
bdyc(10,p,inflow,south,1.45,1,1,nx,1,1,13,nz,3241,3420)
bdyc(10,p,inflow,south,1.38,1,1,5,1,1,1,12,3421,4320)
bdyc(10,p,inflow,south,1.38,1,73,nx,1,1,1,12,3421,4320)
bdyc(10,p,inflow,south,1.38,1,1,nx,1,1,13,nz,3421,4320)

bdyc(10,u,inflow,south,0.73,0.73,1,5,1,1,1,12,1,1260)
bdyc(10,u,inflow,south,0.73,0.73,73,nx,1,1,1,12,1,1260)
bdyc(10,u,inflow,south,0.73,0.73,1,nx,1,1,13,nz,1,1260)
bdyc(10,u,inflow,south,1.09,1.09,1,5,1,1,1,12,1261,1440)
bdyc(10,u,inflow,south,1.09,1.09,73,nx,1,1,1,12,1261,1440)
bdyc(10,u,inflow,south,1.09,1.09,1,nx,1,1,13,nz,1261,1440)
bdyc(10,u,inflow,south,1.45,1.45,1,5,1,1,1,12,1441,1620)
bdyc(10,u,inflow,south,1.45,1.45,73,nx,1,1,1,12,1441,1620)
bdyc(10,u,inflow,south,1.45,1.45,1,nx,1,1,13,nz,1441,1620)
bdyc(10,u,inflow,south,1.45,1.45,1,5,1,1,1,12,1621,1800)
bdyc(10,u,inflow,south,1.45,1.45,73,nx,1,1,1,12,1621,1800)
bdyc(10,u,inflow,south,1.45,1.45,1,nx,1,1,13,nz,1621,1800)
bdyc(10,u,inflow,south,1.39,1.39,1,5,1,1,1,12,1801,2880)

```

bduc(10,u,inflow,south,1.39,1.39,73,nx,1,1,1,12,1801,2880)  
bduc(10,u,inflow,south,1.39,1.39,1,nx,1,1,13,nz,1801,2880)  
bduc(10,u,inflow,south,1.82,1.82,1,5,1,1,1,12,2881,3060)  
bduc(10,u,inflow,south,1.82,1.82,73,nx,1,1,1,12,2881,3060)  
bduc(10,u,inflow,south,1.82,1.82,1,nx,1,1,13,nz,2881,3060)  
bduc(10,u,inflow,south,1.09,1.09,1,5,1,1,1,12,3061,3240)  
bduc(10,u,inflow,south,1.09,1.09,73,nx,1,1,1,12,3061,3240)  
bduc(10,u,inflow,south,1.09,1.09,1,nx,1,1,13,nz,3061,3240)  
bduc(10,u,inflow,south,1.45,1.45,1,5,1,1,1,12,3241,3420)  
bduc(10,u,inflow,south,1.45,1.45,73,nx,1,1,1,12,3241,3420)  
bduc(10,u,inflow,south,1.45,1.45,1,nx,1,1,13,nz,3241,3420)  
bduc(10,u,inflow,south,1.38,1.38,1,5,1,1,1,12,3421,4320)  
bduc(10,u,inflow,south,1.38,1.38,73,nx,1,1,1,12,3421,4320)  
bduc(10,u,inflow,south,1.38,1.38,1,nx,1,1,13,nz,3421,4320)

bduc(10,v,inflow,south,0.73,0.73,1,5,1,1,1,12,1,1260)  
bduc(10,v,inflow,south,0.73,0.73,73,nx,1,1,1,12,1,1260)  
bduc(10,v,inflow,south,0.73,0.73,1,nx,1,1,13,nz,1,1260)  
bduc(10,v,inflow,south,1.09,1.09,1,5,1,1,1,12,1261,1440)  
bduc(10,v,inflow,south,1.09,1.09,73,nx,1,1,1,12,1261,1440)  
bduc(10,v,inflow,south,1.09,1.09,1,nx,1,1,13,nz,1261,1440)  
bduc(10,v,inflow,south,1.45,1.45,1,5,1,1,1,12,1441,1620)  
bduc(10,v,inflow,south,1.45,1.45,73,nx,1,1,1,12,1441,1620)  
bduc(10,v,inflow,south,1.45,1.45,1,nx,1,1,13,nz,1441,1620)  
bduc(10,v,inflow,south,1.45,1.45,1,5,1,1,1,12,1621,1800)  
bduc(10,v,inflow,south,1.45,1.45,73,nx,1,1,1,12,1621,1800)  
bduc(10,v,inflow,south,1.45,1.45,1,nx,1,1,13,nz,1621,1800)  
bduc(10,v,inflow,south,1.39,1.39,1,5,1,1,1,12,1801,2880)  
bduc(10,v,inflow,south,1.39,1.39,73,nx,1,1,1,12,1801,2880)  
bduc(10,v,inflow,south,1.39,1.39,1,nx,1,1,13,nz,1801,2880)  
bduc(10,v,inflow,south,1.82,1.82,1,5,1,1,1,12,2881,3060)  
bduc(10,v,inflow,south,1.82,1.82,73,nx,1,1,1,12,2881,3060)  
bduc(10,v,inflow,south,1.82,1.82,1,nx,1,1,13,nz,2881,3060)  
bduc(10,v,inflow,south,1.09,1.09,1,5,1,1,1,12,3061,3240)  
bduc(10,v,inflow,south,1.09,1.09,73,nx,1,1,1,12,3061,3240)  
bduc(10,v,inflow,south,1.09,1.09,1,nx,1,1,13,nz,3061,3240)  
bduc(10,v,inflow,south,1.45,1.45,1,5,1,1,1,12,3241,3420)  
bduc(10,v,inflow,south,1.45,1.45,73,nx,1,1,1,12,3241,3420)  
bduc(10,v,inflow,south,1.45,1.45,1,nx,1,1,13,nz,3241,3420)  
bduc(10,v,inflow,south,1.38,1.38,1,5,1,1,1,12,3421,4320)  
bduc(10,v,inflow,south,1.38,1.38,73,nx,1,1,1,12,3421,4320)  
bduc(10,v,inflow,south,1.38,1.38,1,nx,1,1,13,nz,3421,4320)

bduc(10,ke,inflow,south,0.73,0.00132,1,5,1,1,1,12,1,1260)  
bduc(10,ke,inflow,south,0.73,0.00132,73,nx,1,1,1,12,1,1260)  
bduc(10,ke,inflow,south,0.73,0.00132,1,nx,1,1,13,nz,1,1260)  
bduc(10,ke,inflow,south,1.09,0.00297,1,5,1,1,1,12,1261,1440)  
bduc(10,ke,inflow,south,1.09,0.00297,73,nx,1,1,1,12,1261,1440)  
bduc(10,ke,inflow,south,1.09,0.00297,1,nx,1,1,13,nz,1261,1440)  
bduc(10,ke,inflow,south,1.45,0.00529,1,5,1,1,1,12,1441,1620)  
bduc(10,ke,inflow,south,1.45,0.00529,73,nx,1,1,1,12,1441,1620)  
bduc(10,ke,inflow,south,1.45,0.00529,1,nx,1,1,13,nz,1441,1620)  
bduc(10,ke,inflow,south,1.45,0.00529,1,5,1,1,1,12,1621,1800)  
bduc(10,ke,inflow,south,1.45,0.00529,73,nx,1,1,1,12,1621,1800)  
bduc(10,ke,inflow,south,1.45,0.00529,1,nx,1,1,13,nz,1621,1800)  
bduc(10,ke,inflow,south,1.39,0.00485,1,5,1,1,1,12,1801,2880)  
bduc(10,ke,inflow,south,1.39,0.00485,73,nx,1,1,1,12,1801,2880)  
bduc(10,ke,inflow,south,1.39,0.00485,1,nx,1,1,13,nz,1801,2880)  
bduc(10,ke,inflow,south,1.82,0.00826,1,5,1,1,1,12,2881,3060)  
bduc(10,ke,inflow,south,1.82,0.00826,73,nx,1,1,1,12,2881,3060)  
bduc(10,ke,inflow,south,1.82,0.00826,1,nx,1,1,13,nz,2881,3060)  
bduc(10,ke,inflow,south,1.09,0.00297,1,5,1,1,1,12,3061,3240)  
bduc(10,ke,inflow,south,1.09,0.00297,73,nx,1,1,1,12,3061,3240)  
bduc(10,ke,inflow,south,1.09,0.00297,1,nx,1,1,13,nz,3061,3240)  
bduc(10,ke,inflow,south,1.45,0.00529,1,5,1,1,1,12,3241,3420)  
bduc(10,ke,inflow,south,1.45,0.00529,73,nx,1,1,1,12,3241,3420)  
bduc(10,ke,inflow,south,1.45,0.00529,1,nx,1,1,13,nz,3241,3420)  
bduc(10,ke,inflow,south,1.38,0.00477,1,5,1,1,1,12,3421,4320)  
bduc(10,ke,inflow,south,1.38,0.00477,73,nx,1,1,1,12,3421,4320)  
bduc(10,ke,inflow,south,1.38,0.00477,1,nx,1,1,13,nz,3421,4320)

bduc(10,ep,inflow,south,0.73,0.000003,1,5,1,1,1,12,1,1260)  
bduc(10,ep,inflow,south,0.73,0.000003,73,nx,1,1,1,12,1,1260)  
bduc(10,ep,inflow,south,0.73,0.000003,1,nx,1,1,13,nz,1,1260)  
bduc(10,ep,inflow,south,1.09,0.000009,1,5,1,1,1,12,1261,1440)  
bduc(10,ep,inflow,south,1.09,0.000009,73,nx,1,1,1,12,1261,1440)

```

bdyc(10,ep,inflow,south,1.09,0.000009, 1,nx,1,1,13,nz,1261,1440)
bdyc(10,ep,inflow,south,1.45,0.000021, 1, 5,1,1, 1,12,1441,1620)
bdyc(10,ep,inflow,south,1.45,0.000021,73,nx,1,1, 1,12,1441,1620)
bdyc(10,ep,inflow,south,1.45,0.000021, 1,nx,1,1,13,nz,1441,1620)
bdyc(10,ep,inflow,south,1.45,0.000021, 1, 5,1,1, 1,12,1621,1800)
bdyc(10,ep,inflow,south,1.45,0.000021,73,nx,1,1, 1,12,1621,1800)
bdyc(10,ep,inflow,south,1.45,0.000021, 1,nx,1,1,13,nz,1621,1800)
bdyc(10,ep,inflow,south,1.39,0.000019, 1, 5,1,1, 1,12,1801,2880)
bdyc(10,ep,inflow,south,1.39,0.000019,73,nx,1,1, 1,12,1801,2880)
bdyc(10,ep,inflow,south,1.39,0.000019, 1,nx,1,1,13,nz,1801,2880)
bdyc(10,ep,inflow,south,1.82,0.000041, 1, 5,1,1, 1,12,2881,3060)
bdyc(10,ep,inflow,south,1.82,0.000041,73,nx,1,1, 1,12,2881,3060)
bdyc(10,ep,inflow,south,1.82,0.000041, 1,nx,1,1,13,nz,2881,3060)
bdyc(10,ep,inflow,south,1.09,0.000009, 1, 5,1,1, 1,12,3061,3240)
bdyc(10,ep,inflow,south,1.09,0.000009,73,nx,1,1, 1,12,3061,3240)
bdyc(10,ep,inflow,south,1.09,0.000009, 1,nx,1,1,13,nz,3061,3240)
bdyc(10,ep,inflow,south,1.45,0.000021, 1, 5,1,1, 1,12,3241,3420)
bdyc(10,ep,inflow,south,1.45,0.000021,73,nx,1,1, 1,12,3241,3420)
bdyc(10,ep,inflow,south,1.45,0.000021, 1,nx,1,1,13,nz,3241,3420)
bdyc(10,ep,inflow,south,1.38,0.000018, 1, 5,1,1, 1,12,3421,4320)
bdyc(10,ep,inflow,south,1.38,0.000018,73,nx,1,1, 1,12,3421,4320)
bdyc(10,ep,inflow,south,1.38,0.000018, 1,nx,1,1,13,nz,3421,4320)

```

```

bdyc(10,h,inflow,south,0.73,27963, 1, 5,1,1, 1,12,1,1260)
bdyc(10,h,inflow,south,0.73,27963,73,nx,1,1, 1,12,1,1260)
bdyc(10,h,inflow,south,0.73,27963, 1,nx,1,1,13,nz,1,1260)
bdyc(10,h,inflow,south,1.09,28063, 1, 5,1,1, 1,12,1261,1440)
bdyc(10,h,inflow,south,1.09,28063,73,nx,1,1, 1,12,1261,1440)
bdyc(10,h,inflow,south,1.09,28063, 1,nx,1,1,13,nz,1261,1440)
bdyc(10,h,inflow,south,1.45,30068, 1, 5,1,1, 1,12,1441,1620)
bdyc(10,h,inflow,south,1.45,30068,73,nx,1,1, 1,12,1441,1620)
bdyc(10,h,inflow,south,1.45,30068, 1,nx,1,1,13,nz,1441,1620)
bdyc(10,h,inflow,south,1.45,31371, 1, 5,1,1, 1,12,1621,1800)
bdyc(10,h,inflow,south,1.45,31371,73,nx,1,1, 1,12,1621,1800)
bdyc(10,h,inflow,south,1.45,31371, 1,nx,1,1,13,nz,1621,1800)
bdyc(10,h,inflow,south,1.39,33700, 1, 5,1,1, 1,12,1801,2880)
bdyc(10,h,inflow,south,1.39,33700,73,nx,1,1, 1,12,1801,2880)
bdyc(10,h,inflow,south,1.39,33700, 1,nx,1,1,13,nz,1801,2880)
bdyc(10,h,inflow,south,1.82,35079, 1, 5,1,1, 1,12,2881,3060)
bdyc(10,h,inflow,south,1.82,35079,73,nx,1,1, 1,12,2881,3060)
bdyc(10,h,inflow,south,1.82,35079, 1,nx,1,1,13,nz,2881,3060)
bdyc(10,h,inflow,south,1.09,33576, 1, 5,1,1, 1,12,3061,3240)
bdyc(10,h,inflow,south,1.09,33576,73,nx,1,1, 1,12,3061,3240)
bdyc(10,h,inflow,south,1.09,33576, 1,nx,1,1,13,nz,3061,3240)
bdyc(10,h,inflow,south,1.45,32072, 1, 5,1,1, 1,12,3241,3420)
bdyc(10,h,inflow,south,1.45,32072,73,nx,1,1, 1,12,3241,3420)
bdyc(10,h,inflow,south,1.45,32072, 1,nx,1,1,13,nz,3241,3420)
bdyc(10,h,inflow,south,1.38,29847, 1, 5,1,1, 1,12,3421,4320)
bdyc(10,h,inflow,south,1.38,29847,73,nx,1,1, 1,12,3421,4320)
bdyc(10,h,inflow,south,1.38,29847, 1,nx,1,1,13,nz,3421,4320)

```

```

bdyc(20,p,inflow,west,0.73,1,1,1,1,ny,1,nz,1,1260)
bdyc(20,p,inflow,west,1.09,1,1,1,1,ny,1,nz,1261,1440)
bdyc(20,p,inflow,west,1.45,1,1,1,1,ny,1,nz,1441,1620)
bdyc(20,p,inflow,west,1.45,1,1,1,1,ny,1,nz,1621,1800)
bdyc(20,p,inflow,west,1.39,1,1,1,1,ny,1,nz,1801,2880)
bdyc(20,p,inflow,west,1.82,1,1,1,1,ny,1,nz,2881,3060)
bdyc(20,p,inflow,west,1.09,1,1,1,1,ny,1,nz,3061,3240)
bdyc(20,p,inflow,west,1.45,1,1,1,1,ny,1,nz,3241,3420)
bdyc(20,p,inflow,west,1.38,1,1,1,1,ny,1,nz,3421,4320)

```

```

bdyc(20,u,inflow,west,0.73,0.73,1,1,1,ny,1,nz,1,1260)
bdyc(20,u,inflow,west,1.09,1.09,1,1,1,ny,1,nz,1261,1440)
bdyc(20,u,inflow,west,1.45,1.45,1,1,1,ny,1,nz,1441,1620)
bdyc(20,u,inflow,west,1.45,1.45,1,1,1,ny,1,nz,1621,1800)
bdyc(20,u,inflow,west,1.39,1.39,1,1,1,ny,1,nz,1801,2880)
bdyc(20,u,inflow,west,1.82,1.82,1,1,1,ny,1,nz,2881,3060)
bdyc(20,u,inflow,west,1.09,1.09,1,1,1,ny,1,nz,3061,3240)
bdyc(20,u,inflow,west,1.45,1.45,1,1,1,ny,1,nz,3241,3420)
bdyc(20,u,inflow,west,1.38,1.38,1,1,1,ny,1,nz,3421,4320)

```

```

bdyc(20,v,inflow,west,0.73,0.73,1,1,1,ny,1,nz,1,1260)
bdyc(20,v,inflow,west,1.09,1.09,1,1,1,ny,1,nz,1261,1440)
bdyc(20,v,inflow,west,1.45,1.45,1,1,1,ny,1,nz,1441,1620)
bdyc(20,v,inflow,west,1.45,1.45,1,1,1,ny,1,nz,1621,1800)
bdyc(20,v,inflow,west,1.39,1.39,1,1,1,ny,1,nz,1801,2880)

```



```

bdyc(20,v,inflow,west,1.82,1.82,1,1,1,ny,1,nz,2881,3060)
bdyc(20,v,inflow,west,1.09,1.09,1,1,1,ny,1,nz,3061,3240)
bdyc(20,v,inflow,west,1.45,1.45,1,1,1,ny,1,nz,3241,3420)
bdyc(20,v,inflow,west,1.38,1.38,1,1,1,ny,1,nz,3421,4320)

```

```

bdyc(20,ke,inflow,west,0.73,0.00132,1,1,1,ny,1,nz,1,1260)
bdyc(20,ke,inflow,west,1.09,0.00297,1,1,1,ny,1,nz,1261,1440)
bdyc(20,ke,inflow,west,1.45,0.00529,1,1,1,ny,1,nz,1441,1620)
bdyc(20,ke,inflow,west,1.45,0.00529,1,1,1,ny,1,nz,1621,1800)
bdyc(20,ke,inflow,west,1.39,0.00485,1,1,1,ny,1,nz,1801,2880)
bdyc(20,ke,inflow,west,1.82,0.00826,1,1,1,ny,1,nz,2881,3060)
bdyc(20,ke,inflow,west,1.09,0.00297,1,1,1,ny,1,nz,3061,3240)
bdyc(20,ke,inflow,west,1.45,0.00529,1,1,1,ny,1,nz,3241,3420)
bdyc(20,ke,inflow,west,1.38,0.00477,1,1,1,ny,1,nz,3421,4320)

```

```

bdyc(20,ep,inflow,west,0.73,0.000003,1,1,1,ny,1,nz,1,1260)
bdyc(20,ep,inflow,west,1.09,0.000009,1,1,1,ny,1,nz,1261,1440)
bdyc(20,ep,inflow,west,1.45,0.000021,1,1,1,ny,1,nz,1441,1620)
bdyc(20,ep,inflow,west,1.45,0.000021,1,1,1,ny,1,nz,1621,1800)
bdyc(20,ep,inflow,west,1.39,0.000019,1,1,1,ny,1,nz,1801,2880)
bdyc(20,ep,inflow,west,1.82,0.000041,1,1,1,ny,1,nz,2881,3060)
bdyc(20,ep,inflow,west,1.09,0.000009,1,1,1,ny,1,nz,3061,3240)
bdyc(20,ep,inflow,west,1.45,0.000021,1,1,1,ny,1,nz,3241,3420)
bdyc(20,ep,inflow,west,1.38,0.000018,1,1,1,ny,1,nz,3421,4320)

```

```

bdyc(20,h,inflow,west,0.73,27963,1,1,1,ny,1,nz,1,1260)
bdyc(20,h,inflow,west,1.09,28063,1,1,1,ny,1,nz,1261,1440)
bdyc(20,h,inflow,west,1.45,30068,1,1,1,ny,1,nz,1441,1620)
bdyc(20,h,inflow,west,1.45,31371,1,1,1,ny,1,nz,1621,1800)
bdyc(20,h,inflow,west,1.39,33700,1,1,1,ny,1,nz,1801,2880)
bdyc(20,h,inflow,west,1.82,35079,1,1,1,ny,1,nz,2881,3060)
bdyc(20,h,inflow,west,1.09,33576,1,1,1,ny,1,nz,3061,3240)
bdyc(20,h,inflow,west,1.45,32072,1,1,1,ny,1,nz,3241,3420)
bdyc(20,h,inflow,west,1.38,29847,1,1,1,ny,1,nz,3421,4320)

```

```

bdyc(30,p, outflow,north,0.0,0.0,1,nx,ny,ny,1,nz,1,nstep)
bdyc(30,u, outflow,north,0.0,0.0,1,nx,ny,ny,1,nz,1,nstep)
bdyc(30,v, outflow,north,0.0,0.0,1,nx,ny,ny,1,nz,1,nstep)
bdyc(30,w, outflow,north,0.0,0.0,1,nx,ny,ny,1,nz,1,nstep)
bdyc(30,ke,outflow,north,0.0,0.0,1,nx,ny,ny,1,nz,1,nstep)
bdyc(30,ep,outflow,north,0.0,0.0,1,nx,ny,ny,1,nz,1,nstep)
bdyc(30,h, outflow,north,0.0,0.0,1,nx,ny,ny,1,nz,1,nstep)

```

```

bdyc(40,p, outflow,east,0.0,0.0,nx,nx,1,ny,1,nz,1,nstep)
bdyc(40,u, outflow,east,0.0,0.0,nx,nx,1,ny,1,nz,1,nstep)
bdyc(40,v, outflow,east,0.0,0.0,nx,nx,1,ny,1,nz,1,nstep)
bdyc(40,w, outflow,east,0.0,0.0,nx,nx,1,ny,1,nz,1,nstep)
bdyc(40,ke,outflow,east,0.0,0.0,nx,nx,1,ny,1,nz,1,nstep)
bdyc(40,ep,outflow,east,0.0,0.0,nx,nx,1,ny,1,nz,1,nstep)
bdyc(40,h, outflow,east,0.0,0.0,nx,nx,1,ny,1,nz,1,nstep)

```

```
igradp=3 # High order pressure gradient boundary condition helps alot
```

```
# Thats all
```

## E.2 FORTRAN Subroutine Used to Set Up the 3-D Roof Geometry

```

subroutine Atchroof1

c *****
c Author: Atch Sreshthaputra; Copyright 2002.
c Date: July 2000
c Function: To draw roof for the temple (Oblique flow)
c *****
  common fmem(1)
  include 'common'

  krmin=16.0
  krmax=25.0
  jrmin=5.0
  jrmax=24.0
  irmin=6.0
  irmax=61.0

c  print*, 'Chapter 500:peek, start DO-LOOP for the roof'
  do k=krmin-k0, krmax-k0
  do j=jrmin-j0, jrmax-j0
  do i=irmin-j0, irmax-i0
    ijk=i+j*nxp2+k*mxy
    ijmlk=ijk-nxp2
    imljk=ijk-1
    if (i.gt.6 .and. i.lt.61) then
      if (j.ge.5 .and. j.le.14) then
        Zroof=j+11
        if (Zroof.eq.k) then
          fmem(iport+ijk)=0.0
          fmem(iporn+ijmlk)=0.0
        endif
        elseif (j.ge.15 .and. j.le.24) then
          Zroof=-1.0*j+40
          if (Zroof.eq.k) then
            fmem(iport+ijk)=0.0
            fmem(iporn+ijk)=0.0
          endif
        endif

      elseif (i.eq.6) then
        if (j.ge.5 .and. j.le.14) then
          Zroof=j+11
          if (Zroof.ge.k .and. k.gt.15) then
            fmem(ipore+ijk)=0.0
          endif
        elseif (j.ge.15 .and. j.le.24) then
          Zroof=-1.0*j+40
          if (Zroof.ge.k .and. k.gt.15) then
            fmem(ipore+ijk)=0.0
          endif
        endif

      elseif (i.eq.61) then
        if (j.ge.5 .and. j.le.14) then
          Zroof=j+11
          if (Zroof.ge.k .and. k.gt.15) then
            fmem(ipore+imljk)=0.0
          endif
        elseif (j.ge.15 .and. j.le.24) then
          Zroof=-1.0*j+40
          if (Zroof.ge.k .and. k.gt.15) then
            fmem(ipore+imljk)=0.0
          endif
        endif
      endif
    endif
  do
  do
  do
  enddo
  enddo
  enddo

  return
end

```

### E.3 FORTRAN Subroutine Used to Set Up the Wall Function

```

subroutine wallwfn
c *****
c Author: Atch Sreshthaputra; Copyright 2002
c Date: August 2000
c Function: To assign wall function for wall & roof
c *****
common fmem(1)
include 'common'

c print*, 'Start assigning walfn for each wall'

do k=1, 26
do j=1, 31
do i=1, 75

ijk=i+j*nxp2+k*mxy
imljk=ijk-1
ijmlk=ijk-nxp2
ijkpl=ijk+mxy

c East of cell; v=0, w=0
if (fmem(ipore+ijk).eq. 0.0 .and. fmem(ipore+imljk).ne.0.0) then
c print*, 'east', i, j, k
call walphi(iv, ieast, 0.0, i, i, j, j, k, k)
call walphi(iw, ieast, 0.0, i, i, j, j, k, k)
endif

c North of cell; u=0, w=0
if (fmem(iporn+ijmlk).eq. 0.0 .and. fmem(iporn+ijk).ne.0.0) then
c print*, 'north', i, j, k
call walphi(iu, inorth, 0.0, i, i, j, j, k, k)
call walphi(iw, inorth, 0.0, i, i, j, j, k, k)
endif

c West of cell; v=0, w=0
if (fmem(ipore+imljk).eq. 0.0 .and. fmem(ipore+ijk).ne.0.0) then
c print*, 'west', i, j, k
call walphi(iv, iwest, 0.0, i, i, j, j, k, k)
call walphi(iw, iwest, 0.0, i, i, j, j, k, k)
endif

c South of cell; u=0, w=0
if (fmem(iporn+ijmlk).eq. 0.0 .and. fmem(iporn+ijk).ne.0.0) then
c print*, 'south', i, j, k
call walphi(iu, isouth, 0.0, i, i, j, j, k, k)
call walphi(iw, isouth, 0.0, i, i, j, j, k, k)
endif

c Top of cell; u=0, v=0
if (fmem(iport+ijk).eq. 0.0 .and. fmem(iport+ijkpl).ne.0.0) then
c print*, 'top', i, j, k
call walphi(iu, itop, 0.0, i, i, j, j, k, k)
call walphi(iv, itop, 0.0, i, i, j, j, k, k)
endif

c Bottom of cell; u=0, v=0
if (fmem(iport+ijk).eq. 0.0 .and. fmem(iport+ijkpl).ne.0.0) then
c print*, 'bottom', i, j, k
call walphi(iu, ibot, 0.0, i, i, j, j, k+1, k+1)
call walphi(iv, ibot, 0.0, i, i, j, j, k+1, k+1)
endif

enddo
enddo
enddo
c print*, 'Assigning wall function for all walls finished'

return
end
c

```

## E.4 FORTRAN Subroutine Used to Calculate the Heat Transfer

```

subroutine Atchheat3
c *****
c Author: Atch Sreshthaputra; Copyright 2002
c Date: December 2000, Updated-April 2002
c Function: To assign heat transfer through roof & walls
c           for the temple (Oblique flow)
c *****
common fmem(1)
include 'common'
common / atchl / sumdat(25,5),solrN,solrS,solrE,solrW,hr

    krmin=16.0
    krmax=25.0
    jrmin=5.0
    jrmax=24.0
    irmin=6.0
    irmax=61.0

    solrN = 911.0
    solrS = 680.6
    solrE = 350.1
    solrW = 118.2

    absorb1 = 0.75
    absorb2 = 0.75
    QsolN   = absorb1*solrN*dt
    QsolS   = absorb1*solrS*dt
    QsolE   = absorb2*solrE*dt
    QsolW   = absorb2*solrW*dt

c   Hcon = North Outside Conv Coefficient (5.25 W/m2.K) (0.92 Btu/hr.ft2.F)
c   Hcos = South Outside Conv Coefficient (0.83 W/m2.K) (0.147 Btu/hr.ft2.F)
c   Hci  = Inside Conv Coefficient (2.67 W/m2.K) (0.47 Btu/hr.ft2.F)
c   Hco  = East West Outside Conv Coefficient (0.83 W/m2.K) (0.147 Btu/hr.ft2.F)

    Hcon = 5.25
    Hcos = 0.83
    Hci  = 2.67
    Hco  = 0.83

c   U1 = North & South Roof U value (28.40 W/m2.K) (5 Btu/hr.ft2.F)
c   U2 = East & West Roof U value (0.888 W/m2.K) (0.156 Btu/hr.ft2.F)
    U1   = 28.40
    U2   = 0.888
    Rcond1 = 1/U1
    Rcond2 = 1/U2
    Rconvi = 1/Hci
    RconvoN = 1/Hcon
    RconvoS = 1/Hcos
    Rconvo  = 1/Hco
    Rtotal1 = Rcond1+Rconvi
    Rtotal2 = Rcond2+Rconvi
    Rhat1n  = 1+(Rtotal1*Hcon)
    Rhat1s  = 1+(Rtotal1*Hcos)
    Rhat2   = 1+(Rtotal2*Hco)

c   North Roof Coefficient
    B11n   = (1/(Rtotal1*Rhat1n))-(1/Rtotal1)
    B21n   = Hcon/Rhat1n
    Gam1N  = QsolN/Rhat1n
    Gam2N  = QsolN-Gam1N

c   South Roof Coefficient
    B11s   = (1/(Rtotal1*Rhat1s))-(1/Rtotal1)
    B21s   = Hcos/Rhat1s
    Gam1S  = QsolS/Rhat1s
    Gam2S  = QsolS-Gam1S

c   East & West Roof Coefficient
    B12   = (1/(Rtotal2*Rhat2))-(1/Rtotal2)
    B22   = Hco/Rhat2
    Gam1E = QsolE/Rhat2

```

```

Gam2E = QsolE-Gam1E
Gam1W = QsolW/Rhat2
Gam2W = QsolW-Gam1W

c      print*, 'Chapter 1600:peek, Start applying heat transfer'
      do k=krmin-k0, krmax-k0
        do j=jrmin-j0, jrmax-j0
          do i=irmin-j0, irmax-i0

            ijk = i+j*nxp2+k*mxy
            ijkpl = ijk+mxy
            ijmlk = ijk-nxp2
            ijp1k = ijk+nxp2
            imljk = ijk-1
            ip1jk = ijk+1
            ijkml = ijk-mxy

c >>>>Roof Slope (North)

            if (i.gt.6 .and. i.lt.61) then
              if (j.ge.5 .and. j.le.14) then
                Zroof=j+11
                if (Zroof.eq.k) then
                  fmem(icp+ijk) =fmem(icp+ijk) - (0.40*0.566*B11n)
                  fmem(ict+ijk) =fmem(ict+ijk) - (0.40*0.566*B11n)
                  fmem(icp+ijk) =fmem(icp+ijk) - (0.40*0.566*B11n)
                  fmem(ics+ijk) =fmem(ics+ijk) - (0.40*0.566*B11n)
                  fmem(ish+ijk) =fmem(ish+ijk) + (0.40*0.566*2.0*Gam1N)

                  fmem(icp+ijkpl)=fmem(icp+ijkpl)+ (0.40*0.566*B21n)
                  fmem(icb+ijkpl)=fmem(icb+ijkpl)+ (0.40*0.566*B21n)
                  fmem(ish+ijkpl)=fmem(ish+ijkpl)+ (0.40*0.283*2.0*Gam2N)

                  fmem(icp+ijmlk)=fmem(icp+ijmlk)+ (0.40*0.566*B21n)
                  fmem(icn+ijmlk)=fmem(icn+ijmlk)+ (0.40*0.566*B21n)
                  fmem(ish+ijmlk)=fmem(ish+ijmlk)+ (0.40*0.283*2.0*Gam2N)
                endif

c >>>>Roof Slope (South)

                elseif (j.ge.15 .and. j.le.24) then
                  Zroof=-1.0*j+40
                  if (Zroof.eq.k) then
                    fmem(icp+ijk) =fmem(icp+ijk) - (0.40*0.566*B11s)
                    fmem(ict+ijk) =fmem(ict+ijk) - (0.40*0.566*B11s)
                    fmem(icp+ijk) =fmem(icp+ijk) - (0.40*0.566*B11s)
                    fmem(icn+ijk) =fmem(icn+ijk) - (0.40*0.566*B11s)
                    fmem(ish+ijk) =fmem(ish+ijk) + (0.40*0.566*2.0*Gam1S)

                    fmem(icp+ijkpl)=fmem(icp+ijkpl)+ (0.40*0.566*B21s)
                    fmem(icb+ijkpl)=fmem(icb+ijkpl)+ (0.40*0.566*B21s)
                    fmem(ish+ijkpl)=fmem(ish+ijkpl)+ (0.40*0.283*2.0*Gam2S)

                    fmem(icp+ijp1k)=fmem(icp+ijp1k)+ (0.40*0.566*B21s)
                    fmem(ics+ijp1k)=fmem(ics+ijp1k)+ (0.40*0.566*B21s)
                    fmem(ish+ijp1k)=fmem(ish+ijp1k)+ (0.40*0.283*2.0*Gam2S)
                  endif
                endif

c >>>>Roof End (East)

                elseif (i.eq.7) then
                  if (j.ge.5 .and. j.le.14) then
                    Zroof=j+11
                    if (Zroof.ge.k .and. k.gt.15) then
                      fmem(icp+ijk) =fmem(icp+ijk) - (0.64*B12)
                      fmem(icw+ijk) =fmem(icw+ijk) - (0.64*B12)
                      fmem(ish+ijk) =fmem(ish+ijk) + (0.64*Gam1E)

                      fmem(icp+imljk)=fmem(icp+imljk)+ (0.64*B22)
                      fmem(ice+imljk)=fmem(ice+imljk)+ (0.64*B22)
                      fmem(ish+imljk)=fmem(ish+imljk)+ (0.64*Gam2E)
                    endif
                  elseif (j.ge.15 .and. j.le.24) then
                    Zroof=-1.0*j+40
                    if (Zroof.ge.k .and. k.gt.15) then
                      fmem(icp+ijk) =fmem(icp+ijk) - (0.64*B12)

```

```

        fmem(icw+ijk) =fmem(icw+ijk) - (0.64*B12)
        fmem(ish+ijk) =fmem(ish+ijk) + (0.64*Gam1E)

        fmem(icp+imljk)=fmem(icp+imljk)+ (0.64*B22)
        fmem(ice+imljk)=fmem(ice+imljk)+ (0.64*B22)
        fmem(ish+imljk)=fmem(ish+imljk)+ (0.64*Gam2E)

    endif
endif

c >>>>Roof End (West)
    elseif (i.eq.60) then
        if (j.ge.5 .and. j.le.14) then
            Zroof=j+11
            if (Zroof.ge.k .and. k.gt.15) then
                fmem(icp+ijk) =fmem(icp+ijk) - (0.64*B12)
                fmem(ice+ijk) =fmem(ice+ijk) - (0.64*B12)
                fmem(ish+ijk) =fmem(ish+ijk) + (0.64*Gam1W)

                fmem(icp+ipljk)=fmem(icp+ipljk)+ (0.64*B22)
                fmem(icw+ipljk)=fmem(icw+ipljk)+ (0.64*B22)
                fmem(ish+ipljk)=fmem(ish+ipljk)+ (0.64*Gam2W)

            endif
        elseif (j.ge.15 .and. j.le.24) then
            Zroof=-1.0*j+40
            if (Zroof.ge.k .and. k.gt.15) then
                fmem(icp+ijk) =fmem(icp+ijk) - (0.64*B12)
                fmem(ice+ijk) =fmem(ice+ijk) - (0.64*B12)
                fmem(ish+ijk) =fmem(ish+ijk) + (0.64*Gam1W)

                fmem(icp+ipljk)=fmem(icp+ipljk)+ (0.64*B22)
                fmem(icw+ipljk)=fmem(icw+ipljk)+ (0.64*B22)
                fmem(ish+ipljk)=fmem(ish+ipljk)+ (0.64*Gam2W)

            endif
        endif
    endif
endif

c >>>>Ceiling U = 2.036 W/m2 K (0.358 Btu/hr-ft-F)
    if (i.gt.6 .and. i.lt.61) then
        if (j.ge.5 .and. j.le.24) then
            if (k .eq. 16) then
                UA4=0.32*2.036
                fmem(icp+ijk) =fmem(icp+ijk) + UA4
                fmem(icb+ijk) =fmem(icb+ijk) + UA4
                fmem(icp+ijkml)=fmem(icp+ijkml)+ UA4
                fmem(ict+ijkml)=fmem(ict+ijkml)+ UA4
            endif
        endif
    endif

    enddo
enddo
enddo

c-----
c      print*, 'Chapter 1600:peek, Finished'

    return
end

```

## E.5 FORTRAN Subroutine Used to Calculate the Buoyancy in the Attic

### Subroutine Atchbuoy3

```

c *****
c Author: Atch Sreshthaputra; Copyright 2002
c Date: November 2001
c Function: To calculate buoyancy in the attic
c           of the 3D temple (Oblique flow)
c *****
      common fmem(1)
      include 'common'

c print*, 'atch Buoy'

      krmin=16.0
      krmax=25.0
      jrmin=5.0
      jrmax=24.0
      irmin=6.0
      irmax=61.0

      do k=krmin-k0, krmax-k0
        do j=jrmin-j0, jrmax-j0
          do i=irmin-i0, irmax-i0

            ijk = i+j*nxp2+k*mxy

            if (i.gt.6 .and. i.lt.61) then
              if (j.ge.5 .and. j.le.14) then
                Zroof=j+11
                B = -dt*gravz*beta/cph
                if (Zroof.ge.k .and. k .gt. 15) then
                  ubs = fmem(ivol+ijk)*fmem(ih +ijk)*B
                  fmem(isw+ijk) = fmem(isw+ijk) + ubs
                endif
              elseif (j.ge.15 .and. j.le.24) then
                Zroof=-1.0*j+40
                B = -dt*gravz*beta/cph
                if (Zroof.ge.k .and. k .gt. 15) then
                  ubs = fmem(ivol+ijk)*fmem(ih +ijk)*B
                  fmem(isw+ijk) = fmem(isw+ijk) + ubs
                endif
              endif
            endif

          enddo
        enddo
      enddo

      return
      end

```

## E.6 FORTRAN Subroutine Used to Generate a HEATX Output File

```

      subroutine out0100
c
c
c Function:   To dump tecplot files for temple simulations
c Author:    Malcolm Andrews
c Date:      September 1998
c Modified:  Atch Sreshthaputra. January 2001.
c
c
      common fmem(1)
      include 'common'
c
c Dump data
      open(9, file='0100.plt')
      write(9,*) ' TITLE= "0100 data"'
      write(9,*) ' VARIABLES = "X","Y","Z","u","v","w","p","ke",',
&      ' "eps","por","h"'
      write(9,*) ' ZONE I=',nx,', J=',ny,', K=',nz,', F=POINT'
      do k=1-k0,nz-k0
      do j=1-j0,ny-j0
      do i=1-i0,nx-i0

          ijk =i+j*nxp2+k*mxy
          xcen=fmem(ixp+i)
          ycen=fmem(iyp+j)
          zcen=fmem(izp+k)
          velx=fmem(iu+ijk)
          vely=fmem(iv+ijk)
          velz=fmem(iw+ijk)
          vpres=fmem(ip+ijk)
          vke=fmem(ike+ijk)
          vep=fmem(iep+ijk)
          vdiff=(fmem(ijk+ike)**2)/(tiny+fmem(ijk+iep))
          vpor=fmem(ijk+ipor)
          vh=fmem(ijk+ih)
          write(9,111) xcen,ycen,zcen,velx,vely,velz,vpres,vke,vep,
& vpor,vh
111      format(' ',11(1p,e12.4))

          enddo
          enddo
          enddo

      close(9)
c Output drop stuff if there

      return
      end

```



## E.7 HEATX Graphical Output Generation Using TECPLOT

The HEATX graphical output presented in this dissertation was generated by the program named TECPLOT Version 8.0 (Amtec 1998). The FORTRAN subroutine presented in Appendix E.6 is used for writing the HEATX output variables (e.g., air velocity, air temperature, air pressure, kinetic energy, and dissipation rate) into an ASCII data file, which is readable by TECPLOT. Figure E.7.1 shows an example of the HEATX output file in the TECPLOT-readable format. To visualize the simulation results of HEATX graphically, a viewpoint must be specified for TECPLOT in an X-Y-Z coordinate, and the program then generates the results into two types of plot, which are vector plot as shown in Figure E.7.2, and contour plot as shown in Figure E.7.3. In addition, TECPLOT can export the graphical results into picture files in either grayscale or color. For the research, TECPLOT was used to generate two major types of plot, which are 1) vector plots showing airflow in and around the building as presented in Figures 5.8 and 5.9, and 2) contour plots showing air temperature and air pressure inside and outside the building as shown in Figures 5.10 and 5.11a.

```

TITLE= "Temple data"
VARIABLES = "X","Y","Z","u","v","w","p","ke","eps","por","h"
ZONE 1= 79, J= 37, K= 30, F=POINT
1.0000E+00 1.0000E+00 2.0000E-01 1.4097E+00 1.4085E+00 3.1290E-03 6.3995E+00 4.8963E-03 2.8349E-05 1.0000E+00 3.3776E+04
3.0000E+00 1.0000E+00 2.0000E-01 1.2977E+00 1.4597E+00 5.0740E-03 6.4671E+00 5.7954E-03 3.7016E-05 1.0000E+00 3.3776E+04
4.5000E+00 1.0000E+00 2.0000E-01 1.2062E+00 1.7104E+00 6.8943E-03 7.0288E+00 1.0218E-02 1.3204E-04 1.0000E+00 3.3776E+04
5.5000E+00 1.0000E+00 2.0000E-01 9.8500E-01 2.1387E+00 8.4484E-03 7.3833E+00 2.0448E-02 9.9037E-04 1.0000E+00 3.3776E+04
6.5000E+00 1.0000E+00 2.0000E-01 5.1854E-01 3.0486E+00 9.4910E-03 8.6360E+00 2.1633E-02 1.3797E-03 1.0000E+00 3.3776E+04
7.2000E+00 1.0000E+00 2.0000E-01 0.0000E+00 0.0000E+00 0.0000E+00 0.0000E+00 0.0000E+00 0.0000E+00 0.0000E+00 0.0000E+00
7.6000E+00 1.0000E+00 2.0000E-01 0.0000E+00 0.0000E+00 0.0000E+00 0.0000E+00 0.0000E+00 0.0000E+00 0.0000E+00 0.0000E+00
8.0000E+00 1.0000E+00 2.0000E-01 0.0000E+00 0.0000E+00 0.0000E+00 0.0000E+00 0.0000E+00 0.0000E+00 0.0000E+00 0.0000E+00
8.4000E+00 1.0000E+00 2.0000E-01 0.0000E+00 0.0000E+00 0.0000E+00 0.0000E+00 0.0000E+00 0.0000E+00 0.0000E+00 0.0000E+00
8.8000E+00 1.0000E+00 2.0000E-01 0.0000E+00 0.0000E+00 0.0000E+00 0.0000E+00 0.0000E+00 0.0000E+00 0.0000E+00 0.0000E+00
9.2000E+00 1.0000E+00 2.0000E-01 0.0000E+00 0.0000E+00 0.0000E+00 0.0000E+00 0.0000E+00 0.0000E+00 0.0000E+00 0.0000E+00
9.6000E+00 1.0000E+00 2.0000E-01 0.0000E+00 0.0000E+00 0.0000E+00 0.0000E+00 0.0000E+00 0.0000E+00 0.0000E+00 0.0000E+00
1.0000E+01 1.0000E+00 2.0000E-01 0.0000E+00 0.0000E+00 0.0000E+00 0.0000E+00 0.0000E+00 0.0000E+00 0.0000E+00 0.0000E+00
1.0400E+01 1.0000E+00 2.0000E-01 0.0000E+00 0.0000E+00 0.0000E+00 0.0000E+00 0.0000E+00 0.0000E+00 0.0000E+00 0.0000E+00
1.0800E+01 1.0000E+00 2.0000E-01 0.0000E+00 0.0000E+00 0.0000E+00 0.0000E+00 0.0000E+00 0.0000E+00 0.0000E+00 0.0000E+00
1.1200E+01 1.0000E+00 2.0000E-01 0.0000E+00 0.0000E+00 0.0000E+00 0.0000E+00 0.0000E+00 0.0000E+00 0.0000E+00 0.0000E+00
1.1600E+01 1.0000E+00 2.0000E-01 0.0000E+00 0.0000E+00 0.0000E+00 0.0000E+00 0.0000E+00 0.0000E+00 0.0000E+00 0.0000E+00
1.2000E+01 1.0000E+00 2.0000E-01 0.0000E+00 0.0000E+00 0.0000E+00 0.0000E+00 0.0000E+00 0.0000E+00 0.0000E+00 0.0000E+00
1.2400E+01 1.0000E+00 2.0000E-01 0.0000E+00 0.0000E+00 0.0000E+00 0.0000E+00 0.0000E+00 0.0000E+00 0.0000E+00 0.0000E+00
1.2800E+01 1.0000E+00 2.0000E-01 0.0000E+00 0.0000E+00 0.0000E+00 0.0000E+00 0.0000E+00 0.0000E+00 0.0000E+00 0.0000E+00
1.3200E+01 1.0000E+00 2.0000E-01 0.0000E+00 0.0000E+00 0.0000E+00 0.0000E+00 0.0000E+00 0.0000E+00 0.0000E+00 0.0000E+00
1.3600E+01 1.0000E+00 2.0000E-01 0.0000E+00 0.0000E+00 0.0000E+00 0.0000E+00 0.0000E+00 0.0000E+00 0.0000E+00 0.0000E+00
1.4000E+01 1.0000E+00 2.0000E-01 0.0000E+00 0.0000E+00 0.0000E+00 0.0000E+00 0.0000E+00 0.0000E+00 0.0000E+00 0.0000E+00
1.4400E+01 1.0000E+00 2.0000E-01 0.0000E+00 0.0000E+00 0.0000E+00 0.0000E+00 0.0000E+00 0.0000E+00 0.0000E+00 0.0000E+00
1.4800E+01 1.0000E+00 2.0000E-01 0.0000E+00 0.0000E+00 0.0000E+00 0.0000E+00 0.0000E+00 0.0000E+00 0.0000E+00 0.0000E+00

```

*Figure E.7.1 Example of a HEATX Output File in Text Format.*

For the vector plot shown in Figure E.7.2, a longer arrow with larger head indicates a higher air velocity. For the contour plot shown in Figure E.7.3, the areas that are within the same contour line have the same air temperature.

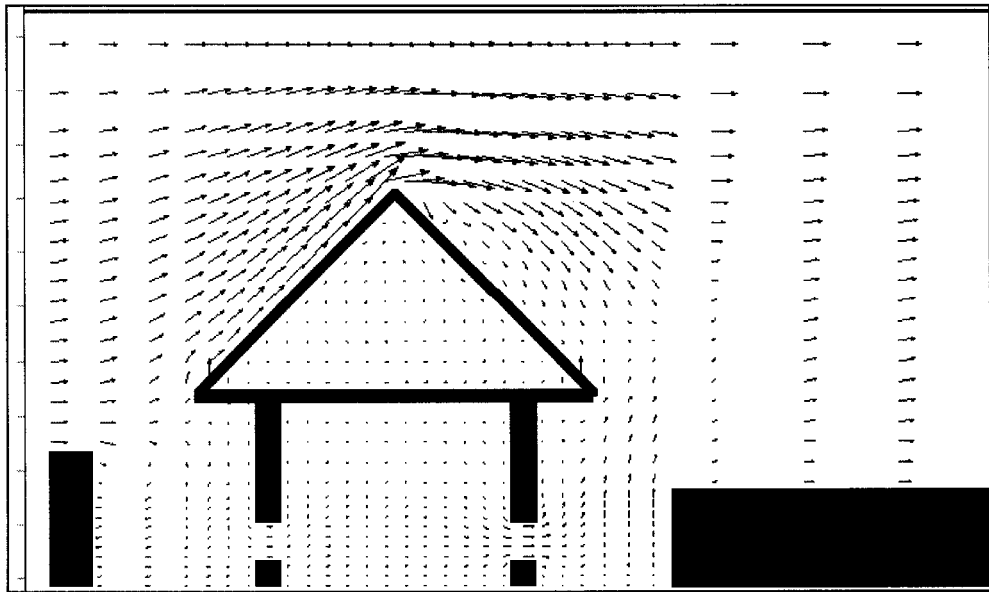


*Figure E.7.2 HEATX Simulation Results in a Vector Plot Generated by TECPLOT.*

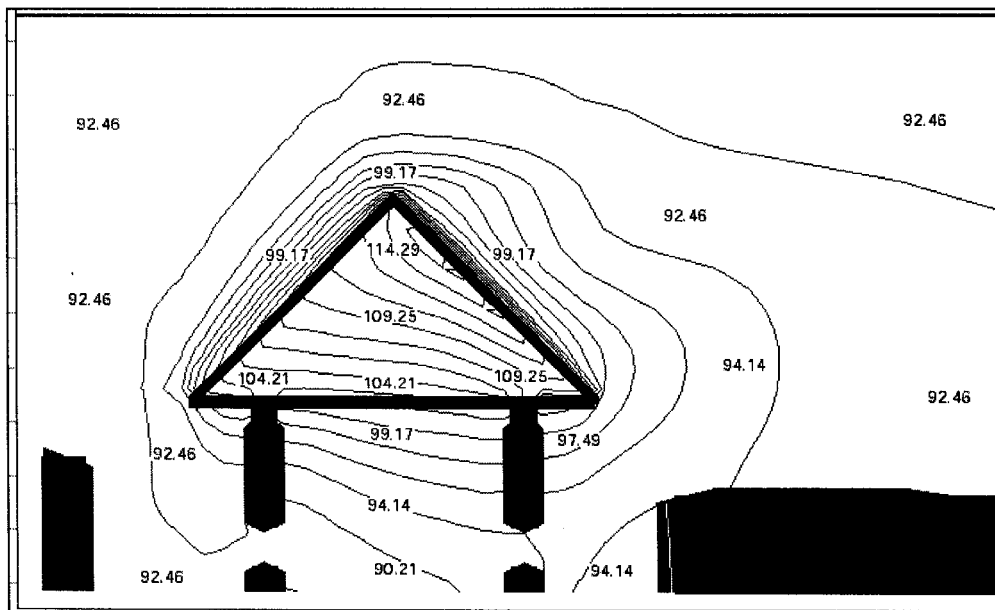


*Figure E.7.3 HEATX Simulation Results in a Contour Plot Generated by TECPLOT.*

## APPENDIX F

### CALIBRATION OF THE INSTRUMENTS

The portable temperature/humidity sensors were calibrated against a calibrated sling psychrometer, a glass thermometer, a calibrated handheld digital temperature/humidity sensor (i.e., Vaisala sensor), and the indoor air quality sensors maintained and calibrated at the Energy Systems Laboratory, Texas A&M University (i.e., ESL canary boxes). Figures F.1 and F.2 show the calibration results of the equipments used in this research against the ESL canary boxes. This calibration was performed at an indoor condition. The errors were found to be within 1 °F for temperature and 1 % for relative humidity. Figures F.3 and F.4 show the calibration results of the equipments at a low-temperature condition. This calibration was performed using a refrigerator. The errors were within 1 °F for temperature and 5 % for relative humidity. Figures F.5 and F.6 show the calibration results of the equipments at a high-temperature condition. The calibration was performed using a kitchen oven. The errors were within 2.5 °F for temperature and 0.5 % for relative humidity. Figures F.7 and F.8 show the calibration results of the equipments at an outdoor condition. The calibration was performed using a calibrated sling psychrometer, and a calibrated Vaisala Temp./RH sensor. The errors were within 1.7 °F for temperature and 2.5 % for relative humidity. Figures F.9 – F.12 show the comparisons of the temperature and relative humidity measured by the instruments used in the research against those measured by the ESL canary boxes. Table F.1 summarizes the results of the calibrations at the three conditions (i.e., the room, the high-temperature, and the low-temperature conditions) in terms of the statistical errors.

**TABLE F.1**

**Statistical Errors between the Temperature/Relative Humidity Measured by the Sensors Used in the Research and those Measured by the ESL Canary Boxes**

	BOX 1		BOX 2	
	Temp.	RH	Temp.	RH
RMSE	1.02	2.21	0.80	3.16
CV-RMSE (%)	1.89	6.78	1.48	9.70
NMBE (%)	1.43	-3.84	0.72	-6.59

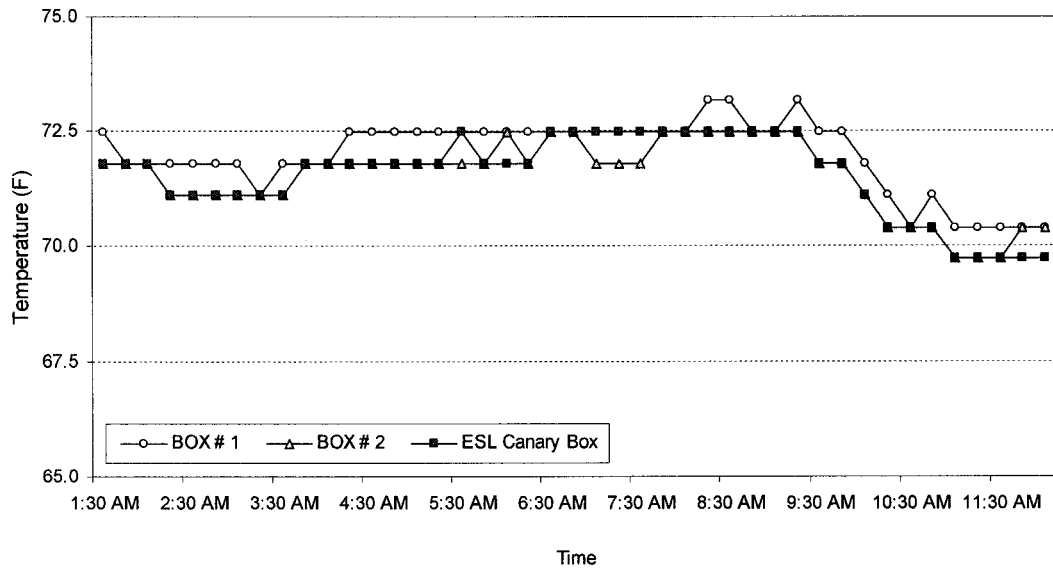


**Figure F.1** Calibration Results of the Temperature Sensors at a Room Condition.

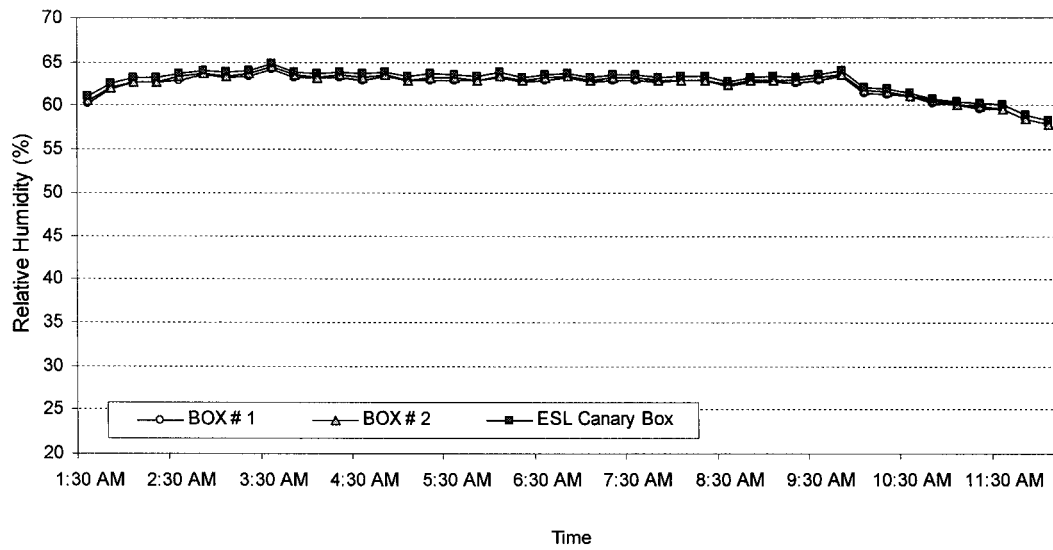


**Figure F.2** Calibration Results of the Relative Humidity Sensors at a Room Condition.

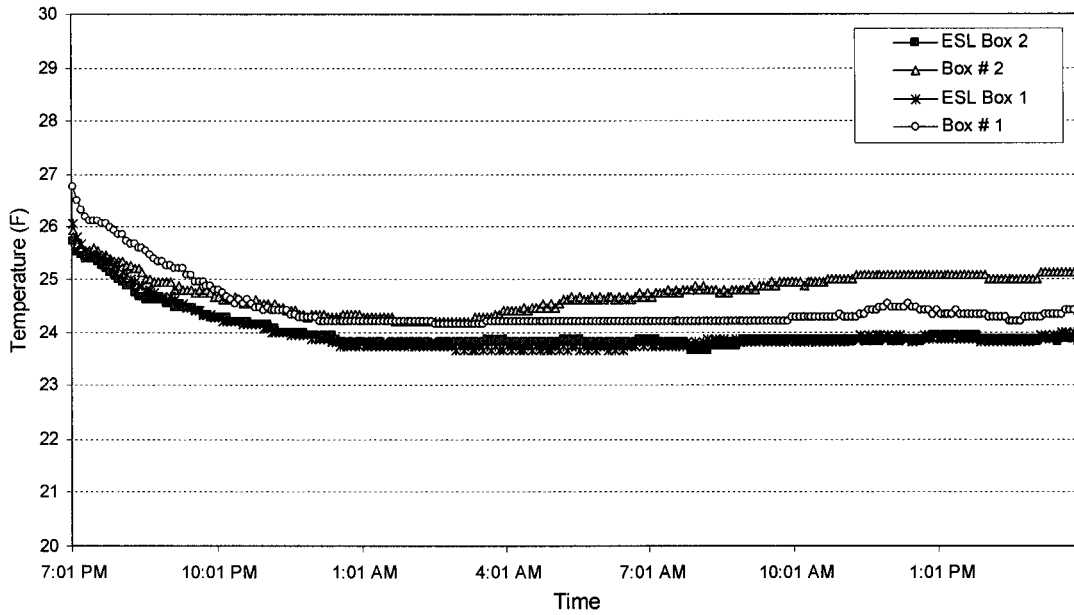


**Figure F.3** Calibration Results of the Temperature Sensors at a Low-Temperature Condition.

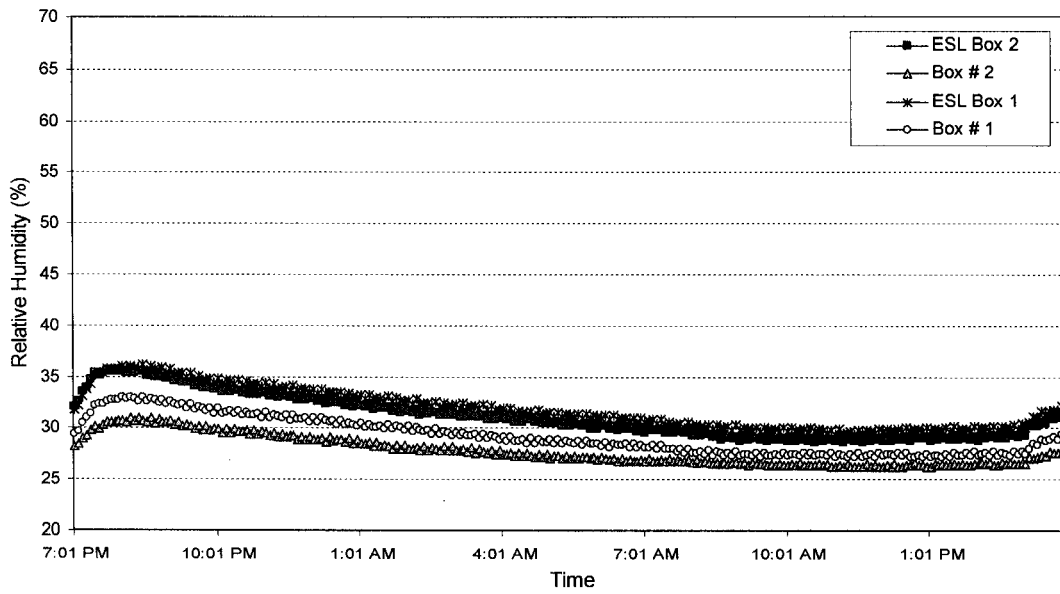


**Figure F.4** Calibration Results of the Relative Humidity Sensors at a Low-Temperature Condition.

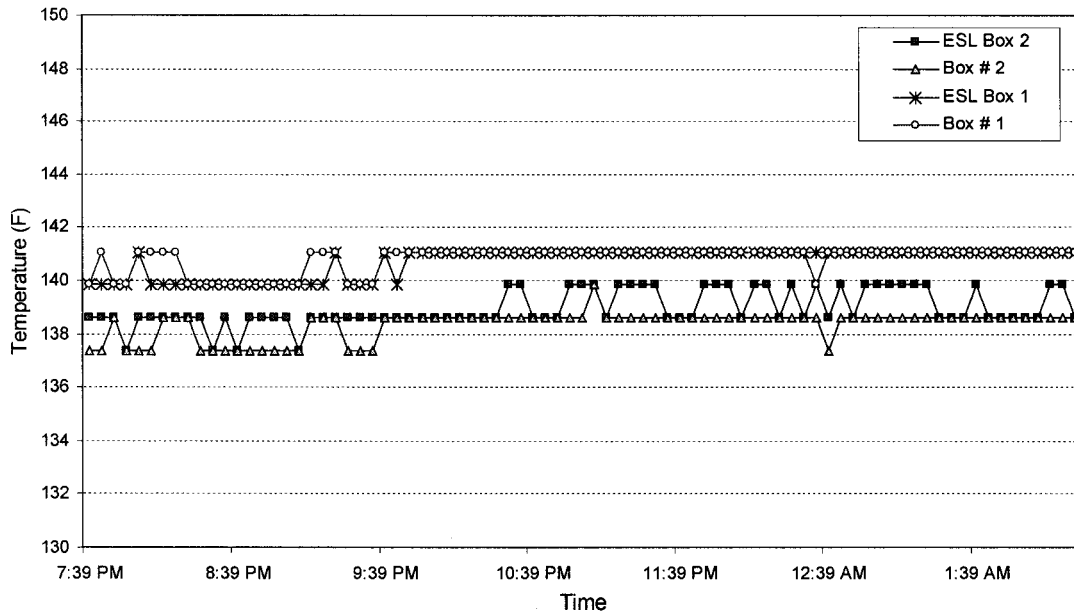


**Figure F.5** Calibration Results of the Temperature Sensors at a High-Temperature Condition.

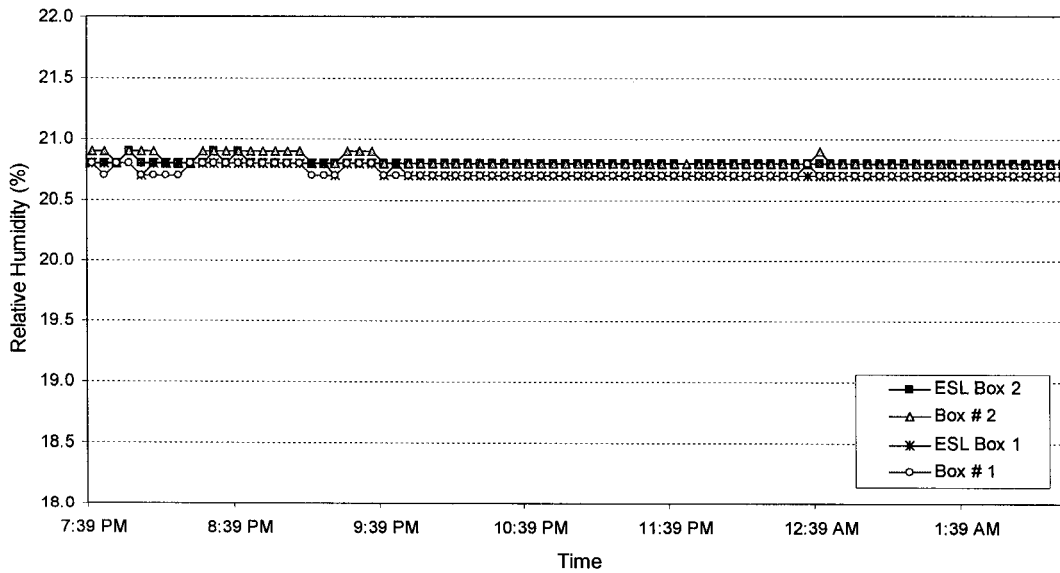


**Figure F.6** Calibration Results of the Relative Humidity Sensors at a High-Temperature Condition.

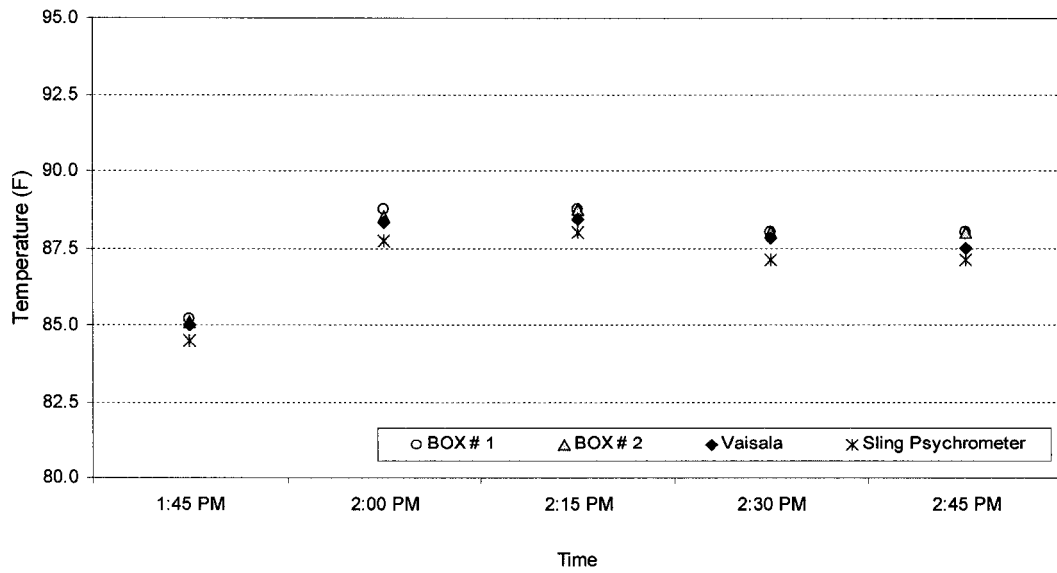


**Figure F.7** Calibration Results of the Temperature Sensors Using Spot Checks Against a Calibrated Vaisala Handheld Temperature/RH Sensor and a Calibrated Sling Psychrometer.

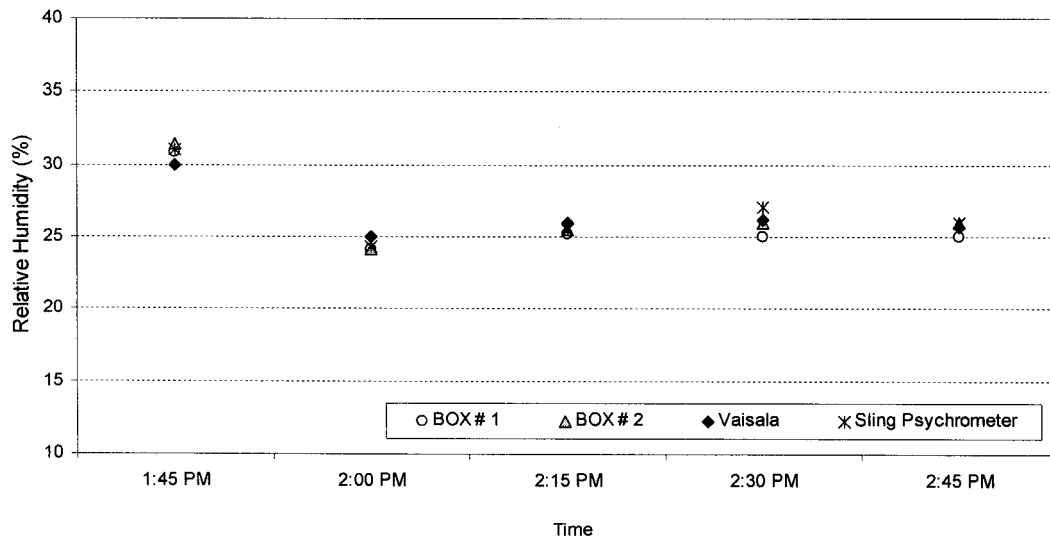


**Figure F.8** Calibration Results of the Relative Humidity Sensors Using Spot Checks Against a Calibrated Vaisala Handheld Temperature/RH Sensor and a Calibrated Sling Psychrometer.

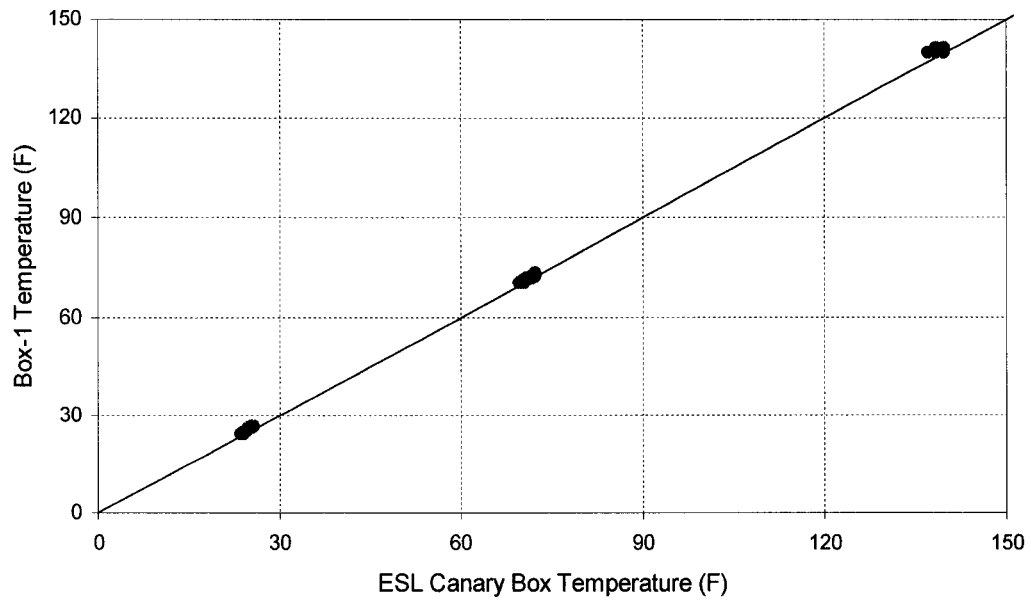


**Figure F.9** Comparisons of the Temperature Measured by the Instrument Used in the Research (Box-1) Against Those Measured by the ESL Canary Boxes.

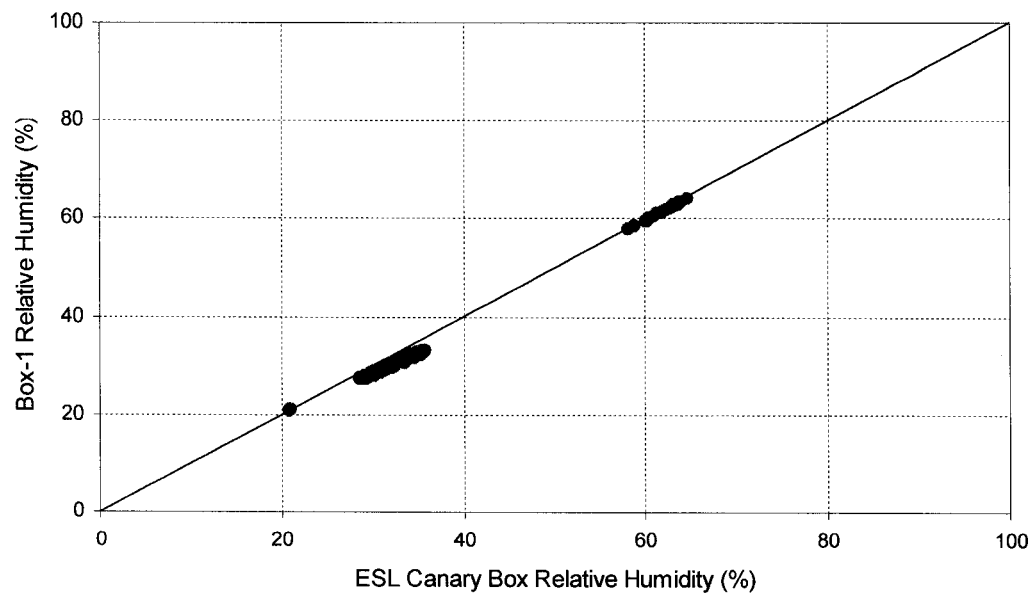


**Figure F.10** Comparisons of the Relative Humidity Measured by the Instrument Used in the Research (Box-1) Against Those Measured by the ESL Canary Boxes.



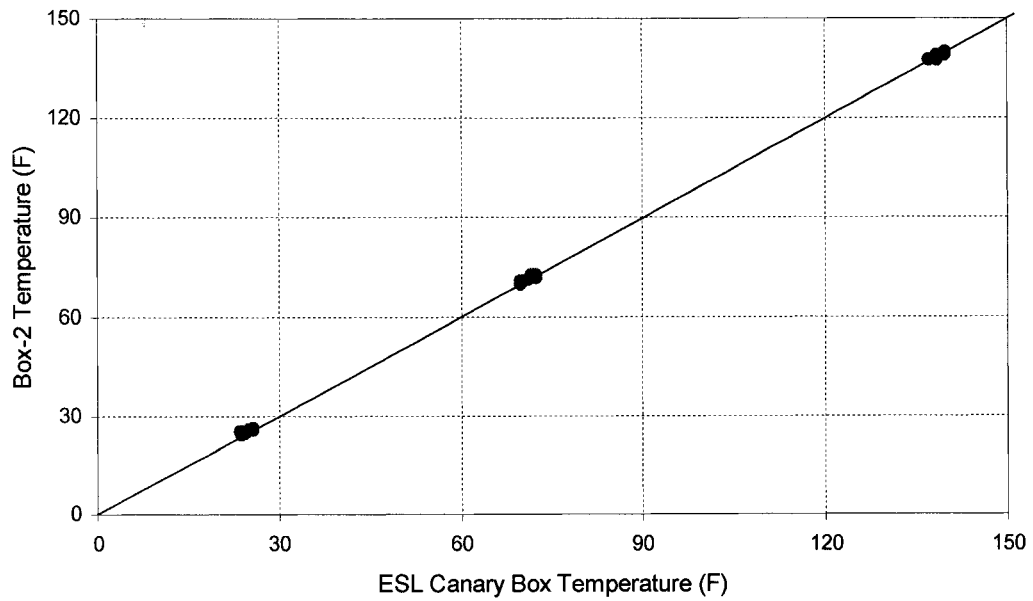


**Figure F.11** Comparisons of the Temperature Measured by the Instrument Used in the Research (Box-2) Against Those Measured by the ESL Canary Boxes..

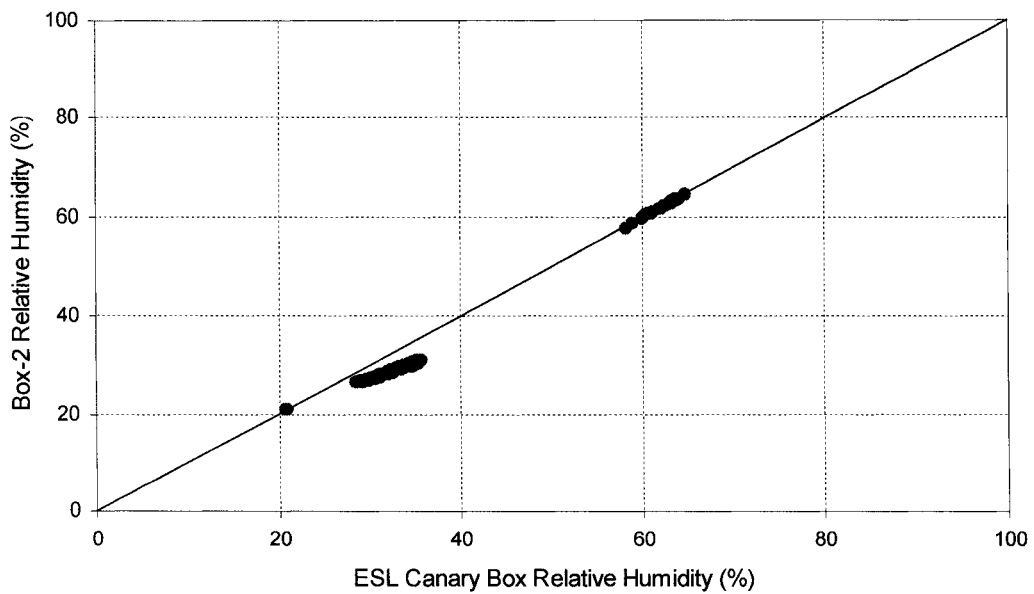


**Figure F.12** Comparisons of the Relative Humidity Measured by the Instrument Used in the Research (Box-1) Against Those Measured by the ESL Canary Boxes.

## APPENDIX G

### PREPARATION OF THE BANGKOK TRY FILE USING LS2TRY

The DOE-2 weather file used in the research was initially prepared by formatting a raw Bangkok weather data into a TRY file using the LS2TRY program developed by Bronson (1992). The LS2TRY program and documentation can be obtained from the Energy Systems Laboratory, Texas A&M University. Using LS2TRY, the TRY file generated from the program is readable by the DOE-2 weather processor, which later transforms this new TRY file into a binary file used only by DOE-2 during the hourly calculation. Basically, the LS2TRY program performs unit conversions of the hourly outdoor weather variables (i.e., dry-bulb temperature, relative humidity, global horizontal solar radiation, and wind speed), and then lays in this new set of data onto a base TRY file (i.e., the Chicago TRY file). To run the program, there are four files needed to be in the same DOS directory:

1. WEATHER\_FILE.DAT (i.e., a raw weather data file to be converted into a TRY file).
2. INSTRUCTION.INS (i.e., an instruction file).
3. BASE\_WEATHER\_FILE.DAT (i.e., a base TRY file, which is the Chicago TRY file).
4. LS2TRY.EXE (i.e., the program executable file).

The following is the format of the raw weather data file (WEATHER\_FILE.DAT)

STATION, MM, DM, YR, JULDY, DECTIME, HD, RH, F, IG, WSP
---

MM	= MONTH
DM	= DAY OF THE MONTH
DECTIME	= DECIMAL TIME/PASSED THRU THE PROGRAM
HD	= HOUR OF THE OBSERVATION
JULDY	= JULIAN DATE
YR	= YEAR
RH	= RELATIVE HUMDITY (%)
F	= DRY BULB TEMPERATURE (F)
IG	= GLOBAL HORIZONTAL RADIATION (W/M <sup>2</sup> )
WSP	= WIND SPEED (MPH)





## VITA

**Name:** Atch Sreshthaputra

**Place of Birth:**

Bangkok, Thailand

**Date of Birth:**

March 25, 1971

**Address:**

259/1 Soi Suan-Oi 2, Sukhothai Rd., Dusit  
Bangkok 10300, Thailand.

**Educational Background:**

Chulalongkorn University, Bangkok, Thailand  
Bachelor of Architecture (1993).

Georgia Institute of Technology, Atlanta, Georgia, USA  
Master of Science in Architecture (1996).

Texas A&M University, College Station, Texas, USA  
Doctor of Philosophy (2003).